Investigating the role of DA1 in growth control

Jack James Dumenil

A thesis submitted to the University of East Anglia in fulfilment of the Degree of Doctor of Philosophy

John Innes Centre, Norwich, Norfolk

September 2013

Abstract

Increasing global demand for food is a major issue facing modern day agriculture. For crops such as wheat and rice, where the seed constitutes the harvestable yield, the engineering of larger seeds provides a possible strategy for yield improvement. A detailed understanding of the growth of plant organs in general is paramount if such advances are to be made. Utilising previously characterised regulators of plant organ growth, this thesis explores the molecular mechanisms involved in the setting of final organ size.

This thesis capitalises on previous studies that have identified *DA1* as a negative regulator of organ growth; it explores the role of the DA1 protein and investigates its interactions with other proteins. *In vitro* studies reveal that DA1 forms homo- and hetero-multimeric complexes with its sister protein DAR1 and *in vitro* and in yeast assays reveal interactions between DA1 and the transcription factor TCP15 and the growth-regulating receptor-like kinase TMK4.

In addition, biochemical assays described in this thesis identify an active ubiquitin interacting motif (UIM) in the N-terminal region of DA1 and an ubiquitin-activated metallopeptidase in its C-terminal region. Further studies reveal that, in addition to being activated by the RING E3 ligases EOD1/BB and DA2, the DA1 peptidase is active towards both EOD1/BB and DA2. *In vitro* and *in vivo* studies demonstrate that DA1 cleaves a peptide fragment from the N-terminus of EOD1 and the C-terminus of DA2.

Finally, this thesis reports two genetic screens carried out in two separate Arabidopsis mapping populations in order to identify novel regulators of organ growth. Analyses of petal and seed phenotypes in the MAGIC RIL-type population and in a natural Swedish population identify novel and *a priori* candidate genes for further characterisation.

List of Contents

List of Figures

List of Tables

List of Supplementary Information

S1 – Supplementary Figures

S2 – Supplementary Tables

Acknowledgements

First and foremost I would like to thank my primary supervisor Professor Mike Bevan for all the assistance that he has given me over the course of my PhD. I believe that Mike's guidance over the last four years, and in particular his demand for both a challenging appetite for progress and a high degree of intellectual freedom, has enabled my work to progress as well as it has. I would also like to thank my secondary supervisors Dr Phil Wigge and Dr Cyril Zipfel, whose assistance has also been invaluable.

My deepest thanks also go to all members (past and present) of the Bevan Lab at the John Innes Centre. To Mathilde Seguela for her essential guidance in my early days in the Lab and to Fiona Corke, Caroline Smith, and Neil Mckenzie for their continued assistance with this work and their encouragement throughout my PhD. I must also say a huge thank you to Joshua Ball and Vladimir Chapman, whose efforts have been central to the progress of the GWA and MAGIC analyses. I cannot forget Cindy Cooper; her media assistance, guidance, cakes and smiles have ensured that I have thoroughly enjoyed my time in the Bevan Lab.

My thanks also go out to those who I have collaborated with, including Yunhai Li at the Chinese Academy of Science, Justin Borevitz and Riyan Cheng at the Australian National University, Canberra, and Andrei Kamenski at the University of York. In particular I would like to thank Matt Box; not just for his assistance with the MAGIC and GWAs studies, but for all his guidance and discussion, both scientific and not.

Most importantly: the family. I would like to say a massive thanks to all those who have put-up with me and supported me through the ups and downs of the last few years, in particular to Mum and Dad. Not forgetting Tim for his words of wisdom.

Finally, I would like to thank the BBSRC and BASF Plant Science who have funded my research. I would like to express particular thanks to BASF whose interest in the DA1 project has been central to developing my interest in the commercial side of science.

Chapter 1 - Introduction

1.1 - Population growth and food production

Global food production is constantly under pressure to keep up with demand from a rapidly growing population. Over the course of human history, events such as the mechanisation of farming during the agricultural revolution of the 17th-18th century, and more recently the Green Revolution of the 1960s, have generated huge advances in productivity. The significant improvements in irrigation, cultivars, fertilisers, and pesticides of the green revolution have allowed agriculture to sustain the huge population increase of the last 40 years (Mitchell and Sheehy, 2006). However, despite these advances, yield increases of key crops – such as rice and wheat– have begun to plateau (Cassman, 1999), with yield potentials (the yield achieved under optimal conditions, free of pathogens and pests) failing to improve over the past 30 years (Mitchell and Sheehy, 2006). The stagnation of the yield-potential increase suggests that increasing crop *productivity* is paramount if the projected population growth is to be sustained. For key food crops such as wheat, rice and maize, and potential fuel crops such as oilseeds, where the seed constitutes the harvestable yield, the engineering of increased seed size and seed number has significant potential benefits for food production and food security.

1.2 – Organ formation in plants

1.2.1 – Plant organs display determinate growth characteristics

Unlike animals, plants are unable to change location in response to environmental fluctuations and as a consequence have evolved a high degree of developmental plasticity to maximise fitness in different environments. Despite this plasticity, and the indeterminate nature of their vegetative growth, organs such as seeds, petals and leaves are determinate in their development. That is to say that they have a pre-determined size and shape. This is shown by the uniformity of final size and morphology of organs *within* species, compared to that found *between* species and between different varieties. In animal systems, organ development is also determinate and although growth of simple organs, such as the *Drosophila* early embryo, can be regulated by cell-counting mechanisms (Edgar et al., 1994), complex organs such as the *Drosophila* wing are thought to be regulated by 'size checkpoints' that detect total organ size rather than cell number (Dong et al., 2007). Current theories to explain how this determinate

development is achieved will be discussed in detail in section 1.5; however the following sections will focus on the developmental processes that underpin organ growth.

It is important to note that, despite considerable similarities, the developmental processes governing the growth of petals and leaves differ markedly from that of seeds. Therefore, in the interest of clarity the bulk of general discussion of 'organ development' in this section will refer to that of petals and leaves, and a separate section (section 1.4) will describe seed-specific regulatory processes.

1.2.2 – Organ initiation and identity

Shoot organs are initiated from the periphery of the shoot apical meristem (SAM) (Fig. 1.1), and the cells committed to form these organ primordia are then replenished by a stem cell population in the central zone of the SAM (reviewed in (Sablowski, 2011)). The maintenance of this stem cell population in the central zone is promoted by the homeodomain transcription factor *WUSCHEL* (*WUS*), which is expressed in the subjacent organising centre (Mayer et al., 1998). *WUS* exists in a regulatory negative feedback loop with the *CLAVATA 1*, (*CLV1*), *CLAVATA 2* (*CLV2*) and *CLAVATA 3* (*CLV3*), which acts to define the size and position of the stem cell population (Schoof et al., 2000, Bleckmann et al., 2010). In this loop, CLV3, a small peptide ligand expressed by stem cells, activates the receptor-proteins CLV1, CLV2 and CORYNE (CRN), which in turn act to repress *WUS* and thereby repress stem-cell identity (Fig. 1.1) (Bleckmann et al., 2010, Schoof et al., 2000).

The pluripotent stem cells of the apical meristem express Class I *KNOTTED1-LIKE HOMEOBOX* (*KNOX*) genes including SHOOTMERISTEMLESS (*STM*) in Arabidopsis and *KNOTTED 1* (*KN1)* in Maize (Jackson et al., 1994, Smith et al., 1992, Long et al., 1996). Non-pluripotent cells within the shoot apical meristem do not express the *KNOX* genes and *KNOX* genes are therefore considered to be markers, and possibly determinants of stem cell identity (Jackson et al., 1994, Smith et al., 1992, Long et al., 1996). Cells recruited into initiating organ primordia have a determinate fate and therefore stem-cell identity cues are repressed prior to organ initiation. This is illustrated by the observation that leaf initiation from the Arabidopsis SAM is promoted by the repression of the *KNOX* gene *BREVIPEDICELLUS* (*BP*) (Hay et al., 2006). *BP* expression in the lateral regions of the SAM is repressed by auxin (Scanlon, 2003, Hay et al., 2006) as well as the Arabidopsis MYB transcription factor *ASYMMETRIC LEAF 1* (*AS1*) and the *LATERAL ORGAN BOUNDARIES* family member *ASYMMETRIC LEAVES 2* (*AS2*) (Guo et al., 2008, Hay et al., 2006). In fact, the exact location of organ initiation from the meristem can be defined by auxin levels,

with auxin maxima observed to form at the precise site of organ primordium formation, and with evidence that exogenous application of auxin is sufficient to promote ectopic organ initiation (Reinhardt et al., 2003).

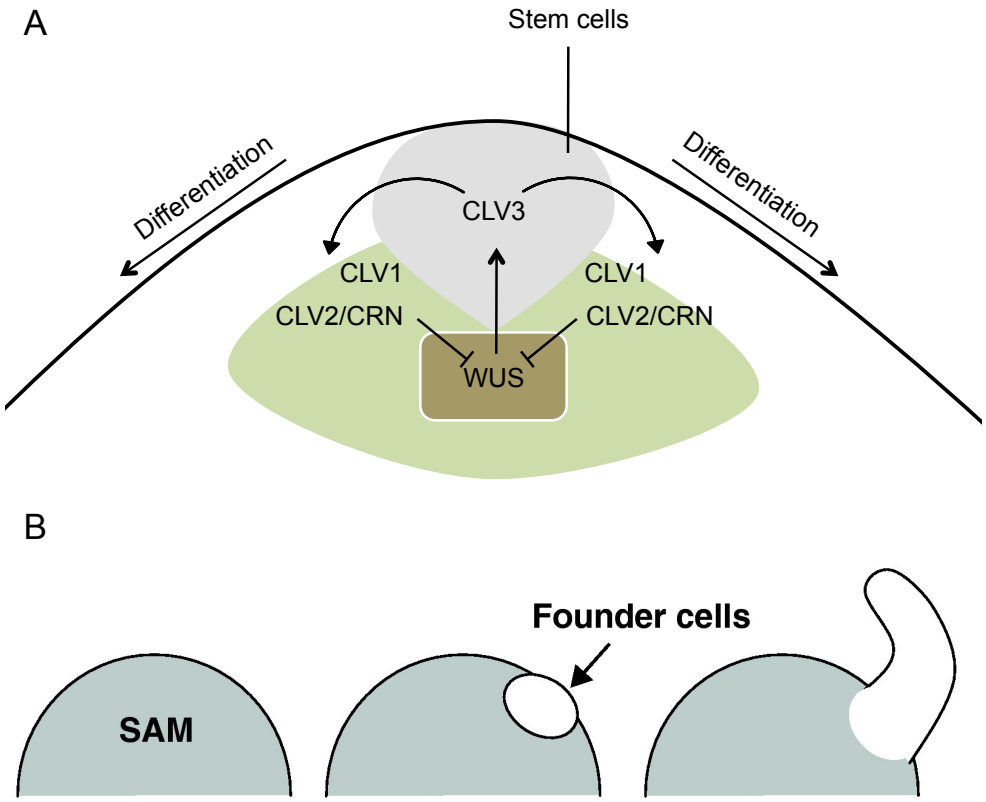

Figure 1.1 – Leaf initiation from the shoot apical meristem

(A) A stem cell population is maintained at the tip of the shoot apical meristem (SAM) by a feedback loop between WUS and CLV1, CLV2, CLV3 and CRN. WUS is expressed in the organising centre (brown shading) and promotes CLV3 activity in the stem cell population (grey shading), which is perceived by CLV1, CLV2 and CRN, whose expression domain is marked by green shading. CLV1, CLV2 and CRN activity represses WUS. (B) Organ primordium formation in Arabidopsis. Founder cells on the flank of the SAM switch from an indeterminate growth programme to a determinate fate, and subsequently develop into organ primordia. (A) Adapted from Sablowski et al (2011), Barton et al (2010) and Bosca et al (2011); (B) from Moon & Hake (2011).

The repression of *KNOX* genes in cells that go on to form organ primordia is thought to represent a switch from indeterminate to determinate growth programmes (Moon and Hake, 2011). The formation and initiation of organ primordia also results in a change in *identity* of founder cells; from a meristem identity to an organ-specific identity (e.g. petal, sepal, leaf precursors). For example, the switch in cell-identity that occurs during sepal initiation results in changes in cell proliferation rate, cell volume changes, heterogeneity in cell volumes, and growth isotropy (Schiessl et al., 2012). These changes are in part mediated by the transcription factor *JAGGED* (*JAG*) (Schiessl et al., 2012). Whereas the growth of wild-type sepal primordia differs from that of the meristem in many ways (mentioned above), *jag-1* sepal primordia do not (Schiessl et al., 2012); suggesting that *JAG* is required for the timely establishment of proper primordium identity (and therefore for appropriate primordium development).

Furthermore, as with plant growth in general, rather than being controlled by the autonomous allocation of individual cellular identities, shoot organ development is controlled by the interaction of different regions in relation to one another. This is highlighted by the Arabidopsis floral-identity triple mutant - *apetala2 (ap2) apetala3 (ap3) agamous (ag),* which results in the conversion of floral organs to leaf-like organs (Bowman et al., 1991). The absence of the respective floral identity genes in these plants results in a loss of floral identity in the floral organs and their consequent reversion to 'leaf-like' organs (Bowman et al., 1991). While these modified floral organs display many leaf-like characteristics, such as their overall morphology, they remain a similar size to organs of the perianth (Bowman et al., 1991), illustrating that the organ-intrinsic leaf-identity cues that result in a canonical leaf morphology interact with the meristem signals that dictate final organ size.

1.2.3 – Organ polarity

Following initiation from the meristem, leaf development occurs on three polar axes (Fig. 1.2); proximal-distal, adaxial-abaxial and medial-lateral (Moon and Hake, 2011), the establishment of all of which are necessary for wild-type leaf form and function.

In the mature leaf, adaxial (dorsal) tissues are often distinct from abaxial (ventral) tissues, and it is therefore important for adaxial-abaxial polarity to be accurately defined. For example, the C4 grass, *Paspalum dilatatum* has a greater stomatal density and higher rates of CO_2 assimilation in its abaxial surface relative to the adaxial surface (Soares et al., 2008). Maintenance of adaxial-abaxial polarity is determined by the antagonistic interaction of adaxially-expressed adaxial-identity promoting genes, and abaxially-expressed abaxial-identity promoting genes. Adaxial-identity promoting genes include *AS1*, *AS2* and the Class III *HOMEO*-

DOMAIN LEUCINE ZIPPER (*HD-ZIPIII*) family (Fu et al., 2007, Lin et al., 2003, Emery et al., 2003) and abaxial-identity promoting genes include members of the *KANADI* (*KAN*) (Eshed et al., 2001, Kerstetter et al., 2001) and *YABBY* (*YAB*) gene families (Eshed et al., 2004). The antagonistic interaction between these two groups of genes serves to restrict their expression to their respective compartments and thereby define an adaxial-abaxial boundary (reviewed in Moon & Hake 2011).

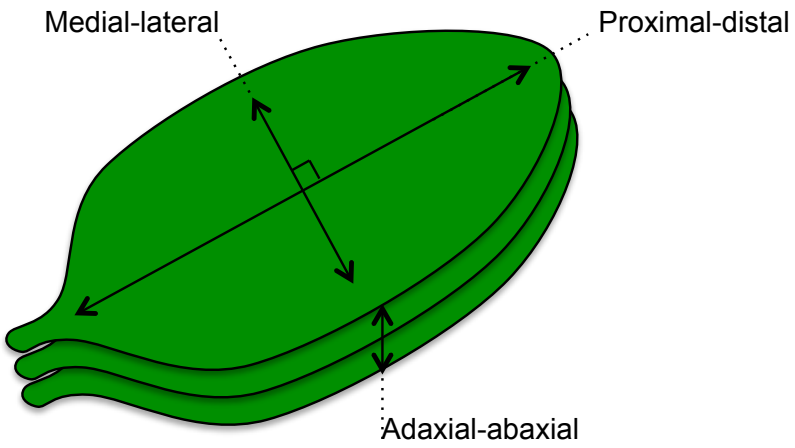

Figure 1.2 – Organ polarity in the leaf

A schematic illustrating the three planes of polarity in the developing organ, using the leaf as an example. The proximal-distal axis runs along the length of the leaf, from petiole to leaf tip; the medial-lateral axis runs perpendicular to the proximal-distal axis, *across* the leaf blade; the adaxial-abaxial axis runs perpendicular to both medial-lateral and proximal-distal axes, through the leaf blade, from one leaf surface to the other.

In simple leaves the proximal-distal axis determines the blade-petiole (in dicots) and blade-sheath (in monocots) organisation. The de-repression of *KNOX* genes in the petioles of the *blade on petiole* (*bop*) mutant results in ectopic leaf blade tissue developing on the petiole (Ha et al., 2004, Norberg et al., 2005). While *KNOX* genes are not normally expressed in developing simple leaves, their expression is required for the lobed shape of compound leaves (Efroni et al., 2010). Indeed a correlation has been observed between the expression of *KNOX* genes and leaf complexity in such plants (Bharathan et al., 2002, Hareven et al., 1996) (reviewed in Efroni

et al., 2010), and ectopic expression of maize *KN1* has been shown to generate super-compound leaves in tomato (Hareven et al., 1996).

Because the modifications to leaf shape along the medial-lateral axis often occur in concert with modification along the proximal-distal axis, it is perhaps more useful to consider these axes as interacting elements of overall leaf *shape*. Indeed, aspect ratio (length:width) has been used as a metric for measuring the *shape* of both Arabidopsis leaves (Kieffer et al., 2011) and petals (Abraham et al., 2013) in recent publications.

While aberrations in adaxial-abaxial polarity can result from mis-expression of tissue-identity genes, aberrations in organ shape result from the mis-regulation of the two driving forces of organ growth: cell proliferation and cell expansion (see section 1.3). Following initiation from the meristem, organ growth is driven by a phase of cell proliferation – during which cells mitotically divide and increase in number – and then a phase of cell expansion, wherein cells exit mitosis and increase in volume (described in detail in section 1.3). The tissue specific mis-regulation of cell proliferation and cell expansion along medial-lateral and proximal-distal axes can affect overall organ shape.

As discussed in detail in section 1.3, cell proliferation in the developing organ is though to be terminated by a basipetal cell-cycle arrest front, which causes cells to exit mitosis and commence cell expansion (Nath et al., 2003). Mutants in the Antirrhinum *TCP* family transcription factor C*INCINNATA* (*CIN*) have an altered pattern of cell-cycle arrest, whereby, compared to wild-type leaves, the marginal tissue grows for longer (Nath et al., 2003). This increase in growth in the leaf margins, results in wider leaves with a negative curvature (2003, Nath et al., 2003).

Members of the Arabidopsis *TCP* family of transcription factors have also been shown to affect leaf shape. Mutations in the Class I *TCPs, TCP14* and *TCP15*, despite having a wild-type final leaf size, have been shown (using a principal component analysis) to have significantly altered shape components (Kieffer et al., 2011). These include an altered aspect ratio component of leaf shape; revealing that in the *tcp14/15* mutants there is a mis-regulation of growth along the proximal-distal axis relative to growth along the medial-lateral axis (Kieffer et al., 2011). More severe *TCP*-related leaf-shape phenotypes can be seen in *JAW-D* plants, which over-express miR319a (a micro-RNA that down-regulates *TCP2, TCP3*, *TCP4*, *TCP10,* and *TCP24*) (Palatnik et al., 2003). Leaves of *JAW-D* plants have significantly altered shape, with a distinctive curled-phenotype (Palatnik et al., 2003).

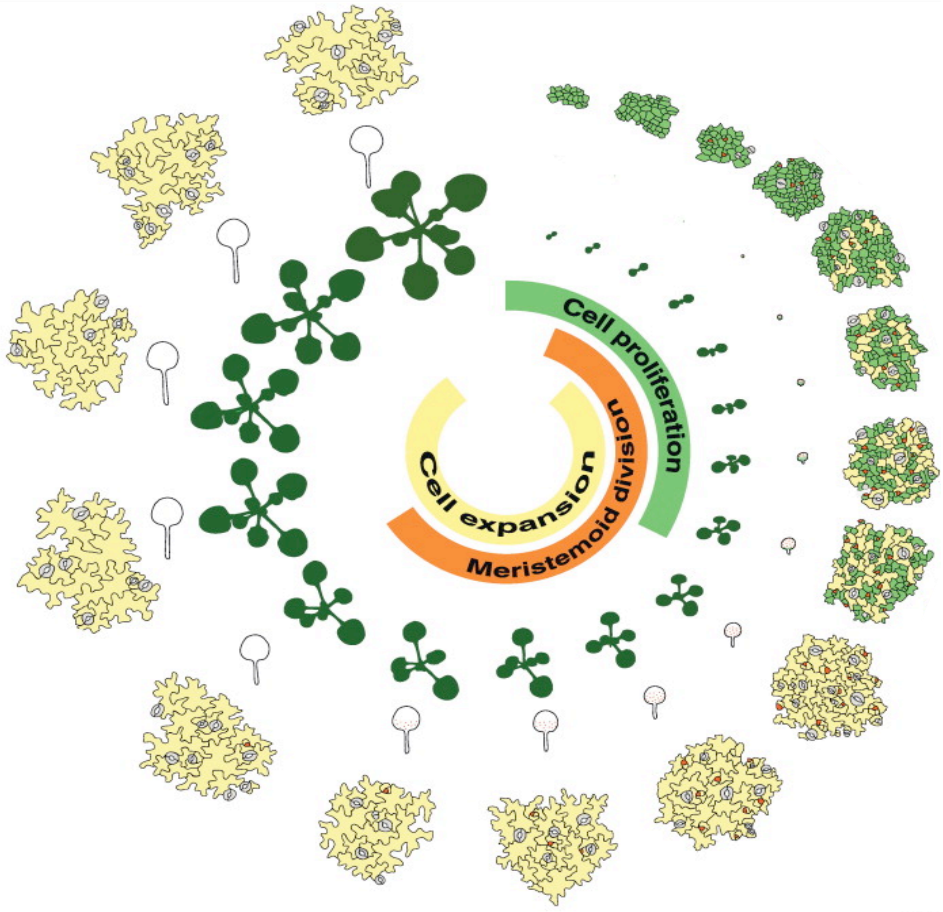

Figure 1.3 – Growth phases during organ development

Overlapping stages of cell proliferation, meristemoid division and cell expansion shown at the cellular, leaf and rosette level. Proliferating cells are represented as green cells, post-mitotic cells are shown in yellow and meristemoid cells are shown in orange. In the early stages of leaf development the majority of cells are mitotically active and proliferate rapidly. This is followed by mitotic arrest and the transition from cell proliferation to cell expansion, such that eventually all cells are in the expansive phase. Overlapping the transition from cell proliferation to cell expansion is a phase of prolonged meristemoid division, which appears to persist after the onset of the cell-cycle arrest front. (From Gonzalez et al (2012)).

1.3 – Organ growth is a multi-phase process

Leaf and petal growth can be generalised into two key cellular processes that occur in phases; an initial period of cell proliferation, followed by a period cell expansion (Fig. 1.3) (Johnson and Lenhard, 2011, Horiguchi et al., 2006a, Bögre et al., 2008). Following initiation from the SAM, cells in the organ primordium divide during a period of cell proliferation, wherein rapid mitotic divisions result in an increase in cell number (Johnson and Lenhard, 2011). This proliferative phase of growth is terminated by a basipetal front of cell-cycle arrest (Nath et al., 2003, Donnelly et al., 1999) that causes cells to exit the mitotic cell-cycle and initiate a phase of cell expansion (Melaragno et al., 1993). In some organs – such as leaves – mitotic exit is concurrent with entry to the endocycle (see Box 1.2) and subsequent endoreduplication.

The following sections (1.3.1 – 1.3.4) describe in detail the importance of organ initiation, cell proliferation, cell expansion, and the transitory growth phase in establishing final organ size.

1.3.1 – Primordial formation from the shoot apical meristem

Organs such as leaves and petals are formed from primordia that initiate from the shoot SAM (see section 1.2.2). When cell proliferation is accelerated in the SAM, such as caused by the overexpression of *Arabidopsis* CDC27a (a subunit of the Anaphase Promoting Complex (APC)) in tobacco, the L1 zone forms with a larger complement of smaller cells (Rojas et al., 2009). As a consequence, more (smaller) cells are recruited into the initiating organ primordia and the resulting mature leaf is significantly larger than the wild-type (Rojas et al., 2009). In addition, the exogenous application of auxin (dissolved in lanolin) to *pin1* mutant SAMs has been shown to be sufficient to induce ectopic organ initiation (Reinhardt et al., 2003). Interestingly, larger droplets of lanolin resulted in the initiation of larger organ primordia from the SAM (Reinhardt et al., 2003).

These data suggest that an increase in the number primordium founder cells can lead to an increase in overall organ size. This is consistent with observations that the *struwwelpeter* (*swp*) mutant in Arabidopsis, has reduced leaf area and cell number from the earliest stages of development (Autran et al., 2002). The reduction in final leaf size and cell number is therefore possibly due to fewer cells being recruited into the initiating leaf primordium (Autran et al., 2002).

In addition to the influence of the *size* of the organ primordium, the *rate* of primordia initiation may also have an impact on final organ size. This has been observed with *klu* mutants, which show an interaction between an accelerated plastochron and a reduced final organ size

(Anastasiou et al., 2007), as well as in rice *pla1* (*plastochron 1)* mutants, which have an increased plastochron and smaller leaves (Miyoshi et al., 2004).

1.3.2 – Cell proliferation

The proliferative stage of organ growth occurs early in the development of the organ (Andriankaja et al., 2012), and is responsible for determining the population of cells that will enter the expansive phase. As the expansive phase contributes to the majority of organ size increase, the *rate* and *duration* of cell proliferation in young organ primordia can significantly influence final organ size. The *rate* of cell proliferation refers to the average number of mitotic cycles per unit time during the proliferative phase; with an elevated proliferation rate generating a larger population of cells in a fixed time interval. The proliferative phase commences when primordia initiate from the SAM and it is terminated when cells exit the mitotic cell cycle. The *duration* of cell proliferation therefore refers to the average duration of mitotic activity within the developing organ.

Many genes have been shown to influence cell proliferation during organ formation; these include genes that affect the *rate* of cell proliferation as well as genes that influence the *duration* of cell proliferation (reviewed in (Breuninger and Lenhard, 2010)). Genes that influence the *rate* of cell proliferation include the *GIF1/2/3* (*GRF-interacting factor)* triplet. The *gif1/2/3* triple mutant has a reduction in final leaf size, which is concurrent with a reduction in cell number (Lee et al., 2009). Kinematic analysis of growth revealed that this reduction in cell number is due to a reduction in cell-proliferation *rate* rather than a temporal mis-regulation of proliferation initiation and termination (Lee et al., 2009). Arabidopsis GIF proteins have been shown to directly physically interact with the GROWTH-REGULATING FACTOR (GRF) family of proteins, a relationship that is thought to reflect the fact that GRFs and GIFs are transcriptional coactivators (Horiguchi et al., 2005, Kim et al., 2003). Similarly to the *gif1/2/3* triple knockout (Lee et al., 2009), the *grf5* single mutant and the *grf1/grf2/grf3* triple mutant have smaller leaves with fewer cells (Horiguchi et al., 2005, Kim et al., 2003, Kim and Kende, 2004). Based on the observed interactions between GRFs and GIFs (Horiguchi et al., 2005, Kim et al., 2003, Kim and Kende, 2004), this reduction in leaf size is expected to be a consequence of a reduction in the *rate* of cell proliferation during leaf development.

A similar effect is seen with *sleepy1* (*sly1*) mutant plants, which are defective in an F-BOX E3 ligase subunit (see section 1.7.4 for details). In *sly1* plants, leaf area is also reduced as consequence of a reduction in cell proliferation rate (McGinnis et al., 2003, Achard et al., 2009). The molecular basis of this phenotype is discussed in more detail in section 1.5.1.

In contrast to influencing the *rate* of cell proliferation, three genes, all with links to the ubiquitin system, have been shown to negatively influence the *duration* of cell proliferation (Li et al., 2008, Xia, 2013, Disch et al., 2006). Loss of function mutations in two RING E3 ligases, *BB/EOD1* and *DA2,* result in an increase in leaf area as a consequence of an increase in cell number (Disch et al., 2006, Xia, 2013). Kinematic analysis of leaf growth in these mutants reveals that the cell-proliferation rate is not increased; instead the duration of the proliferative phase of organ growth is increased (Disch et al., 2006, Xia, 2013). E3 ligases are involved in the post-translational modification of substrate proteins with ubiquitin (see section 1.7.4), which can act as both an enhancing and a repressive signal (Mallery et al., 2002, Fang et al., 2000, Stevenson et al., 2007). It is possible that DA2 and EOD1 repress organ growth through the ubiquitin-directed proteolysis of factors that promote cell proliferation, or through the ubiquitin-dependent activation of factors that promote cell expansion.

A similar phenotype is also seen with the dominant negative *da1-1* allele of *DA1*, encoding a UIM (ubiquitin interaction motif)-containing peptidase. *da1-1* plants have enlarged leaves, petals and seeds as a consequence of an extended duration of cell proliferation (Li et al., 2008). In the case of *da1-1*, cells in the developing leaf were mitotically active for almost 50% longer than in wild-type plants, resulting in a increased number of cells leading into the phase of expansive cell growth (Li et al., 2008).

Although *EOD1* and *DA2* do not genetically interact, recent data has revealed a genetic interaction between *DA1* and both E3 ligases; *EOD1* and *DA2* (Li et al., 2008, Xia, 2013). This interaction, and the link to the ubiquitin system held by all three genes, presents the possibility that all these genes might influence cell proliferation through the same mechanism.

In contrast to the negative effect on the duration of proliferation exhibited by *DA1*, *EOD1* and *DA2; KLUH* (*KLU*) – a cytochrome P450 – has been revealed as a positive regulator of the duration of cell proliferation in developing organs (Anastasiou et al., 2007). *Klu-2* knockout plants display reduced leaf, sepal and petal area (Anastasiou et al., 2007), and a reduction in final seed size (Adamski et al., 2009). The reduction in lateral organ area does not coincide with a reduction in cell size or cell proliferation *rate*, instead cells in *klu-2* organs have a reduced *duration* of cell proliferation during organ growth (Anastasiou et al., 2007). Interestingly, in *KLU*/*klu-2* chimeric plants *KLU* appears to function non-cell-autonomously; influencing the development of neighbouring *klu-2* tissues in chimeric organs and influencing *klu*-2 organs in chimeric inflorescences (Eriksson et al., 2010). These observations are reminiscent of data from the study of the developing Drosophila wing disc, which reveal the

coordinated growth of adjacent cell populations. In these studies, targeted inhibition of growth in the anterior or posterior territory of the Drosophila wing disc resulted in a non-cell-autonomous reduction in cell proliferation in the adjacent, unaffected territory (Mesquita et al., 2010). This coordinated reduction in cell proliferation across the entire organ results in the formation of well-proportioned wings despite growth inhibition in only one territory (Mesquita et al., 2010). This is similar to the coordinated, well-proportioned morphology observed in *KLU*/*klu-2* chimeric petals, which occurs despite the absence of *KLU* in one petal region (Eriksson et al., 2010). These data suggest that *KLU* might influence organ growth via a diffusible signal molecule (Eriksson et al., 2010, Kazama et al., 2010); this is discussed in detail in section 1.5.2.

Evidence that the basipetal arrest front (responsible for triggering exit from the proliferative phase) persists at a fixed distance from the leaf blade base (Kazama et al., 2010) suggests that, as well as the regulation of *rate* and *duration* of cell proliferation, regulation of the *area* of mitotic competence within the developing leaf might also determine final organ size. For example, an enlarged proliferative region in the developing leaves of the *spatula* (*spt*) mutant is thought to contribute to an increase in final leaf size (Ichihashi et al., 2010). In *spt* leaves (deficient in the *SPT* bHLH transcription factor), an increase in cell number with no change in cell size suggests that mis-regulation of cell proliferation is responsible for the larger final leaf size (Ichihashi et al., 2010). The fact that a size difference is only visible five days after sowing (DAS), and not at 3 DAS (during the proliferative phase), suggests that the rate of proliferation is in fact not altered (Ichihashi et al., 2010). Despite the lack of direct evidence that the duration of proliferation is unaffected, evidence that the proliferative region of the leaf is larger in *spt* plants supports the idea that *SPT* could influence the spatial regulation of proliferative competence within the developing leaf. Based on this data, there are two potential mechanisms of action of the *spt* mutant. Firstly, *SPT* could influence the range of a purported diffusible growth signal, thereby extending the influence of a pro-proliferation factor. Alternatively, it could adjust the sensitivity of all cells in the leaf to such a growth factor, and therefore alter the growth factor's active range (a more detailed discussion of these concepts is presented in section 1.5).

As well as the uniform regulation of cell proliferation across the entire organ, some genes have been revealed to control cell proliferation in a tissue-specific manner. For example, the zinc-finger transcription factor, *JAG,* which has narrower and shorter petals and sepals than wild-type plants, affects the *duration* of cell proliferation of certain, specific petal tissues (Dinneny

et al., 2004, Ohno et al., 2004). *JAG* appears to promote petal growth by maintaining the mitotic competence of the distal regions of the petal (Dinneny et al., 2004), revealing a differential regulation of cell proliferation along the proximal-distal axis. In a similar way, the Antirrhinum *CIN* gene appears to regulate the duration of cell proliferation along the medial-lateral axis, with leaf margins proliferating for longer in *cin* mutants (2003). Leaves of *cin* plants are larger than the wild-type and, like *jag* petals, have an aberrant morphology (2003, Dinneny et al., 2004, Ohno et al., 2004), revealing a role for tissue-specific regulation of cell proliferation in the patterning of organs.

Additional tissue-specific regulation of cell proliferation in the developing organ can be seen for meristemoid cells, which are guard cell precursors (Fig. 1.3). Meristemoid cells typically undergo one to three rounds of asymmetric division before forming the guard mother cell (GMC), which then undergoes one further symmetric division to form two guard cells (Peterson et al., 2010). This means that a single meristemoid cell can generate up to three pavement cells and two guard cells, and their population therefore makes a significant contribution to overall leaf size. Importantly, regulation of meristemoid division appears to be largely independent of the mechanisms controlling pavement cell proliferation (Andriankaja et al., 2012), and therefore it is perhaps appropriate to consider meristemoid division as a separate growth phase.

Only one example of the mis-regulation of meristemoid cell division is known for Arabidopsis: *PEAPOD* (*PPD*). The *ppd* loss-of-function mutant has increased leaf lamina size and generates curved leaves due to increased proliferation within the leaf blade (White, 2006). However, unlike the *da1-1* mutant or the *gif1/2/3* triple mutant (Lee et al., 2009, Li et al., 2008), the observed increase in proliferation is not a consequence of a *general* increase in proliferation, but specifically a mis-regulation of meristemoid cell proliferation.

It is noteworthy that the absence of meristemoid cells in petals makes the petal a considerably simpler organ for the study of growth and development.

1.3.3 – Cell expansion

During organ growth, cell expansion occurs through either an endoreduplication-correlated mechanism, or an endoreduplication-independent mechanism. In the former system, cells enter a modified cell-cycle called the endocycle (see Box 1.2), and every endocycle is accompanied by a concurrent increase in cell volume. The latter system involves cell expansion that is independent of the endocycle, and is primarily dependent on biophysical expansion.

1.3.3.1 – Endoreduplication-correlated cell expansion

Analysis of cell types from many different organisms - from endoreduplicated plant cells to multi-nucleate somatic syncytia in *Caenorhabditis elegans* – reveals a positive correlation between cell size and ploidy, with larger cells having an increased DNA content (Sugimoto-Shirasu and Roberts, 2003, Flemming et al., 2000, Nagl, 1976). The molecular basis of this correlation is not well understood (Sugimoto-Shirasu and Roberts, 2003), however it is possible that high ploidy is simply a requirement of increased cell size. It has been suggested that cell *division* is a consequence of organ growth rather than a cause; i.e. a high density of nuclei is needed to provide "information" (RNA and proteins) over suitable distances to the developing organ (Mizukami, 2001). Based on this logic, it would follow that endoreduplication would be necessary to sustain large cell sizes. This is supported by observations in crop plants such as wheat and sugarcane, in which genome duplication events are associated with increased cell size.

The endocycle (the cell-cycle that drives endoreduplication) is a modified cell-cycle in which DNA replication is un-coupled from cytokinesis (see Box 1.2). For this reason, regulation of cell expansion can also occur at the level of the cell-cycle. For example, a mutation in RPT2a, a subunit of the 26S proteasome regulatory particle, has been shown to increase final leaf size as a result of increased cell expansion and endoreplication (Sonoda et al., 2009). The 26S proteasome plays a key role in the cell-cycle by rapidly degrading cell-cycle regulators and ensuring a unidirectional progression through the cycle (see section 1.6 for a detailed discussion of the cell-cycle). *rpt2a* mutants show elevated expression of G1- and S-phase specific factors and an uncoupling of the G2/M transition (see section 1.6), both of which act to promote endoreplication (Sonoda et al., 2009). Additional genes, such as *ARL* (*ARGOS-LIKE*) and *ZINC FINGER HOMEODOMAIN5* (*ZHD5*), have been shown to increase leaf size by influencing cell expansion (Hu et al., 2006, Hong et al., 2011). However, in these examples there is no clear causative link to the mis-regulation of the cell-cycle.

1.3.3.1 – Biophysical regulation of cell expansion

The cell wall of plants exerts major constraints on cell expansion, and emerging evidence shows that there is a complex interplay between the constraint of cell expansion by the cell wall, and genes that control cell size.

A striking example of this is the *transparent testa glabra 2* (*ttg2*) mutation, which causes a biophysical constraint in one tissue type that results in an overall reduction in the size of the entire organ (Garcia et al., 2005). *TTG2* is a seed-coat expressed gene that is thought to

influence seed size through the integument-mediated physical restriction of endosperm growth (Garcia et al., 2005). *TTG2* is discussed in more detail in section 1.4. In addition to this example, which documents the physical restriction of whole organs, there are also examples of physical constraints acting on individual cells. These forces, which influence cells of the SAM and the developing leaf primordium, have been shown to affect both leaf initiation and final size. In tomato, the exogenous application of expansin – a cell wall loosening protein (Sampedro and Cosgrove, 2005) – to the SAM causes ectopic primordia formation (Fleming et al., 1999, Fleming et al., 1997). This is thought to occur through the loosening of the L1 layer of the SAM, relaxing its physical constraint to the over-proliferation of subjacent cell layers and allowing *de novo* leaf primordia to develop (Kessler and Sinha, 2004). In support of this work is data demonstrating that, in addition to the exogenous application of expansins, the over-expression of *EXPANSIN 10* (*EXP10*) in Arabidopsis is sufficient to increase leaf size (Cho and Cosgrove, 2000).

Work has also revealed that changes in the methyl-ester status of pectin polysaccharides in the cell walls of the SAM contributes to organ primordia formation and phyllotaxis (Peaucelle et al., 2008). This is thought to be due to the increased tissue elasticity that accompanies demethylesterification (Peaucelle et al., 2011), and supports predictions that elastic domains in the SAM form mechanical signals that promote organ initiation (Kierzkowski et al., 2012). This regulatory effect of the SAM on overall plant growth can be seen through the manipulation of the SAM in *brassinosteroid insensitive1* (*bri1*) plants, which exhibit a dwarfed phenotype as a consequence of defects in cell expansion (Clouse et al., 1996). Over-expression of *BRI1* in the L1 layer of the SAM of *bri1* plants is sufficient to completely rescue the dwarfed phenotype (Savaldi-Goldstein et al., 2007). In addition, targeted depletion of brassinosteroids in the L1 layer of wild-type plants is sufficient to generate a dwarfed phenotype, revealing that the SAM epidermis is able to both promote and restrict plant shoot growth (Savaldi-Goldstein et al., 2007).

Finally, there is also evidence that cortical microtubule dynamics control organ growth and development through a biophysical mechanism. The observation that the long and narrow leaf phenotype of the *angustifolia* (*an*) mutant is due to the promotion of cell-expansion along the apical-basal axis, and that this is concurrent with altered cortical microtubule arrangements, suggests that the regulation of microtubules at the cellular level may influence overall organ size (Kim et al., 2002). This link between individual cell growth and whole-organ development

is important, as it demonstrates that cell-autonomous mechanisms can provide considerable control of overall growth (see section 1.5).

1.3.4. – The transition phase: controlling the 'stock' of cells entering expansion

For organs that undergo endocycle-correlated cell expansion, organ growth can be simplified into an initial phase of cell proliferation followed by a phase of endocycle-driven cell expansion. While these phases may overlap at the whole-organ level (i.e. at a specific time point during organ formation some cells will be cycling through the mitotic cell cycle and others will be cycling through the endocycle), individual cells can only either be mitotically cycling *or* endocycling. As a consequence, cells undergo a decision-making process, with some factors influencing them to remain proliferating, and others promoting the switch to the endocycle (see section 1.6 for detailed review of this topic).

Genes such as *DA1*, *EOD1, DA2*, and *KLU* (Disch et al., 2006, Li et al., 2008, Xia, 2013, Anastasiou et al., 2007) control the temporal dynamics of this decision and thereby alter the timing of the switch to cell expansion. *DA1* and *EOD1* for example, both promote the onset of cell expansion, and cells in which these genes are absent take longer to execute the decision to enter the expansive phase (Li et al., 2008, Disch et al., 2006). Conversely, genes such as *KLU* and *CYCD3* appear to negatively regulate the onset of cell expansion (Adamski et al., 2009, Anastasiou et al., 2007, Dewitte et al., 2007). This reveals the existence of antagonistic signalling pathways, which possibly influence cell proliferation through the decision-making of individual cells (to divide or to expand) during organ growth.

As discussed in section 1.3.2, the Antirrhinum *CIN* gene is also thought to increase the sensitivity of cells to the basipetal arrest front (Nath et al., 2003). However in this example, the effect is enhanced only in the leaf margins where *CIN* is most strongly expressed (Nath et al., 2003), further highlighting the importance of cell-autonomous factors during the transition phase.

Conversely, genes such as *SPT* regulate the spatial dynamics of the transition from cell proliferation to cell expansion; influencing the distance of the arrest front from the leaf base during the arrest front *pausing* phase (Ichihashi et al., 2010, Andriankaja et al., 2012, Kazama et al., 2010). The re-location of the arrest front in the *spt* mutant could be due to either an extension of the field of a mobile growth signal (see section 1.5.2 for a discussion), or the increased sensitivity of leaf cells to this signal. In both models, the balance of factors influencing proliferation and expansion would be influenced in the direction of cell proliferation (along the apical-basal axis), and thus result in an enlarged proliferative region.

Typically, genes such as *DA1* and *EOD1* (Li et al., 2008, Disch et al., 2006) – whose mutants result in enlarged organs – are considered to be *negative regulators of the duration of cell proliferation*. However as this section highlights, ultimately, it is the molecular decision-making of individual cells that will determine final organ size and therefore it is perhaps more accurate to consider these genes as *promoters of the transition to expansion*, thereby considering the role of these genes from a cell-centric viewpoint.

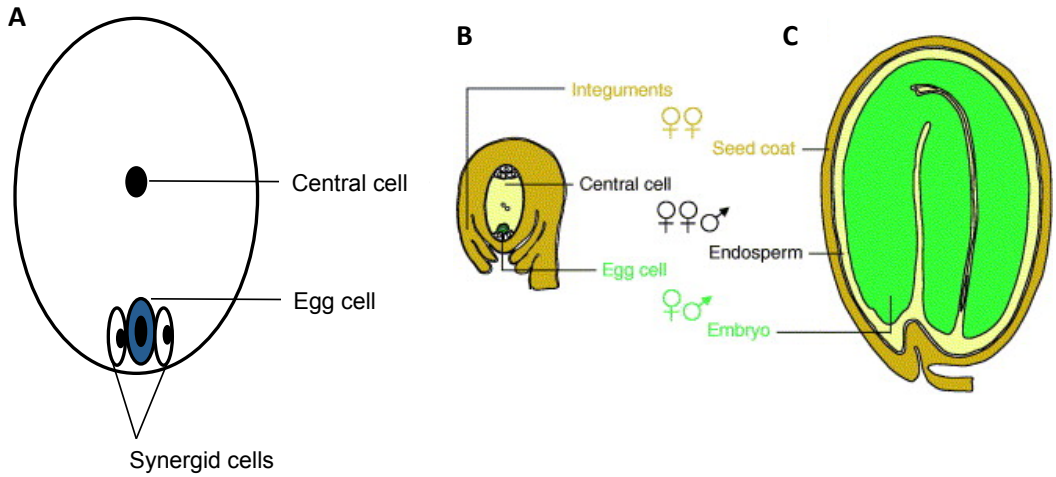

Figure 1.4 – The mature Arabidopsis female gametophyte and the developing seed

(A) The embryo sac contains one homodiploid central cell, one haploid egg cell, and two haploid synergid cells. (B,C) The Arabidopsis gametophyte prior to fertilisation (B) and the developing seed (C). Maternal tissues are labelled in gold, diploid zygotic tissues are labelled in green and triploid zygotic tissues in yellow. Before and after fertilisation the maternal sporophytic tissue (either the integuments (B) or the seed coat (C)) is intimately associated with the gametophytically derived tissue of the central cell and egg cell, which becomes the endosperm and embryo respectively. (B,C) Adapted from (Haughn and Chaudhury, 2005)

1.4 – Seed growth

Seed development requires the integration of three genetically distinct tissues, all of which are not found in other aerial organs (Fig. 1.4). All angiosperms undergo double fertilisation, whereby two sperm cells enter the embryo sac, with one fertilising the haploid egg cell and one fertilising the homodiploid central cell (Berger et al., 2008). This results in the fertilised seed consisting of three genetically distinct components (see Box 1.1); the embryo (2N), the endosperm (3N) and the seed coat - derived from the ovule integuments (2N). Due to their intricate inter-dependence, the growth of all three tissues is tightly coordinated during seed

development. For example, the developing embryo relies on the provision of nutrients and support from the endosperm (Hirner et al., 1998, Lopes and Larkins, 1993), and the endosperm in turn depends on the accurate development of, and nutrient flow from the integuments (Garcia et al., 2005, Lopes and Larkins, 1993). This interdependence can be seen through the highly complex developmental regulation in the seed, whereby changes in an individual tissue can have pleiotropic effects on the other tissues, as well as on seed size in general.

BOX 1.1 – Genetic composition of the seed

Sporophyte and gametophyte

The Arabidopsis female gametophyte; the embryo sac, contains two synergid cells, one haploid egg cell, and a homodiploid central cell. It exists in intimate contact with the sporophytic tissue of the seed coat, which is derived from the maternal ovule integuments (Chaudhury et al., 1998).

Maternal and zygotic

The partition between maternal and zygotic tissue is not as distinctive as the sporophyte – gametophyte split. Zygotic tissue is that derived from the fertilised egg cell; the embryo (2N), and from the fertilised central cell; the endosperm(3N) (Berger et al., 2008). The only true maternal tissue is the sporophytic tissue of the seed coat (2N), however, maternal gametophytic regulation also exists. This is from maternally inherited alleles that act through the gametophytic tissue, even after the fertilisation events (Grossniklaus et al., 2001). Within the zygote, the genetic differences between embryo and endosperm are more complex than just 2N Vs 3N.

Maternal regulation of seed development can occur in different ways. One such mechanism is the maternal regulation of seed nutrition, which occurs through the chalazal tissue. Impairment to this tissue (the site of nutrient transport) in the *Seg 1*, *3*, *6*, and *7* barley mutants has been shown to significantly reduce overall seed size (Felker et al., 1985). Maternal regulation of seed development can also occur via the integuments, as illustrated by *ttg2*; a mutation in an integument-expressed proanthocyanin synthesis gene. *ttg2* plants produce smaller and rounder seeds as a direct consequence of reduced cell elongation in the integuments (Garcia et al., 2005). In these seeds, through either biophysical constraint, or through proanthocyanin-mediated poisoning of the endosperm, the *ttg2* integuments act to restrict endosperm growth, thereby reducing final seed size (Garcia et al., 2005). Furthermore, and highlighting the intricate relationship between all genetic compartments within the seed, this reduction in endosperm restricts embryo growth (Garcia et al., 2005).

Conversely, gametophytic regulation of sporophytic tissues can also occur. Autonomous endosperm proliferation in the gametophytic *multicopy suppressor of ira* (*msi1)* mutant, leads to the enlargement and partial differentiation of the integuments (Ingouff et al., 2006). It is not clear whether this gametophytic effect on integument development is of a biophysical nature or due to cross talk between the two compartments, however it clearly shows that the development of the endosperm and the integuments are intricately linked. One further example is the sporophytic recessive *haiku* (*iku*) mutation (Garcia et al., 2003), which, like *msi1*, reduces integument development through a reduction in endosperm growth. However, unlike the *msi1* allele, the *iku* allele is zygotically expressed. This demonstrates that partitioning of the developing seed into the gametophyte and the sporophyte, or maternal and zygotic tissue, is probably not sufficient to understand the complexities, coordination, and compartmental cross-talk involved in seed development.

1.5 – Coordinating cell division and expansion during organ growth

1.5.1 – Hormonal regulation of organ growth

Auxin, brassinosteroids, gibberellic acid and cytokinins are long-range signalling molecules that have widespread effects in plant development and play a key role in regulating organ growth (Johnson and Lenhard, 2011). As small signalling molecules, they have the potential to coordinate the activities of large populations of cells throughout the developing plant, and as a consequence aberrations in synthesis, perception and degradation of phytohormones often results in systemic phenotypes.

Auxins have been shown to influence both cell expansion and cell proliferation (Chen et al., 2001), and to be involved in regulating many developmental processes, including embryo development, organ initiation, leaf vascular development and patterning, and root growth (reviewed in Teale et al 2006). Auxins appear to influence leaf expansion via changes to the cell wall and the plasma membrane (Overvoorde et al., 2005, Teale et al., 2006), suggesting that auxin-dependent cell expansion changes are due to biophysical effects. Auxin-mediated regulation of cell proliferation, however, is less well understood, although there is evidence that auxin regulates the expression of several cell-cycle genes (reviewed in (Vanneste et al., 2005)).

The effect of auxin on cell expansion in leaves can be seen by over-expressing Arabidopsis *AUXIN BINDING PROTEIN1* (*ABP1*) in tobacco. Over-expression of *ABP1* is sufficient to promote cell expansion, and generates leaves with larger cells (Jones et al., 1998). In addition, the

auxin-inducible gene, *ARGOS* has been revealed as a negative regulator of organ growth. Unlike for *ABP1*, *ARGOS* over-expression primarily affects cell number; generating larger leaves with more cells (Hu et al., 2003). This suggests that *ARGOS* promotes either the *rate* or *duration* of cell proliferation in developing organs. Interestingly *ARGOS* appears to function upstream of *ANT* and *CYCD3*, and its over-expression results in the prolonged expression of *ANT* and *CYCD3* (Hu et al., 2003). The role of *CYCD3* in the maintenance of the mitotic cell cycle (Dewitte et al., 2007) suggests that perhaps *ARGOS* influences organ growth via the auxin-dependent promotion of the duration of cell proliferation.

A related gene, *ARGOS-LIKE* (*ARL*) also affects organ growth, but in response to brassinosteroids. *ARL* is up-regulated by brassinosteroids, and demonstrates a role for brassinosteroids in the setting of final organ size. Over-expression of *ARL* results in larger leaves and cotyledons, a phenotype that is largely due to an increase in cell size; indicating that *ARL* promotes cell expansion in the developing leaf (Hu et al., 2006). Brassinosteroids have also been shown to affect organ development as part of systemic changes to cell expansion rates. The *bri* (*brassinosteroid insensitive1)* and the *dwf4* (*dwarf4*) mutants have severe dwarfed phenotypes with smaller leaves, that are thicker and curled in *bri1* plants (Clouse et al., 1996, Azpiroz et al., 1998). Both *BRI1* and *DWF4* reduce organ size through reduced cell expansion rates, an effect that can be reversed in *bri1* plants by expressing wild-type BRI1 in the L1 layer of the SAM (Savaldi-Goldstein et al., 2007), which suggests that brassinosteroids might regulate organ size exclusively through altered expansion rates in the SAM.

Much like in the case of auxin, cytokinins influence a wide variety of plant responses including the pathogen response, apical dominance, organ development and vascular development (reviewed in Choi and Hwang (2007)). The effect of cytokinins on organ growth can be seen in the *ahk2/ahk3/ahk4* mutant, which is defective for three cytokinin receptors. This mutant has fewer leaves, which are smaller than wild-type leaves due to a reduction in cell number (cell area is the same as the wild-type), indicating that cytokinins promote leaf growth via an increase in cell proliferation (Higuchi et al., 2004, Nishimura et al., 2004). This is supported by the observation that disruption of cytokinin metabolism has also been shown to affect petal growth. Knock-down of two cytokinin oxidase/dehydrogenase (*CKX*) genes, *CKX3* and *CHX5* (responsible for catalysing the degradation of cytokinins) results in an increase in petal area (Bartrina et al., 2011). The increase in petal area is a consequence of an increased number of

wild-type sized cells, revealing that the large organ phenotype is achieved through promotion of cell proliferation in the developing petal (Bartrina et al., 2011).

The role of gibberellins in organ growth and development was revealed through the identification of the DELLA proteins (Koornneef and Van der Veen, 1980), which are negative regulators of gibberellin-dependent growth promotion (Hauvermale et al., 2012, Davière and Achard, 2013, Dixit, 2013). DELLA knockout mutations increase leaf area through an increase in cell number, which is a consequence of elevated cell expansion and proliferation rates (Achard et al., 2009). As with brassinosteroids, constitutively desensitising plants to gibberellins results in a systemic dwarf phenotype (Peng et al., 1997). DELLAs are destabilised by ubiquitin-directed, proteasome-mediated degradation (Alvey and Harberd, 2005), and knockdown of *SLY1*, an F-BOX subunit of the SCF E3 ubiquitin ligase (McGinnis et al., 2003) (see section 1.7.4 and 5.1.1) leads to a reduced leaf area as a result of decreased cell proliferation (Achard et al., 2009). Interestingly, gibberellins have also been shown to affect cell expansion, with overexpression of the gibberellin biosynthetic gene, *GIBBERELLIN 20-OXIDASE1* (*GA20OX*) increasing leaf area through increased cell size and cell number (Gonzalez et al., 2010).

Abscisic acid (ABA) is less well characterised as a regulator of growth and development, however there is evidence that it might regulate organ growth through *DA1* and *DAR1* (Li et al., 2008). *DA1* expression is induced by ABA and *da1-1* seedlings are partially insensitive to ABA-inhibition, indicating that ABA might be involved in regulating the duration of cell proliferation in the developing organ (Li et al., 2008).

1.5.2 – Evidence for additional long-range growth factors in organ development

The type of spatial coordination revealed by the compensation mechanism (described in section 1.5.3) may be due to a diffusible, threshold-dependent, long-range growth-signal such as Drosophila WINGLESS (WG), which is involved in coordinating *Drosophila* embryogenesis (Zecca et al., 1996). In this system, a gradient of WG accumulates in cells surrounding the WG-expressing cells, and cells in this field respond quantitatively; resulting in the differential expression of additional growth factors (Zecca et al., 1996). Interestingly, the study of a cytochrome p450 enzyme encoded by the *KLU* gene has provided evidence for a similar diffusible signal in the regulation of Arabidopsis floral development. At the single organ level – in the regulation of petals – *KLU* functions in a non-cell autonomous manner (Adamski et al., 2009, Anastasiou et al., 2007); with the *KLU* genotype able to influence the development of adjacent *klu-2* tissues. Further work with *KLU*/*klu-2* chimeric inflorescences has revealed that *KLU* has an effect beyond individual flowers and can influence the development of *klu-2*

flowers in the same inflorescence (Eriksson et al., 2010). *KLU* cytochrome P450 is a member of a large superfamily of genes involved the oxidation of many diverse substrates including steroids and fatty acids (Pinot and Beisson, 2011); suggesting that KLU may be involved in the synthesis or modification of a lipid or steroidal signal molecule. Indeed, in animal systems cytochrome P450s are involved in the modification of retinoic acid (vitamin A), which is an important morphogen during vertebrate embryonic development (Nebert and Russell, 2002). Taken together, these data suggest that targets of KLU may be diffusible signalling molecules involved in the coordination of cell proliferation in lateral organ growth. There is strong data to support the role of a *KLU*-dependent signal in the long distance coordination of organ growth (Adamski et al., 2009, Anastasiou et al., 2007, Eriksson et al., 2010), however there is little direct evidence that a similar diffusible signal is responsible for coordinating the arrest front in developing organs (see section 1.5.5).

1.5.3 – A compensation mechanism regulates final organ size

Sections 1.3.1 and 1.3.2 describe genes that mis-regulate cell proliferation or cell-expansion and in doing so alter final organ size. Interestingly, there are also genes that mis-regulate cell proliferation and cell expansion *without* influencing overall organ size. These genes reveal the phenomenon of *compensation*, which is the ability of the developing organ to compensate for fluctuations in cell number with changes cell size (and *vice versa*); such that final organ size remains constant. For example, as discussed in section 1.3.2 and in a similar fashion to *KLU, CYCLIND3;1-3* are thought to positively regulate the duration of cell proliferation in developing organs (Dewitte et al., 2007). However, whereas the reduction in cell number in *klu-2* petals results in an over-all reduction in petal size, the reduction in cell number in *cycd3;1-3* leaves does not affect leaf area (Dewitte et al., 2007). This is due to a compensatory increase in cell expansion in *cycd3;1-3* leaves that results in cells that are considerably larger that the wild type (Dewitte et al., 2007). A similar compensatory effect can be seen when *Arabidopsis* AUXIN BINDING-PROTEIN 1(ABP1) – involved in the promotion of auxin-mediated cell-expansion – is over-expressed in tobacco (Jones et al., 1998). In this case, despite an increase in cell area, there is an apparent reduction in cell number that causes the leaves to remain morphologically identical to the wild-type (Jones et al., 1998). This compensation effect suggests that developing organs possess an intrinsic 'measure' of organ size, and, that throughout their growth they are able to access this pre-determined spatial information that sets the final size.

Investigation of the compensation mechanism by Ferjani et al (2007) revealed that there are three distinct routes by which the developing leaf can compensate for a reduction in cell

proliferation. The first route involves the initiation of cell expansion during the proliferative phase, as seen in *KRP2* overexpressing lines (Ferjani et al., 2007). The second and third routes involve post-mitotic compensation, where enhanced cell expansion follows the termination of the proliferative phase (Ferjani et al., 2007). One route – that utilised by *fugu2-1* mutants – involves an elevated *rate* of post-mitotic cell expansion, and the other route – that utilised by *fugu5* mutants – involves an elevated *duration* of post mitotic cell expansion (Ferjani et al., 2007).

1.5.4 – Models to explain the compensatory mechanism

A non-cell-autonomous model provides one explanation of why certain mutations affecting cell proliferation are compensated, and why others lead to a change in final organ size. It predicts that there are two classes of genes involved in organ size regulation; those involved in spatial sensing (signal propagation, transduction and perception), and those that operate outside of the sensing mechanism - involved in performing core cellular activities only (such as cell expansion and cell proliferation) (Fig. 1.5).

In this scenario genes involved in these *core* cellular processes would be independent of the sensing mechanism and therefore any aberrant growth that resulted from mutations in these *core* genes would be detected and compensated. Conversely, mutations in components of the sensing mechanism would have effects that cannot be compensated, because the detection and response mechanisms would themselves be aberrant. This can be explored by comparison of the effect of *da1-1* and *cycd3;1-3* mutations. Both of these mutations alter the duration of cell proliferation during organ formation, but only the *cycd3;1-3* mutant is compensated (Li et al., 2008, Dewitte et al., 2007). *CYCD3;1-3* are key cell-cycle genes responsible for negatively regulating the switch from the mitotic cell-cycle to the endocycle (Dewitte et al., 2007). In *cycd3;3* mutants, the absence of the negative influence of the *CYCLIND3* genes causes cells to be released early from the proliferative phase. However, perhaps because *cycd3;3* cells are still able to accurately sense their position in the developing organ, development is adjusted according to the still correct spatial cues (resulting in increased expansion), and the pre-determined final organ size is achieved.

The *da1-1* large organ phenotype suggests that *da1-1* cells have an increased sensitivity to a potential proliferation-promoting signal. This would lead to proliferation at lower signal levels, therefore a later exit from the proliferative phase and consequently an increased organ size. According to this model, if DA1 were involved in the process of signal perception, the

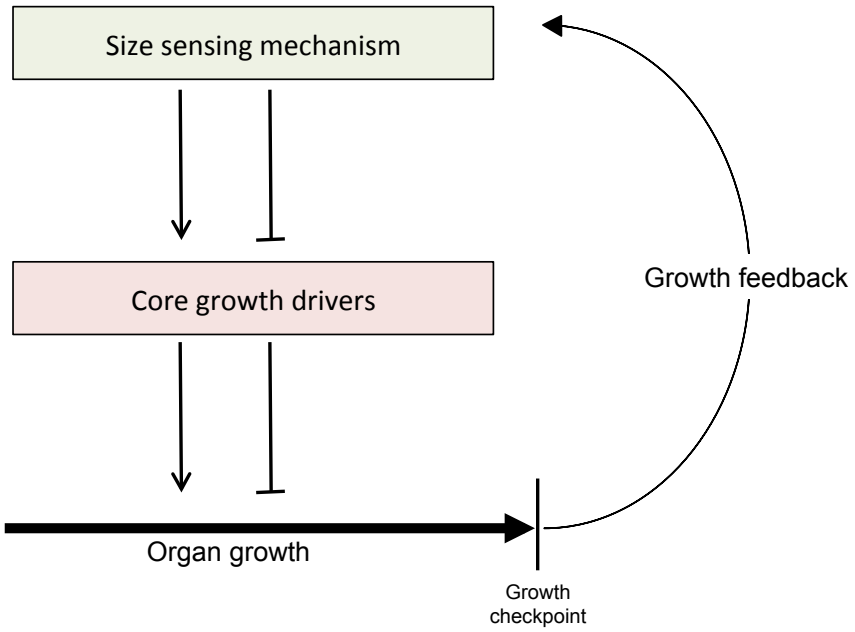

Figure 1.5 – A model to explain the compensation effect

This model predicts that there are two groups of genes involved in organ growth: genes involved in a size-sensing mechanism and genes involved in downstream core growth processes. It predicts that spatial cues are received and transduced by a sensing machinery that in turn influences the activity of down-stream core growth drivers (which indirectly or directly influence organ growth). The model predicts that while mutation of core growth drivers might affect organ growth, accurate perception of aberrant growth by an intact size sensing mechanism would buffer against developmental abnormalities. Conversely, this model predicts that growth-altering mutations in elements of the size sensing machinery might also render the organ unable to perceive the consequent aberrant growth, and would therefore result in uncompensated abnormal growth.

da1-1 developing organ would be unable to detect the aberrant growth that results from the *da1-1* mutation. As a consequence, the developing organ would not undergo a compensatory reduction in cell expansion.

This model predicts that genes with non-compensated mutations (such as *DA1, BB/EOD1*, *KLUH* and *SPT* (Li et al., 2008, Disch et al., 2006, Anastasiou et al., 2007, Ichihashi et al., 2010)) are likely to be involved in responding to or regulating the size-sensing mechanism, and that genes that are compensated (such as *CYCD3;1-3*, and *CYCD2;1* (Qi and John, 2007, Dewitte et al., 2007)) are involved in core developmental processes downstream of the sensing mechanism.

1.5.5 – Coordination of growth at the organ level

Evidence of a compensation mechanism in the setting of final organ size (section 1.5.3) suggests that throughout organ development, constituent cells can map their position relative to the other cells in the organ. This allows cells to alter their growth such that a pre-determined final organ size can be reached. This positional mapping could be achieved through one of two systems: a non-cell-autonomous signal 'field' that generates spatial information to constituent cells, or a cell-autonomous system in which individual progenitor cells have a fixed growth potential such that they divide a certain number of times and then expand to a fixed size (Fig. 1.6). It is also possible that a combination of both mechanisms function during organ formation.

The cell-autonomous model (Fig. 1.6a) is based on observations that the growth potential of certain structures can be pre-determined by *pre-loading* with a fixed amount of growth factor. The maternal provision of *CYCLINB* mRNA to the Drosophila early embryo is one such example (Edgar et al., 1994). The *Drosophila* early embryo is preloaded with a pool of maternal CYCLIN B, which acts as a regulator of nuclear proliferation (Edgar et al., 1994). CYCLIN B is degraded on the mitotic spindle and therefore levels fall with every nuclear division. This means that the maternal 'loading' of the embryo is able to pre-determine exactly how many nuclear divisions will occur regardless of their frequency; allowing the developing embryo to compensate for any changes in the rate of cell division (Edgar et al., 1994) In this model, if nuclear division rate was accelerated, although more nuclear divisions could occur per unit time, the growth factor would run out after the pre-determined number of divisions and nuclear division would be halted. It is tempting to speculate that this model extends to cellularised organs. In such a system, initial progenitor cells might be 'loaded' with a cell-autonomous signal that accurately regulates proliferation in a similar mitosis-dependent way to establish an intrinsic measure of organ size.

Examples of an alternative (non-cell-autonomous) model (Fig. 1.6b) can also be found in animal systems. In Drosophila, a gradient of either the mRNA or the protein of the transcription factor *BICOID*, defines spatial boundaries in the developing embryo (Lipshitz, 2009), and it is thought that a similar system might be responsible for coordinating the proliferation arrest front in Arabidopsis lateral organs (Lenhard, 2012). Evidence that the arrest front is held at a fixed distance from the base of the leaf (Andriankaja et al., 2012, Kazama et al., 2010) suggests that a proliferation promoting signal field, originating from the

leaf base, may be responsible for maintaining mitotic competence and cell proliferation. Such a morphogen, emitted from the leaf base, would promote cell proliferation in the leaf basal region only, as a consequence of its purported threshold-dependent activity (Lenhard, 2012). In more distal regions, where the morphogen concentration is reduced, cells would be released from mitosis (Lenhard, 2012). This proposed mechanism predicts that cell proliferation drives cells in the organ out of the morphogen field and thereby causes their exit from the mitotic cell-cycle (Lenhard, 2012).

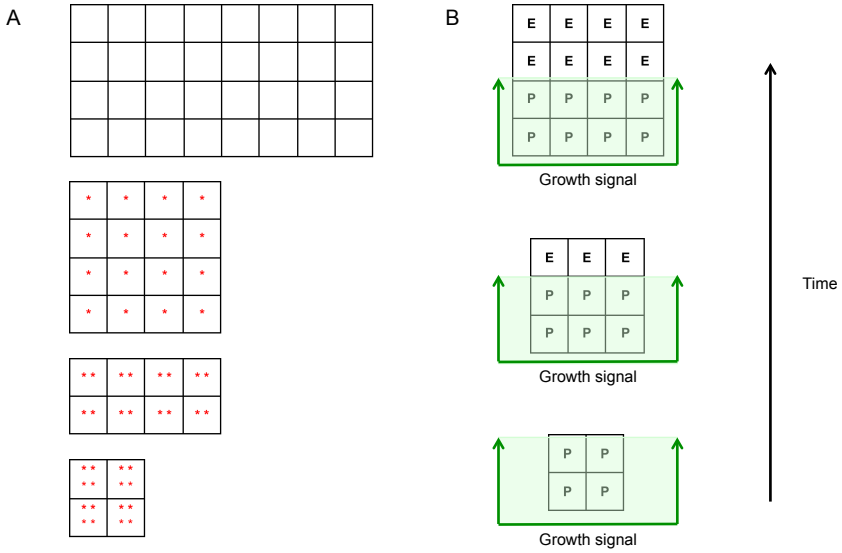

Figure 1.6 – Cell-autonomous and non-cell-autonomous coordination of organ growth

(A) The cell-autonomous model of organ growth involves the pre-loading of progenitor cells with a fixed degree of growth potential. In this example, the cells (white squares) are pre-loaded with growth factor (red stars; each star conferring the ability to divide once), and when no growth factor remains, cell division is arrested. (B) Non-cell-autonomous growth regulation via a diffusible growth signal. In this example, a cell-proliferation-promoting growth factor is expressed from the base of the organ. Cells located within this signal field (green shading) are stimulated to proliferate (denoted by 'P'), whereas cells outside the signal field cease proliferation and begin cell expansion (denoted by 'E'). In this model, as cells divide they are mechanically forced out of the signal field, thereby reducing the relative proportion of the organ that is in the proliferative state.

Examples of pro-proliferative diffusible signals regulating organ growth exist in animal systems. These include DECAPENTAPLEGIC (DPP), which is a diffusible long-range signal involved in

drosophila wing disc growth and patterning, and whose gradient has been shown to influence cell proliferation (Rogulja et al., 2008, Lecuit et al., 1996, Rogulja and Irvine, 2005). One response to DPP signalling, is the phosphorylation of the transcription factor, MAD, to form MAD^{Phos}, which then influences downstream targets in a concentration-dependent manner (Rogulja et al., 2008). Cells that cannot respond to DPP signalling do not proliferate and die, and those that show over-sensitivity to DPP over-proliferate (Burke and Basler, 1996, Capdevila and Guerrero, 1994). DPP signalling has been tentatively linked (Rogulja et al., 2008) to another pathway, the hippo pathway, that is thought to be a size-checkpoint for wing disc development (Zhao et al., 2010, Pan, 2007, Dong et al., 2007). The Hippo pathway (the Yap pathway in mammals) is a kinase cascade of negative growth regulators that is activated by high cell density and results in the repression of cell proliferation and the promotion of apoptosis (Zhao et al., 2010). The signalling molecules responsible for activating the Hippo-Yap pathway are not yet known. However the activated pathway results in the phosphorylation and inactivation of YORKIE, which is a promoter of cell proliferation and cell survival (Zhao et al., 2010, Pan, 2007). Interference with the Hippo-pathway results in over-proliferation and tumourogenesis (Dong et al., 2007), which is perhaps reminiscent of interference with the *DA1*, *EOD1*, and *DA2* pathways; all of which result in over-proliferation and enlarged organs (Xia, 2013, Li et al., 2008, Disch et al., 2006).

BOX 1.2 – The cell cycle and its regulation during development

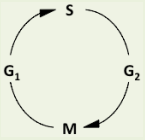

The mitotic cell cycle is a highly-regulated, unidirectional progression through a series of stages required for cell growth and division. G_1 phase - when much of the cell machinery is replicated, S phase- when genetic material is replicated, G_2- a proof-reading stage involving the double-checking of replicated DNA, M-phase – mitosis, followed by cytokinesis.

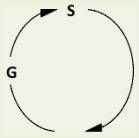

The endocycle is a modified cell cycle with mitosis and cytokinesis absent. The cycle consists purely of growth and synthesis, which results in large, high ploidy cells.

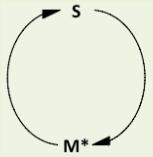

The syncytial cell cycle is modified such that there are no growth phases or cytokinesis. This allows

1.6 – Organ growth and the cell-cycle

As discussed in section 1.3, organ growth is driven by a combination of cell proliferation and cell expansion. Cell proliferation and endoreduplication-dependent cell expansion are both processes that have the cell cycle as their core. In the leaf, proliferating cells progress through the mitotic cell-cycle and expanding cells can progress through the endocycle, a modified cell-cycle where mitosis and cytokinesis are absent (see Box 1.2). In both cases, the number of cycles can affect the final size of the organ, and therefore mis-regulation of the *rate* or *duration* of either the mitotic cell-cycle or the endocycle may influence final organ size.

1.6.1 – The cell-cycle: a brief overview

1.6.1.1 – The Mitotic cell-cycle

The cell-cycle is a cyclical, unidirectional progression through different growth stages. Mitotic cells progress through a DNA synthesis phase (S-phase), which is preceded and proceeded by two gap phases (G1- and G2-phase respectively). G_1-phase is required for the replication of cell machinery in preparation for the DNA synthesis of S-phase, and G_2-phase is required for checking and proof-reading the DNA after replication. Following the completion of G1, S and G2, cells then progress through the mitotic phase (M-phase), where cells divide through cytokinesis. Cell-cycle checkpoints exist at the boundaries between these different phases to ensure that the preceding phases have been completed and that there is no premature entry into the next phase. Importantly, these checkpoints are unidirectional (i.e. cells can only progress in one direction), which ensures that cells progress through the cell-cycle in the correct order.

The accurate and timely progression of the cell-cycle is mediated by a family of serine/threonine kinases, the CYCLIN DEPENDENT KINASES (CDKs), and their CYCLIN subunits, which are required for CDK activity (van den Heuvel, 2005). The regulation of CDKs is tight and multi-layered, and includes phosphorylation events (both activating and repressive), strict control of protein expression and degradation, and regulation by CDK inhibitors (CKIs) (Dewitte and Murray, 2003). Five classes of CDK (termed CDKA-E) (Joubes et al., 2000), and five classes of cyclin (termed CYCLIN A, B, C, D and H) have been identified in plants (Dewitte and Murray, 2003). Cyclins, so named due to their periodic cyclical expression patterns, are the chief regulatory influence on CDKs, and individual cyclins have roles at specific cell-cycle checkpoints. For example, A-type cyclins regulate S-phase progression, B-type cyclins regulate the G_2/M transition, and D-type cyclins regulate the G_1/S transition (Dewitte and Murray, 2003). Unlike

A- and B-type cyclins, D-type cyclins do not have a cyclical pattern of abundance, and are thought to be controlled by higher-order signalling in the regulation of cell division (Dewitte and Murray, 2003). There are seven identified Arabidopsis CDK inhibitors with homology to animal CKIs; these are termed ICK/KRP proteins (INHIBITOR OF CDK/KIP-RELATED PROTEIN) and they inhibit CDK activity through their binding to CDK-CYCLIN complexes (Dewitte and Murray, 2003, De Veylder et al., 2001). Four CKIs have also been characterised in Arabidopsis belonging to the SIAMESE (SIM) and SIAMESE-RELATED (SMR) protein families (Churchman et al., 2006).

Cell-cycle unidirectionality is maintained by ubiquitin-mediated degradation of cyclins, which ensures that once a checkpoint is passed, components required for the previous stage are destroyed (Dewitte and Murray, 2003). A- and B-type cyclins are directed for destruction through ubiquitination by the Anaphase Promoting Complex (APC), and D-type cyclins by an SCF-type E3 ligase, (Dewitte and Murray, 2003). In addition to cyclins, CDK inhibitors are also regulated by ubiquitin-dependent proteolysis; thereby de-repressing the respective CDK (King et al., 1996).

1.6.1.2 – Cell-cycle variations

Excluding the meiotic cell cycle – where S-phase is followed by a modified M-phase, with two rounds of chromosome segregation (van den Heuvel, 2005) – there are two significant variations of the mitotic cell cycle; the endocycle and the syncytial cell-cycle.

Cells in the syncytial cell-cycle rapidly cycle between S-phase and a modified M-phase that lacks cytokinesis. The absence of G_1 and G_2 permits rapid cycling, and the lack of cytokinesis results in syncytial growth to produce multiple nuclei dividing without cellularisation. The lack of G_1 and G_2 means that syncytial tissues are highly dependent on the extracellular provision of DNA and protein, and their development is often governed by the nucleo-cytoplasmic ratio (Edgar et al., 1986, Edgar and Datar, 1996). In plants the early stages of endosperm development involves the syncytial cell cycle.

The endocycle consists of an S-phase followed by a single G-phase and no mitosis, resulting in a doubling of ploidy level with each cycle (van den Heuvel, 2005). Down-regulation of the M-phase components, CYCA1, CYCA2, CYCBs and CDKB have been reported in endocycling cells (Dewitte and Murray, 2003). Work has also implicated CYCD3;1-3 in the maintenance of the mitotic cell cycle (Dewitte et al., 2007), suggesting that CYCD3 acts as a mitotic cyclin that drives cells from G_2 to M, rather than allowing them to exit (to the endocycle) from G_2 – S-phase (Dewitte et al., 2007). Interestingly elevated levels of CYCD3 have been identified in

endoreduplicating tomato tissues (Joubes and Chevalier, 2000) , suggesting that CYCD3 may be a general promoter of all cell cycles (mitotic and endocycles) as a consequence of a promotion of the G_1/S-phase transition (Dewitte et al., 2007).

1.6.2 – Regulating cell proliferation via the mitotic cell-cycle

As described in section 1.5.1, quadruple DELLA knockout plants exhibit an increased leaf area due to an increased rate of cell proliferation (Achard et al., 2009). Further investigation of this phenotype revealed that DELLAs promote the expression of several CKIs; *KRP2*, *SIM1*, *SMR1*, *SMR2* (Achard et al., 2009). As CKIs negatively regulate the progression of the cell-cycle, the absence of DELLA activity in the quadruple DELLA knockout is therefore thought to drive an increase cell-proliferation through a de-repression CKI-mediated cell-cycle inhibition. Over-expression of the APC subunits, CDC27a and APC10 has also been shown to increase the rate of cell proliferation in the developing leaf (Rojas et al., 2009, Eloy et al., 2011). As the APC is required for mitotic progression, an increase in APC activity (through increased abundance of its subunits), leads to an elevated mitotic rate.

As well as explaining observed increases in proliferation *rate* during organ growth, manipulation of the cell-cycle machinery has also been shown to affect the *duration* of cell proliferation during organ formation. As described in section 1.5.4, *cyc3;1-3* triple knockout leaves and petals have a reduced duration of cell proliferation (Dewitte et al., 2007). This has led to a suggestion that CYCLIN D3s act as gatekeeper proteins, promoting the maintenance of the mitotic cell-cycle and blocking entrance into the endocycle (Dewitte et al., 2007). Consistent with this is the observation that the large organ-size phenotype of plants over-expressing *AINTEGUMENTA* (*ANT*), is associated with increased *CYCD3* expression (Mizukami and Fischer, 2000). Over-expression of *ANT* – an AP2-domain transcription factor – results in enlarged leaves with more cells, and conversely *ant* mutant leaves are smaller and have fewer cell (Mizukami and Fischer, 2000). *ANT* over-expression causes an increased duration of cell proliferation, which is consistent with the observed increase in *CYCD3* expression, further supporting a role for *CYCD3* in the maintenance of mitotic competence (Mizukami and Fischer, 2000).

1.6.3 – Regulating cell expansion via the endocycle

As discussed in section 1.3.3, some mechanisms of cell expansion are accompanied by endoreduplication (Sugimoto-Shirasu and Roberts, 2003). It is therefore possible that regulation of the switch to, and the persistence of the endocycle will have a significant impact on cell expansion in developing organs.

The switch from the mitotic cell-cycle to the endocycle may be governed by the antagonistic influences of factors that promote mitosis and endocycling respectively. Because exit from the mitotic cell cycle is a pre-requisite for entry to the endocycle, cell cycle regulators described in section 1.6.2 that influence the *duration of cell proliferation* are also likely to be important in determining the onset of the endocycle. The blurring of the boundaries between what is negative regulation of the mitotic cell-cycle and promotion of the endocycle (and *vice versa*) has made studies in this area difficult. For example, three recent papers disagree as to whether the class I *TCP*, *TCP15*, is involved in the regulation of cell *proliferation* or cell *expansion* (Kieffer et al., 2011, Li et al., 2012, Uberti-Manassero et al., 2012). Using quantitative imaging, Kieffer et al report that *TCP15* influences the expansion of the leaf blade as a consequence of repressed cell proliferation in the developing leaf epidermis. Conversely, Li et al (2012) suggest that *TCP15* represses endoreduplication in trichomes and cotyledon cells. This disagreement is consistent with the apparent context-dependent role of the class I *TCPs* (Kieffer et al., 2011, Li et al., 2012, Uberti-Manassero et al., 2012), however it also likely reflects the coupled nature of the mitotic cell-cycle and the endocycle. The mitotic cell-cycle and the endocycle both have G- and S-phases, and therefore factors that can promote either of these shared phases might enhance both types of cell-cycle. It is also worthwhile considering that *TCP15*-dependent growth factors are likely only a subset of the total population of growth factors that influence the cell-cycle. As such, the precise effect of altered *TCP15* expression is likely to be dependent on the background (in terms of cell-cycle regulation) of each treatment and tissue. Indeed, Li et al (2012) only reported six cell-cycle regulators differentially regulated by *TCP15* (Li et al., 2012).

Knockout of RPT2a, a 26S proteasome regulatory subunit (see section 1.3.3), increases the duration of cell expansion and, as a consequence, increases leaf size through an increase in cell size (Sonoda et al., 2009). Further investigation of this mutant revealed that the G_1 regulator, *CYCD3;1* and the S-phase regulators, *CDC6b*, *CDT1a*, *CDT1b*, *HISH4* and *CYCA3;1*, were up-regulated in *rpt2a-2* mutants (Sonoda et al., 2009). The number of cells in *rpt2a-2* leaves remains similar to the wild-type throughout development, suggesting that the increase in cell size is a consequence of enhanced endocycling (rate or duration), but not due to a consequence of early mitotic exit (Sonoda et al., 2009). As the endocycle consists only of a G-phase and an S-phase, up-regulation of these G_1- and S-phase specific factors reflects the increased persistence and/or up-regulation of the endocycle.

Recent work has pointed to chloroplast retrograde signalling promoting the onset of cell expansion in the developing leaf (Andriankaja et al., 2012). This work showed that genes involved in chloroplast differentiation were up-regulated prior to the appearance of the cell-cycle arrest front, and that chemical inhibition of chloroplast differentiation blocked the cell-cycle arrest front (Andriankaja et al., 2012). Chloroplast retrograde signalling in cultures of the red algae, *Cyanidioschyzon merolae* activates CDKA and thereby initiates nuclear DNA replication (Kobayashi et al., 2009). The reliance of nuclear DNA replication on chloroplast differentiation shown by these studies may reflect a requirement for active plastids during S-phase. The inhibition of cell proliferation by chloroplast differentiation can be uncoupled by the addition of CDK inhibitors (aphidicolin or nalidixic acid), which permits chloroplast differentiation without subsequent nuclear DNA replication (Kobayashi et al., 2009). Arabidopsis CDKA levels are elevated in G_1- and S-phase (Dewitte and Murray, 2003) and thus the up-regulation of CDKA in response to retrograde signalling is reminiscent of the up-regulation of other G_1- and S-phase specific factors in the *rpt2a-2* mutant, which has increased endocycling and larger leaves (Sonoda et al., 2009).

1.7 – The ubiquitin system

The characterisation of the E3 ligases, DA2, EOD1 and SLY as *bona fide* regulators of organ growth (McGinnis et al., 2003, Disch et al., 2006, Xia, 2013), as well as the identification of other members of the ubiquitin pathway as growth regulators (Li et al., 2008, Rojas et al., 2009), suggests that ubiquitination probably plays a key role in regulating organ growth, as in most other biological processes. Furthermore, the importance of ubiquitin-dependent proteolysis in the cell-cycle, a centrally important process at the heart of organ development (section 1.6), further stresses the significance of ubiquitination in the establishment of final organ size.

Ubiquitination is a reversible post-translation modification akin to phosphorylation, which involves the ligation of ubiquitin (a short peptide molecule) to lysine residues on the surface of substrate proteins (Hershko and Ciechanover, 1998). The ligation mechanism is a three-step enzymatic process involving three classes of enzyme: E1-activating enzymes, E2-conjugating enzymes and E3-ligases (Fig. 1.7). The ligation of ubiquitin can occur in variety of forms, from single mono-ubiquitin molecules, to long-chain poly-ubiquitin molecules (Woelk et al., 2006, Mallery et al., 2002, Disch et al., 2006, Petroski and Deshaies, 2003). Moreover, the inter-molecular couplings and lengths of these chains can impart different signals, ranging from enhancing modifications to labels for destruction (Mallery et al., 2002, Fang et al., 2000,

Stevenson et al., 2007). The following section describes the ubiquitination cascade and key enzymatic steps, and explores the roles played by these enzymes in the regulation of organ growth. Importantly, this section leverages the wealth of knowledge present in metazoan and yeast ubiquitin-biology, and uses it to improve our understanding of the hitherto less advanced field of plant ubiquitin-biology. Ubiquitination has a centrally important role in cell-cycle regulation (Hershko and Ciechanover, 1998), which is a process at the core of both cancer progression in animals (Vermeulen et al., 2003, Hartwell and Kastan, 1994) and organ growth in plants (Inzé and De Veylder, 2006, Beemster et al., 2003).

1.7.1 – Ubiquitin: a small peptide with multiple signalling roles

Ubiquitin is a highly conserved 76 amino acid protein, whose structure is 100% conserved in higher plants and differs by only three residues from animal ubiquitin (Callis et al., 1995). It is expressed as an inactive precursor, as either an ubiquitin polymer, or fused to other peptide sequences (Wiborg et al., 1985, Ozkaynak et al., 1987, Callis et al., 1995). Ubiquitin oligomers are formed through the creation of an isopeptide linkage between a C-terminal glycine of ubiquitin (Gly76) and a lysine residue on the substrate protein (Pickart and Fushman, 2004). These can be single mono-ubiquitin moieties, such as those involved in the regulation of EPS15 (Woelk et al., 2006). They can also be long chain poly-ubiquitin signals, such as those seen on BRCA2 and MDM2 in animals and EOD1 and DA2 in Arabidopsis (Mallery et al., 2002, Disch et al., 2006, Xia, 2013, Fang et al., 2000).

Poly-ubiquitin chains can be formed through two distinct processes; an isopeptide linkage between the C-terminal Gly76 and a lysine residue on the preceding ubiquitin (Pickart and Fushman, 2004), or through head-to-tail 'linear' chains where the N-terminal Met1 is conjugated to Gly76 through a peptide linkage (Kirisako et al., 2006). There are seven lysine residues on ubiquitin (K6, K11, K27, K29, K31, K48 and K63), therefore seven possible (non-linear) poly-ubiquitin architectures are available. All seven linkages have been identified *in vivo* in yeast (Peng et al., 2003), and all but K6 and K27 have been identified in Arabidopsis (Saracco et al., 2009). The different linkages are thought to confer different signals to the substrate protein, with K48 linked chains generally associated with signalling proteasome-mediated degradation (Jacobson et al., 2009), and other linkages thought to have a variety of functions including enzyme activation (Mallery et al., 2002, Woelk et al., 2006). The structure and function of poly-ubiquitin chains is discussed in detail in section 5.1.3.

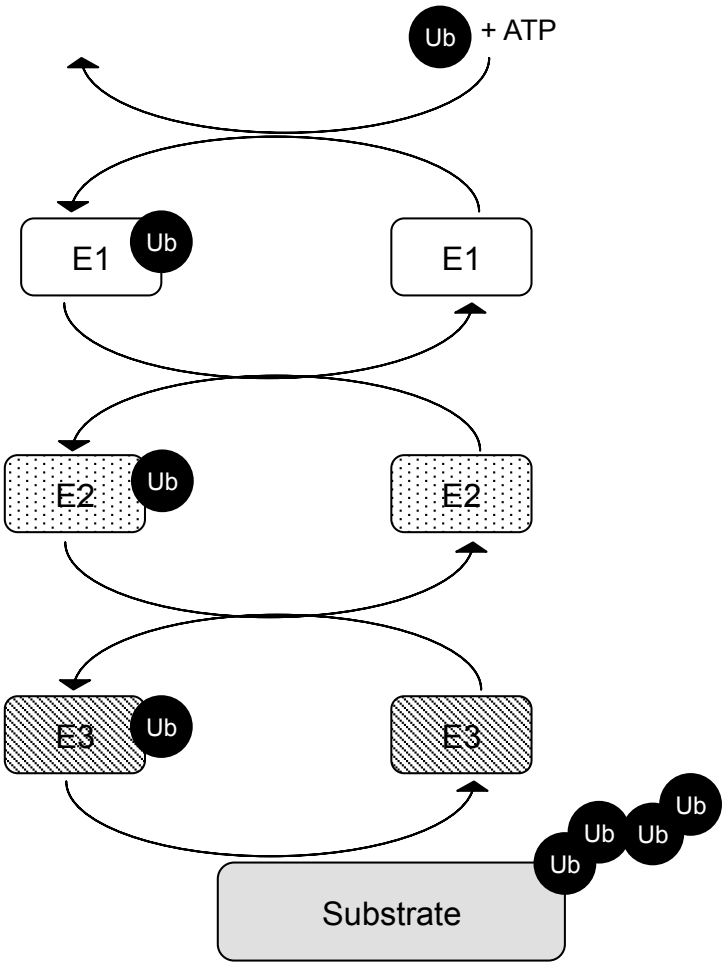

Figure 1.7 – The ubiquitin cascade

An illustration of the ubiquitin cascade, using the HECT family of E3 ligases as an example. The ubiquitin cascade is initiated by an ATP consuming reaction in which the E1 activating enzyme forms a thioester bond with the C-terminal glycine of ubiquitin, this is followed by transfer of the E1 conjugated ubiquitin molecule to the active site of the E2 conjugating enzyme. The E2 then transfers the ubiquitin molecule to the E3, which ligates it to the substrate protein, via an isopeptide linkage between the C-terminal Gly76 and a lysine residue on the substrate protein. Poly-ubiquitin chains are formed through the ligation of ubiquitin molecules onto lysine residues on additional ubiquitin molecules. Non HECT-family E3 ligases do not form a covalent intermediate with the ubiquitin molecule; instead they cooperate with the E2 to ligate the ubiquitin molecule directly to the substrate.

1.7.2 – E1 activating enzymes: ATP-dependent ubiquitin activation

As described above, the mechanism of ligating an ubiquitin molecule to its substrate is a three-step process involving three classes of enzyme (Fig. 1.7). The first step in this process is the conjugation of free ubiquitin to the E1 activating enzyme in an ATP-consuming step. This reaction, via an ubiquitin-adenylate intermediate, results in the formation of a high energy thiolester linkage between the ubiquitin and a catalytic cysteine residue on the E1 (Hatfield et al., 1997, Hershko and Ciechanover, 1998).

The Arabidopsis genome encodes two E1 genes (UBA1 and UBA2) (Hatfield et al., 1997), one of which has been shown to play a role in plant innate immunity and to have an organ-size phenotype in certain genetic backgrounds (Goritschnig et al., 2007). A 15bp deletion in the C-terminal region of Arabidopsis UBA1 (named *mos5* (*modifier of snc1 5*)) was able to rescue the dwarf phenotype of the *npr1-1 snc1* double mutant, which has constitutively activated defence responses (Goritschnig et al., 2007). Reduced plant growth is a characteristic defence response and can be seen in various assays for pathogen challenge (Gómez‐Gómez et al., 1999, Gómez-Gómez and Boller, 2000, Zipfel et al., 2006). This highlights an overlap between plant development and the pathogen response, which is supported by observations that the well characterised growth regulator, *TCP14* (Kieffer et al., 2011) is also a central hub in the plant immune system network (Mukhtar et al., 2011). Therefore, in addition to the *mos5* phenotype implicating *UBA1* in the defence response, it may reveal a potential link to core developmental growth control.

1.7.3 – E2 conjugating enzymes: transferring ubiquitin to substrates

After activation of the ubiquitin monomer, the E1-thiolester-bound ubiquitin is transferred to a thiol group on the active site cysteine of the E2 enzyme. In spite of there being only two E1 enzymes in Arabidopsis, the fact that only *UBA1* has a pathogen response phenotype, suggests that there may be some degree of selectivity in its downstream interactions with E2s (Goritschnig et al., 2007). Indeed, data from animal systems demonstrates that the Human E1s, UBA1 and UBE6, have different E2 binding preferences (Jin et al., 2007). This idea that the E1-E2 interaction is to some extent specific, is supported by observations that UBA1 binds to E2 enzymes with a greater affinity when it is ubiquitinated (Haas et al., 1988, Ye and Rape, 2009). This in turn suggests that the thiolester-ubiquitin status of the E1 might serve to recruit the E2 to the E1 (Ye and Rape, 2009). Perhaps in a similar fashion to the proposed recruitment of UIM-containing proteins by E3-bound ubiquitin, in the process of coupled mono-ubiquitination (Woelk et al., 2006).

The E2 conjugating step is the second tier of the ubiquitin cascade and E2 enzymes have a significant influence on target protein specificity. This is reflected in the increased number of E2s (relative to E1s); analysis of the Arabidopsis genome sequence predicted 37 E2s in 12 subfamilies (Vierstra, 1996, Sadanandom et al., 2012). E2 conjugating enzymes are responsible for catalysing the transfer of ubiquitin to the substrate proteins, and E3 enzymes, although often necessary, are typically only required to *coordinate* the E2-substrate interaction. Indeed, although most E2s appear to be inactive without an E3, the Arabidopsis E2s, UBCE, UBC2 and UBC8 have all been shown to ubiquitinate substrates *in vitro* in the absence of E3 enzymes (Wiborg et al., 2008).

In animal systems, E2 enzymes have been shown to influence cell proliferation rate and cancer progression. Over-expression of the human E2, UBCH10, the expression of which is elevated in many primary tumours, results in an increase in cell proliferation (Okamoto et al., 2003). This increase in cell proliferation is likely to be a direct consequence of UBCH10 being the preferential binding partner of the APC E3 ligase (Summers et al., 2008), and therefore its over-expression is likely to lead to accelerated mitotic cell-cycling. Indeed UBCH10 over-expression was shown to be sufficient to promote APC-mediated degradation of securin, a key anaphase inhibitor (Pellman and Christman, 2001, Summers et al., 2008).

1.7.4 – E3 ligases: coordinating and specifying the ligation of ubiquitin to substrates

E3 ligase enzymes are responsible for the final step of the ubiquitin cascade, where they coordinate the E2-mediated ligation of ubiquitin to the target protein. Due to their role in *specifying* the ligation of ubiquitin, there are large numbers of E3 genes; for example there are 1415 predicted in Arabidopsis (Mazzucotelli et al., 2006). E3 ligases are unified by their biochemical function and not their structure or sequence. Whereas all E3 ligases act to facilitate the ligation of E2-ubiquitin to the relevant target protein, their group as a whole contains both monomeric and multimeric proteins of varying sequence divergence (Mazzucotelli et al., 2006).

Despite their functional conservation, E3 ligases are an extremely diverse group of enzymes. In terms of structure, there are two groups of E3 ligase; monomeric E3s, where E2-binding domains and substrate binding domains are on the same polypeptide, and multimeric E3s. Multimeric E3s consist of an E2-interacting module, and a target-specifying module joined by a CUL (CULLIN) or CUL-like protein; (Mazzucotelli et al., 2006) (Fig. 5.1).

E3 ligases can also be split into two groups based on their E2-binding domains, characterised by the presence of either a HECT (Homology to E6-AP C-Terminus) domain or a RING (Really

Interesting New Gene)/U-box domain. All HECT E3s, including UPL3 (UBIQUITIN PROTEIN LIGASE 3) - a regulator of trichome development (Downes et al., 2003), are monomeric E3s; whereas RING E3s exist as both monomeric E3s and as subunits in multimeric modular E3 complexes (Mazzucotelli et al., 2006). Some RING E3s, such as EOD1 (Disch et al., 2006) and the negative regulator of ABA signalling KEG (KEEP ON GOING) (Stone et al., 2006), as well as the closely related PLANT U-BOX (PUB) E3s, including PUB12 and PUB13 (Lu et al., 2011), are single polypeptide E3s. Whereas the RING protein atRBX1 (RING BOX PROTEIN1), the knockdown of which causes severe developmental phenotypes such as poorly developed leaves and loss of apical dominance (Lechner et al., 2002), is part of a multimeric E3 ligase. RBX1 is the E2-binding subunit of SCF (SKP1-CULLIN-F-BOX), CUL3-BTB/POZ (CULLIN-3 – BRIC-A-BRAC, TRAMTRACK and BROAD COMPLEX/POX VIRUS and ZINC FINGER), and CUL4-DDB1 (UV-DAMAGED DNA-BINDING PROTEIN1) E3 ligases; henceforth termed the cullin-ring ligases (CRLs) (Mazzucotelli et al., 2006). All E3 ligases, except HECT E3s, simply act to *coordinate* the ligation of the E2-conjugated ubiquitin to the substrate, without themselves covalently binding the ubiquitin. HECT E3 ligases, however, form a thioester intermediate with the ubiquitin molecule before ligation to the substrate.

As discussed in section 1.7.4, the activity of the human APC, a multimeric E3 ligase, can influence the rate of cell proliferation through manipulating the spindle checkpoint arrest (Okamoto et al., 2003, Summers et al., 2008). This is consistent with evidence that over-expression of Arabidopsis *CDC27a* (an APC subunit) in tobacco is sufficient to increase cell proliferation in the SAM (see section 1.3.1) (Rojas et al., 2009). The Arabidopsis APC has at least 11 subunits (Capron et al., 2003, Gieffers et al., 2001) and a multitude of interacting proteins (Fülöp et al., 2005), presenting multiple possibilities for manipulating cell-proliferation rate. The molecular basis of the *CDC27a* overexpression-dependent increase in cell proliferation is thought to be an increase in APC-mediated ubiquitin-directed degradation of mitotic cyclins (Irniger et al., 1995), anaphase inhibitors (Pellman and Christman, 2001), and regulators of DNA replication (Capron et al., 2003), which together accelerate the exit from M-phase and increase the rate of cell proliferation.

Another example relating ubiquitination to growth in Arabidopsis is that of the F-BOX protein *SLY1* (see section 1.5.1). Its knockdown causes reduction in leaf area through a decrease in cell proliferation rate (McGinnis et al., 2003, Dill et al., 2004). Unlike the APC, the targets of *SLY1* are not at the level of the cell-cycle, instead they are DELLA proteins (Dill et al., 2004), which are negative regulators of gibberellin-dependent growth promotion (Hauvermale et al., 2012,

Davière and Achard, 2013, Dixit, 2013). This indicates that E3 ligases mediate multiple processes that influence growth.

Knockout mutations of two E3 ligases, EOD1/BB and DA2 (Disch et al., 2006, Xia, 2013), have large-organ phenotypes, which are caused by a prolonged duration of cell proliferation during organ formation. Despite their well-characterised organ size phenotypes, little is known about their targets. As discussed in section 1.5.4, the observation that mutations in these genes are not compensated for by decreased cell expansion might suggest that their substrates are involved in spatial sensing during organ growth.

As well as those E3 ligases that have well characterised organ-size phenotypes (already discussed in this section), there are also E3 ligases and complex components that are involved in pathways linking organ growth and development. These include the RING E3 ligase, KEEP ON GOING (KEG), which is a negative regulator of ABA signalling (Stone et al., 2006) and the F-BOX proteins EBF1 and EBF2 (EIN3-BINDING F-BOX), which promote growth via repression of ethylene action (Gagne et al., 2004); both of which are linked to phytohormone growth responses. The F-BOX protein, UFO (UNUSUAL FLORAL ORGANS) is a regulator of meristem development and floral organ identity in Arabidopsis (Levin and Meyerowitz, 1995), and due to the intimate relationship between organ size, shape and identity (discussed in section 1.2.2), its activities are also relevant to organ development in general.

Studies of cancer cell biology are much more advanced that those of plant development, and as a consequence have identified many E3 ligases involved in the regulation of cell proliferation (Nakayama and Nakayama, 2006). Despite significant differences between cancer progression and the establishment of final organ size in plants, because they share the process of cell proliferation, some degree of comparison is likely to be fruitful. Furthermore, as regulation of the cell-cycle is centrally important for cell-proliferation control in both systems, understanding the involvement of E3 ligases in the regulation of the cell-cycle in cancer progression may shed valuable light on the role of ubiquitination in the control of final organ size.

The F-BOX protein SKP2 is an oncogenic E3 ligase subunit in humans, and has been shown to promote cell proliferation by targeting several CKIs for proteolytic degradation (Nakayama and Nakayama, 2006). Although there are thought to be many targets of SKP2 (Nakayama and Nakayama, 2006), its primary target is considered to be p27 (Sutterlüty et al., 1999), which is a CKI involved in negatively regulating the G_1-S-phase transition and whose over-expression represses cell proliferation (Vlach et al., 1996). Conversely, the F-BOX E3 subunit FBW7 is a

tumour suppressor and acts to restrict cell proliferation through the negative regulation of cell-cycle promoters including CYCLIN E (Nakayama and Nakayama, 2006, Tetzlaff et al., 2004). CYCLIN E is a promoter of the G_1-S-phase transition and therefore its ubiquitin-directed degradation, mediated by FBW7, is thought to repress cell-cycling (Tetzlaff et al., 2004, Nakayama and Nakayama, 2006).

These examples from mammalian cancer biology demonstrate the potential roles played by E3 ligases in the promotion and repression of cell proliferation through direct regulation of cell-cycle promoters and repressors. Despite the fact that some mammalian E3 ligases and cell-cycle regulators do not have homologs in higher plants, the overall close similarities in the regulation of cell cycle progression, such as the common functions of proliferation promoting cyclins and repressive CKIs (Dewitte and Murray, 2003), indicates that exploring these systems may lead to the identification of new E3 ligases.

1.7.6 – Ubiquitin-like proteins also modulate protein function

In addition to ubiquitin, many organisms including higher plants encode ubiquitin-like proteins (UBLs). Although their sequences are relatively diverse, with sequence similarity ranging from ~50% (RUB (RELATED TO UBIQUITIN)) to ~20% (mammalian AUT7) (Jentsch and Pyrowolakis, 2000, Schwartz and Hochstrasser, 2003), all UBLs share a similar tertiary structure known as the ubiquitin fold (Miura and Hasegawa, 2010, Hochstrasser, 2009). All UBLs are also conjugated in to their substrate in a similar way to ubiquitin; through an ε-amido linkage or isopeptide bond between the C-terminal glycine of the UBL and a lysine on the target protein (Miura and Hasegawa, 2010, Kerscher et al., 2006). In addition, all UBL conjugation pathways also involve E1-like, E2-like and E3-like proteins in a conjugation cascade.

The UBL, HUB1, which is involved in yeast cell polarisation (Dittmar et al., 2002), and which has also been identified in Arabidopsis (Downes and Vierstra, 2005), has a relatively poorly understood conjugation cascade. SUMO (SMALL UBIQUITIN-RELATED MODIFIER) and RUB have been relatively well characterised in animals and plants and use hetero-dimeric E1 complexes and specialist E2-conjugating enzymes (Miura and Hasegawa, 2010). SUMO and RUB are activated by the hetero-dimeric E1 complexes SAE1-SAE2 (Castaño-Miquel et al., 2013) and AXR1-ECR1/AXL1-ECR1 (Hotton et al., 2011) respectively. In addition SUMO and RUB utilise the specialised E2-conjugating enzymes SCE1 and RCE1 respectively (Dharmasiri et al., 2007, Miura and Hasegawa, 2010, Jentsch and Pyrowolakis, 2000). Specialist E3-ligase enzymes are also required for ligating UBLs; SIZ1 and HPY2 are involved in sumoylation (Ishida et al., 2009, Miura et al., 2010) and RBX1/ROC in rubylation (Miura and Hasegawa, 2010).

Although rubylation and sumoylation are the best-studied processes in plant UBL biology, rubylation appears to be a significantly more restricted process as its only known substrates are the cullin subunits of multimeric E3 ligases (Miura and Hasegawa, 2010). Here it plays a significant role in the regulation of multimeric E3 activity and specificity (Duda et al., 2008, Merlet et al., 2009). This is discussed in more detail in section 5.1.2. In contrast, sumoylation has been shown to be involved in a variety of biological processes including phytohormone signalling, cold-tolerance, meiosis, DNA damage responses and chloroplast development (Miura et al., 2007, Budhiraja et al., 2009, Miura et al., 2009, Miura and Hasegawa, 2010). Furthermore, sumoylation plays a role in regulating the transition from cell-proliferation to cell-expansion, with the SUMO E3 ligase HIGH PLOIDY 2 (HPY2) characterised as a negative regulator of the endocycle in Arabidopsis (Ishida et al., 2009). This study revealed that *hpy2* mutants suffer premature mitotic exit and, as a consequence, have a dwarfed phenotype with defective meristems (Ishida et al., 2009). In addition, the SUMO E3 ligase SIZ1 is involved in regulating the salicylic-acid-mediated growth response, with *siz1* mutants exhibiting a dwarfed phenotype (Miura et al., 2010). This phenotype includes a reduced leaf area and reduced root biomass, as a consequence of altered cell proliferation and cell expansion respectively (Miura et al., 2010).

This chapter has reviewed the current state of knowledge surrounding the processes governing organ formation and the setting of organ size in animals and plants. It has focused on the contribution made by cell proliferation and cell expansion in the developing organ, and detailed the identities and mechanisms of action of the key regulators of these processes. Drawing on studies from animal systems, this chapter has explored possible models to explain the apparent size-checkpoint system that is evidenced by the presence of a compensation mechanism in plant organ development. It has also focused on the role played by the cell cycle in the regulation of organ size, and in particular on how modification of the cell cycle can drive changes in the *rate* and *duration* of both cell proliferation and cell expansion. The importance of the process of ubiquitination in the cell-cycle and other organ-growth regulatory pathways has also been explored and the enzymatic processes underpinning ubiquitination have been discussed in detail.

This thesis focuses on the role played by DA1 in the regulation of organ size in Arabidopsis. Chapter 3, the first results chapter, focuses on the structure of the DA1 protein and the role played by its individual domains in DA1 biochemistry and *DA1*-dependent growth regulation.

Chapter 4 explores the DA1 interactome through a yeast-2-hybrid screen and seeks to link DA1 to upstream signalling events as well as to downstream regulation of the cell-cycle. Chapter 5 looks in detail at the *DA1-EOD1* and *DA1-DA2* interactions and explores the role played by DA1 in the regulation of growth through the Arabidopsis ubiquitin system. Complementing the function analysis of DA1 in Chapters 3-5, Chapter 6 describes two large scale genetic analyses conducted to screen for novel regulators of organ growth in Arabidopsis, as well as to investigate whether natural variation at the *DA1* locus is utilised as a growth regulator by natural populations.

Chapter 2 - Materials and Methods

2.1 – Reagents

General reagents used in this thesis were purchased from Merk Chemicals Ltd. (Nottingham, UK), Sigma-Aldrich Company Ltd. (Gillingham UK), Melford Laboratories Ltd. (Ipswich, UK), New England Biolabs UK Ltd. (Herts, UK), Qiagen Ltd. (Manchester, UK), Bio-Rad Laboratories Ltd. (Herts, UK), and Santa Cruz Biotechnology Inc. (Texas, USA). Reagents used for ubiquitin biochemistry were obtained from Boston Biochem Inc. (Massachusetts, USA).

2.2 – Recombinant DNA work

Some constructs described in this thesis were made by Neil McKenzie (Bevan Lab).

2.2.1 – Agarose gel electrophoresis

0.8% or 1% agarose gels were made by dissolving agarose in 1x TRIS-acetate-EDTA (TAE). The agarose was mixed with TAE and heated in a microwave oven until boiling and dissolution of the agarose. The solution was cooled at room temperature before being mixed with 0.005% (v/v) ethidium bromide and poured into a custom gel tray. The gel was then left to set at room temperature. When set, the gel was placed in a custom gel tank and immersed in 1% TAE. Samples were mixed with 10X DNA loading buffer (0.25% (w/v) Bromophenol Blue, 0.01% (w/v) SDS , 4% (w/v) glycerol, and 0.5 mM EDTA) and loaded in either 10µl or 20µl aliquots onto the gel. Samples were run in parallel with 3µl of 1Kb DNA Ladder (New England BioLabs) at 80-150V. Gels were analysed using an AlphaImager EP gel analyser (Alpha Innotech, USA).

2.2.2 – PCR amplification of DNA

All PCR protocols used dNTP solutions made from a 100mM dNTP stock solution consisting of dATP, dGTP, dCTP, dTTP (Promega U1240). PCRs were carried out in either individual PCR tubes (4titude 4TI-0790), strips of eight PCR tubes (4titude 4TI-0780) or 96 well PCR plates (Fisher Scientific 11757533), and were run using the PTC200 PCR machine (MJ Research).

2.2.2.1 – High fidelity PCR amplification of DNA

High fidelity PCR was used to amplify cDNA in the cloning of whole gene coding sequences. The cDNA used in this thesis was kindly provided by Mathilde Seguela. This protocol uses the Phusion® High-Fidelity DNA Polymerase kit from New England BioLabs Ltd (M0530S). It is a

'Hot-Start' protocol and requires the addition of Phusion® High-Fidelity DNA Polymerase once the sample has reached 98 °C in step 1.

Reagent	Volume (µl)
Ultra-pure Water	34
Phusion® HF Buffer	10
dNTPs (10mM)	1
Forward Primer	2
Reverse Primer	2
Template DNA	0.5
Phusion® High-Fidelity DNA Polymerase	0.5
TOTAL	**50**

STEP	Temperature	Time (minutes)
	98°C	3
2	98°C	0.5
3	60°C	0.5
4	72°C	1
	30x repeats of steps 2-4	
5	72°C	5

Table 2.1 – High Fidelity PCR protocol

2.2.2.2 – Colony PCR

This PCR protocol was used to assay for successful transformation of *Escherichia coli* (*E. coli*).

Using a 10µl pipette tip, 1µl of either liquid culture or plated culture was added to each PCR tube. PCR tubes were then vortex for 10 seconds and loaded into the PCR machine.

Reagent	Volume (µl)
Ultra-pure Water	15
10X PCR Buffer (Qiagen 201203)	2
Forward Primer	0.4
Reverse Primer	0.4
dNTPs (10mM)	0.4
Taq Polymerase (Qiagen 201203)	0.8
Template DNA	1
TOTAL	**20**

STEP	Temperature	Time (minutes)
1	98°C	3
2	98°C	0.5
3	55°C	0.5
4	72°C	2
	29x repeats of steps 2-4	
5	72°C	5

Table 2.2 – Colony PCR protocol

2.2.2.3 – YeastAmp PCR

This PCR protocol was used to amplify DNA from yeast miniprep products.

Reagent	Volume (µl)
Ultra-pure Water	36.25
10X PCR Buffer (Invitrogen 18067-017)	5
MgCl (50mM)	1.5
Forward Primer	2.5
Reverse Primer	2.5
dNTPs (10mM)	1
TaqPolymerase(Invitrogen 10342)	0.25
TOTAL	**50**

STEP	Temperature	Time (minutes)
1	94°C	3
2	94°C	0.5
3	56°C	0.5
4	72°C	2
	30x repeats of steps 2-4	
5	72°C	5

Table 2.3 – YeastAmp PCR protocol

2.2.2.4 – Sequencing PCR reaction

DNA was submitted to The Genome Analysis Centre (Norwich, UK) for sequencing as 'ready-reactions'. Prior to submission, the sequencing sample was prepared using the PCR based BigDye® Terminator v3.1 Cycle Sequencing Kit from Invitrogen (Invitrogen 28002870). Sequencing data was analysed using the VectorNTI contigExpress software (Invitrogen A14470).

Reagent	Volume (µl)
Template DNA	1
Primer	0.32
BigDye	1
Ultrapure water	6.18
TOTAL	**50**

STEP	Temperature	Time (minutes)
1	96°C	0.5
2	50°C	0.25
3	60°C	4
	30x repeats of steps 2-4	
5	14°C	5

Table 2.4 – Sequencing PCR protocol

2.2.2.5 – Site-directed mutagenesis of DNA

This technique was used for the site-directed mutagenesis of the DA1 peptidase domain. It was carried out using Primers for the 3' and 5' termini of DA1 as well as mutagenic primers for the peptidase domain (see section 2.2.8).

Two first-step PCRs were carried out using the high-fidelity PCR documented in section 2.2.2.1; the first containing the DA1 5' forward primer and the reverse peptidase mutagenic primer,

and the second containing the forward peptidase mutagenic primer and the DA1 3'terminus reverse primer. PCR products from each reaction were purified using the PCR purification technique described in section 2.3.3.2. A second high fidelity PCR reaction was carried out using the products of both first-step PCRs and the DA1 5' forward and 3' reverse primers.

2.2.2.5 – Genotyping of transgenic plants

Using genomic DNA extracted from the appropriate plants (section 2.2.3.4) and the Colony PCR protocol (2.2.2.2). PCRs using the T-DNA border primer (BP) and the right genomic primer (RP) were used to detect the T-DNA insert, whereas PCRs using the left genomic primer (LP) and RP were used to confirm no insertion. Homozygotes for the T-DNA insertion contained a BP-RP PCR fragment only, heterozygotes contained both BP-RP and LP-RP PCR fragments, and wild-type plants contained only LP-RP PCR fragments.

A similar technique was used to detect binary vector insertions in genomic DNA.

2.2.3 – DNA Purification

2.2.3.1 – DNA extraction from E.coli

Miniprep DNA extraction from *E. coli* was carried out using the Qiagen Spin Miniprep Kit (Qiagen 27104), according to the manufacturer's instructions. Samples were eluted in 30µl of Qiagen Buffer EB.

Large quantities of DNA were extracted from *E. coli* using the Qiagen Plasmid Maxi Kit (Qiagen 12162), according to the manufacturer's instructions. The DNA pellet was resuspended in 200µl in 1x ultrapure water.

2.2.3.2 – DNA extraction from PCR solutions and agarose gels

DNA was extracted from completed PCR reactions using the QIAquick PCR Purification Kit (Qiagen 28104), according to the manufacturer's instructions. Samples were eluted in 30µl Qiagen Buffer EB.

Specific DNA fragments were extracted from completed PCR reactions and restriction digests using the QIAquick Gel Extraction Kit (Qiagen Ltd 28704), according to the manufacturer's instructions. Samples were eluted in 30µl Qiagen Buffer EB.

2.2.3.3 – DNA extraction from yeast

DNA was extracted from yeast using the Qiagen Spin Miniprep Kit (Qiagen Ltd 27104) and a modified protocol.

1.5ml of an overnight yeast culture (see section 2.7) was pelleted at 600x g for 2 minutes and the supernatant discarded. 250µl Qiagen Buffer P1 (RNAase added) was mixed with 3µl Zymolase (Zymo Research E1004) and added to the pelleted yeast. The pellet was resuspended and incubated at 37 °C for one hour. Following incubation, the remainder or the Qiagen Spin Miniprep Kit manufacturer's protocol was followed (beginning with the addition of 250µl Qiagen Buffer P2). Samples were eluted in 30µl Qiagen Buffer EB.

2.2.3.4 – DNA extraction from plants

A single leaf was placed in a 1.5ml eppendorf tube and ground with a disposable grinder in 150µl REB buffer (50mM TRIS-HCL pH8, 25mM EDTA, 250mM NaCl, 0.5% (w/v) SDS). 150µl Phenol:Chlorophorm:Isoamyl alcohol (Sigma-Aldrich P3803) was added to each tube and vortexed for 10 seconds, before centrifuging for 5minutes at 16 000x g. 130µl of the aqueous phase was then transferred to a clean 1.5ml eppendorf tube, where the addition 110µl of isopropanol was followed by centrifuging for 30 minutes at 16 000x g. The supernatant was discarded, the pellet was washed with 50µl 70% ethanol, and the tube was centrifuged for a further minute at 16 000x g. The ethanol supernatant was discarded and the pellet was left to dry at room temperature for one hour, before being resuspended in 50µl of ultrapure water.

2.2.4 – Subcloning

2.2.4.1 – Restriction digestion of DNA

Restriction digests were carried out using restriction endonuclease enzymes purchased from New England BioLabs (BamHI (R3136T/M), XhoI (R0146M), NotI (R3189M), SalI (R3138T/M), NdeI (R0111S), NheI (R0131S), EcoRI (R0101S)) using the appropriate, designated buffers. Restriction digests were carried out in a 20µl reaction volumes containing 1µl restriction endonuclease, 2µl manufacturer's reaction buffer and made up to 20µl with sample DNA or ultrapure water. Restriction digests were carried out for two hours at 37°C.

2.2.4.2 – DNA ligation

DNA ligations were carried out using the LigaFast Rapid DNA Ligation System from Promega. Reactions were carried out in a volume of 10µl, including 5µl 2x LigaFast Rapid Ligation Buffer (Promega C671A) and 1µl T4 DNA ligase (Promega M1801). The amount of vector and insert DNA was calculated using the following formula (from Promega) and the reaction volume was made up to 10µl with nuclease-free water. Ligation reactions were incubated for 30 minutes at room temperature.

$$\frac{\text{ng of vector x size of insert (kb)}}{\text{Size of vector (kb)}} \times \text{ratio of } \frac{\text{Insert}}{\text{vector}} = \text{ng of insert}$$

Figure 2.1 – Equation for DNA ligation reaction

Equation used to calculate the mass of vector and insert DNA for DNA ligation reactions. Equation adapted from the Promega Subcloning Notebook (http://www.promega.co.uk).

2.2.4.3 –Klenow reaction

The Klenow polymerase reaction was used to blunt 5' overhangs (created from restriction digestion), prior to ligation. The DNA Polymerase I, Large (Klenow) Fragment kit from New England BioLabs Ltd (M0210S) was used for this work. A 20µl reaction was used containing 1-4µg template DNA, 2µl NEBuffer 2, 0.8µl 1mM dNTPs (see section 2.2.2), 1µl DNA Polymerase I, Large (Klenow) Fragment and nuclease-free water. The reaction was run for 30 minutes at room temperature.

2.2.5 – Transforming bacteria

2.2.5.1 – Bacterial strains

Subcloning efficiency DH5α competent *E. coli* (Invitrogen 18265017) were used for general subcloning and DNA generation for protoplast work. ONE SHOT BL21 (DE3) pLYSs *E. coli* (Invitrogen C606010) were used for *in vitro* protein expression. TOP10 One Shot competent *E. coli* (Invitrogen C404003) were used in the Yeast-2-Hybrid analysis. GV3101 *Agrobacterium tumefaciens* (kindly provided by Kim Johnston) were used for stable transformation of Arabidopsis.

2.2.5.2 – Preparation of electro-competent GV3101 A. tumefaciens

A 50ml LB culture of GV3101 was grown overnight at 28°C with the appropriate antibiotics (see section 2.2.5.5). The following day 400ml of fresh LB was inoculated with 4ml of the overnight culture and grown at 28°C until the OD_{600} value was between 0.4 and 0.7. At this point, the entire 400ml culture was stored on ice for 15 minutes before centrifuging at 3000x g for 10 minutes (at 4°C). The supernatant was discarded and the pellet re-suspended in 10ml ultrapure water, before being centrifuged for 10 minutes at 3000x g (4°C). The supernatant

was discarded and the pellet re-suspended once more in 10ml ultrapure water. This supernatant was then discarded and the pellet re-suspended in 10ml 10% (v/v) glycerol before being transferred to a 50ml Falcon tube and centrifuged at 3000x g for 10 minutes. The pellet was re-suspended in 1ml of 10% (v/v) glycerol, aliquoted into 40µl volumes, frozen in liquid nitrogen and stored at -80°C. This method was adapted from the John Innes Centre Standard Operating Procedure (CDB-SC-023) written by Nicola Stacey.

2.2.5.3 – Chemical transformation of bacteria

This technique was used for DH5α competent *E. coli* (Invitrogen 18265017), ONE SHOT BL21 (DE3) pLYSs *E. coli* (Invitrogen Ltd C606010) and TOP10 One Shot competent *E. coli* (Invitrogen C404003).

1-10µg (in 1-5µl) of DNA was added to a 50µl aliquot of bacteria in a 1.5ml tube and incubated on ice for 30 minutes. The tube was heat-shocked for 30 seconds at 42°C and returned to ice for two minutes. 250µl of S.O.C medium (Invitrogen 15544-034) was added to each tube and then the tubes were incubated at 37°C for one hour at 220rpm. After this incubation step, 50µl of the transformation solution was pipetted onto an appropriate plate (see section 2.2.5.5) and incubated overnight at 37°C.

2.2.5.4 – Electro-transformation of bacteria

This technique was used for the transformation of GV3101 *A. tumefaciens*.

1-10µg (in 1-5µl) of DNA was added to a 40µl aliquot of electro-competent bacteria in an electroporation cuvette (Geneflow E6-0060) on ice. An electric pulse was applied (field strength: 1.25kv/mm, capacitance: 25uF, resistance: 400Ω, pulse length: 8-12milliseconds), immediately followed by the transfer of cells to 1ml of LB in a 1.5ml tube. The bacterial solution was then incubated at 28°C for one hour followed by plating 10µl and 100µl on appropriate plates (see section 2.2.5.5) and incubation at 28°C for three days.

2.2.5.5 – Making plates

LB	1% (w/v)	Tryptone
	0.5% (w/v)	Yeast Extract
	1% (w/v)	NaCl
	1% (w/v)	Agar (for solid LB)
	Adjusted to pH 7.0 with NaOH	

Table 2.5 – LB Formula

100ml of LB agar (sufficient volume for three 90mm petri dishes) was melted in a microwave and left to cool at room temperature. When cooled, relevant antibiotics were added to their respective final concentrations (kanamycin 50µg.ml^{-1}, ampicillin 100µg.ml^{-1}, gentamycin 10µg.ml^{-1}, spectinomycin 50µg.ml^{-1}, carbenicillin 100µg.ml^{-1}, rifampicin 25µg.ml^{-1}) and plates were poured. When making plates for *A. tumefaciens*, all antibiotics, with the exception of rifampicin, were added at half the concentrations stated above.

2.2.6 – Vectors

The vectors used in this thesis are listed in the following table. Their vector maps can be seen in (Fig.S1).

Vector Name	Vector Type	Vector Layout	Reference
pAM-GW-YFPc	Binary Vector	35S-Gateway-YFPc	Lefebvre et al, 2010
pAM-GW-YFPn	Binary Vector	35S-Gateway-YFPn	Lefebvre et al, 2010
pAM-YFPn-GW	Binary Vector	35S-YFPn-Gateway-	Lefebvre et al, 2010
pAM-YFPc-GW	Binary Vector	35S-YFPc-Gateway-	Lefebvre et al, 2010
pEarleyGate 201	Binary Vector	35S-HA tag-Gateway-	Earley et al, 2006
pw1211	Binary Vector	35S-Gateway-FLAG tag	Phil Wigge, SLCU
pMDC32	Binary Vector	35S-Gateway-FLAG tag	(Curtis and Grossniklaus, 2003)
pAmiR	Binary Vector	35S-amiRNA	(Schwab et al., 2006)
pGEX4T2	In vitro expression	Ptac-GST-polylinker	GE Life Science
pGEX4T1	In vitro expression	Ptac-GST-polylinker	GE Life Science
pET24a	In vitro expression	T7-polylinker-HIS	Novagen
peTnT	In vitro expression	T7-FLAG-HA-polylinker-HIS	Adapted from Novagem

Table 2.6 – Vectors used in this thesis

2.2.7 – Primers

All primers used in this thesis were purchased from either from Sigma Genosys (Sigma-Aldrich) or Metabion International AG, Germany.

Primer Identity		Primer sequence
Primers for pGEX4T2 cloning		
DA1	Forward	gcgggatccGGTTGGTTTAACAAGATCTT
	Reverse	cgccgctcgagTTAAACCGGGAATCTAC
DAR1	Forward	gcgggatccGGGTGGCTAACTAAAATCCTTA
	Reverse	ccgctcgagTTAAGGAAATGTACCGGTCAAG
GUS	Forward	cggGGATCCgtccgtcctgtagaaaccc
	Reverse	ggcCTCGAGttgtttgcctccctgctg
DA2	Forward	CGAggatccGTAATAAGTTGGGAAGGAAGAG
	Reverse	ccgCTCGAGttattgccaggtaacttcagtt
Primers for pETnT cloning		
DA1	Forward	gcgggatccGGTTGGTTTAACAAGATCTT
	Reverse	cgccgctcgagAACCGGGAATCTACCGGTC
GUS	Forward	cggGGATCCgtccgtcctgtagaaaccc
	Reverse	ggcCTCGAGttgtttgcctccctgctg
Nterm	Forward	gcgggatccGGTTGGTTTAACAAGATCTT
	Reverse	ggcCTCGAGaggatgatatctctccctgtaac
Cterm	Forward	cggGGATCCaaatgtgatgtctgcagccacttt
	Reverse	ggcCTCGAGaaccgggaatctaccggtcatct
TCP15	Forward	gcggtcgacaATGGATCCGGATCCGGATCA
	Reverse	cgtctcgagGGAATGATGACTGGTGC
LRRfrag	Forward	gtgaattcGCAGGCACATTCGGTTAT
	Reverse	gtgctcgagCCGACCATCAGCTGAATCG
DA2	Forward	CGAggatccGTAATAAGTTGGGAAGGAAGAG
	Reverse	ccgCTCGAGTTGCCAGGTAACTTCAGTTG
EOD1	Forward	cgaggatccAATGGAGATAATAGACCAGTGGA
	Reverse	ccgctcgagATGAATGCTGGGCTCCCCA
BBR	Forward	TATAGAATTCATGCCCATGGAGAACGACA
	Reverse	TATACTCGAGGCTTTGTCCAGAGGTCGAAG
DA1pep	Forward (mutagenic)	GGTTCGATTCTAGCTGCAGAGATGATGGCAGCGT GGATGAGGCTC
	Reverse (mutagenic)	GAGCCTCATCCACGCTGCCATCATCTCTGCAGCTA GAATCGAACC
SIS3	Forward	TATAGGATCCATGGCGATGAGAGGTGTC
	Reverse	TATACTCGAGTCTCCGAGATGGAGATAGATCG
Primers for pDBleu cloning		
DA1(truncated)	Forward	gaggtcgaCTATTACTTTTCAAATGGATTTC
	Reverse	aaagcggccgcTTAAACCGGGAATCTACCGG
Primers for pEXP-AD502 cloning		
TCP15	Forward	gcggtcgacaATGGATCCGGATCCGGATCA
	Reverse	ggtgcggccgcCTAGGAATGATGACTGGTG
LRR	Forward	ttgtcgaccATGGAGGCTCCTACGCC
	Reverse	atgcggccgcTCACCGACCATCAGCTG

Table 2.7 – Primers used in this thesis

Primers for Sequencing		
T7	Forward	AATACGACTCACTATAGG
	Reverse	GCTAGTTATTGCTCAGCG
pDBleu	Forward	CAAGCTATACCAAGCATACAATC
	Reverse	ACCTCTGGCGAAGAAGTCCAAAGC
pEXP-AD502	Forward	Tataacgcgtttggaatcact
	Reverse	Taaatttctggcaaggtagac
pAMIR	Forward	ATATAAGGAAGTTCATTTCATTTGGAG
	Reverse	Gagcctcgacatgttgtcgc
p35S	Forward	Tcgcaagacccttcctctatataagga
M13	Forward	Gtaaaacgacggccag
	Reverse	Caggaaacagctatgac
Primers for pENTr cloning		
DA1	Forward	caccATGGGTTGGTTTAACAAGATC
	Reverse (STOP)	TTAAACCGGGAATCTACCGGTC
	Reverse (NO STOP)	AACCGGGAATCTACCGGTCATC
DA2	Forward	caccATGGGTAATAAGTTGGGAAGGA
	Reverse (STOP)	ccgCTCGAGttattgccaggtaacttcagtt
	Reverse (NO STOP)	ccgCTCGAGTTGCCAGGTAACTTCAGTTG
EOD1	Forward	caccATGAATGGAGATAATAGA
	Reverse (STOP)	TCAATGAATGCTGGGCTCC
	Reverse (NO STOP)	ATGAATGCTGGGCTCCCCA
BBR	Forward	caccATGCCCATGGAGAACGAC
	Reverse (NO STOP)	GCTTTGTCCAGAGGTCGAAG
Primers for plant genotyping		
da1ko1	Salk_126092 LP	AAGCCAGCTAAATATGATTGG
	Salk_126092 RP	AATCCGTTTGGAACTCGTTTG
tcp14	N108688 SMLP	CGCTTCCACTTTTAGCCCTAATAACATA
	N108688 SMRP	TGTTTTTGTGTGTGTCTAATCTTGCTGAT
	N108688 3'dSpm32	TACGAATAAGAGCGTCCATTTTAGAGTGA
tcp15	SALK_011491 LP	AGAACCACGTAAGCCCATCTC
	SALK_011491 RP	CACCACTACTCCAAAACGGTG
eod1-2	SALK_045169 LP	GAGCGATGCATCTCTAACCAC
	SALK_045169 RP	AGTAGGAACAGAAAGCAGGGG
da2-1	SALK_150003 LP	AGATGATGAAGACGGTGTTGC
	SALK_150003 RP	AGCTCGGCCTACTCAGTATCC
dar1-1	SALK_067100 LP	ATTTAGTCGAAGCCATGCATG
	SALK_067100 RP	TTACAAGGAGCAGCATCATCC
tcp22	Salk 027490 LP	CGCATGAAGTACCAAGCTCTC
	Salk 027490 RP	AATGTGGTGCCTCAACCTATG
LBb1		GCGTGGACCGCTTGCTGCAACT
LBa1		TGGTTCACGTAGTGGGCCATCG

Table 2.7 – Primers used in this thesis

2.3 – Plant growth

2.3.1 – Plant material

All Arabidopsis lines used in this work were accessions, RILs, mutants or T-DNA insertion lines of *Arabidopsis thaliana* (assistance with Arabidopsis work was kindly provided by Caroline Smith and Fiona Corke from the Bevan Lab).

The lines used in Chapters 3-5 are listed in Table 2.8. T-DNA insertion lines were genotyped using the DNA extraction protocol in section 2.2.3.4, the colony PCR protocol in section 2.2.2.2 and the primers listed in section 2.2.8.

The analysis described in Chapter 6 uses the Multiparent Advanced Generation Inter-Cross (MAGIC) population described in Kover et al (2009), and a Swedish subset of the 1001 genomes project population (Weigel & Mott 2009). The MAGIC lines were kindly provided by Phil Wigge at the Sainsbury Laboratory Cambridge University, Cambridge. The Swedish accessions were kindly provided by Caroline Dean at the John Innes Centre, Norwich. The identities of the Swedish accessions used in the GWAs analysis are listed in Table. S2.

Arabidopsis Line	**T-DNA/Mutation**
Col-0	N/A
da1ko1	Salk_126092
tcp14	N108688
tcp15	SALK_011491
bak1-4	SALK_116202.39.60
eod1-2	SALK_045169
da2-1	SALK_150003
dar1-1	SALK_067100
tcp22	SALK_027490
da1-1	Mutant (Li et al 2009)

Table 2.8 – Arabidopsis lines used in this thesis

2.3.2 – Growth conditions

All mature Arabidopsis plants were grown in compost composing of eight parts peat-based compost (Levington F2 soil, N150:P200: K200mg/L, pH=5.3-5.7) and one part grit.

For the GWAs analysis, five seeds of each accession were sown into randomised strips of five P40 pots (five seeds per pot, 25 seeds per accession). Plants were stratified at 4°C for three

days and vernalised at for six weeks under 30µM white light (seedlings were thinned after one week of vernalisation to leave one seedling per plot). After vernalisation plants were moved to growth chambers until flowering (16h light / 8h dark cycle, 20°C day, 80% humidity, 170µM white light). During growth, pots were moved (randomly) to different positions within the growth chamber.

For the MAGIC analysis, plants were stratified for three days and vernalised for 4 weeks in short days under 30µM white light. After vernalisation plants were moved to growth chambers until flowering (16h light / 8h dark cycle, 21°C day/17°C night, 80% humidity, 170µM white light).

For the phenotyping of plants in Chapters 3-5, seeds were sown in FP9 pots, stratified for three days at 4°C and then moved directly to growth chambers (20°C, 16 hours light, 8 hours dark). After one week of growth, seedlings were pricked out into randomly assigned positions in P24 trays and moved back into the same growth chamber.

For the Agrobacterium-mediated transformation of plants (see section 2.3.3), seeds were sown in FP9 pots, stratified for three days at 4°C and then moved directly to glass-house conditions (16h light / 8h dark cycle supplemented with 120 µmol m-2 s-1 fluorescent lighting, 21-23°C day, 16°C night). After one week, 12 seedlings were transplanted to individual pots in P24 trays and returned to the same glass-house conditions until inflorescence bolts emerged. For cross pollination of Arabidopsis, a similar procedure was followed, except that individual seedlings were pricked out into individual F7 pots.

2.3.3 – Agrobacterium-mediated transformation of Arabidopsis

10ml LB (with appropriate antibiotics (see section 2.2.5.5)) was inoculated with *A. tumefaciens* and incubated at 28°C for 2 days at 200rpm. 1ml of this 10ml culture was used to inoculate a new 400ml culture, which was then incubated overnight at 28°C and 200rpm.

The following day the culture was centrifuged for 10 minutes at 3000x g and the supernatant discarded. The pellet was resuspended in 400ml transformation buffer (0.5xMS salts, 0.5g.l^{-1} MES, 5% sucrose, 300µl.l^{-1} Silwet L-77 (Lehle Seeds, Texas, USA VIS-01) and prepared plants (see section2.3.2) were dipped into this solution for 30 seconds (with gentle agitation). After dipping, plants were laid on their sides and covered with plastic to maintain humidity. Plants were left overnight and then returned to an upright position and moved into the glasshouse conditions described in section 2.3.2.

When ripe, seed was manually threshed. Threshed seed was sterilised by shaking 100µl of seed in a 1.5ml tube containing 1ml sterilisation solution (50% (v/v) ethanol and 0.625% (w/v) dichloroisocyanuric acid) for 18 minutes. Immediately afterwards, the sterilisation solution was removed and seeds were washed with 3x 1ml 100% ethanol. Seeds were left to dry on sterile filter paper. Once sterile, seeds were sown on GM plates (0.43% (w/v) Murashige and Skoog, 1% (w/v) sucrose, 0.01% (w/v) inositol, 10ppm (w/v) thiamine, 50ppm (w/v) pyridoxine, 50ppm (w/v) nicotinic acid, 0.05% (w/v) MES, 9% (w/v) agar, pH 5.7) with the appropriate final concentration of antibiotic (spectinomycin- 25µl.µl^{-1}) and incubated at 20°C, in 24 hour light, for 10-15 days. Transformed seedlings were selected based on their antibiotic resistance.

2.3.4 – Crossing plants

Maternal flowers (see section 2.3.2 for growth conditions) were selected before opening, and the immature anthers were removed from all flowers of a single inflorescence, then a mature paternal flower was introduced (using forceps) to the paternal flower and the paternal anther was rubbed on the stigmatic surface of the maternal plant. The relevant inflorescence was labelled seeds were harvested when ripe. Seedlings were grown in individual P40 pots (in glass-house conditions documented in section 2.3.2) and genotyped as described in section 2.3.1.

2.3.5 – Phenotyping plants

2.3.5.1 – Petal and seed area measurements

Individual petals were harvested from the first flowers to form on each plant. These were then stuck to a custom black perspex background using transparent adhesive tape. Petals were scanned using a desktop scanner (Hewlett Packard Scanjet 4370) at a high resolution (<3600dpi). Images were stored as black and white 8-bit images, and subjected to image analysis using the ImageJ software (http://rsbweb.nih.gov/ij/) - see Box 2.3.5.1 for details.

Seed area was measured using the same protocol, with the exception that seeds were scattered in a petri dish and scanned against a white background.

2.3.5.2 – Inflorescence stem height

Inflorescence stem height was measured a 28 days after bolting (rather than after sowing) to ensure that all plants were at a developmentally equivalent stage. The length of the stem was measured from its base to its most distal tip, using a ruler.

Box 2.1 - Instructions for ImageJ analysis

Open image in ImageJ and set threshold (Ctrl+Shift+T) such that all petals are completely red and most other structures are not. Select all petals with the "rectangular selection" tool and chose the analyse option (Analyze > Analyze Particles). In the dialog box set a size threshold to exclude smaller (non-petal) structures and large structures such as aggregations of petals. Do this by choosing a minimum value of half the mean petal size and a maximum value of twice the mean petal size (check by eye to ensure accuracy). Additionally, ensure that "Display results", "Exclude on edges" and "Include holes" are enabled and click "OK".

This protocol is adapted from the John Innes Centre standard operating procedure CDB-SC-022, written by Nicola Stacey.

2.4 – Brassinosteroid root growth assay

Seeds were sterilised using the protocol described in section 2.3.3 and then added to a 1.5ml tube with 1ml sterile water. The tube was vortexed for 10 seconds, then wrapped in tin foil and left at 4°C for seven days to stratify. 100mm square plates were made with modified ½ MS (0.22% (w/v) Murashige and Skoog, 1% (w/v) sucrose, 0.8% (w/v) phytoagar, pH5.7) including epibrassinolide (Sigma-Aldrich E1641) at the appropriate concentration. Seeds were placed on to plates at a rate of ten per treatment per genotype (a total of 30 seeds per plate). Plates were placed upright in a growth chamber (20°C, 16 hours light, 8 hours dark) for 9 days. Roots were carefully unravelled, plates were scanned in a desktop scanner (Hewlett Packard Scanjet 4370), and root lengths calculated using ImageJ software (http://rsbweb.nih.gov/ij/). This method was kindly provided by the Zipfel Group, The Sainsbury Lab, Norwich, UK.

2.5 – *In vitro* protein biochemistry

2.5.1 – Western Blots

20%, 12% or 4-20% precast SDS-polyacrylamide gels (RunBlue NXG02012, NXG01227, NXG42027) were submerged in RunBlue SDS-TRIS-tricine run buffer (RunBlue NXB0500), in a gel tank (Atto Japan AE6450) Samples were mixed with 2x Laemmli sample buffer (Bio-Rad Ltd 161-0737) placed in a heat block for 10 minutes at 96°C and then loaded into rinsed wells in the gel in either 10µl or 20µl aliquots. The gels were run at 160V for 60 minutes along with a

3ul aliquot of PageRuler Plus Prestained Protein Ladder, 10 to 250kDa (Fermentas 26619). If appropriate, gels were stained at this stage (see section 2.5.1.1).

Transfers were carried out using the Bio-Rad Mini Trans-Blot® Cell kit (Bio-Rad 170-3836). Gels were removed from their glass casing and laid on top of a sponge (from Bio-Rad Mini Trans-Blot® Cell kit), two pieces of chromatography paper (VWR WHAT3030-917) and a methanol-washed PVDF membrane (Roche Diagnostics 03010040001). Air bubbles were removed from between the gel and membrane and then two further pieces of Whatman paper and a sponge were applied to the gel. This was enclosed in a gel holder cassette (from Bio-Rad Mini Trans-Blot® Cell kit), submerged in transfer buffer (25mM TRIS, 192mM glycine, 10% (v/v) methanol) and run at 90V for 70 minutes at 4°C.

Following the transfer the membrane was washed for 10 minutes in 50ml PBS (140mM NaCl, 2.7mM KCl, 10mM Na_2HPO_4, 1.8mM KH_2PO_4, pH 7.3) at room temperature, before being agitated in 50ml blocking solution (5% (w/v) milk powder, 0.1% (v/v) Tween-20) for either one hour at room temperature or overnight at 4°C. Primary antibodies were diluted to their appropriate concentration (see Table 2.9) in blocking solution and incubated with the membrane (10ml per membrane with gentle agitation) for one hour before five washes with 50ml PBST (140mM NaCl, 2.7mM KCl, 10mM Na_2HPO_4, 1.8mM KH_2PO_4, 0.1% (v/v) Tween-20,pH 7.3) at room temperature. If secondary antibody was required, staining and washing steps were repeated.

The washed membrane was held with forceps and carefully one corner was blotted onto blue-roll to remove excess moisture. It was then laid in a petri dish and treated with peroxidise substrate (SuperSignal West FEMTO Max. Sensitivity substrate (Fisher Scientific PN34095)) at a rate of 800µl substrate per membrane. Membranes were left in this substrate for five minutes, dried as before and placed in an X-ray cassette under a piece of X-ray film (Fuji Film X-RAY 18x24cm – (FujiFilm 497772RXNO)). X-ray films were developed using a Konica SRX-101 Table Top X-ray film developer (Konica 106931659).

Subsequent to analysis, if required, membranes were washed in 50ml PBST and stained with 10ml Ponceau S solution (Sigma-Aldrich P7170) for 30 minutes, followed by a single wash in 50ml PBST and drying at room temperature.

2.5.1.1 – Staining protein gels

Protein gels were stained by agitation with InstantBlue Coomassie stain (Expedeon ISB1L) for 30 minutes at room temperature (20ml per gel).

Epitope	Host	Manufacturer	Working dilution
a-FLAG®M2-HRP	Mouse monoclonal	Sigma-Aldrich A8592. Lot: 060M6000	1:1000
a-HIS^{6} HRP	Mouse monoclonal	Sigma-Aldrich A7058, Lot: 101M4765	1:4000
a-HA-HRP	Mouse monoclonal	Sigma-Aldrich H6533. Lot: 030M4814	1:1000
a-Ubiquitin	Mouse monoclonal	BostonBiochem AB-001. Lot: 027A37010	1:1000
a-Ubiquitin	Mouse monoclonal	Sigma-Aldrich U0508. Lot: 110M1664	1:1000
a-GST-HRP	Mouse monoclonal	Santa Cruz Biotechnology SC-138. Lot:A2513	1:1000
a-GST rabbit	Goat polyclonal	GE Healthcare UK Ltd, Bucks 27-4577-50	1:1000
a-Goat-HRP	Donkey	Santa Cruz Biotechnology sc-2020	1:6000
a-Mouse-HRP	Goat	Santa Cruz Biotechnology sc-2005. Lot:C2011	1:6000

Table 2.9 – Antibodies used in this thesis

2.5.2 – Co-Immunoprecipitation analysis

All bait proteins for these studies were GST-tagged and glutathione sepharose beads (GE Life Science 17-0756-01) were used for their pull-down.

A flask of 10ml LB with appropriate antibiotics (see section 2.2.5.5) was inoculated with a BL21 (see section 2.2.5.1) glycerol stock of the appropriate expression construct and left to grow overnight at 37°C and 220rpm. The following morning the 10ml preculture was used to inoculate an 100ml LB flask (at a ratio of 1:100), and this culture was incubated at 37°C for two hours at 220rpm. The flask was removed from the incubator, IPTG (Melford MB1008) was added to a final concentration of 1mM before the culture was incubated at 28°C (and 220rpm) for another three hours. Following this growth phase, the cultures were centrifuged at 4500x g for 10 minutes, the supernatants were discarded and the pellets resuspended at 4°C in 2.5ml TGH Buffer (50mM HEPES (pH7.5), 150mM NaCl, 1% Triton-X-100, 10% Glycerol, 1mM DTT, 1 cOmplete EDTA-free protease inhibitor tablet (per 50ml) (Roche 11873580001)). The bacterial suspension was then sonicated (on ice) for four bursts of ten seconds, separated by 20-second intervals, before being centrifuged at 12 000x g for 20minutes to pellet any cellular debris. Cleared sonicates were then stored on ice while a 50% slurry of washed glutathione sepharose beads (GE Life Sciences 17-0756-01) was prepared according to the manufacturer's instructions. 20µl of the 50% glutathione sepharose slurry was then combined with 2.5ml of protein extract from bait protein (GST-tagged) expressing cells and 2.5ml of protein extract from prey protein (HA-/FLAG-/HIS-tagged) expressing cells. This mixture was incubated for 30 minutes at 4°C on a rotating wheel and then the glutathione sepharose beads were washed five times with an excess (500µl) of TGH buffer (following manufacturer's instructions). After

washing, proteins were eluted with 35µl GST-elution buffer (50mM TRIS-glycine (pH8.0), 10mM reduced glutathione) over 30 minutes at 4°C before being analysed by western blot analysis (see section 2.5.1).

2.5.3 – UIM binding assays

Proteins in this assay were GST-tagged and glutathione sepharose beads (GE Life Sciences 17-0756-01) were used for their purification.

Bacteria was grown, induced and lysed as described in section 2.5.2 and the cleared sonicate was subjected to Bradford analysis to calculate protein content (see section 2.5.6). A volume of sonicate containing 4mg of protein was added to 20µl 50% glutathione sepharose (prepared as in section 2.5.2) and incubated on a rotating wheel at 4°C for 30 minutes. The beads were then washed with 1ml of TGH buffer and then added to 10µg ubiquitin (Boston Biochem, USA-U100) to a volume of 100µl (Fisher et al., 2003). This was followed by rotation for two hours at 4°C. The beads were washed four times with 1ml TGH buffer and then added directly to 50µl 2x Laemmli sample buffer (Bio-Rad Ltd 161-0737) followed by western blot analysis (see section 2.5.1).

2.5.4 – Ubiquitination assays

Proteins used in this assay were either GST-tagged, FLAG-tagged, or HIS-tagged. Purification of these proteins used glutathione sepharose beads (GE Life Sciences 17-0756-01), Anti-FLAG M2 Magnetic Beads (Sigma-Aldrich M8823), and Dynabeads His-Tag Isolation & Pulldown (Invitrogen Ltd 101-04D) respectively.

Bacteria were grown, induced and lysed as described in section 2.5.2, apart from the pellets being re-suspended in *5ml* TGH buffer *without* DTT. Cleared sonicates were then incubated (by rotation) with either 100µl of 50% glutathione sepharose slurry or 100µl of the appropriate magnetic bead (all of which were prepared according to the respective manufacturer's instructions) for 30 minutes at 4°C. Beads were then washed twice with 1ml TGH buffer (without DTT) and twice with 1ml modified TGH buffer (*without* cOmplete EDTA-free protease inhibitor tablet, DTT and Triton-X-100). Proteins were eluted from beads by incubating (by rotation) for 30 minutes at 4°C with 100µl elution buffer (see Table 2.10). Purified proteins were assessed for protein content using Bradfords assay (see section 2.5.6) and were aliquoted and frozen at -80°C.

Glutathione Sepharose Beads	
50mM	TRIS-glycine (pH8.0)
10mM	Reduced glutathione
10% (v/v)	Glycerol
Anti-FLAG M2 Magnetic Beads	
50mM	TRIS-glycine (pH8.0)
100µg.ml^{-1}	3xFLAG Peptide (Sigma-Aldrich, F4799)
10% (v/v)	Glycerol
Dynabeads His-Tag Isolation & Pulldown	
300mM	Imidazole
50mM	Na_2HPO_4
300mM	NaCl
0.01% (v/v)	Tween-20
10% (v/v)	Glycerol

Table 2.10 – Elution buffers

Basic ubiquitination assays were made according to the scheme in Table 2.11 in a final volume of 30µl in reaction buffer (See Table 2.12). Reactions were run for two hours at 30°C, then terminated by incubation for ten minutes at 4°C before being subjected to western blot analysis (see section 2.5.1).

Enzyme	Amount	Source
E1	100ng	Human UBE1 (Boston Biochem E-304, E-305, E-306)
E2	500ng	GST-UBC10 (plasmid kindly provided by Michal Lenhard) OR Human UbcH5b/UBE2D2 (Boston Biochem USA E2-622)
E3	200ng	See Chapter 5

Table 2.11 – Ubiquitination assay protocol

50mM	TRIS-HCl (pH7.4)
5mM	$MgCl_2$
2mM	ATP
2mM	DTT

Table 2.12 – Ubiquitination assay reaction buffer

Other modifications of this basic ubiquitination assay were made. These are described in the following sections.

2.5.4.1 – DA1-ubiquitination assays and E3 cleavage assays

These assays share exactly the same experimental lay-out and differ from the basic ubiquitination assay (section 2.5.4) by the addition of 200ng DA1 only.

2.5.4.2 – Two-step EOD1 cleavage assay

This assay involves the generation of ubiquitinated DA1 from a DA1-ubiquitination assay (section 2.5.4.1), the purification of this ubiquitinated DA1, and its addition to a second reaction containing only E3 ligase. This assay uses pETnT-DA1.

A 300µl first reaction is carried out as described in section 2.5.4.1, except that the reaction buffer *does not* contain DTT. After two hours at 30°C and 10 minutes at 4°C, 20µl Anti-FLAG M2 Magnetic Beads (Sigma-Aldrich M8823) were added to the 300µl reaction and incubated (rotating) for one hour at 4°C. The beads were washed twice with 1ml TGH buffer (without DTT) and twice with 1ml modified TGH buffer (*without* cOmplete EDTA-free protease inhibitor tablet, DTT and Triton-X-100) before elution with 20µl elution buffer (see Table 2.10).

5µl of the purified DA1 from the first reaction was added to a 30µl second reaction containing 200ng E3 ligase and reaction buffer (50mM TRIS-HCL (pH7.4), 5mM $MgCl_2$, 2mM ATP, 2mM DTT). This reaction was run for two hours at 30°C, before being terminated by 10 minutes at 4°C and samples subjected to western blot analysis.

2.5.4.3 – Assays using modified ubiquitin molecules

Two assays involved the addition of modified ubiquitin. These assays follow exactly the same protocol of the basic ubiquitination assay (section 2.5.4) and include either methylated ubiquitin (Boston Biochem U-502), K48R ubiquitin (Boston Biochem UM-K48R) or K63R ubiquitin (Boston Biochem UM-K63R).

2.5.5 – De-ubiquitinase assay

200ng GST-DA1 or 200ng empty vector was incubated with 500ng of K63-linked poly ubiquitin (Recombinant Human His6-PolyUb WT Chains (2-7,K63-linked) – Boston Biochem USA: UCH-330-100) or K48- linked poly-ubiquitin (Recombinant Human His6-PolyUb WT Chains (2-7,K63-linked) – Boston Biochem: UCH-230-100) for 2hr at 30°C in a 30µl reaction with reaction buffer (50mM TRIS-HCL pH7.4, 5mM MgCL2, 2mM ATP and 2mM DTT). Reactions were stopped by the addition of 30µl 2x Laemmli sample buffer (Bio-Rad Ltd, 161-0737) and samples subjected to western blot analysis.

2.5.6 – Bradford Assay

A standard curve was created by diluting BSA (New England BioLabs B9001S) in aliquots of the lysis buffer (TGH) used to extract proteins on the day of use. Dilutions for standard curves were only used once and also made fresh every day. 5µl of each dilution was added to a single well of a 96 well plate (Fischer Scientific TKT-180-070U) with 245µl of Bradford reagent (one

part Bio-Rad Protein Assay Dye Reagent Concentrate (Bio-Rad Ltd 500-0006), five parts ultra-pure water). All protein standards were made in triplicate. 5µl aliquots of purified proteins were added to single wells of the same 96 well plate along with 245µl of the same Bradford reagent (also in triplicate). All samples were analysed at 595nm using a Tecan Safire microplate reader (Tecan Instruments).

2.6 – Arabidopsis protoplast work

Assistance with Arabidopsis protoplast work was kindly provided by Caroline Smith (Bevan Lab).

2.6.1 – Protoplast harvesting

Protoplasts were prepared from leaves of 4-5 week old plants grown in 16hrs light (20°C) and 8hrs dark (18°C). Leaves were stuck by their upper epidermis to Sellotape (Henkel Limited, UK) while Magic tape (3M UK Plc) was pressed down onto the lower epidermis and then pulled away and discarded. The remaining leaf material was placed in a petri dish containing 10ml enzyme solution (20mM MES(pH5.7), 20mM KCl, 0.4M mannitol, 1.0% cellulose R10 (Yakult), 0.25% macerozyme (Yakult), 10mM $CaCl_2$, 0.1% (w/v)BSA) and shaken for 120 minutes at room temperature at 40rpm. The leaf fragments were discarded and the liberated protoplasts were filtered through 70µm mesh (Falcon 352350) into a 50ml tube and centrifuged for three minutes at 100x g. The protoplasts were then washed twice with 10ml ice cold W5 solution (2mM MES (pH 5.7), 154mM NaCl, 125mM CaCl2, 5mM KCl). The protoplasts were resuspended in 5ml ice cold W5 solution and kept on ice for 30 minutes before resuspending them in a concentration of 2-5 x 105cells/ml with buffer MMg (4mM MES (pH 5.7), 0.4M mannitol,15mM $MgCl_2$).

2.6.2 – Protoplast Transformation

20µg (20µl) of plasmid (see section 2.2.3.1) was added to a 1.5ml tube with 100µl protoplasts (protoplasts were aliquoted with a cut off 1000µl pipette tip). 120µl PEG/Ca solution (40% (v/v) PEG 4,000, 0.2M mannitol, 100mM $CaCl_2$) was added to the protoplasts and mixed gently by inverting the tube, before incubating for 10 minutes at room temperature. The protoplasts were then diluted with 600µl W5 solution, mixed slowly (by inverting the tube) and then diluted with a further 600µl W5 and mixed again. The tube was then centrifuged at 100x g for one minute and as much supernatant as possible was removed before re-suspending pellets in 250µl W5 and aliquoting into a 24 well plate . For the EOD1 and DA2 cleavage assays (section 5.3.4.2) 50µM MG132 (Sigma-Aldrich C2211) was included in the final treatment of W5. Protoplasts were left for 16 hours at 20°C before analysis.

This method was adapted from (Wu et al., 2009).

2.6.3 – Spit-YFP analysis in protoplasts

Protoplasts were aliquoted onto standard microscopy slides (Skan Ltd 631-0114) covered with a cover slip, and sealed by nail polish. Protoplasts were analysed using a Leica SP5 (II) confocal microscope with an excitation wavelength of 488nm and emission wavelengths 505nm-550nm. Images were processed using the ImageJ software (http://rsbweb.nih.gov/ij/) and are presented as individual and overlay images.

2.6.3 – EOD1 and DA2 cleavage assays

Protoplasts were transferred to a 1.5ml tube, the tubes were centrifuged at 100x g for one minute and the supernatant was discarded. 50µl extraction buffer was added (100mM TRIS HCl pH7.5, 150mM NaCl, 5mM EDTA, 5% (v/v) glycerol, 10mM DTT, 1% (v/v) protease inhibitor cocktail (Sigma-Aldrich, P9599), 0.5% (v/v) Triton-X-100, 1% (v/v) Igepal, 50µm MG132 (Sigma-Aldrich, C2211)) and the tubes were vortexed for 30 seconds before being centrifuged for 20 minutes at 12 000x g and 4°C. The supernatant was harvested and subjected to western blot analysis as described in section 2.5.1.

2.7 – Yeast-2-Hybrid screen

2.7.1 – Yeast strain and media

The yeast strain used was PJ69-4α (James et al., 1996), bait genes were inserted into the pDBleu vector and the prey library (kindly provided by Phil Wigge) was present in the pEXP-AD502 vector (see section 2.2.7), both of which are both part of the ProQuest™ Two-Hybrid System from Invitrogen. The screen was a co-transformation screen.

YPD	1% (w/v)	Peptone
	1% (w/v)	Yeast Extract
	0.5% (w/v)	NaCl
	2% (w/v)	Sucrose
	(2% (w/v)	Agar)
SC	0.67% (w/v)	Yeast Nitrogen Base without amino acids (Becton, Dickinson & Co 291940)
	2% (w/v)	Sucrose
	Appropriate %	Amino acid DO supplement (Clontech 8619-1, 8609-1,8605-1, 8610-1, 8680-1, 8604)
	(2% (w/v)	Agar)

Table 2.13 – Yeast Media

2.7.2 –Preliminary transformation

A lithium acetate transformation protocol was used to generated the bait expressing strain (pDBLeu-DA1), to test for auto-activation of strains expressing non-interacting bait and prey proteins (pDBleu-DA1, pEXP-AD502-Ø) on $SC^{-Leu-Trp-His}$, and to perform the drop-tests used to validate the interactions. No autoactivation of the *HIS3* reporter was detected.

2.7.2.1 – Transformation protocol

DAY1

A 50ml liquid culture was inoculated with a single colony of yeast and grown overnight at 28°C at 220rpm.

DAY2

The overnight culture was diluted to OD_{600}=0.4 with fresh media and grown at 30°C (220rpm) until OD_{600}=0.3-1.0, then cells were harvested by centrifuging for 5 minutes at 4000x g.

Cells were washed with 50ml sterile water, centrifuged for 5 minutes at 4000x g and the remaining pellet was re-suspended in solution A at a rate of 100µl per transformation.

5µl carrier DNA was mixed with 5µg transforming DNA (keeping total volume ≤ 20µl) and added to the 100µl yeast solution along with 700µl of Solution B.

Samples were shaken for 30 minutes at 28°C and then heat shocked for 15 minutes at 42°C in a waterbath. Cells were then centrifuged for five seconds, re-suspended in 200µl TE (10mM TRIS-Cl pH7.5, 1mM EDTA) and spread onto appropriate plates (stored at 28°C).

Solution A	100mM	LiAc pH7.5
	10mM	TRIS-HCl pH7.5
	1mM	EDTA
Solution B	40% (w/v)	PEG-4000
	10mM	TRIS-HCl pH7.5
	1mM	EDTA
	100mM	LiAc pH7.5
Carrier DNA	$10mg.ml^{-1}$	Salmon Sperm DNA (Fluka 31149)

Table 2.14 – Materials for preliminary yeast transformation

2.7.3 – Library screen

Solution C	100mM	LiAc pH7.5
	10mM	TRIS-HCl pH7.5
	1mM	EDTA
	1M	Sorbitol
Solution D	33% (w/v)	PEG-4000
	100mM	LiAc pH7.5
	27.6µg	Salmon Sperm DNA (Sigma-Aldrich AM9680)

Table 2.15 – Materials for library transformation

DAY1

Four 3ml liquid cultures of SC^{-Leu} were inoculated with yeast expressing pDBleu-DA1. Cultures were grown overnight at 28°C (at 220rpm).

DAY2

All overnight cultures were combined and diluted with SC^{-Leu} to form 100ml culture of OD_{600}=0.1. This culture was grown for seven hours (28°C and 220rpm), before diluting to form a 200ml culture of OD_{600}=0.1. This culture was grown overnight at 28°C and 220rpm.

DAY3

When the OD_{600} reached1.3, the overnight culture was diluted to form a 200ml culture of OD_{600}=0.4 and then grown at 28°C and 220rpm until the OD_{600} reached 0.85. The 200ml culture was split into four 50ml falcon tubes, which were centrifuged at 1800x g for five minutes. The pellets were washed twice with 5ml solution C and then the contents of the four tubes were combined in 1ml Solution C and kept on ice for 10 minutes.

Cells were then centrifuged at 1800x g for five minutes, the pellet was resuspended in 720µl Solution C and then split into two tubes containing 360µl each. 10µg of library DNA was added to each tube and mixed by vortexing, followed by heating at 28°C for 30 minutes and then heatshocking for 40 minutes at 42°C.

Cells were centrifuged at 1800x g for five minutes and the pellet re-suspended in 1000µl water. 100µl aliquots were spread on 140mm $SC^{-Leu-Trp-His}$ plates and left out of sunlight at room temperature. Additionally, the re-suspended pellet was diluted one in four and one in ten, and

spread on SC-$^{Leu-Trp}$ plates in order to calculate transformational efficiency. Transformational efficiency was 263,200 transformational events per screen. Two screens were carried out, resulting in 526 400 transformational events in total.

2.7.3.1 – Selecting colonies

Colonies that grew on SC$^{-Leu-Trp-His}$ plates were used to inoculate 3ml SC$^{-Leu-Trp-His}$ liquid cultures, which were then subjected to miniprep (section 2.2.3.3), PCR (section 2.2.2.3) and sequencing (section 2.2.2.4) analyses. Sequenced colonies were screened for those with genes in-frame with the GAL4 activation domain present in pEXP-AD502. Only these colonies were reported in Chapter 4.

2.7.3.2 - Drop testing

Candidate genes selected for further study were subject to drop testing. The respective pEXP-AD502 prey constructs (isolated from colonies) were transformed into TOP10 One Shot competent cells (Invitrogen C404003) and subjected to a further round of sequencing analysis (section 2.2.2.4). Complete coding sequences, generated from cDNA (section 2.2.2.1) were cloned into empty pEXP-AD502 vector (section 2.2) and re-transformed into yeast using the protocol described in section 2.7.2.1. Transformed yeast were diluted and grown on SC$^{-Leu-Trp}$, SC$^{-Leu-Trp-His}$, and SC$^{-Leu-Trp-His-Ade}$ plates and incubated at both room temperature and 28°C (data presented in Chapter 4 is from growth at 28°C). Drop tests were repeated a total of four times.

2.8 – MAGIC analysis

The lines used in this study are described in section 2.3.1 and the growth conditions used are described in section 2.3.2. Organs were phenotyped following the protocols documented in section 2.3.5.

The MAGIC analysis was kindly performed in collaboration with Mathew Box at the Sainsbury Laboratory Cambridge University, Cambridge. QTLs were identified using HAPPY: 'a software package for multipoint QTL mapping in genetically heterogeneous animals' (Mott, 2000, Mott et al., 2000). The genotype information used in the HAPPY analysis was from 1250 SNPs, spaced roughly 100Kb apart (Kover et al., 2009, Mott et al., 2011). Genotype interrogation of parental lines used publicly available sequence data (Gan et al., 2011) and the Rätsch lab GBrowse platform (http://gbrowse.cbio.mskcc.org/gb/gbrowse/thaliana-19magic/).

2.9 – GWAS analysis

The accessions used in this study are listed in Table S2 and the growth conditions used are described in section 2.3.2. Organs were phenotyped following the protocols documented in section 2.3.5.

The genome wide association (GWA) analysis was performed in collaboration with Mathew Box at the Sainsbury Laboratory Cambridge University, and Justin Borevitz and Riyan Cheng at the Australian National University, Canberra, Australia. The analysis was carried out using the QTLRel package (Cheng et al., 2011) and call_method_75_ TAIR9 SNP data (Horton et al., 2012). Alleles with a frequency of less than 0.05 were excluded from the analysis.

Chapter 3 - A Structural Analysis of the DA1 Protein

3.1 Introduction

The aim of the research conducted in this Chapter was to achieve a greater understanding of DA1 function, beyond the preliminary observations of growth and developmental effects seen in genetic studies (Li et al., 2008). The initial research demonstrated clearly that *DA1* is a key regulator of organ growth (Li et al., 2008), however it did not identify the mechanism through which DA1 controls this growth. The work described in this Chapter uses the conserved protein domains found in DA1 to uncover the biochemical functions of DA1, and thereby to gain a deeper understanding of the mechanisms controlling growth in Arabidopsis. Moreover, due to the extensive similarity in protein structure shared between DA1 and other DA1 family members, progress made in this Chapter is likely to be relevant to the study of other family members (Fig. 3.1). This work may therefore be of significant interest to research areas including cold tolerance, pathogen response and the regulation of root meristem size (Yang et al., 2010, Bi et al., 2011, Peng et al., 2013).

As illustrated in Fig. 3.1 DA1 is predicted to contain 4 identifiable protein domains: two UIM domains, one LIM domain and a C-terminal metallopeptidase domain embedded in the highly conserved C terminal region.

3.1.1 - The Ubiquitin-Interacting Motif (UIM)

The UIM is a specific type of ubiquitin binding domain (UBD) made up of a short motif containing the highly conserved sequence: Φ-x-x-Ala-x-x-x-Ser-x-x-Ac at its core (where Φ is a large hydrophobic residue, and 'Ac' acidic residue) (Hofmann and Falquet, 2001). The UIM moiety is thought to form an short alpha-helix, which is able to insert into protein folds and bind ubiquitin (Hofmann and Falquet, 2001). Interestingly the ubiquitin binding capacity of UIMs is not limited to one molecule per domain, with recent work illustrating that UIMs are able to bind two ubiquitin molecules; one on either face of the helix (Harper and Schulman, 2006). Although a diverse variety of proteins contain UIMs, it is particularly pertinent to this work that UIMs have been shown to be present in many proteins involved in the proteasomal and lysosomal degradation pathway (Hofmann and Falquet, 2001).

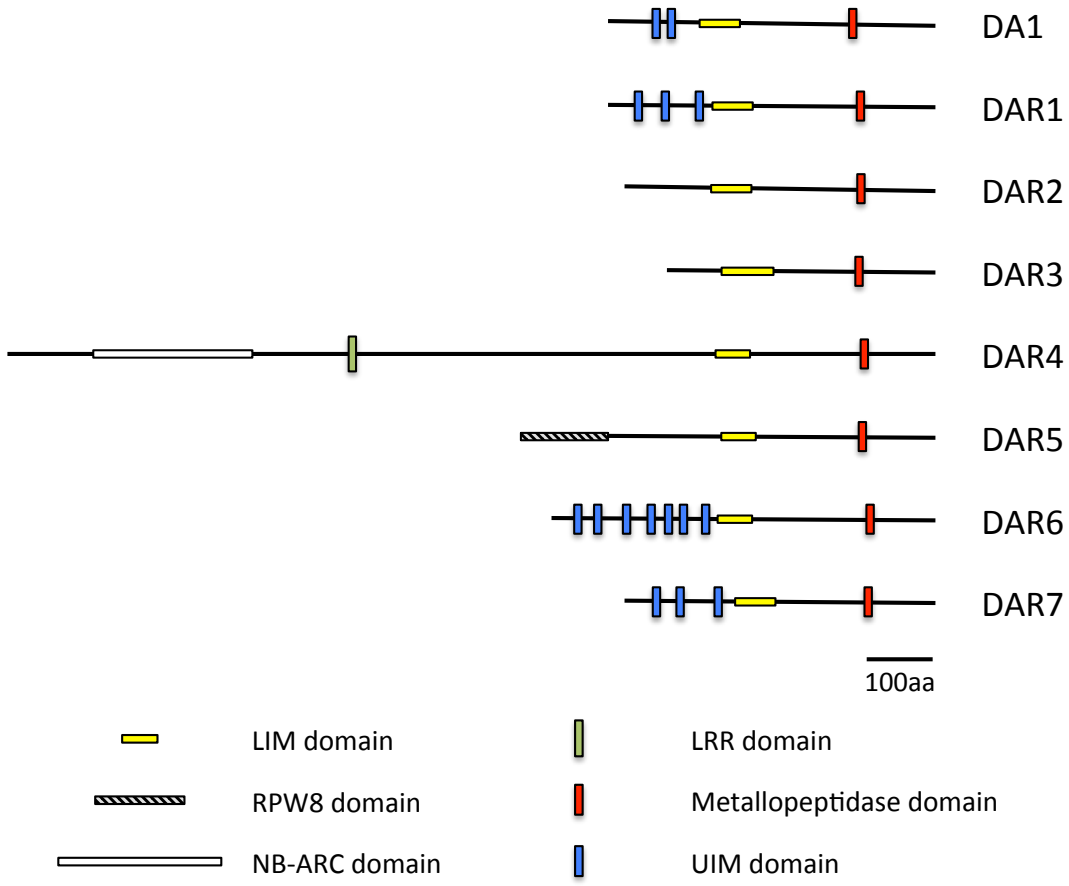

Figure 3.1 – The DA1 protein family

All DA1 family members possess a C-terminal zinc metallopeptidase domain and central or C-terminal LIM domain. Four members contain UIM domains and two specialised members contain unique domains; DAR4 a NB-ARC and LRR domain, and DAR5 an RPW8 domain - all three of which are characterised pathogen response domains (Bi et al., 2001, Xiao et al., 2001).

A further feature of UIM containing proteins (but not exclusive to UIMs) is their ability to promote cis-mono-ubiquitination at a location distinct from that of the UIM (Oldham et al., 2002). This process is termed coupled mono-ubiquitination and has been observed for the mammalian UBD-containing proteins, STS1, STS2, EPS15 and HRS (Hoeller et al., 2006). This process involves the mono-ubiquitination of UBD containing proteins, which results in a UBD-cis-ubiquitin interaction, and generates a change in protein confirmation (Woelk et al., 2006, Haglund and Stenmark, 2006, Hoeller et al., 2006). UIMs have been shown to be *sufficient* for

coupled mono-ubiquitination, with GST-UIM chimeric proteins capable of causing mono-ubiquitination of the GST (Oldham et al., 2002). The exact mechanism is unclear, although it has been shown for the human protein EPS15 that a UIM interaction with an E3 ligase-conjugated ubiquitin is necessary to recruit the E3 ligase to EPS15 (Woelk et al., 2006). As for the role of coupled mono-ubiquitination, it is possible that the UIMs preferentially interact with ubiquitin in *cis*, and therefore their mono-ubiquitination serves to modify the confirmation of the protein they are in and alter its biochemical activity.

In addition to these *cis*-mediated mechanisms, UIMs have been showed to play a role in the *trans*-regulation of target proteins, such as the ubiquitin dependent recognition and internalisation of plasma membrane signal receptors (Hofmann and Falquet, 2001). In this system it is postulated that UIM proteins act as adaptors and cargo receptors, and direct the specific movement of ubiquitinated proteins through the endosomal pathway to specific destinations. It is thought that the covalently attached ubiquitin on the target protein acts as a bait that draws the UIM-containing adaptor protein into specific intimate contact.

Of particular interest to this work is the abundance of UIM domains in de-ubiquitinating enzymes (DUBs). These enzymes specifically remove ubiquitin from proteins and reverse the biological consequences of ubiquitination. The ubiquitin specific protease (USP), Josephin, and ovarian tumour protease (OTU) families (Komander et al., 2009), show similarities in protein structure to DA1 as they all contain UIM and peptidase domains. For many UIM- containing DUBs the UIMs are necessary for de-ubiquitinating activity (Mao et al., 2005, Meulmeester et al., 2008), and in some cases UIMs determine the specificity of the DUB. For example, the UIM present in mammalian DUB, ATXN3 confers specificity towards K63 linked poly-ubiquitin chains (Winborn et al., 2008). In addition, there is evidence that different UIM domains have different affinities for different ubiquitin chain lengths (Woelk et al., 2006).

3.1.2 - The LIM domain

The LIM (Lin11, Isi1 and Mec-3) domain (Prosite: PS00478) is a highly conserved tandem zinc finger domain that acts as a platform for highly specific protein-protein interactions in many organisms (Schmeichel and Beckerle, 1994, Kadrmas and Beckerle, 2004, Agulnick et al., 1996). Characterised by the sequence C-x_2-C-x_{16-23}-H-x_2-C-x_2-C-x_2-C-x_{16-21}-C-x_2-(C/H/D), two quartets of cysteine and histidine residues co-ordinate the zinc ions at the core of the two zinc fingers (Kadrmas and Beckerle, 2004) (Fig. 3.2).

LIM proteins are involved in a wide variety of cellular roles, from actin binding to transcriptional regulation (Maul et al., 2003, Shirasaki and Pfaff, 2002, Moes et al., 2012). This

diversity in function makes it difficult to infer any specific functions of DA1 from the presence of a LIM domain alone. For example the LIM domains present in LIM-Homeodomain (LIM-HD) protein are involved in mediating the *trans*-interaction with its binding partner LBD1 (Agulnick et al., 1996), whereas the LIM domain in LIM kinase-1 is thought to *cis*-regulate kinase activity by auto-inhibition of the kinase domain (Nagata et al., 1999). Because it is difficult to infer the biological function of members of the DA1 family from the presence of a LIM domain alone, a detailed functional investigation is required.

Although the core LIM motif – the zinc coordinating sequence – is highly conserved amongst protein species, the flanking protein sequence is thought to be that which determines the specificity of the LIM interaction, and mutations in these regions are sufficient to abolish LIM function. For example, mutations in residues in, and immediately adjacent to, the zinc-coordinating region of the LMX1B LIM domain in Humans, are sufficient to generate the loss-of-function phenotype responsible for Nail-Patella Syndrome (NPS) (Clough et al., 1999, Hamlington et al., 2001, McIntosh et al., 1998).

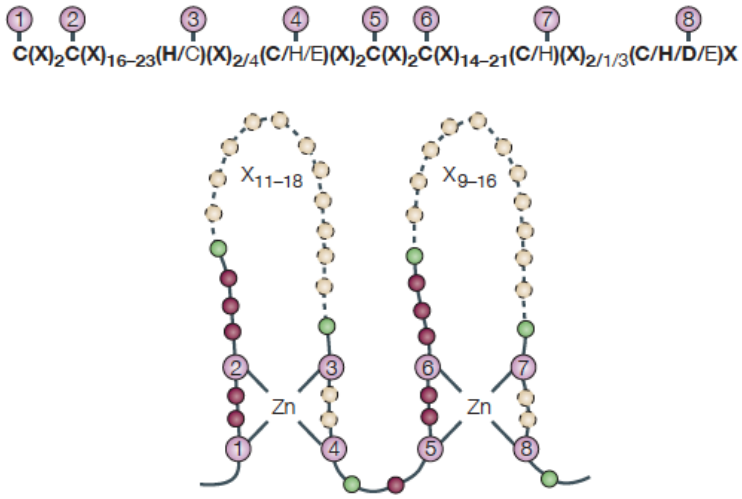

Figure 3.2 – The LIM domain

Eight highly conserved histidine and cysteine residues (purple circles) coordinate two zinc ions that form the core of the zinc fingers. Variation in the length and composition of the finger domains and the peripheral protein sequence determines the specificity of the LIM domain. (Figure from Kadrmas and Beckerle, (2004))

3.1.3. – The C-terminal peptidase

The C-terminal region of DA1 is the most distinctive yet most enigmatic domain in the protein. The published *da1-1* mutation, with a single amino acid transition in the highly conserved C-terminal region, is sufficient to generate a dominant negative-interfering growth phenotype (Li et al., 2008). This indicates that conserved regions of the C-terminal domain are probably essential for DA1 function.

The dominant negative nature of *da1-1*, and the functional redundancy between DA1 and DAR1 (Li et al., 2008) suggest that the *da1-1* phenotype may be a consequence of the non-functional da1-1 protein forming a complex with a binding partner – for example DA1 or DAR1 – and forming a non-functional complex (Fig. 3.4a,b). This explanation would be similar to the proposed mechanism for the dominant negative effects of the *ERECTA ΔKinase* mutant, where the formation of a non-functional receptor heterodimer is thought to cause the observed developmental phenotypes (Shpak et al., 2003). Therefore, one prediction to be tested is that DA1 homo- and hetero-oligomerises with DA1 and DAR1.

An alternative explanation for the observed dominant negative phenotype of the *da1-1* mutant is that the non-functional da1-1 protein binds to its target protein and competes with both DA1 and DAR1 for their common target protein (Fig. 3.4c,d). This form of substrate competition is similar to that observed for the mammalian peptidase SPP (Schrul et al., 2010).

The C-terminal domain (Pfam:PF12315) is highly conserved amongst DA1 family members and defines the DA1 family (Fig. 3.1). It has strong homology over a short region with members of the higher-order peptidase MA clan (Pfam:CL0126), containing proteins from a wide diversity organisms including archaea, bacteria, metazoans, fungi and plants (Pfam). Members of this clan are defined by a neutral zinc metallopeptidase domain (PROSITE:PS00142), characterised by an H-E-x-x-H motif (henceforth termed HExxH), where the two histidine residues coordinate a zinc atom to form the active site of the peptidase (Matthews et al., 1972, Devault et al., 1988, Jongeneel et al., 1989). The peptidase MA clan contains diverse proteins with a wide variety of functions. For example, members of the WLM family (PF08325) have been shown to have de-ubiquitination and de-sumoylation activities (Iyer et al., 2004, Su and Hochstrasser, 2010, Mullen et al., 2010). Other clan members include virus expressed enhancin peptidases, whose function is to facilitate infections (Wang and Granados, 1997, Lepore et al., 1996); reprolysin-family snake venom endopeptidases (Fox and Serrano, 2005); and astacin, a crustacean digestive enzyme (Bond and Beynon, 1995).

The presence of two UIM domains and a zinc metallopeptidase active site suggests that DA1 and related family members may have a peptidase function *and* be involved in an as yet unknown aspect of the ubiquitin system. Therefore the functional characterisation of the activities of these domains, together with the LIM domain, will provide new information to help understand the functions of members of the DA1 family.

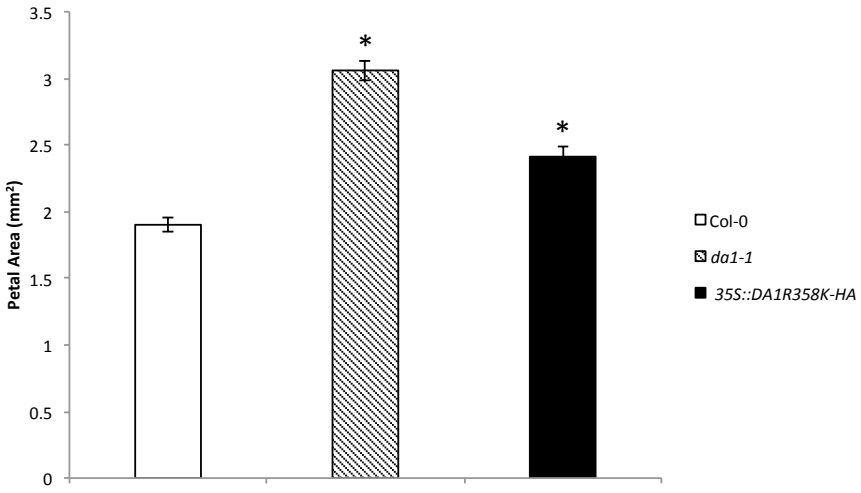

Figure 3.3 – The DA1R358K mutation is negatively interfering towards DA1 and DAR1

Over-expression of DA1R358K-HA in Col-0 partially phenocopies the da1-1 large organ phenotype. (*) Petals of both *da1-1* and 35S:DA1R358K-HA plants are significantly larger than Col-0 (Student's T-test, $p<0.05$; n=25). Similar results were observed by Li et al (2008). The 35S::DA1R358K-HA construct was kindly provided by Yunhai Li and the relative expression level of DA1R358K in these lines is eight times wild-type levels (Li et al., 2008).

3.2 – DA1 interacts with DA1 and DAR1 *in vitro*, in a LIM-independent manner

3.2.1 – Overexpressing DA1^{R358K}-HA partially phenocopies *da1-1*

The observed genetic redundancy between *DA1* and *DAR1*, and the dominant negative nature of the *da1-1* mutation (Li et al., 2008), suggests that the da1-1 protein may interfere with the function of wild-type DAR1, leading to its large organ phenotype (Li et al., 2008)(Fig. 3.4). To explore whether the da1-1 protein also had a negative interfering activity towards wild-type DA1, DA1^{R358K} (incorporating the da1-1 R^{358}K transition) was overexpressed in Col-0 plants, in which there are wild-type levels of DA1. To achieve this, DA1^{R358K}-HA was cloned into the pMDC32 vector (Curtis and Grossniklaus, 2003), where it was under the control of 35S promoter, and transformed into Col-0. Data presented in Fig. 3.3, shows that expression of

p35S::*DA1*^{R358K}*-HA* in a Col-0 background generates a large organ phenotype that partially phenocopies the *da1-1* mutation. This large petal phenotype, although not as severe as the *da1-1* phenotype, was present in a wild-type DA1 and DAR1 background suggesting that the DA1^{R358K} protein has a negative interfering effect towards *both* DA1 and DAR1. The increased level of expression of *DA1*^{R358K}*-HA* in this line relative to wild-type DA1 (eightfold; Li et al (2008)) suggests that *da1-1* might not have a true dosage dependent effect. However, the high level of instability of DA1 protein expression in Arabidopsis tissues that leads to it being undetectable in stable transgenics (Yunhai Li, personal communication), may mean that higher gene expression does not correspond to higher protein levels.

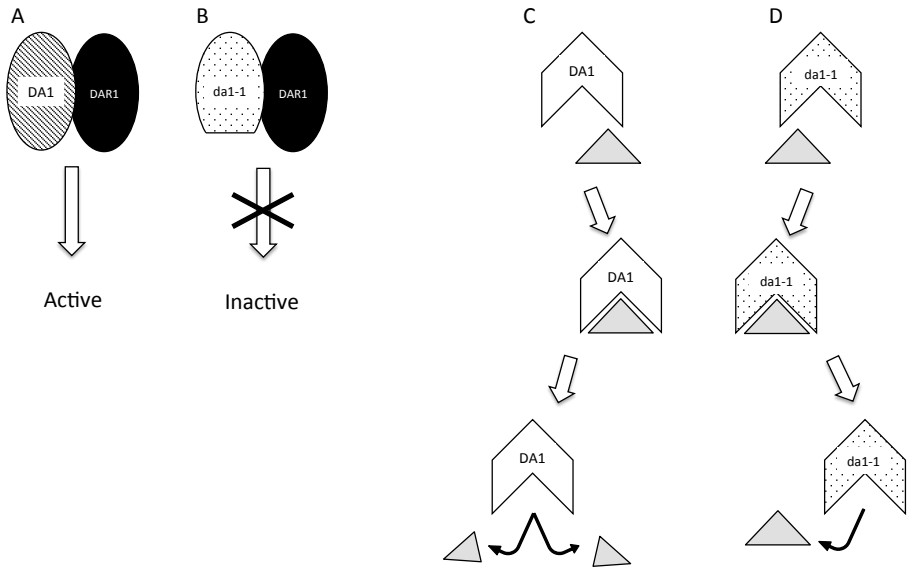

Figure 3.4 – Models for explaining the *da1-1* dominant negative phenotype

(A,B) The non-functional complex model: in wild-type cells, a DA1-DAR1 oligomer functions as an active complex (A), however, the da1-1-DAR1 complex is inactive (B), which results in a reduction in overall DA1 (and DAR1) activity. (C,D) The substrate competition model: DA1 binds to and processes a substrate molecule (large grey triangle) into its product (small grey triangles) (C). However, da1-1 is only able to bind the substrate molecule and not able to process it (D). The inactive da1-1 protein competes with wild-type DA1 (and DAR1) for substrate binding, and therefore reduces DA1 activity.

There are at least two possible explanations of the observed dominant negative phenotype of *da1-1* plants (Fig. 3.4). One is that DA1 and DAR1 interact physically as well as genetically, and therefore the possibility of physical interactions between DA1 and both DA1 and DAR1 was explored.

Box 3.1 – Methods of assaying for protein-protein interactions

***In vitro* co-Immunoprecipitation (co-IP)**
This tests for direct physical interactions between proteins in the absence of species-specific proteins. The artificial nature of this system ensures that co-purifications are due to direct interaction between bait and prey and not intermediate adaptor proteins or higher order protein complexes.

***In planta* co-Immunoprecipitation (co-IP)**
The endogenous conditions in this system give added confidence to the validity of any observed *in vitro* interaction. However this endogenous background allows for the formation of naturally occurring higher-order protein complexes and therefore does not allow one to infer direct bait-prey physical interactions.

***In planta* bimolecular fluorescence complementation (BiFC)**
Unlike *in planta* co-IP experiments, due to the requirements for protein-protein proximity for positive BiFC results, this system gives more confidence that an observed interaction is a direct bait-prey interaction. It is however, still possible for positive results to be due to candidate proteins being in extremely close proximity through higher-order protein complexes and not through a direct physical interaction.

3.2.2 – FLAG-DA1 physically interacts with GST-DAR1 and GST-DA1 *in vitro*

There are several methods that can be used to investigate putative protein interactions; the strengths and weaknesses of these methods are discussed in Box 3.1. In this experiment the primary goal was to establish whether or not DA1 and DAR1 were able to directly interact. Based on the observation that DA1 was undetectable in stable transgenic Arabidopsis lines (Yunhai Li, personal communication), an *in vitro* approach was chosen.

In this *in vitro* system, recombinant GST-tagged bait proteins were incubated with recombinant FLAG-tagged prey proteins before precipitation of GST-tagged bait proteins on glutathione sepharose beads. The purified proteins were then eluted and subjected to SDS-PAGE and immunoblot analysis. The ability of β-glucuronidase (GUS) to form a homo-tetramer was utilised to design a positive control of GST-GUS vs FLAG-GUS. Two sets of negative controls were also used; these were GST-GUS vs FLAG-prey, and GST-bait vs FLAG-GUS.

From Fig. 3.5 it can be seen clearly that GST-DA1 directly interacts with both FLAG-DA1 and FLAG-DAR1. These data show that DA1 is able to both homo- and hetero-oligomerise, indicating that the 'non-functional complex' hypothesis for explaining the DA1 dominant negative phenotype (Fig. 3.4a,b) is feasible. However, it is not clear from this data whether the complexes formed are dimeric or oligomeric, so henceforth products of the DA1-DA1 and DA1-DAR1 interactions will be referred to as *oligomers*.

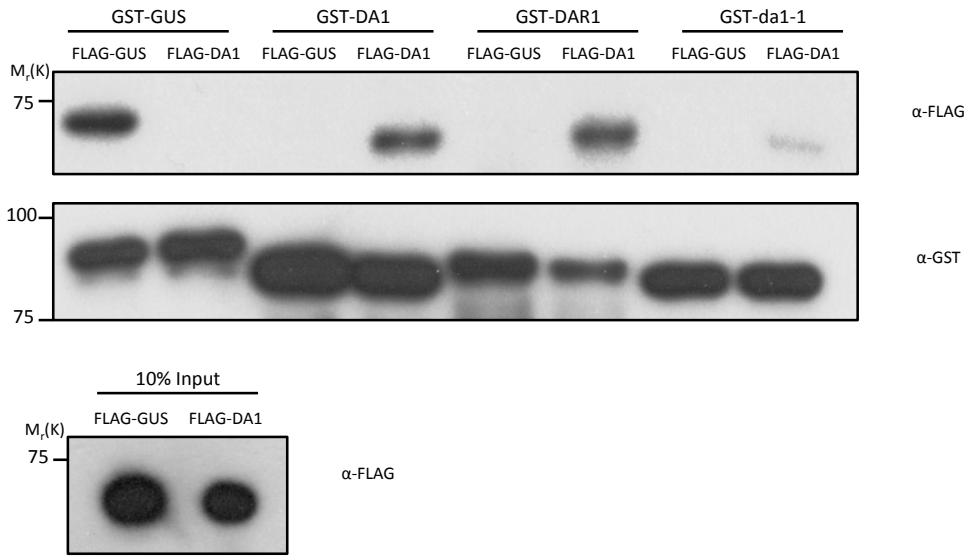

Figure 3.5 – FLAG-DA1 interacts with GST- DA1, GST-DAR1 and GST-da1-1 *in vitro*

E. coli expressed GST-tagged bait proteins were incubated with *E. coli* expressed FLAG-tagged prey proteins before purification on glutathione sepharose beads and immunoblotting for GST and FLAG. FLAG-DA1 co-purified with GST-DA1 (lane 4), GST-DAR1 (lane 6) and GST-da1-1 (lane 8) but not with the negative control GST-GUS (lane 2). The GST-da1-1 – FLAG-DA1 interaction (lane 8) was significantly weaker than all other positive interactions, but stronger than the negative control (lane 2).

3.2.3 – The LIM domain is not necessary for the DA1-DA1 interaction

Due to its widely documented role in protein-protein interactions (reviewed in Kadrmas & Beckerle (2004)), the LIM domain was a promising candidate region for mediating DA1 oligomerisation. To investigate this hypothesis, DA1 proteins with mutated LIM domains were assayed *in vitro* for their ability to homo-oligomerise with wild-type DA1.

This work used the DA1lim8 mutant (originally designed by Yunhai Li), which incorporates four Cys-Gly transitions into four of the eight zinc-coordinating positions of the LIM domain (C172, C175, C199 and C202). This mutation was predicted to abrogate LIM function based on evidence that individual amino acid changes at these positions are sufficient to interfere with and abolish LIM function (Taira et al., 1994, Agulnick et al., 1996). Taira et al (1994) showed that, by making a single Cys-Gly transition at the fourth zinc-coordinating position of both LIM domains in the XLIM-1 protein, the negative regulatory capacity of the LIM domains were abolished. They also showed that this effect is equivalent to deleting both entire LIM domains. This observation is supported by Agulnick et al (1996), who showed that a Cys-Gly transition in the equivalent position of both LIM domains in the LHX1 protein, almost completely abolishes its ability to interact with its binding partner LBD1.

The experimental format for this work was similar to that used to investigate DA1-DAR1 oligomerisation in section 3.2.2. However, when designing this experiment it was important to consider the hypothesised role the LIM might play in the interaction; whether the LIM domain interacted with the LIM domain of its partner, or a different protein region. To ensure that the assay was robust to the possibility of the LIM domain binding a non-LIM region of its partner, lim8 mutations were included in both bait and prey constructs.

The data presented in Fig. 3.6 show that mutating the LIM domain in either one or both of the interacting partners did not abolish their interaction. This suggests that the LIM domain is not involved in mediating the DA1-DA1 oligomerisation event. This also indicates that the LIM domain may have other roles; perhaps mediating interactions with other proteins or mediating intramolecular interactions.

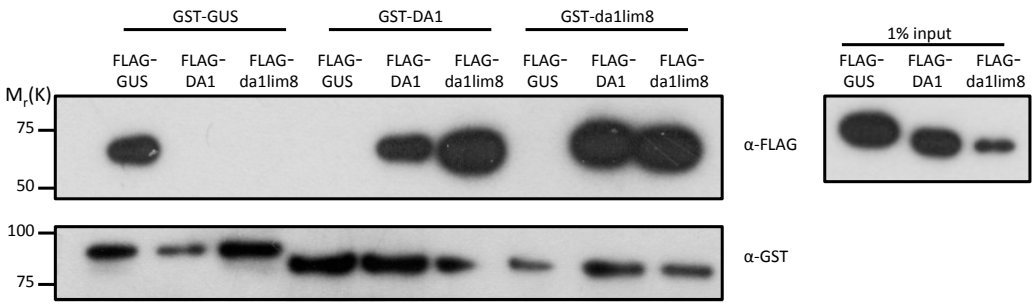

Figure 3.6 – The DA1 LIM domain is not necessary for DA1 homo-oligomerisation

E. coli expressed GST-tagged bait proteins were incubated with *E. coli* expressed FLAG-tagged prey proteins before purification on glutathione sepharose beads and immunoblotting for GST and FLAG. FLAG-DA1 and FLAG-da1lim8 co-purified with GST-DA1 and GST-da1lim8 (lanes 5,6,8,9) but not with the negative control GST-GUS (lanes 2,3); revealing that mutating the LIM domain in DA1 is not sufficient to abolish the physical interaction between DA1 proteins.

3.2.4 – DA1 interacts with da1-1 *in vitro*

To investigate whether the $R^{358}K$ mutation affects the ability of DA1 to form a putative homo-oligomer, an interaction between DA1 and da1-1 was tested. Using the *in vitro* co-immunoprecipitation analysis described in section 3.2.2, GST-DA1 bait protein was incubated with FLAG-da1-1 prey protein before immunoprecipitation and western blot analysis.

These data demonstrate that GST-DA1 physically interacts with FLAG-da1-1 (Fig. 3.5). The band in lane eight demonstrates that, compared to the negative controls (lanes two and seven) there is a clear GST-DA1 – FLAG-da1-1 interaction *in vitro*. However, it is notable that the DA1-da1-1 band (lane eight) in this blot is considerably weaker than that of the DA1-DA1 positive control. The relative weakness of the DA1-da1-1 interaction was surprising considering the genetics and biochemistry studies suggested that the 'non-functional complex' model (Fig. 3.4) might explain the *da1-1* phenotype. Nevertheless, it is still conceivable that the reduced affinity of da1-1 for DA1 (and DAR1) shown in Fig. 3.5 is sufficient to enable the incorporation of the da1-1 protein in the majority of DA1 oligomers in *da1-1* mutant tissues.

This data is nonetheless consistent with the genetic data presented in Fig. 3.3, which shows that overexpression of the $DA1^{R358K}$ protein in a Col-0 background only *partially* rescued the da1-1 phenotype. If the $DA1^{R358K}$ mutant protein had a weaker binding affinity than its wild-

type counterpart, then added wild-type DA1 in the Col-0 background might reduce the relative abundance of the DA1^{R358K} protein in the predicted DA1-DAR1 oligomers.

A

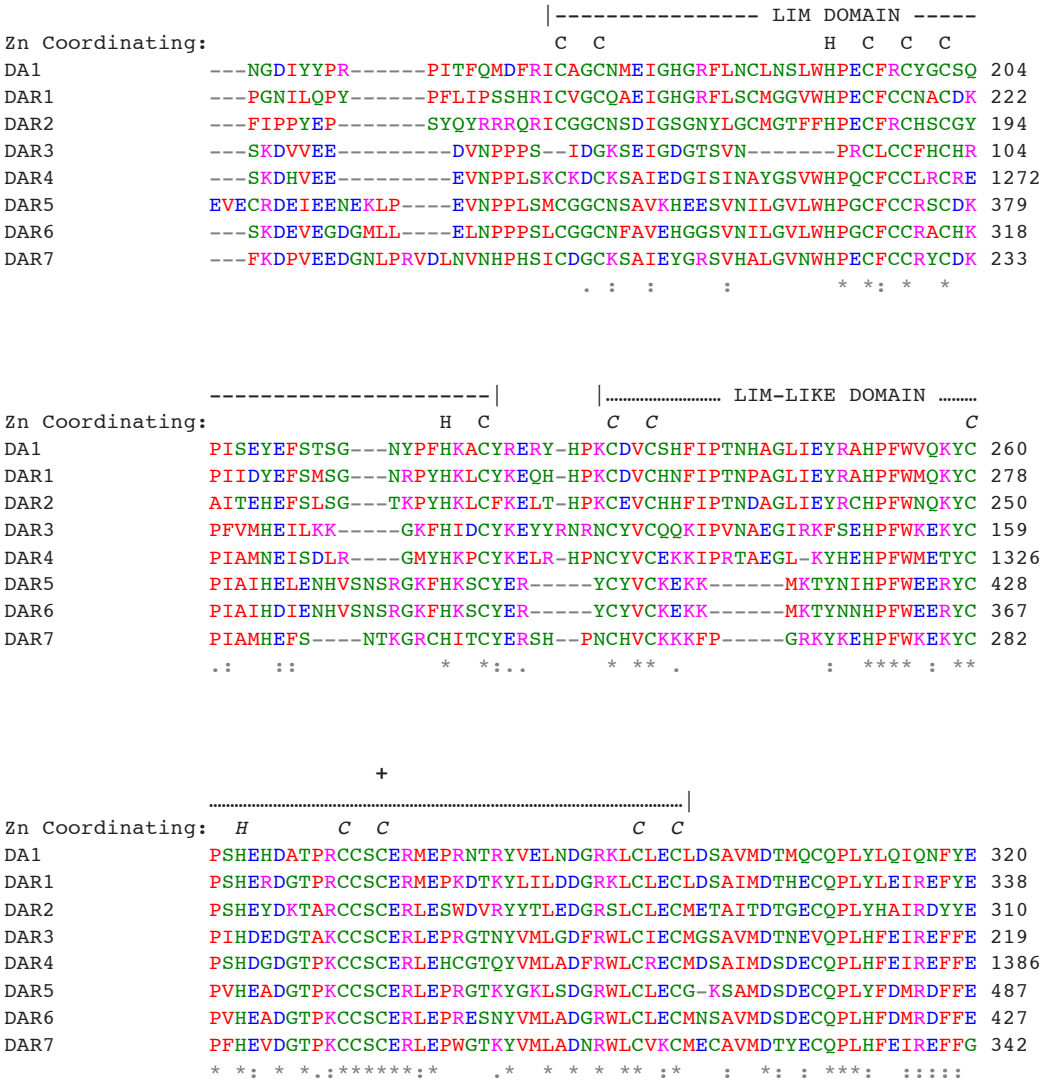

B

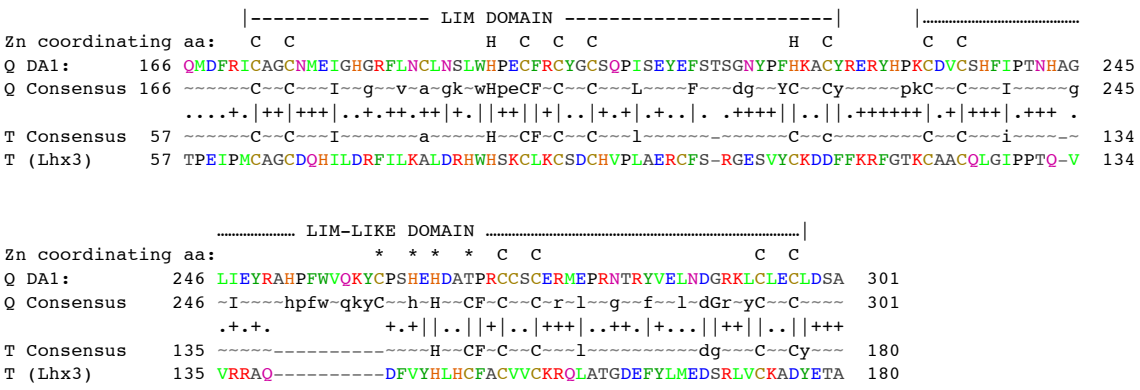

Figure 3.7 – DA1 contains a cryptic LIM-like domain

(A) ClustalW alignment of the DA1 family members' LIM and LIM-like domains. LIM domain zinc-coordinating residues and LIM-like domain putative zinc-coordinating residues are indicated by 'H/C'; '+' denotes the cysteine residue mutated to tyrosine in the chs3-2D protein (Bi et al., 2011, Larkin MA et al., 2007, Goujon et al., 2010, Larkin et al., 2007). For explanation of colour codes used see supplementary information (Table S3). (B) HMM-HMM alignment of DA1 and mouse LHX3 based on structural predictions and protein homology, generated by HHpred (Biegert A et al., 2006, Remmert et al., 2011, Söding, 2005, Söding et al., 2005). Conserved zinc-coordinating residues are indicated by 'H/C' and uncertain residues are marked with a '*'. The alignment reveals similarity between DA1 and both LIM domains of LHX3.

3.2.5 – DA1 family proteins contain a LIM-like domain

Because *in vitro* experiments demonstrated that the LIM domain was not necessary for a DA1-DA1 interaction (section 3.2.3), more effort was placed on *in silico* analysis of the DA1 structure in order to identify other domains with a potential role in protein-protein interactions.

Typical web-based domain prediction software (R.D. Finn et al., 2012, Schultz J et al., 1998, De Castro E et al., 2006), search target protein sequences for known domains with a relatively high stringency. For this reason, such programmes may fail to identify novel, divergent domains that differ from the canonical motif by a small number of conserved residues. In the case of DA1, these tools predict the presence of four domains shown in Fig. 3.1; in particular they predict only one LIM domain (170aa-230aa) (Fig. 3.7a). To relax the stringency of these software searches, a simple two-step analysis was carried out. First, an initial homology detection screen (Biegert A et al., 2006) was carried out to identify proteins with similar domains and structures. This was then followed by a domain prediction screen (R.D. Finn et al.,

2012, Schultz J et al., 1998, De Castro E et al., 2006), which used these proteins as query sequences. This strategy revealed that a large region of DA1 (167aa-303aa) had significant structural similarities with a number of other proteins. In particular, the region 230aa-297aa shared significant structural homology with the LIM domains of other proteins (including the mouse LIM/homeobox protein LHX3 (Zhadanov et al., 1995)), as illustrated in Fig. 3.7b. This new putative domain was termed the *LIM-like domain*.

The purported second pair of zinc coordinating amino acids in the LIM-like domain of DA1 was not detected by classical domain prediction software (R.D. Finn et al., 2012, Schultz J et al., 1998, De Castro E et al., 2006) because of significant sequence divergence from the canonical LIM pattern. By considering a CxxH pairing at position 261aa-264aa, it was apparent that an insertion in the first zinc finger domain and the inter-finger region causes the sequence to deviate significantly from the LIM consensus pattern. This results in a finger length of 24aa and an inter-finger region of 7aa (rather that 16-23aa and 2aa respectively). Currently it is not known if these changes result in a functional domain or whether they abolish LIM function. Observations from a recent publication on another member of the DA1 family, CHS3/DAR4, suggest that this *LIM-like* domain is both functional and essential for DAR4 function (Bi et al., 2011). They showed that a single Cys-Tyr transition at position 1340aa in the *chs3-2D* allele has a dominant gain-of-function phenotype, with plants showing severe stunting, curled leaves, constitutive expression of *PATHOGENESIS-RELATED* (*PR*) genes and accumulation of salicylic acid. Fig. 3.7a shows that this cysteine residue is predicted to form the second zinc-coordinating residue of the second zinc-finger in the LIM-like domain. The fact that this mutation causes such a significant phenotype suggests that this LIM-like domain is indeed functional. It is therefore possible that the LIM-like domain in DA1 plays an important role in DA1 function, and that mutations in this domain in DA1 may also generate a dominant negative phenotype. This opens up additional approaches to the structure-functional analysis of DA1.

3.3 – Only one DA1 UIM domain binds mono-ubiquitin

Four members of the DA1 family contain predicted UIM domains (Fig3.1), but it is unclear whether these are functional UIM domains or relics. For example in DAR1 (Fig. 3.8) inspection of UIM2 shows that it lacks the highly conserved serine residue in the C-terminal section of the domain. This divergence in sequence presents the possibility that the UIM is non-functional. In order to determine whether the UIMs are indeed functional and to determine their role in

organ size control, a semi-quantitative *in vitro* ubiquitin-binding assay was conducted to test the functionality of the UIM domains. This assay focussed exclusively on the DA1 UIMs.

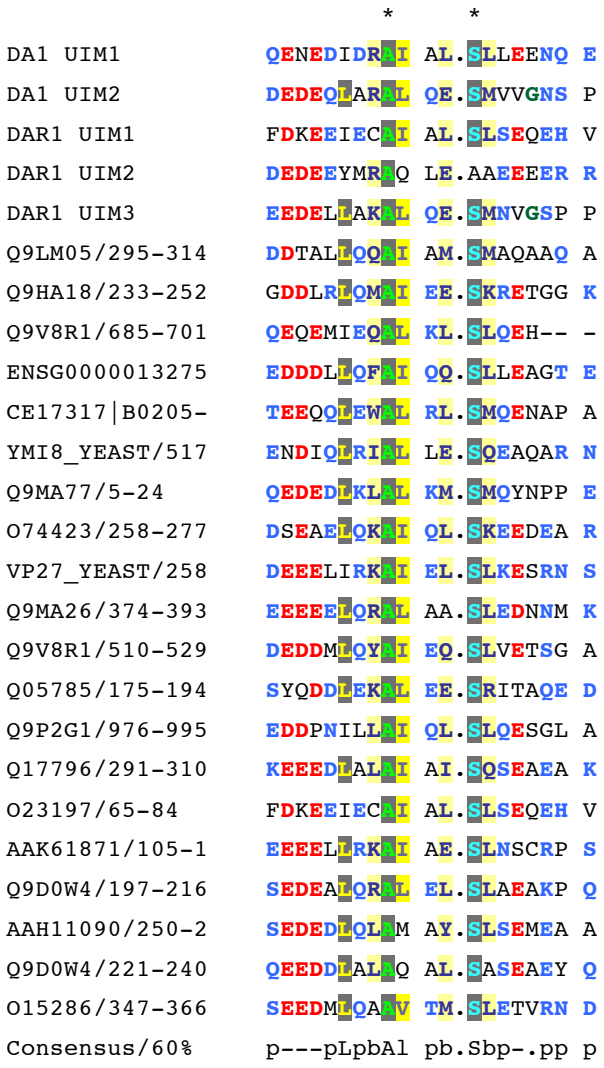

Figure 3.8 – SMART alignment of DA1 and DAR1 UIM domains

Highly conserved Alanine and Serine residues marked with * were converted to Glycines in order to generate UIM mutants. Considerable variation can be seen in the DA1 and DAR1 samples. Colour code is CHROMA (see supplementary information Table S4)

This investigation used a similar approach similar to that used by Oldham et al (2002) in their study of the UIMs in Epsin. An N-terminal GST tag was fused to a 52aa DA1 fragment spanning both UIM domains. Each UIM domain was mutated separately and in combination, to generate a total of four constructs (Fig. 3.9). The mutations introduced in order to abrogate UIM function were Ala-Gly and Ser-Ala transitions at the highly conserved residues indicated in Fig. 3.8. GST-UIM^{wt} contained both wild-type UIM domains; GST-uim1 contained a mutated UIM1 and a wild-type UIM2; GST-uim2 contained a wild-type UIM1 and a mutated UIM2; and GST-uim12 had both UIMs mutated. These constructs were kindly provided by Yunhai Li from the Bevan lab.

Figure 3.10 shows that GST-UIM^{wt} and GST-uim1 were both able to bind mono-ubiquitin, whereas GST-uim2 and GST-uim12 were not. The lack of ubiquitin binding by GST-uim2 (where only UIM1 is active) suggests that UIM1 does not bind mono-ubiquitin and may be non-functional.

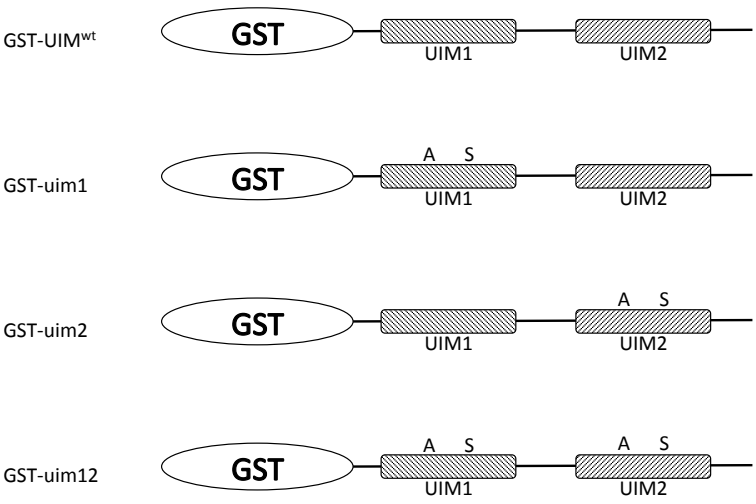

Figure 3.9 – *E. coli* UIM expression constructs

A 52aa fragment of DA1 spanning both UIM domains was subcloned into the pGEX$_4$T$_2$ expression vector. Mutated constructs were made by introducing serine-alanine and alanine-glycine transitions at the residues marked S and A respectively. In total four constructs were made: one wild-type (GST-UIM^{wt}), one with UIM1 mutated (GST-uim1), one with UIM2 mutated (GST-uim2), and one with both UIMs mutated (GST-uim12). These constructs were kindly provided by Yunhai Li.

The UIMs in the human de-ubiquitinating enzyme ATXN3 preferentially target the enzyme to K63- (rather than K48-) linked ubiquitin chains, which suggests that the UIMs have a preference to binding a particular ubiquitin chain architecture (Winborn et al., 2008). Furthermore, the UIM domain of the human 26S proteasome subunit, S5a, has a significantly reduced affinity towards mono-ubiquitin compared to the UIMs of EPS15 and HRS (Woelk et al., 2006). This difference may be because the 26S proteasome is involved in binding and degrading poly-ubiquitinated substrate proteins (Voges et al., 1999, Young et al., 1998), and EPS15 and HRS are well characterised targets of coupled mono-ubiquitination (Woelk et al., 2006, Hoeller et al., 2006). It is therefore possible that S5a UIMs have a preference for poly-ubiquitin, and EPS15 and HRS have a preference to mono-ubiquitin.

Based on these observations, the inability of DA1 UIM1 to bind mono-ubiquitin does not confirm that the UIM is non-functional. Instead, it may be that DA1 UIM1 is specialised to binding poly-ubiquitin chains or perhaps chains attached to specific substrate proteins. The observation that DA1 is ubiquitinated (section 5.3.3), raises the possibility that UIM2 may bind cis-ubiquitin in a coupled mono-ubiquitination mechanism that regulates DA1 activity, in a similar way to that exhibited by EPS15 and Hrs (Hoeller et al., 2006, Woelk et al., 2006).

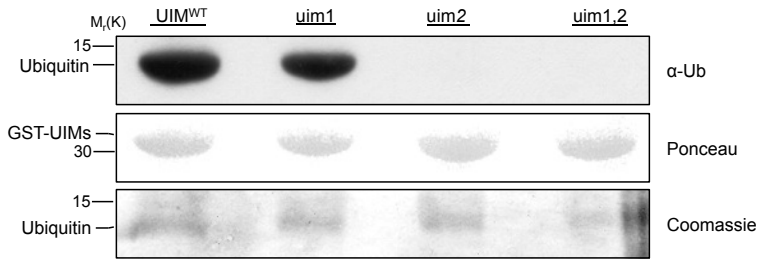

Figure 3.10 – DA1 UIM2 binds mono-ubiquitin *in vitro*

Recombinant GST-tagged UIM fragments were incubated with mono-ubiquitin before purification on glutathione sepharose beads and immunoblot analysis. Mono-ubiquitin co-purified with GST-UIM^{wt} and GST-uim1 only, revealing that UIM2 is the only UIM domain present in DA1 capable of binding mono-ubiquitin *in vitro*.

3.4 – DA1 metallopeptidase is not active towards K48 or K63 poly-ubiquitin

The DA1 C-terminal peptidase domain belongs to the MA clan of peptidases that includes the WLM family of proteins, which have been shown to be involved in de-sumoylation and de-ubiquitination (Iyer et al., 2004, Su and Hochstrasser, 2010, Mullen et al., 2010). Because both DA1 and WLM DUBs contain UIMs and a peptidase domain, it was hypothesised that DA1 was a de-ubiquitinating enzyme. To test this hypothesis the ability of DA1 to hydrolyse poly-ubiquitin was assayed in an *in vitro* system. Recombinant GST-DA1 was incubated with poly-ubiquitin chains (a mixture of 2-7mers) for two hours at 30°C, before aliquots were run on SDS-PAGE and subjected to western blot analysis. Because K48 and K63 linked ubiquitin chains are the most abundant forms of poly-ubiquitin in nature (Peng et al., 2003, Saracco et al., 2009), only poly-ubiquitin chains joined by these linkages were tested in this assay. Empty GST vector (GST-Φ) was used as a negative control in this assay.

The western blots in Fig. 3.11 showed that DA1 had no de-ubiquitinating activity towards either K63 and K48 linked ubiquitin in these experimental conditions. Although it remained a possibility that DA1 possessed a de-ubiquitinating activity towards other poly-ubiquitin structures, the identification of other substrates for the DA1 peptidase in Chapter 5 led to the decision not to pursue this avenue of research.

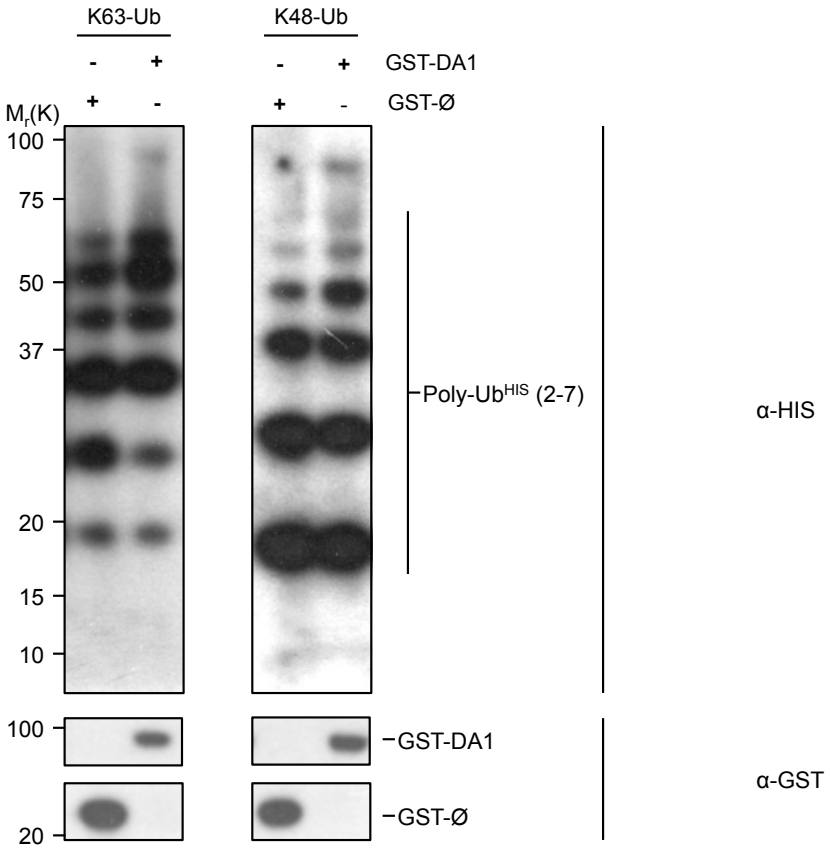

Figure 3.11 – DA1 is not able to cleave K48- and K63- linked poly-ubiquitin *in vitro*

Poly-ubiquitin chains of various lengths (2-7mers) were incubated with either GST-DA1 or GST, before SDS-PAGE and immunoblot analysis. The addition of GST-DA1 did not result in an accumulation mono-ubiquitin or lower-molecular weight ubiquitin chains, demonstrating that GST-DA1 does not have a de-ubiquitinase activity towards K48- and K63-linked poly-ubiquitin.

3.5 - Discussion

The biochemical analyses reported in this chapter have improved our understanding of DA1 protein function, provided plausible explanations for its genetic interactions, and helped to focus research on promising leads.

Based on predictions from *da1-1* genetic interactions, it was shown that DA1 and DAR1 physically interact *in vitro*. This suggests that the active forms of these proteins may be hetero- and homo-oligomeric complexes. The genetic analysis carried out by Li et al (2008) revealed that DA1 and DAR1 redundantly influence the duration of cell proliferation in developing organs. The analysis also showed that the da1-1 protein had a negative influence on the activity of DAR1 (Li et al., 2008). Together these observations suggested that DA1 and DAR1 might be active in a multimeric complex, which is rendered non-functional with the inclusion of the da1-1 protein. The evidence in section 3.2.2 that DA1 and DAR1 interact *in vitro* supports the prediction that DA1 and DAR1 operate in a multimeric complex. In addition, the *in vitro* observation that da1-1 binds both DA1 and DAR1 supports the prediction that da1-1 is able to interact physically with wild-type DA1 and DAR1 in this multimeric complex.

By integrating this genetic and biochemical evidence it is possible to postulate that members of the DA1 family may act together, as interchangeable subunits. For example, DA1 and DAR1 may form a complex whose functions are different from those of the respective homo-oligomeric complexes. This idea is supported by the significant sequence similarity between family members, and emerging evidence of different roles for the different family members (Bi et al., 2011, Yang et al., 2010, Peng et al., 2013). This ability of different family members to form into different complexes could serve to integrate different stimuli into a single coordinated biological response.

The human muscle differentiation cofactors CRP1 and CRP2 are an example of LIM domain containing proteins that form modular complexes (Chang et al., 2003). These proteins utilise their dual LIM domains to bind different interacting partners; SRF at the N-terminal LIM and GATA4/6 at the C-terminal LIM (Chang et al., 2003). The identification of the LIM-like domain in DA1, and evidence of its significance in DAR4 (Yang et al., 2010), suggests that the dual LIM and LIM-like domains in DA1 may act as a scaffold for modular complex formation, akin to that seen for CRP1 and CRP2 (Chang et al., 2003). In support of this, the *in vitro* da1lim8 binding studies show that the LIM domain is not required for the DA1-DA1 interaction, which suggests that it has a role in the binding of other DA1 family members or putative substrates.

As the LIM domain is not required for DA1-DA1 interactions, it is possible that it may have a role in either intramolecular interactions (perhaps associated with coupled mono-ubiquitination and controlling peptidase activity) or in mediating interactions of DA1 with other as yet unknown proteins. The well characterised role of LIM domains in mediating protein-protein interactions (Schmeichel and Beckerle, 1994, Kadrmas and Beckerle, 2004, Agulnick et al., 1996) and the evidence that the DA1-DA1 interaction is independent of LIM function, suggests that the DA1 LIM domain could be utilised to identify *de novo* DA1 interacting partners. Such interactors could be upstream regulators of DA1, other components of DA1 complexes, or the downstream targets of DA1 complex activity. To explore these possibilities, a truncated version of DA1 containing the LIM and C-terminal domain was used in Chapter 4 to identify binding partners in a yeast-2-hybrid screen.

Finally, evidence that DA1 has no de-ubiquitinating activity *in vitro* suggested that the putative DA1 peptidase may have other substrates. This observation, together with the identification of UIM2 as a functional ubiquitin-binding motif, has helped to focus functional analysis of DA1 on the observed genetic interactions with the E3 ubiquitin ligases, EOD1/BB and DA2 (Li et al., 2008, Disch et al., 2006, Xia, 2013). This is explored further in Chapter 5. The revelation that DA1 is probably not a de-ubiquitinating enzyme suggests that it may have alternative roles within the ubiquitin system. For example DA1 may act as an E3 ligase adaptor protein that may recruit its cognate E3 ligase to a target. This is seen with the mammalian UIM-containing protein RAP80, which recruits BRCA1 to double-strand breaks (Sobhian et al., 2007). An alternative possibility is that the DA1 UIMs recruit a cognate E3 ligase by binding to its ubiquitinated from and consequently initiate a coupled mono-ubiquitination reaction that subsequently alters DA1 activity (Woelk et al., 2006, Komander et al., 2009). The role of the putative DA1 peptidase activity in these mechanisms is not yet known, but it could involve the modification of E3 behaviour, as is the case for the human E3 ligases, RNF13 and Parkin (Burchell et al., 2012, Bocock et al., 2010).

Chapter 4 - A yeast-2-hybrid screen for DA1 interacting proteins

4.1 Introduction

Current understanding of DA1 function has been obtained from knowledge of DA1 protein structure, DA1 biochemistry (Chapter 3), genetic analysis of the *da1*-1 mutant (Li et al., 2008), and two observed genetic interactions with *EOD1/BB* (Li et al., 2008) and *MED25/PFT1 (Xu and Li, 2011).* Biochemical work has yielded significant insights into the relationship between DA1 and DAR1, as well as the role of DA1 in the ubiquitin system (Chapter 3). The observed genetic interaction between *DA1* and the E3 ligase *EOD1* (Li et al., 2008) suggested DA1 might have a role in the regulation of EOD1 (Chapter 5), which emphasises the potential significance and promise of identifying DA1 interacting proteins for advancing the understanding of the regulation of growth control. This is the subject of research described in this Chapter.

4.1.1 – Identifying *physical* interactors of DA1

To complement and extend the observations of a *genetic* interaction between *DA1* and *EOD1*, work in this Chapter focussed on identifying *physical* interactions between DA1 and other proteins. The reasons for screening for *physical* interactors rather than *genetic* interactors are as follows: first, growth and developmental phenotypes are often highly pleiotropic, and there is considerable risk that enhancer and suppressor screens may identify non-related genes. For example, the *da1-1* enhancer *EOD3* was recently shown to be independent of *DA1* (Fang et al., 2012). Second, a genetic interaction does not indicate biochemical or developmental *proximity*; it can establish that the two genes in question may be in the same pathway, but not that they function at the same step within that pathway. Therefore, depending on the complexity of a pathway, a genetic interaction can be relatively uninformative, such as the observed interaction between *MED25/PFT1* and *DA1* (Xu and Li, 2011).

In contrast, the identification of physical interactions between proteins provides the foundations for a variety of informative biochemical and genetic experiments that can define, in molecular detail, the cellular functions of the interaction and the partner proteins. A good example of this power is the discovery, through a Y2H screen (see section 4.1.2), that the Arabidopsis F-box protein AtFBS1 interacts with 14-3-3 proteins (Sepúlveda-García and Rocha-

Sosa, 2012). This observation has led to new hypotheses for the dimerization and auto-ubiquitination of AtFBS1, which will undoubtedly be tested in the near future.

A further reason for screening for physical interactions is an interest in the significance of the DA1 peptidase. The presence of this domain in DA1 suggests a role in the irreversible modification of target proteins; a process known to play a critical role in regulating the uni-directionality of the cell-cycle and cell proliferation in human cancer cells (Elledge, 1996, Mason and Joyce, 2011). The irreversible nature of this modification indicates that potential substrates of DA1 identified through interaction screens may be novel candidate regulators of the progression of cell proliferation. Therefore such screens for DA1-interacting proteins form a necessary part of our work towards understanding the control of organ and seed growth.

4.1.2 – Yeast-2-Hybrid – An overview

Two key methods are suitable for identifying the physical interactors of DA1: a Yeast-2-Hybrid screen (henceforth Y2H) and an *in planta* co-immunoprecipitation screen. The latter involves the immunopurification of epitope-tagged bait protein from transgenic plant tissue and the subsequent proteomic identification of binding partners. This method relies on the stability of the bait protein *in planta*, however as the DA1 protein is unstable *in planta* (Yunhai Li, personal communication) this technique was unsuitable. For this reason a Y2H based experimental strategy was used.

The Y2H screen, originally developed in the 1980s (Fields and Song, 1989), is a yeast-based method for identifying physically interacting proteins. As illustrated in Fig. 4.1, the transcriptional activation of a specific set of reporter genes is dependent upon the interaction of both a bait and a prey protein. Using the Invitrogen Pro-Quest™ system, the coding sequence of the bait protein (DA1) was fused in-frame to the DNA-binding domain of the GAL4 transcription factor (GAL4-DB), and a library of coding sequences of potential prey proteins was fused to the activation domain of GAL4 (GAL4-AD). The prey library was generated from cDNA from Arabidopsis inflorescences and kindly provided by Phil Wigge and Vinod Kumar at the John Innes Centre, Norwich. The physical interaction of DA1 and its prey brings GAL4-DB and GAL4-AD into close proximity such that a functional GAL4 transcription factor is reconstituted, leading to activation of the reporter genes. In order to reduce the occurrence of false-positives in the screen, two independent reporter genes were used in this screen. The yeast strain used in this assay (PJ69-4α), had its *HIS3* and *ADE2* genes under the control of the *GAL4* transcription factor (see fig. 4.2) (James et al., 1996). These genes enable autotrophy for histidine and adenine respectively, and therefore a bait and prey interaction is required for

yeast to grow on media deficient for histidine and adenine. In the screen described in this Chapter, growth on a histidine deficient medium was initially used to identify positive interactors. This was then followed by a further validating screen on medium deficient for both histidine and adenine.

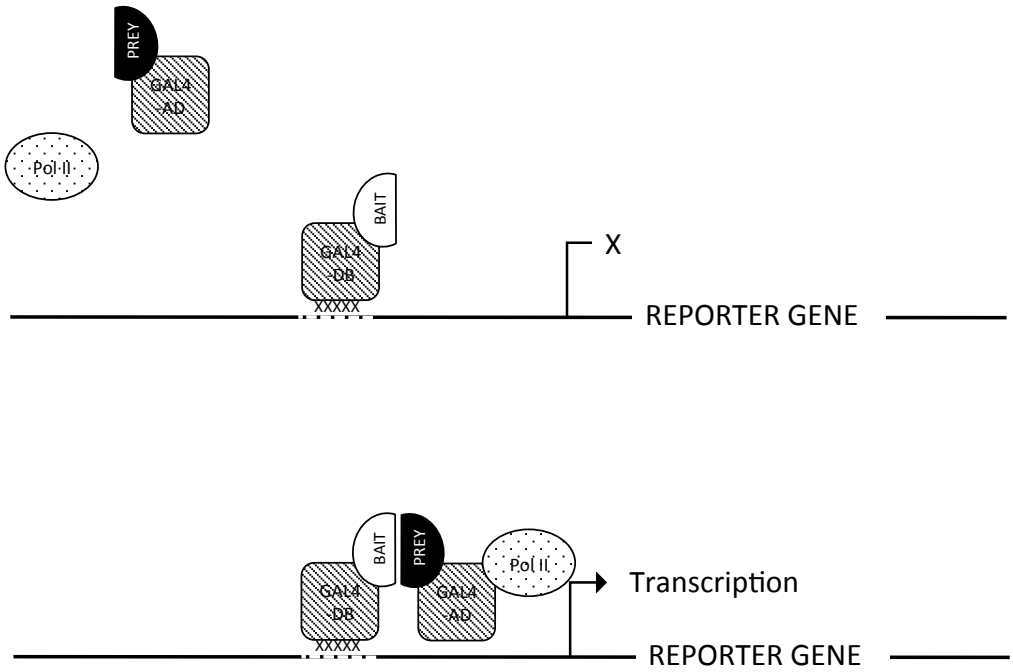

Figure 4.1 – The yeast-2-hybrid screen

The bait gene is fused to the GAL4 DNA binding domain (GAL4-DB) and the prey gene to the GAL4 activation domain (GAL4-AD). Both GAL4 domains are required for the activation of the GAL4 reported gene. When bait and prey proteins interact, bait-GAL4-DB recruits the prey-GAL4-AD to the promoter of the reported gene and transcription is initiated. In yeast where there is no bait-prey interaction, the reporter gene is not activated.

4.2 – DA1 Yeast-2-Hybrid identifies 31 candidate interactors

4.2.1 – Experimental strategy

The experiments were carried out in three steps:

1. A first-round screen was used to identify a pool of positive interactors. This was done by initially selecting all colonies that were able to grow on SC-Leu-Trp-His medium (see Box 4.1). This pool of 117 primary transformants was then assessed – based on known biochemical and developmental roles – for promising candidates.
2. Candidate interactors were taken forward for a second-round of Y2H to confirm the initial interaction. This was done through a re-transformation of the yeast with both bait and prey, followed by selection on SC-Leu-Trp-His-Ade medium (see Box 4.1). This added confidence to the original interaction through the use of -Ade selection, which has a background level two orders of magnitude lower than -His selection (James et al., 1996). Negative controls consisting of empty vectors (GAL4-DB and GAL4-AD) were used to assay for specific interactions.
3. Following this second round, remaining candidate interactors were cloned into bacterial expression vectors and tested for interaction with DA1 *in vitro.* Only at his stage were candidates taken forward for genetic analyses.

Box 4.1 – Yeast-2-hybrid selection genes

The PJ69-4a yeast strain used in this screen is deficient for *LEU2* and *TRP1*, and has the *HIS3* and *ADE2* genes under the control of GAL4. The bait vector, pDBleu contains the *LEU2* gene and the prey vector, pEXP-AD502 contains the *TRP1* gene. Interaction of bait and prey constructs results in an active GAL4 protein and therefore the transcription of *HIS3* and *ADE2*

LEU2	Confers ability to grow on SC-Leu media Selects for presence of bait construct (pDBleu)
TRP1	Confers ability to grow on SC-Trp media Selects for the prey construct (pEXP-AD-502)
GAL1-HIS3	Confers ability to grow on SC-His media Selecting for a bait:prey interaction
GAL2-ADE2	Confers ability to grow on SC-Ade media Selecting for a bait:prey interaction Stringent selection (two orders of magnitude less background than *HIS3)*

4.2.2 – Truncated DA1 was used to reduce false positives

As demonstrated in section 3.3, DA1 UIM2 interacts non-covalently with ubiquitin, and both UIMs may have the potential to bind poly-ubiquitin. In order to reduce false positives arising from non-specific binding between DA1 UIMs and endogenous yeast ubiquitin (free ubiquitin and ubiquitinated proteins), a truncated DA1 bait protein was used in the Y-2-H screen. The construct had the N-terminal 162aa removed, leaving both the LIM domain and the C-terminal peptidase domain. The removal of such a large protein fragment had the potential to increase the number of false negatives. However biochemical data suggesting the LIM and LIM-like domains may be involved in binding non-DA1 family members (section 3.2) gave confidence that this construct could identify candidate binding partners.

4.2.3 – DA1 interacts with 31 candidate genes

Adjusted to remove multiple colonies of the same clone, Fig. 4.1 displays identities of the in-frame prey proteins that were fused to GAL4-AD in colonies that grew robustly on SC-Leu-Trp-His medium. The table lists many genes that initially appear to be involved in growth and development. UNFERTILISED EMBRYO SAC 16 (UNE16), and MATERNAL EFFECT EMBRYO ARREST 14 (MEE14) both have published seed development phenotypes (Pagnussat et al., 2005), and were considered to be potential candidates for further study. ARABIDOPSIS THALIANA UBIQUITIN ACTIVATING ENZYME (ATUBA1) is also an interesting candidate, as it is one of only two E1 activating enzymes in Arabidopsis and has a published pathogen-related growth-response phenotype (Goritschnig et al., 2007). This is particularly interesting as it shows biochemical and developmental overlap with DA1 – through the ubiquitin system, and growth and development respectively.

The *LOB DOMAIN-CONTAINING PROTEIN 41* (*LBD41*) was also of interest. This gene is related to the LOB-domain containing protein, *ASYMMETRIC LEAVES 2* (*AS2*), the knockout of which causes leaf lobing, short petioles and the formation of leaflet-like structures (Semiarti et al., 2001). *AS2* is involved in the repression of *KNOX* gene expression in the lateral regions of the SAM (Guo et al., 2008, Hay et al., 2006), and influences leaf development and the establishment of adaxial-abaxial polarity (Semiarti et al., 2001, Xu et al., 2003, Lin et al., 2003). Over-expression of the *LBD41* homolog in *Celosia cristata* has been shown induce leaf lobing and ectopic leaf blade formation on the petiole (Meng et al., 2010).

It is also noteworthy that 15 out of the 31 interacting proteins have a predicted chloroplast localisation. These included genes involved in photosynthesis , such as PSAE-1 (Varotto et al.,

2000), FERREDOXIN 2 (Hanke et al., 2004) and two RUBISCO subunits (Spreitzer and Salvucci, 2002) as well as non-photosynthetic genes such as the transcription factor *TCP15* (Uberti-Manassero et al., 2012, Li et al., 2012, Kieffer et al., 2011) and the DNA binding storekeeper protein-related gene AT4G00270.

Despite the potential interest of many of these genes, the candidates selected for further characterisation were TCP15 and the Leucine Rich Repeat Receptor-Like Kinase (LRR-RLK) TMK4. The decision to pursue TCP15 was largely based on observations from whole-proteome screens of protein interactions relevant to plant pathology, which appeared to suggest an interaction between DARs and the TCPs (Mukhtar et al., 2011). Furthermore, TCPs have a well-described role in organ growth and development (Kieffer et al., 2011, Koyama et al., 2010, Li et al., 2012, Steiner et al., 2012, Uberti-Manassero et al., 2012).

The decision to pursue TMK4 was based on observations that TMK4 is a promoter of organ growth, through both cell proliferation and cell expansion, and has a reduced sensitivity to auxin. Moreover, preliminary data showing a genetic interaction between da1-1 and the LRR-RLK FLAGELLIN SENSITIVE2 (FLS2) (Cyril Zipfel, personal communication), and data from animal systems implicating UIM containing proteins in the processing of LRR-RLKs (Marmor and Yarden, 2004) suggested that TMK4 and DA1 may interact to influence organ growth and development.

Additional reasons for pursuing TCP15 and TMK4 will be described in further detail in section 4.3 and section 4.4 respectively.

Clone	Locus	Gene name	Gene description	Predicted Location
1	AT2G22230		Beta-Hydroxyacyl-ACP Dehydratase, Putative	CW, CH
2	AT4G00270		DNA-Binding Storekeeper Protein-Related	CH
3	AT1G30460	ATCPSF30	Cleavage And Polyadenylation Specificity Factor Subunit	NU
4	AT5G35100		Peptidyl-Prolyl Cis-Trans Isomerase	CH
5	AT5G60390		Elongation factor Tu family protein	PM, VC, MT, NU, CY
6	AT4G36260	SHR2	SHI Related Sequence 2	NU
7	AT4G13640	UNE16	Unfertilized Embryo Sac 16	NU
8	AT1G69690	TCP15	TCP Family Transcription Factor	CH
9	AT2G15890	MEE14	Maternal Effect Embryo Arrest 14	CH
10	AT2G28790		Osmotin-Like Protein, Putative	CW
11	AT4G28750	PSAE-1	PSA E1 Knockout,	CH
12	AT2G30110	ATUBA1	Ubiquitin-Activating Enzyme 1	CY, NU, PM, PD
13	AT1G67090	RBCS1a	Ribulose Bisphosphate Carboxylase Small Chain 1a	CH
14	AT3G23750	TMK4	LRR-RLK Family Protein	PM
15	AT3G04120	GAPC1	Glyceraldehyde-3-Phosphate Dehydrogenase C Subunit	CY, MT, CH, NU,PM,AP
16	AT5G38410	RBCS3B	Ribulose Bisphosphate Carboxylase Small Chain 3B	CH
17	AT1G74030	ENO1	Enolase 1	CH
18	AT5G65950		Unknown Protein	Unknown
19	AT2G23350	PAB4	Poly(A) Binding Protein 4	CY
20	AT3G15360	ATHM4	Arabidopsis Thioredoxin M-Type 4	CW,CH
21	AT1G54630	ACP3	Acyl Carrier Protein 3	CH
22	AT1G36390		Co-Chaperone Grpe Family Protein	CH
23	AT1G60950	ATFD2	Ferredoxin 2	CH
24	AT5G60670		60S Ribosomal Protein L12	RB
25	AT5G08160	ATPK3	Arabidopsis Thaliana Serine/Threonine Protein Kinase 3	Unknown
26	AT5G49460	ACLB-2	ATP Citrate Lyase Subunit B 2	CY, PM
27	AT2G18030		Peptide Methionine Sulfoxide Reductase Family Protein	EM
28	AT4G32880	HTHB8	Homeobox Gene 8	NU
29	AT3G02550	LBD41	Lob Domain-Containing Protein 41	NU
30	AT5G24490		30S Ribosomal Protein, Putative	RB,CH
31	AT3G04940	ATCYSD1	Cysteine Synthase D1	CW,CH

Table 4.1 - List of DA1-interacting proteins identified from the first round of the yeast-2-hybrid screen.

(CY=cytosol; CW=cell wall; NU=nucleus; CH=chloroplast; PM=plasma membrane; PD=plasmodesmata; MT=mitochondria; AP=apoplast; RB=ribosome; VC=vacuole; EM=endomembrane system).

4.3 – DA1 interacts with TCP15

4.3.1 – TCPs – An overview

4.3.1.1 – TCP biochemistry

TCPs are a family of transcription factors named after their first characterised members; *TEOSINTE BRANCHED 1* (*TB1*), *CYCLOIDEA* (*CYC*), and *PROLIFERATING CELL FACTORS 1* and *2* (*PCF1* and *PCF2*) (Cubas et al., 1999). They are characterised by the presence of an atypical basic-Helix-Loop-Helix structure that is capable of DNA binding and protein-protein interaction (Kosugi and Ohashi, 1997). The TCP family (of which there are 24 members in Arabidopsis) forms two distinct groups with distinctive effects on growth: Class I *TCP*s, which are most similar to *PCF1* and *PCF2*; and Class II *TCP*s, which are more similar to *CYC* and *TB1*; Figure 4.2 shows the relationships between TCP family members defined by protein sequence similarities across the TCP domain. TCPs have been shown to bind DNA as well as homo-and hetero-dimerise (Viola et al., 2011, Kosugi and Ohashi, 2002, Masuda et al., 2008, Kosugi and Ohashi, 1997). Both classes of TCPs are thought to bind DNA through the basic region of their TCP domain (Kosugi and Ohashi, 1997), and consensus sequences for both classes have been described as GGNCCCAG and GTGGNCCC for class I and II respectively (Kosugi and Ohashi, 2002). The biochemistry of TCP protein-protein interactions, however, is less clear; the presence of an ΦxxLL sequence (where Φ is an hydrophobic amino acid) in the second helix of the TCP domain is thought to be a good candidate region based on its similarity to the LxxLL motif shown to mediate the binding of transcriptional co-activators to nuclear receptors in animals (Martín-Trillo and Cubas, 2010, Heery et al., 1997). However, the high level of sequence conservation within the TCP domain and the large degree of diversity amongst binding partners, suggests that – as with the LIM domain – binding specificity might be determined by the sequences immediately adjacent to the TCP domain.

4.3.1.2 – TCPs influence organ growth and development

As a family, the TCPs are well characterised as regulators of growth and development. Family members have been classified as class I, which are thought to promote growth and

development, and class II TCPs, which have been shown to repress growth and development. Severe developmental defects in overexpression lines and a high-level of genetic redundancy amongst class I TCPs, such as *TCP15* and *TCP20*, means that developmental phenotypes have been extremely hard to interpret (Hervé et al., 2009, Kieffer et al., 2011). For this reason, the notion that class I TCPs *promote* growth and development needs to be taken with caution (Martín-Trillo and Cubas, 2010). Conversely, class II TCPs have well documented growth and developmental phenotypes. For example hyper-activation of *TCP4,* by fusing it to the C-terminal activation domain of VP16 (Sadowski et al., 1988), results in a significant reduction in leaf size, which is thought to be a consequence of a reduction of the duration of the growth period (Sarvepalli and Nath, 2011). Moreover, enhanced expression of miR319a – a microRNA known to down-regulate *TCP2, TCP3*, *TCP4*, *TCP10,* and *TCP24* – results in a distinctive curled-leaf phenotype (Palatnik et al., 2003), and the *miR319a*^{129} loss-of-function mutant shows floral development defects such as significantly reduced sepal length (Nag et al., 2009). In addition, *Antirrhinum cin* mutants show increased leaf area and curvature (Nath et al., 2003).

The mechanism through which mutations in class II TCPs cause these phenotypes is still unclear, however some evidence points to the direct regulation of cell-cycle genes. For example, *TCP24* binds to the promoter regions of the pre-replication complex (pre-RC) control factors *CDT1a* and *CDT1b*, and there is good evidence to suggest that this interaction reduces expression of the genes (Masuda et al., 2008). The pre-RC genes are required for S phase licensing, and therefore their repression is likely to result in slower S phase progression and reduced cell proliferation. Similarly, there is evidence that suggests the class I TCPs *TCP20* and *TCP15* activate the expression of the cell cycle effectors. These include: *CYCA1;1*, *CYCB1;1*, *CYCB1;2*, *CDC20*, and *CDKB2;1* (Li et al., 2005a, Kieffer et al., 2011).

TCPs have also been shown to influence SAM development, with gain of function (miR319-resistant) *TCP3*-expressing plants unable to develop a functional SAM (Koyama et al., 2010a, Koyama et al., 2007). It has been shown that *TCP3* supresses the expression of the *CUC* (*CUP SHAPED COTELYDON*) genes (Koyama et al., 2010a, Koyama et al., 2007), which have been shown to promote SAM formation (Hibara et al., 2006, Aida et al., 1997). In particular, this suppression of *CUC* genes is thought to be a consequence of the induced expression of *AS1*, miR164, *IAA3/SHY2* (*INDOLE-3-ACETIC ACID3/SHORT HYPOCOTYL2*) and SAUR (*SMALL AUXIN UP RNA*), all of which appear to negatively regulate *CUC* expression (Koyama et al.).

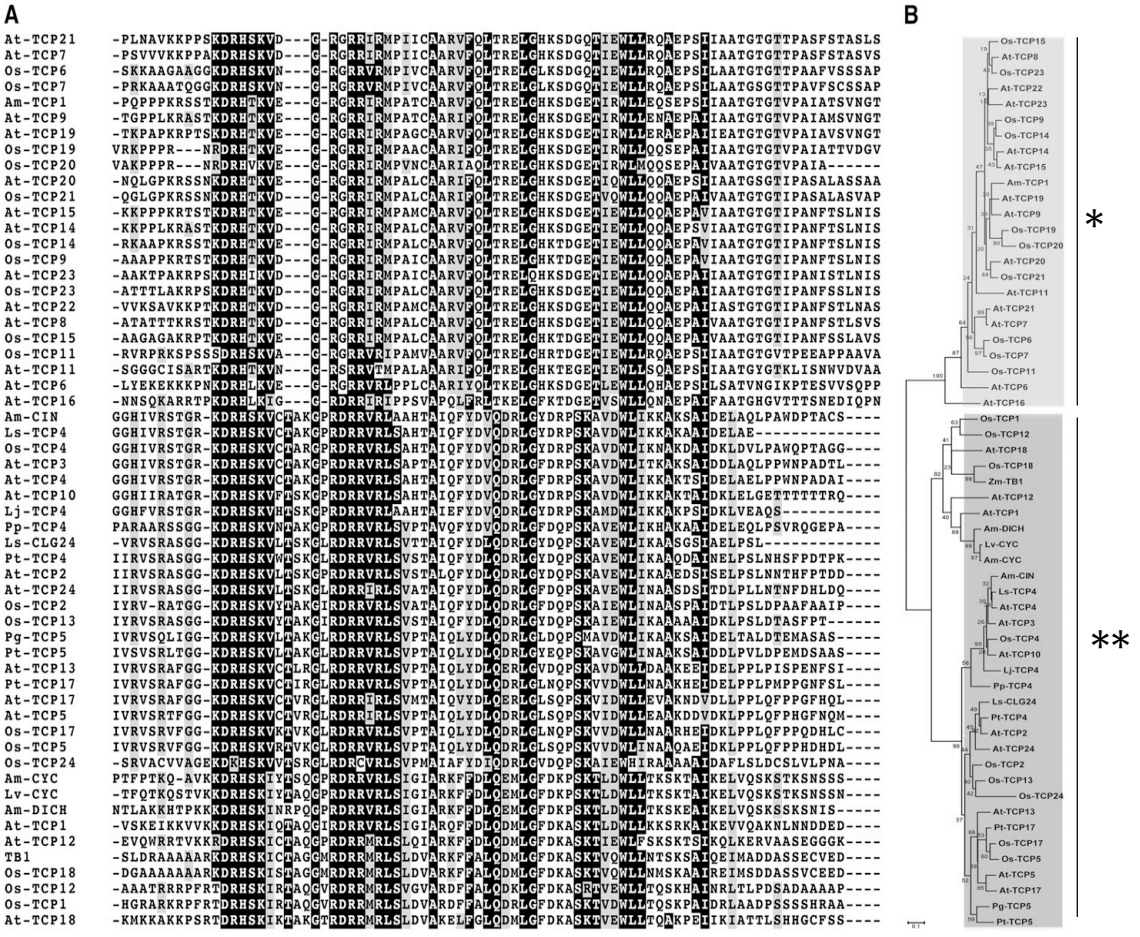

Figure 4.2 – The TCP family of transcription factors

(A) An alignment of the TCP domain of the TCP family of transcription factors and (B) a neighbour-joining phylogram with midpoint rooting based on sequence analysis of the TCP domain. Adapted from Aggarwal et al (2010). '*' indicates the class I TCP clade and '**' indicates the class II TCP clade.

4.3.1.3 – *TCP15* influences organ growth and development

Recently, several publications have described the developmental significance of *TCP14* and *TCP15* (Kieffer et al., 2011, Li et al., 2012, Uberti-Manassero et al., 2012). However, as evidence of the complexity of *TCP* genetics, there is considerable conflict within the data and it is difficult to draw many firm conclusions. Nonetheless, it is clear that both *TCP14* and *TCP15* are expressed in young developing organs, in a pattern consistent with that of proliferating tissue (Kieffer et al., 2011, Uberti-Manassero et al., 2012). Indeed the leaf GUS staining data from Uberti-Manassero et al (2012) is reminiscent of that seen for *DA1* (Li et al., 2008).

Another point of agreement between Kieffer et al (2011), Li et al (2012), and Uberti-Manassero et al (2012) is that the redundancy amongst the most closely related *TCP*s limits the insight that can be gained from the use of single gene knock-out mutations. Using a double knock-out approach, Kieffer et al (2011) report that the *tcp14/tcp15* double mutant has reduced internode length (resulting in a reduced inflorescence height), reduced pedicel length and a quantitative effect on leaf blade expansion. The reduction in internode and pedicel length appears to agree with the perceived role of *TCP14* and *TCP15* as class I TCPs, in the promotion of growth and development. Another strategy used by Kieffer et al (2011), Li et al (2012), and Uberti-Manassero et al (2012), in order to overcome the problem of redundancy, was the fusion of EAR (SRDX) domains to the C-termini of the proteins, which turned them into dominant transcriptional repressors (Hiratsu et al., 2003). However, taking into account the evidence that TCP proteins form hetero-dimers with family and non-family members (Viola et al., 2011, Kosugi and Ohashi, 2002, Masuda et al., 2008), the observed phenotypes are likely to be significantly more complex than those resulting from single gene *tcp* knockouts. In addition to leaf curling and leaf shape phenotypes, *pTCP15:TCP15SDRX* expressing plants had smaller rosette leaves early on in development, which were made up of smaller cells (Uberti-Manassero et al., 2012, Li et al., 2012). These data further support the notion that *TCP15* promotes organ growth, and more specifically, also predict that it does so through increasing the initial rate of cell expansion. This is supported by the observation that in *pTCP15:TCP15SDRX* plants, cotyledon cell size is reduced (Li et al., 2012).

Surprisingly, and contradicting the *pTCP15:TCP15SDRX* data showing reduced growth (Uberti-Manassero et al., 2012, Li et al., 2012), evidence from DEX-inducible over-expression of wild-type *TCP15* reveals a reduction in epidermal cell size and a reduction of high ploidy cells in rosette leaves (Li et al., 2012). This, along with evidence that *pTCP15:TCP15SDRX* plants have increased trichome branching (Li et al., 2012), suggested that *TCP15* may also act to negatively regulate cell size and endoreduplication.

4.3.1.4 – *TCP14* and *TCP15* are implicated in pathogen response pathways

Recently, two sets of evidence have linked *TCP15* and its closest relative, *TCP14*, to pathogen response pathways. Firstly, a partial correlation analysis of microarray data, carried out by Dan Maclean in The Sainsbury Laboratory, identified DA1 as a hub in a network of interactions in response to flg22 (the pathogen-associated molecular pattern (PAMP) for flagellin) (Fig. S2). This network predicted a directional relationship from *DA1* to *TCP15*, suggesting that *DA1* was upstream of *TCP15*.

Secondly, a recent large scale Y2H screen investigating the interactome network of plant-pathogen effectors, identified TCP14 as a hub in response to both *Pseudomonas syringae* and *Hyaloperonospora arabidopsidis* infection (Mukhtar et al., 2011). Interestingly, this study also identified a physical interaction between TCP14 and DAR1. This link between the TCPs and pathogen response is not surprising when one considers that treatment of seedlings with the bacterial peptides flg22 (flagellin), and elf18 (EF-Tu), results in an inhibition of growth (Gómez - Gómez et al., 1999, Gómez-Gómez and Boller, 2000, Zipfel et al., 2006).

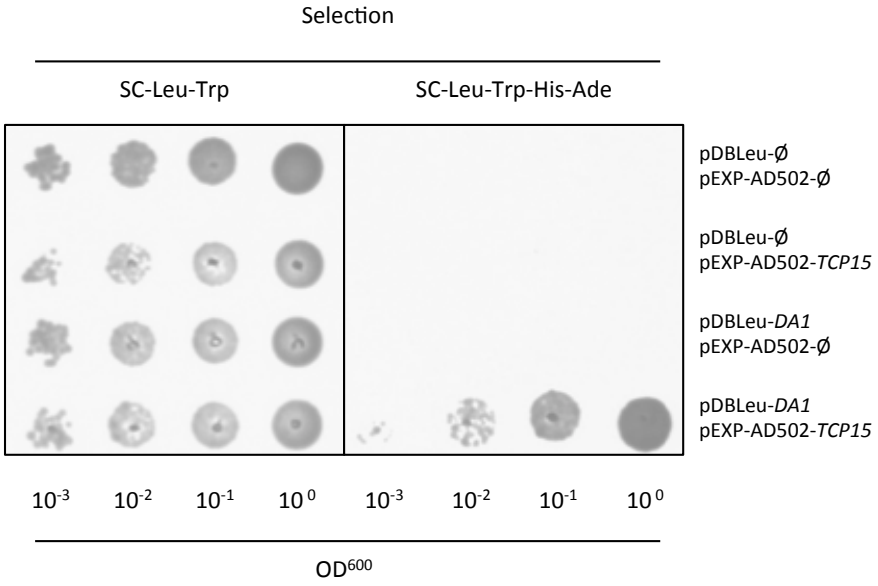

Figure 4.3 – In yeast drop-test: DA1 interacts with TCP15 in yeast

Yeast co-expressing pDBLeu-DA1 and pEXP-AD-502-TCP15 were able to grow on $SC^{-Leu-Trp-His-Ade}$ medium, demonstrating a physical interaction. All negative controls, including DA1 with empty vector, and TCP15 with empty vector were unable to grow on $SC^{-Leu-Trp-His-Ade}$ medium. All treatments were able to grow on $SC^{-Leu-Trp}$ medium, demonstrating that both bait and prey constructs were being expressed.

4.3.2 – DA1 physically interacts with TCP15

Sequencing of the interacting Y2H clone revealed that the full-length TCP15 sequence was fused to the GAL4-AD fragment. To re-test the interaction in yeast, full length *TCP15*-GAL4-AD was re-transformed into yeast and screened for an interaction with DA1. TCPs have been shown to auto-activate in Y2H screens (Kosugi and Ohashi, 2002) and therefore ensure TCP15 auto-activation was not generating a false positive, a negative control of the TCP15 and an empty bait vector was used. The drop test shown in Fig. 4.3 demonstrates a strong interaction between DA1 and TCP15, and no interaction between any of the three negative controls.

Following this observation, *TCP15* was cloned into the pETnT bacterial expression vector for *in vitro* analysis. Following the procedure described in section 3.2.2; recombinant GST-tagged bait proteins were incubated with recombinant FLAG-tagged prey proteins before precipitation of GST-tagged bait proteins on glutathione sepharose beads. The purified proteins were then eluted and subjected to SDS-PAGE and immunoblot analysis. The ability of β-glucuronidase (GUS) to form a homo-tetramer was utilised to design a positive control of GST-GUS vs FLAG-GUS. Two sets of negative controls were also used; these were GST-GUS vs FLAG-TCP15, and GST-DA1 vs FLAG-GUS.

Fig. 4.6 shows that, *in vitro,* DA1 physically interacts with TCP15. This observation, combined with the Y2H data suggested that the DA1-TCP15 relationship is a *bona fide* physical interaction.

4.3.3 – *DA1-TCP15* genetic interactions

Due to the large degree of redundancy among TCP family members, and in agreement with recent publications (Kieffer et al., 2011, Li et al., 2012, Uberti-Manassero et al., 2012), very few developmental phenotypes were visible with the single *tcp15* knockout mutant. In order to overcome this, double knockout lines were generated with the most closely related family member of *TCP15; TCP14* (Martín-Trillo and Cubas, 2010, Aggarwal et al., 2010). Using these lines, and a triple knockout line incorporating the *da1-1* mutation, plants were phenotyped for petal size, seed size and inflorescence stem height.

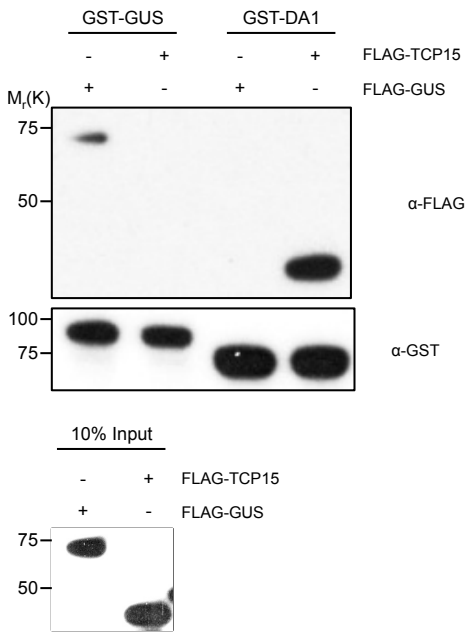

Figure 4.4 - DA1 interacts with TCP15 *in vitro*

E. coli expressed GST-tagged bait proteins were incubated with *E. coli* expressed FLAG-tagged prey proteins before purification on glutathione sepharose beads and immunoblotting for GST and FLAG. FLAG-TCP15 co-purifies with GST-DA1 (lane 4) but not GST-GUS (lane 2).

4.3.3.1 – DA1 interacts with TCP14 and TCP15 to control stem height

Fig. 4.5c shows that *da1-1* plants have significantly longer inflorescence stems than Col-0 (Student's T-test, p=0.034), revealing that *da1-1* is a negative regulator of inflorescence stem growth. It also shows that, in agreement with Kieffer et al (2011), *tcp14/tcp15* plants exhibit a significantly shorter inflorescence stem than Col-0 (Student's T-test, p<0.001). This reveals that, as is predicted for class I *TCPs* (Martín-Trillo and Cubas, 2010), *TCP14* and *TCP*15 are positive regulators of growth and development, promoting the elongation of inflorescence stems. Interestingly, the *da1-1* related increase in stem height is abolished in the *tcp14/tcp15/da1-1* triple mutant, which has a phenotype equivalent to the *tcp14/tcp15* double knockout. This suggests that in the regulation of inflorescence stem height, *DA1, TCP14* and *TCP15* are in the same pathway, and that the *TCPs* may function downstream of *DA1.*

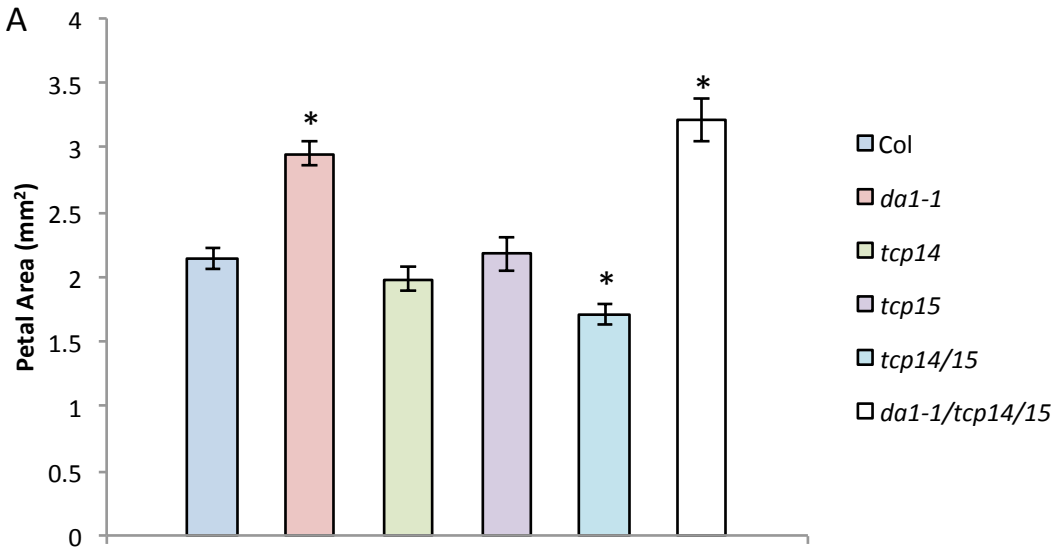
A
Petal Area (mm²)
4
3.5
3
2.5
2
1.5
1
0.5
0
*
*
*
Col
da1-1
tcp14
tcp15
tcp14/15
da1-1/tcp14/15

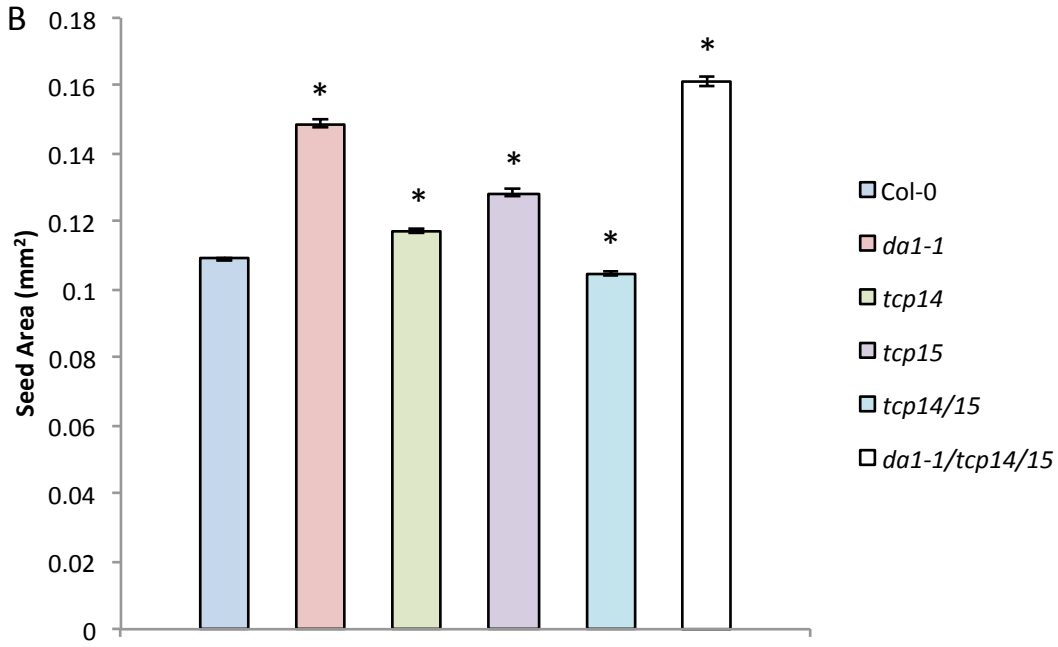
B
Seed Area (mm²)
0.18
0.16
0.14
0.12
0.1
0.08
0.06
0.04
0.02
0
*
*
*
*
*
Col-0
da1-1
tcp14
tcp15
tcp14/15
da1-1/tcp14/15

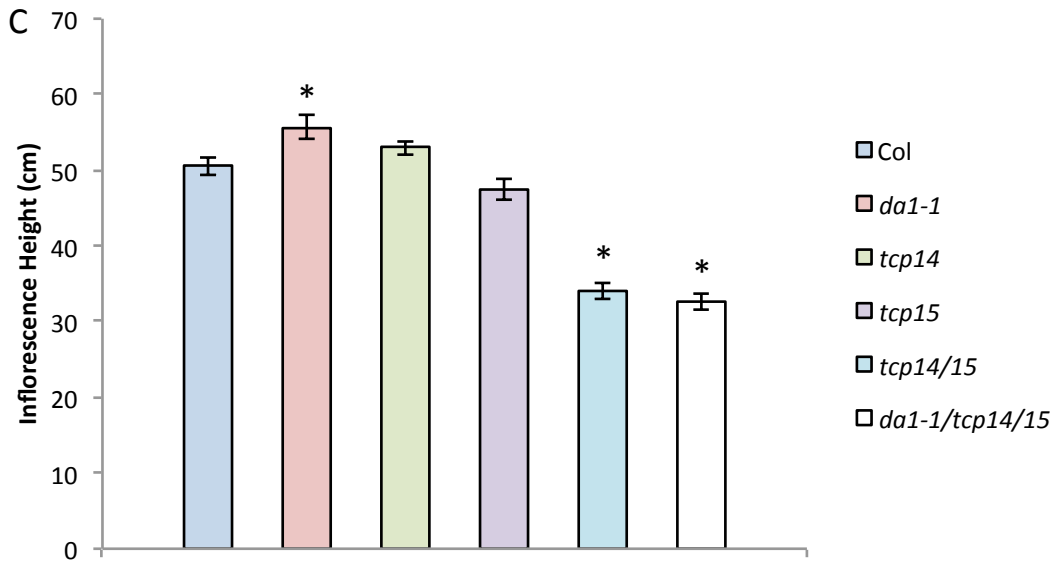

Figure 4.5 – *TCP15* genetic interactions

(A-E) Phenotypes of Col-0, *da1-1*, *tcp14*, *tcp15*, *tcp14/tcp15* and *da1-1/tcp14/tcp15* plants. (A) Petal area (n=10), (B) seed area (n=600), (C) inflorescence stem height (n=6). Values are presented as mean ± SE. (*) Denotes values that are significantly different from Col-0 (Student's T-test $p<0.05$).

4.3.3.2 – DA1 and TCP15 genetically interact to control petal area

Analysis of petal area (Fig. 4.5a) showed that *tcp14/tcp15* plants had significantly smaller petals that Col-0 (Student's T-test, $p<0.001$). This is consistent with the *a priori* expectation that class I TCPs are promoters of petal growth and development (Martín-Trillo and Cubas, 2010). Consistent with the original research (Li et al., 2008), *da1-1* plants had enlarged petals (Students T-test, $p<0.001$), however *tcp14/tcp15/da1-1* plants also had this phenotype (Student's T-test, $p<0.001$). In fact there was no significant difference between petal size in the *da1-1* and *tcp14/tcp15/da1-1* lines, indicating that the negative effect of the *tcp14/tcp15* genotype had been completely abolished by the *da1-1* allele. This suggested that TCP15 may function upstream of DA1, which is inconsistent with the interpretation that TCP15 functions downstream of DA1 with respect to inflorescence height.

Nonetheless, it is still possible that the data is consistent with TCP15 functioning downstream of DA1 in determining petal area. The petal area increase in *da1-1* lines is significantly greater that the decrease observed in *tcp14/tcp15* lines (Fig. 4.5a), suggesting the effect of DA1 is stronger than that of TCP14/15. As DA1 may have multiple effects on growth through several peptidase substrates (see Chapter 5), TCP14/TCP15 could be just be one of its targets. The relatively small phenotypic effect of the *tcp14/tcp15* mutation compared to the *da1-1* phenotype is consistent with this interpretation.

4.3.3.3 – DA1 and TCP15 do not genetically interact to regulate seed area

As displayed in Fig. 4.5b, seed area for all genotypes (*da1-1*, *tcp14*, *tcp15*, *tcp14/tcp15*, *tcp14/tcp15/da1-1*) was significantly different from that of Col-0 (Student's T-test, $p<0.001$). Consistent with published data (Li et al., 2008), *da1-1* plants had larger seeds, and consistent with section 4.3.3.2 and the notion that class I TCPs are promoters of growth and development, *tcp14/tcp15* plants had smaller seeds than Col-0. In agreement with petal data (section 4.3.3.2), *tcp14/tcp15/da1-1* seed resembled *da1-1* seed, with the effect of the *tcp14/tcp15* genotype being completely abolished. However, interestingly the *tcp14* and *tcp15* single knockouts had significantly enlarged seeds relative to Col-0, influencing seed size in the opposite direction to the double knock-out.

This contradictory effect of the single and double *tcp* mutants may be due to the ability of the TCPs to hetero-dimerise (Viola et al., 2011, Kosugi and Ohashi, 2002, Masuda et al., 2008). This suggests that other binding partners may be involved with TCP14 and TCP15 in the regulation of seed development. Furthermore the prospect that the TCPs are differentialy regulated through their phosphorylatable residues (Martín-Trillo and Cubas, 2010) allows for the possibility that hetero-complex members are differentialy regulated. A speculative model exists to explain the observed phenotypes in which; TCP14, TCP15 and possible other as yet unknown factors oligomerise to promote seed growth, and where the TCPs are also targets for repressive phosphorylation. This leads to a possible model in which, when TCP14 and TCP15 are present in complexes, seed growth is promoted, but under tight control. In single *tcp* knockout lines, less repressive phosphorylation is present and growth is accelerated, and in *tcp14/tcp15* double knockout lines, insufficient transcription factors are present to promote growth, and growth is repressed.

4.3.3.4 - Summary

With the exception of the *tcp14* and *tcp15* seed phenotype, these data collectively support a role for TCP14 and TCP15 in the *promotion* of growth and development. However, in line with

recent work (Kieffer et al., 2011), these TCPs also appear to have contradictory tissue-specific effects. They exhibited no genetic interaction to regulate seed area, and the observed genetic interaction for petal size may be misleading, and possibly due to an epistatic interaction between *da1-1* and *tcp14/tcp15*. Despite this, a genetic interaction was observed between *DA1* and *TCP14/15* in the regulation of inflorescence height. Previous work investigating the relationship between *TCP14* and *TCP15,* and *SPINDLY* (Steiner et al., 2012) highlights the difficulty in observing genetic interactions with TCP family members. Genetic redundancy amongst family members and lethality of gene over-expression resulted in Steiner et al (2012) using tissue-specific overexpression of *TCP14*, in order to identify an interaction. This publication supports section 4.3.3.2 in arguing that due to the complexities of *TCP* genetics, and the fact that DA1 has other *bona fide* target proteins (Chapter 5), further biochemical and functional evidence will be required to establish the biological significance of the interactions between DA1 and TCP15.

4.4 – DA1 interacts with the C-terminal domain of the LRR-RLK, TMK4

4.4.1 – Leucine-rich repeat receptor-like kinases (LRR-RLKs) – an overview

Leucine-rich repeat receptor-like kinases (LRR-RLKs) are the largest sub-family of the receptor-like kinase (RLK) family in Arabidopsis (Diévart and Clark, 2003). Of the 610 predicted RLKs, 216 are LRR-RLKs (Diévart and Clark, 2003). RLKs are defined as membrane spanning proteins with C-terminal Ser/Thr kinases, and "versatile" N-terminal extra-cellular domains (Shiu and Bleecker, 2003) and the LRR-RLKs are characterised by the presence of LRR motifs present in their N-terminal domains (Diévart and Clark, 2003).

4.4.1.1 – LRR-RLKs are involved in plant development and pathogen response

The LRR-RLK family includes key regulators of growth and development such as CLAVATA1 (CLV1), BRASSINOSTEROID-INSENSITIVE1 (BRI1), ERECTA (ER) and TMK1-4 (Clark et al., 1997, Clouse et al., 1996, Torii et al., 1996, Dai et al., 2013). CLV1, a regulator of shoot apical meristem (SAM) size (Clark et al., 1997, Schoof et al., 2000), has recently been linked to *DA1.* Work carried out by Yunhai Li at the Chinese Academy of Sciences in Beijing (personal communication) has shown that the expression domain of WUSCHEL is greatly increased in da1-1 mutants, akin to the effect in *clv* mutants (Schoof et al., 2000).

Also of relevance to this work is BRI1, a receptor in the brassinosteroid signalling pathway, whose mutants show severe developmental defects including dwarfed stature and thickened leaves (Clouse et al., 1996). BRI1 is activated by the binding of brassinosteroids to its extra-

cellular domain (Kinoshita et al., 2005), which in turn causes the release of the inhibitory BRI1 KINASE INHIBITOR 1 (BKI1) from the cytoplasmic domain (Wang and Chory, 2006). This results in the recruitment of the LRR-RLK, BRI1-ASSOCIATED RECEPTOR KINASE1 (BAK1), which binds to BRI1 to form the active signal complex (Li et al., 2002a, Nam and Li, 2002). Importantly BAK1 also complexes with FLS2, the pattern recognition receptor (PRR) for flagellin in Arabidopsis, to initiate the defence response (Chinchilla et al., 2006, Chinchilla et al., 2007a, Gómez-Gómez and Boller, 2000). BAK1 also appears to have a role in brassinosteroid-independent cell death (Kemmerling et al., 2007), however, its association with both BRI1 and FLS2 is of most interest to this work.

4.4.1.2 – da1-1 partially phenocopies bak1-4 in brassinosteroid response assays

As described in section 4.3.1.4, a recent partial correlation analysis (Fig. S2) (Maclean, unpublished) identified *DA1* as a hub in a transcriptome network in response to flg22 treatment; suggesting a role for DA1 in the flg22 PAMP response. Based on the role of BAK1 in both flg22 PAMP responses and brassinosteroid signalling, a potential link between *DA1* and brassinosteroids was investigated.

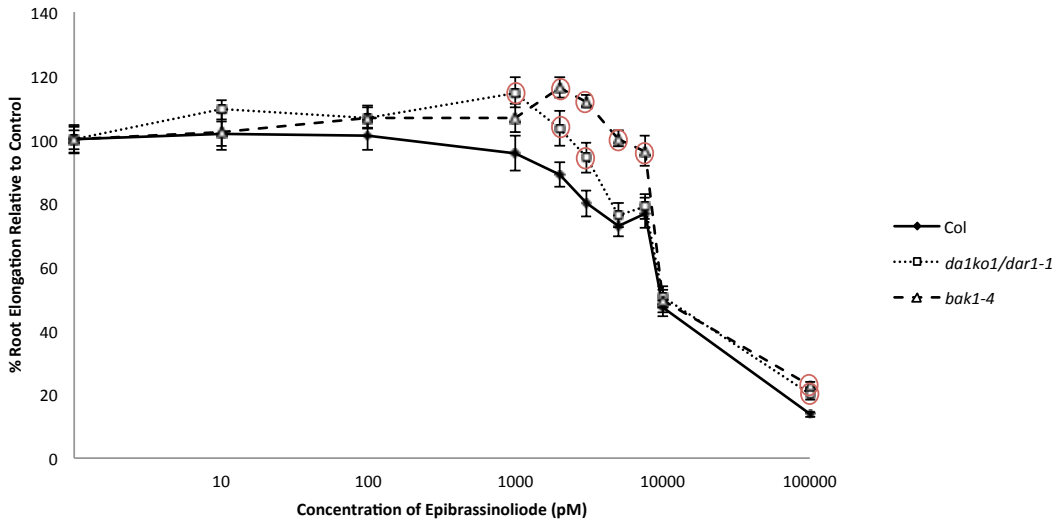

Figure 4.6 – *da1-1* seedlings have reduced sensitivity to epibrassinolide

Root lengths of 9-day old seedlings of Col-0, *da1ko1/dar1-1* and *bak1-4* in response to varying concentrations of epibrassinolide (n=20). Values are presented as means ± SE, relative to root length in the absence of epibrassinolide. Red circles denote values that are significantly different from Col-0 at the equivalent epibrassinolide concentration (Student's T-test $p<0.05$).

In order to do this, a seedling root growth experiment, assaying for sensitivity to epibrassinolide, was carried out. Increasing concentrations of epibrassinolide cause a reduction in root length in seedlings, however seedlings that are insensitive to brassinosteroids show a smaller reduction in root growth. *bak1-4* seedlings are partially insensitive to brassinosteroids, and over intermediate concentrations of epibrassinolide, their root length is significantly longer that Col-0 (Kemmerling et al., 2007). Fig. 4.6 shows that, although not as severe as the *bak1-4* phenotype, *da1-1* seedlings have a reduced sensitivity to epibrassinolide relative to Col-0 in epibrassinolide concentrations between 1nM to 100nM (Student's T-test, $p<0.02$). These data suggest that *da1-1* affects *sensitivity* to brassinosteroids, and therefore DA1 may be involved in fine-tuning the transduction of brassinosteroid signalling. Furthermore, based on a potential role for DA1 in FLS2 response signalling, this 'fine-tuning' may indicate a relationship between DA1 and BAK1.

One potential role of DA1 in LRR-RLK mediated signalling may involve the processing of ubiquitinated LRR-RLKs. Many plasma membrane signal receptors are internalised by endocytosis subsequent to activation by the signal ligand (Marmor and Yarden, 2004). This internalization can either lead to attenuation of signal transduction or the facilitation of a further signalling step once internalised. In both processes, following endocytosis a decision is made to direct the internalised signal receptor to the multivesicular body (MVB) for degradation, or to recycle the receptor back to the membrane (Marmor and Yarden, 2004). Many mammalian membrane receptor tyrosine kinases (RTKs) such as human epidermal growth factor receptor (EGFR) require ubiquitination for internalisation (Haglund et al., 2003), and others require ubiquitination of endocytotic machinery (Dunn and Hicke, 2001). The abundance of UIMs in proteins involved in the processing of RTKs in animal systems has led to the postulation of an 'UIM-cycle', where UIM-containing adaptor proteins recognise and mediate the internalisation of activated RTKs (Marmor and Yarden, 2004). The presence of an active UIM domain in DA1 indicates that DA1 may be involved in the ubiquitin mediated processing of LRR-RLKs, particularly in light of evidence that FLS2 is ubiquitinated (Lu et al., 2011).

4.4.1.3 – TMK4 (TRANSMEMBRANE KINASE 4)

BLAST analysis of the TMK4 protein sequence reveals that it is a member of sub-family IX of the LRR-RLK family and is most closely related to TRANSMEMBRANE KINASE1 (TMK1).

```
  1 MEAPTPLLLLVLLTTITFFTTSVADDQTAMLALAKSFNPPPSDWSSTTDFCKWSGVRCTG 60

 61 GRVTTISLADKSLTGFIAPEISTLSELKSVSIQRNKLSGTIPSFAKLSSLQEIYMDENNF 120

121 VGVETGAFAGLTSLQILSLSDNNNITTWSFPSELVDSTSLTTIYLDNTNIAGVLPDIFDS 180

181 LASLQNLRLSYNNITGVLPPSLGKSSIQNLWINNQDLGMSGTIEVLSSMTSLSQAWLHKN 240

241 HFFGPIPDLSKSENLFDLQLRDNDLTGIVPPTLLTLASLKNISLDNNKFQGPLPLFSPEV 300

301 KVTIDHNVFCTTKAGQSCSPQVMTLLAVAGGLGYPSMLAESWQGDDACSGWAYVSCDSAG 360

361 KNVVTLNLGKHGFTGFISPAIANLTSLKSLYLNGNDLTGVIPKELTFMTSLQLIDVSNNN 420

                                                        TMD>>
421 LRGEIPKFPATVKFSYKPGNALLGTNGGDGSSPGTGGASGGPGGSSGGGGSKVGVIVGVI 480

481 VAVLVFLAILGFVVYKFVMKRKYGRFNRTDPEKVGKILVSDAVSNGGSGNGGYANGHGAN 540

                                          KINASE DOMAIN>>
541 NFNALNSPSSGDNSDRFLLEGGSVTIPMEVLRQVTNNFSEDNILGRGGFGVVYAGELHDG 600

601 TKTAVKRMECAAMGNKGMSEFQAEIAVLTKVRHRHLVALLGYCVNGNERLLVYEYMPQGN 660

661 LGQHLFEWSELGYSPLTWKQRVSIALDVARGVEYLHSLAQQSFIHRDLKPSNILLGDDMR 720

                          |-----------------------------------
721 AKVADFGLVKNAPDGKYSVETRLAGTFGYLAPEYAATGRVTTKVDVYAFGVVLMEILTGR 780

    --------Yeast-2-Hybrid Fragment (185aa)----------------------
781 KALDDSLPDERSHLVTWFRRILINKENIPKALDQTLEADEETMESIYRVAELAGHCTARE 840

    ------------------------------------------------------------
841 PQQRPDMGHAVNVLGPLVEKWKPSCQEEEESFGIDVNMSLPQALQRWQNEGTSSSTMFHG 900

    ----------------------------|
901 DFSYSQTQSSIPPKASGFPNTFDSADGR* 929
```

Figure 4.7 – Protein sequence of AT3G23750

The protein sequence of AT3G23750 (TMK4) with the transmembrane domain (TMD) marked in blue, the kinase domain marked in red, and the fragment identified in the DA1 Y2H marked with a superjacent dashed line ('|----|').

TMK4 has recently been identified as a positive regulator of growth and development through the study of combinational knockouts mutations with its most closely related proteins (Dai et al., 2013). *tmk1/tmk4* double mutants display reduced root and aerial organ size, and a dwarf-like phenotype. All of these phenotypes are more severe in the *tmk1/tmk3/tmk4* triple and *tmk1/tmk2/tmk3/tmk4* quadruple mutants (Dai et al., 2013). The reduced root length in these mutants is primarily a consequence of reduced cell expansion, however the reduction in leaf area is primarily a consequence of reduced cell proliferation (Dai et al., 2013). Dai et al (2013) also demonstrated that *tmk1/tmk4* mutants had reduced sensitivity to auxin (reminiscent of *da1-1* and *bak1-4* to brassinosteroids), and that the *tmk1/tmk3/tmk4* triple mutant is insensitive to auxin.

Recent data also revealed that TMK4 may be involved in the flg22 PAMP response. flg22 treatment of Arabidopsis cell cultures resulted in the enrichment of TMK4 in lipid rafts with FLS2 (Keinath et al., 2011).

4.4.2 – DA1 physically interacts with the C-terminal fragment of TMK4

Sequencing of the Y2H colony 14 (Table 4.1) revealed that the 185aa C-terminal fragment of TMK4 (Fig.4.7) was fused in-frame to the GAL4-AD. The fragment extends from the extreme C-terminus of TMK4 into the kinase domain (Fig. 4.7). Subsequent to identification of the interacting colony containing a region of TMK4, the gene fragment was cloned and re-transformed into yeast and a second-round screen was run. Fig. 4.11 shows the positive drop test results, demonstrating that only yeast containing both pDBleu-*DA1* and pEXPAD-502-TMK4frag could grow on SC-Leu-Trp-His-Ade selective media.

Following confirmation of the interaction in yeast, the TMK4 C-terminal fragment was cloned into the pETnT bacterial expression vector and expressed in *E. coli* as an N-terminal HA epitope fusion protein for *in vitro* coIP analysis.

Following the procedure described in section 3.2.2; recombinant GST-tagged bait proteins were incubated with recombinant HA-tagged prey proteins before precipitation of GST-tagged bait proteins on glutathione sepharose beads. The purified proteins were then eluted and subjected to SDS-PAGE and immunoblot analysis. The ability of DA1 to form a homo-oligomer was utilised to design a positive control of GST-DA1 vs FLAG-DA1. Two sets of negative controls were also used; these were GST- Ø vs FLAG-TCP15, and GST-DA1 vs HA- Ø. Fig. 4.9 shows that GST-DA1 is able to pull down HA-DA1 (positive control) and the HA-tagged TMK4 C-terminal fragment. GST alone did not pull-down the HA-tagged DA1 protein.

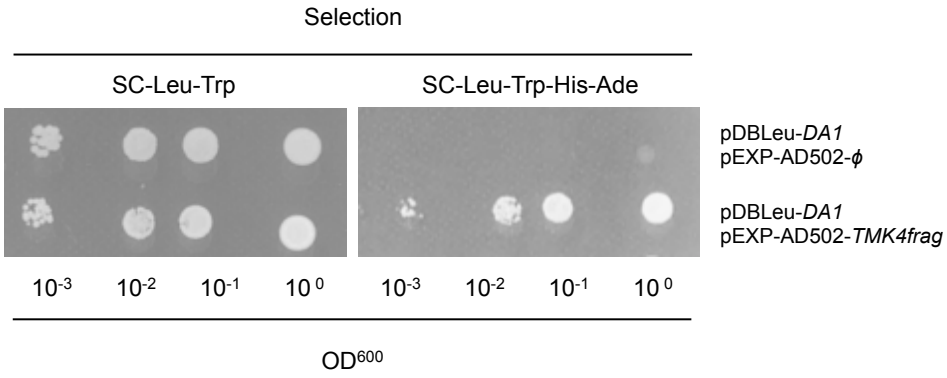

Figure 4.8 – In yeast drop-test: DA1 interacts with the C-terminus of TMK4

Yeast co-expressing pDBLeu-DA1 and pEXP-AD-502-TMK4frag (C-terminal fragment of TMK4) were able to grow on $SC^{-Leu-Trp-His-Ade}$ medium, demonstrating a physical interaction. The negative control, DA1 with empty vector, was unable to grow on $SC^{-Leu-Trp-His-Ade}$ medium. Both treatments were able to grow on $SC^{-Leu-Trp}$ medium, demonstrating that both bait and prey constructs were being expressed.

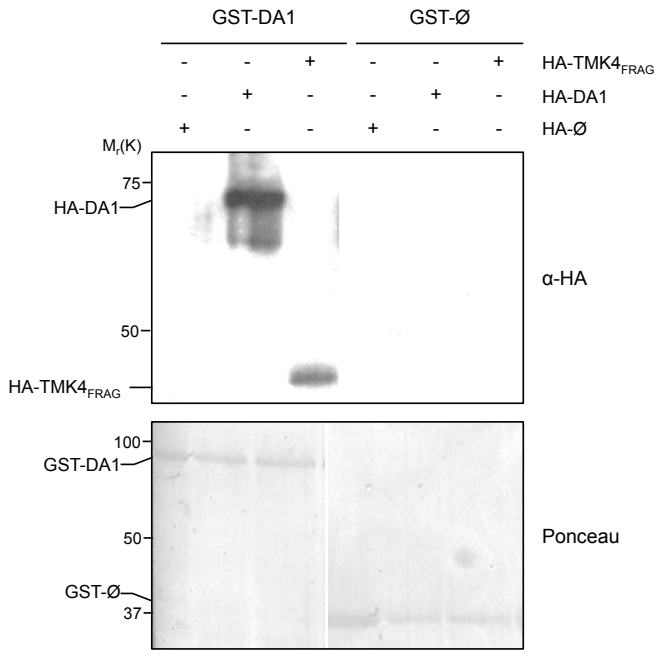

Figure 4.9 – DA1 interacts with TMK4 *in vitro*

E. coli expressed GST-tagged bait proteins were incubated with *E. coli* expressed HA-tagged prey proteins before purification on glutathione sepharose beads and immunoblotting for HA. HA-$TMK4_{FRAG}$ co-purified with GST-DA1 (lane 3) but not with GST-Ø (lane 6).

4.4.3 – Cloning of full-length TMK4

Repeating the Y2H and *in vitro* interaction studies (section 4.4.2) with a full-length TMK4 protein would confirm that the observed interaction is not an artefact of the truncated protein. PCR amplification of the 2.8 Kb coding sequence of *TMK4* from cDNA was straightforward. However upon subcloning the construct into *E. coli*, no intact full-length clones were recovered. This may be because the cells were unable to tolerate the kinase domain of TMK4, perhaps reflected in the fact that any full-length genes that were successfully cloned were extensively mutated in the C-terminal kinase domain. Despite employing strategies involving two-step cloning of the gene and the growth of *E. coli* at 28°C, no full-length non-mutated construct could be stably maintained in *E. coli*.

An alternative strategy to validate the observed in yeast and *in vitro* interactions was to carry out an *in planta* co-IP (see Box 3.1) with full-length protein. In order to achieve this, and thereby avoid the problems with the accumulation of *E. coli* derived mutations in the kinase domain, the genomic DNA was used and the gene was cloned with its intron intact. Unfortunately TMK4 only has one intron, located downstream of the kinase active site. Despite the absence of a bacterial promoter and the growth of bacteria at 28°C, the kinase domain still accumulated mutations. This meant that despite occasionally successfully sub-cloning a full-length intact gene into an entry vector (pDONR), the additional cloning steps into the destination vector led to mutations in the kinase domain. For this reason, and due to progress made in other areas, validation of the observed interaction with DA1 (section 4.4.2) was not carried out with full-length protein.

4.4.4 – amiRNA *TMK4* knockdown lines reveal developmental defects

For genetic analysis of TMK4, T-DNA insertion lines were acquired to assay for developmental phenotypes and a putative genetic interaction with *DA1.* Unfortunately, at the time this work was carried out no TMK insertion lines were publicly available. As a consequence an amiRNA knockdown approach was taken.

An amiRNA construct was acquired from the *Arabidopsis thaliana* amiRNA library at Open Biosystems (Thermo Scientific). The library was developed by Dr. Greg Hannon at Cold Spring Harbour laboratories and the amiRNA design is based on work by Detlef Weigel at the Max Planck Institute for Developmental Biology (Open_Biosystems). Based on this, the construct was designed to be targeted specifically to *TMK4* and none of its closest relatives (Schwab et al., 2006).The amiRNA construct is expressed in a mi319a backbone, under the control of a 35S promoter, in the pAmiR binary vector (see supplementary information Fig. S1).

Wild-type Col-0 plants were transformed with this construct and transformants assessed for their phenotypes. Fig. 4.13 shows the phenotypes of four T1 amiRNA transformants. Preliminary observations showed that these T1 plants exhibited severe developmental defects, ranging from dwarfed overall stature and serrated leaves, to later flowering with rounder leaves. It is possible that the differences in severity of phenotype are due to variation in the level of amiRNA expression. The different phenotypes depicted in Fig. 4.13 shows that the amiRNA construct strongly influences plant development. These data show that amiRNA knockdown of TMK4 largely phenocopies the *tmk1/tmk4, tmk1/tmk3/tmk4* and *tmk1/tmk2/tmk3/tmk4* mutants (Dai et al., 2013). It is interesting that the variation in developmental defects is not simply a linear escalation of a particular phenotype (for example leaf curling), but rather a wide variety of different phenotypes of varying severity. This implies that TMK4 may have a general, higher-order role in regulating growth and development, and as its expression is reduced, its effect becomes more severe and pleiotropic.

Due to progress being made in other areas of my research, further investigation of this area was not continued. The Y2H and *in vitro* data provide strong evidence of an interaction between DA1 and TMK4, and amiRNA knockdown and mutant (Dai et al., 2013) phenotypes show that TMK4 is a promoter of growth and development. Taken together with predictions that *DA1* is involved in the flg22 response (Fig. S2), and that *da1-1* seedlings are partially insensitive to epibrassinolide (Fig. 4.6), it is possible that DA1 may be involved in the processing of LRR-RLKs. Moreover, based on work in animal systems highlighting the importance of UIM-containing proteins in the processing of RTKs (Marmor and Yarden, 2004), and *in vitro* evidence that DA1 binds to the cytoplasmic domain of TMK4 (Fig. 4.9), it is reasonable to suggest a model whereby DA1 is involved in the ubiquitin-mediated regulation and processing of LRR-RLKs. The UIM-cycle postulated by Marmor and Yarden (2004) implies that DA1 may play a role as an ubiquitin-targeted adaptor protein, however recent data showing that FLS2 is ubiquitinated by the E3 ligases PUB12 and PUB13 in a BAK1-dependent manner (Lu et al., 2011) suggests another possibility. In light of data from Chapter 5 that demonstrates DA1 is able to proteolytically process two E3 ligases *in vitro* and *in planta*, it is possible that DA1 regulates the activity of E3 ligases recruited to process LRR-RLKs. Although PUB12 and PUB13 are not necessary for flg22 perception, they effect the *sensitivity* of perception (Marino et al., 2012, Lu et al., 2011). This is similar to the effect of *da1-1* on epibrassinolide perception, and presents an interesting and intriguing possibility that DA1 influences the activity of E3 ligases involved in the regulation of FLS2, BRI1 and TMK4 signalling.

Figure 4.10 – Preliminary evidence of developmental phenotypes of TMK4 amiRNA knockdown lines

Four T1 Col-0 lines expressing an AT3G23750 (TMK4) amiRNA knockdown construct. The plants exhibit a variety of developmental phenotypes including; dwarfed stature, and narrow and crinkly leaves. This figure presents preliminary data and contains only a subset of the transformants generated.

4.5 - Discussion

The Y2H screen described in this Chapter identified several interacting proteins that implicate DA1 in growth and development and possibly pathogen responses (Table 4.1). Two interacting proteins, TCP15 and TMK4, were selected for further study based on their potential links to growth and development *and* the flagellin PAMP response. For TCP15; a clear role in the regulation of cell proliferation and growth (Kieffer et al., 2011, Li et al., 2012, Uberti-Manassero et al., 2012, Steiner et al., 2012) has recently been combined with data from TCP14 (Mukhtar et al., 2011) and transcriptomic analysis (Maclean, unpublished) that suggests a role in the response to the bacterial elicitor flagellin. TMK4 has been demonstrated to negatively regulate cell expansion (in roots) and cell proliferation (in leaves) (Dai et al., 2013) and has a possible connection to FLS2 and the flagellin PAMP response (Keinath et al., 2011). Combined with evidence that *da1-1* partially phenocopies *bak1-4* in response to epibrassinolide (section

4.4.1.2), it may be that the LRR-RLK link provided by TMK4 can be extended to both FLS2 and BRI1. Future experiments, based on improved knowledge of DA1 function, will include detailed analyses of phenotypes and genetic interactions of the amiRNA lines and analysis of TMK4 protein levels, modifications and localization during organ growth.

Control of the cell cycle is fundamentally important for plant growth as it establishes the numbers and sizes of cells that comprise a growing organ. The interaction between TCP15 and DA1, and evidence that *TCP15* directly regulates the expression of key cell-cycle genes (Kieffer et al., 2011, Li et al., 2012), provides a promising link between DA1 function and the cell-cycle. The *da1-1* large organ phenotype is due to developing organs being mitotically active for longer (Li et al., 2008). The interaction of DA1 with a transcription factor that has been shown to repress cell proliferation in leaf and floral tissues (Kieffer et al., 2011) reveals a possible mechanism for this phenotype. However, the often-contradictory phenotypes revealed from genetic studies of *TCP15* (Fig. 4.5) (Kieffer et al., 2011, Li et al., 2012, Uberti-Manassero et al., 2012), have made it difficult to establish direct genetic evidence of a role of DA1 in TCP15 function. Speculatively, assuming that TCP15, as a canonical class I TCP, is a promoter of growth, and that the dependence of its function on DA1 indicated by the partial correlation analysis is correct, then a model can be proposed in which DA1 negatively regulates the growth promoting activity of TCP15. This model is supported by data showing a genetic interaction to regulate inflorescence stem height (section 4.3.3.1), but contradicted by data from other sources that report a growth repressing activity of TCP15 (Kieffer et al., 2011). Despite the uncertainty surrounding the details of the interaction, the observation that DAR1 has also been shown to interact with TCP14 (Mukhtar et al., 2011) supports the observed DA1-TCP15 interaction, generating important insight that may allow us to explain certain aspects of the *da1-1* phenotype.

The observation that DA1 physically interacts with the cytoplasmic domain of TMK4, an LRR-RLK, provides sufficient insight to be able to propose a tentative role for DA1 in LRR-RLK-mediated regulation of growth and development. The 'UIM-cycle' model for the ubiquitin dependent processing of RTKs in animal systems (Marmor and Yarden, 2004) predicts a role for DA1 as an adaptor protein in the internalisation or recycling of LRR-RLKs. However, evidence that the DA1 peptidase is active towards two E3 ligases (Chapter 5), and evidence that FLS2 is ubiquitinated by PUB12 and PUB13 (Lu et al., 2011), suggests that DA1 may be involved in the proteolytic regulation of E3 ligases involved in RLK-mediated signal transduction. Indeed, the way that PUB12 and PUB13 affect the *sensitivity* of the flg22

response (Marino et al., 2012, Lu et al., 2011) is reminiscent of how DA1 affects *sensitivity* of brassinosteroid perception (section 4.4.1.2). It is possible that ubiquitination of some LRR-RLKs is required for their activity and that DA1 acts to recruit and regulate E3 ligases at the cytoplasmic domain of the respective RLK. Due to the fact that BAK1 is involved in both the flg22 and brassinosteroid responses, it is tempting to speculate that DA1 also interacts with the C-terminal domain of BAK1.

Although it is possible that DA1 regulates TCP15 and TMK4 independently and at distinct cellular locations, it is also possible that DA1 interacts with both proteins in the same location. Evidence from animal systems reveals that the sterol regulatory element binding proteins (SREBPs), ER-membrane bound transcription factors, are 'activated' by a proteolytic cleavage event that liberates the DNA-binding domain from the membrane, before transition the nucleus (Brown and Goldstein, 1997, Eberle et al., 2004). This example suggests a possible mechanism of DA1 action, involving ligand binding of LRR-RLKs resulting in the RLK-proximal ubiquitin-mediated regulation of TCP15 activity. This model, although very speculative, is supported by strong evidence that TCP14 is a network hub in response to pathogen response (Mukhtar et al., 2011), and that TCP15 interacts physically with the E3 ligase PUB14 (Dreze et al., 2011). Detailed genetic analysis would help to dissect these interactions, but they may be very complex due to substantial genetic redundancy of *TCP* genes.

The suggestion that DA1 may play a role in growth and development and the pathogen response is supported by the identification of the E1-activating enzyme ATUBA1 in the Y2H screen. A 15bp deletion in the C-terminal region of ATUBA1 (named *mos5* (*modifier of snc1 5*)) was able to rescue the dwarf phenotype of the *npr1-1 snc1* double mutant, which has constitutively activated defence responses (Goritschnig et al., 2007). *mos5* has enhanced disease susceptibility, which suggests that ATUBA1 is involved in activating pathogen response pathways (Goritschnig et al., 2007). The ability of *mos5* to rescue the dwarf phenotype of the *npr1-1 snc1* double mutant suggests that ATUBA1 negatively regulates a growth control pathway (Goritschnig et al., 2007); something that is well characterised in defence responses (Gómez‐Gómez et al., 1999, Gómez-Gómez and Boller, 2000, Zipfel et al., 2006).

The regulation of a specific set of pathways by an E1-activating enzyme is surprising, seeing as specificity in the ubiquitination cascade is considered to be determined by E3 enzymes (Hershko and Ciechanover, 1998). Based on observations in Chapter 5, that reveal DA1 interacts with two E3 ligases, it is difficult to see how DA1 may also interact with an E1 enzyme. One explanation would be if the E1, E2 and E3 enzymes form a temporary complex that

shuttles ubiquitin through the ubiquitin cascade to the substrate. Regardless of the explanation, the identification of ATUBA1 as an interactor of DA1 unifies the ubiquitin system, the pathogen response, and growth and development pathways; all pathways that DA1 has been links to.

Other candidate DA1-interacting proteins from the Y2H screen include the Class III homeodomain-leucine zipper (HD-Zip III) protein ATHB8 (HOMEOBOX GENE 8), which is part of a small gene family shown to be involved in leaf development, meristem regulation, vascular development and auxin transport (reviewed in (Prigge et al., 2005)). *ATHB8* expression has been shown to promote cell differentiation during vascular development (Baima et al., 2001) and to be highly correlated with cell division in the developing vascular system (Kang and Dengler, 2002). Consistent with its role in vascular development, there is also evidence that *ATHB8* expression is positively regulated by auxin (Baima et al., 1995, Mattsson et al., 2003). In addition, there is evidence that *ATHB8* antagonises the effect of *REVOLUTA* (*REV*), and promotes meristem and floral organ development (Prigge et al., 2005). The fact that this growth promoting transcription factor is auxin-responsive (Baima et al., 1995, Mattsson et al., 2003), presents the possibility that it may operate in a similar pathway to TMK4, which is involved in auxin sensing (Dai et al., 2013). It is therefore conceivable that any interaction between DA1 and ATHB8, may be related to the DA1-TMK4 interaction.

Also identified in the first round of the Y2H screen was *LOB DOMAIN-CONTROLING PROTEIN 41* (*LBD41*), related to the LOB-domain containing protein, *ASYMMETRIC LEAVES 2* (*AS2*), which affects leaf lobing, petiole length and the ectopic formation of leaflet-like structures (Semiarti et al., 2001). The *LBD41* homolog in *Celosia cristata* has also been shown induce leaf lobing and ectopic leaf blade formation on the petiole (Meng et al., 2010). This is possibly due to a similar repression of *KNOX* gene activity as that seen with *AS2* (Guo et al., 2008, Hay et al., 2006).

4.5.1 – DA1, TCP15 and the chloroplast: a role in retrograde signalling?

Finally, the abundance of chloroplast localised proteins in the Y2H screen (Table 4.1) suggests that DA1 may function in the chloroplast. Recent work by Andriankaja et al (2012) revealed that the cell proliferation arrest front appears to be induced by chloroplast retrograde signalling. It was shown that genes involved in the synthesis of chlorophylls and hemes, whose action is thought to promote retrograde signalling (Voigt et al., 2010), were up-regulated prior to the onset of cell expansion (Andriankaja et al., 2012). It was also shown that the group of

genes that was differentially expressed during the transition from cell proliferation to expansion was enriched in for genes also shown to be differentially regulated in response to Norflurazon (NF), a chemical inhibitor of chloroplast differentiation (Andriankaja et al., 2012). Moreover, the transition from cell proliferation to cell expansion in the leaf tip was inhibited when NF was applied (Andriankaja et al., 2012), further supporting a role of chloroplast retrograde signalling in the promotion of cell expansion in the developing leaf.

Although the precise details of chloroplast retrograde signal *transduction* remain unclear (Nott et al., 2006, Leister, 2012, Caldana et al., 2012), reactive oxygen species (ROS), tetrapyrrole biosynthesis and plastid gene expression are all thought to play a role in signal initiation (Galvez‐Valdivieso and Mullineaux, 2010, Voigt et al., 2010). As the onset of the cell-proliferation arrest front is delayed in *da1-1* organs, it is possible that *DA1* acts to promote the onset of arrest and thereby accelerate the transition from proliferation to expansion across the developing organ. It is possible that *DA1* might promote this transition by promoting chloroplast retrograde signalling. This hypothesis is supported by preliminary data from the Y2H screen, which shows that DA1 interacts with 15 chloroplast localised proteins including, FERREDOXIN 2 and PSAE-1 (Fig. 4.3), both of which are involved in linear photophosphorylation (Allen, 2003, Nott et al., 2006). Interference with linear photophosphorylation can induce the rapid accumulation of singlet oxygen ($^1O_2$), which is thought to be involved in initiating retrograde signalling (Galvez‐Valdivieso and Mullineaux, 2010). This suggests that any DA1-mediated inhibition of either FERREDOXIN or PSAE-1 might promote retrograde signalling and therefore promote the onset of the cell proliferation arrest front. Additionally, because TCP15 is predicted to be localised to the chloroplast (Wagner and Pfannschmidt, 2006), it is possible that DA1-TCP15 interactions might promote the expression of chloroplast genes, and thereby activate retrograde signalling (Voigt et al., 2010).

Consistent with the possibility that DA1 promotes retrograde signalling through elevated ROS levels, is evidence from microarray analyses that shows enhanced expression of *FSD1* (IRON SUPEROXIDE DISMUTASE 1) in *da1-1* plants (Yunhai Li, personal communication). FSD1 is involved in protecting chloroplasts from oxidative stress (Myouga et al., 2008) and is involved in de-toxifying $^1O_2$ by converting it to H_2O_2; the first of a two-step pathway resulting in H_2O. It may be, therefore, that *DA1* negatively regulates *FSD1*; thereby promoting $^1O_2$-induced retrograde signalling and positively regulating the arrest front.

Chapter 5 - DA1 is an ubiquitin-activated peptidase

5.1 – Introduction

This chapter identifies functions of the DA1 metallopeptidase domain and its role in the processing and regulation of E3 ligases. Through a combination of genetics and biochemistry, these experiments identify the E3 ligases EOD1 and DA2 as targets of DA1 peptidase activity, and reveal a novel mechanism for the ubiquitin-dependent peptidase-mediated regulation of E3 ligases.

5.1.1 – E3 Ligases: a diverse group of proteins unified by functional similarity

The final step in the ubiquitin cascade (see section 1.7) is the targeted transfer of E2-conjugated ubiquitin molecules to substrate proteins. E3 ubiquitin ligases are responsible for determining the specificity of this E2-mediated ubiquitin transfer; a centrally important function consistent with the identification of 1415 E3 ubiquitin ligases in Arabidopsis (Mazzucotelli et al., 2006). In the most general terms, an E3 ubiquitin ligase is an enzyme that facilitates, directly or indirectly, the transfer of E2-conjugated ubiquitin molecules to a specific substrate. However despite this functional conservation, E3 ligases are an exceptionally diverse group of enzymes. According to their protein structures, there are two general groups of E3 ligase: monomeric E3s, where E2-binding domains and substrate binding domains are on the same polypeptide; and multimeric E3s, which consist of an E2-interacting module and a target-specifying module joined by a CUL (CULLIN) or CUL-like protein (Mazzucotelli et al., 2006) (Fig. 5.1).

E3 ligases can also be categorized according to their E2-binding domains. These are either a HECT (Homology to E6-AP C-Terminus) domain or a RING (Really Interesting New Gene)/U-box domain. All HECT E3s, including UPL3 (UBIQUITIN PROTEIN LIGASE 3) - a regulator of trichome development in Arabidopsis (Downes et al., 2003), are monomeric E3s; whereas RING E3s exist as both monomeric E3s and as subunits in multimeric modular E3 complexes (Mazzucotelli et al., 2006). Some RING E3s, such as BB/EOD1 (Disch et al., 2006) and the negative regulator of ABA signalling KEG (KEEP ON GOING) (Stone et al., 2006), as well as the closely related PLANT U-BOX (PUB) E3s, including PUB12 and PUB13 (Lu et al., 2011), are single polypeptide E3s. In contrast the RING protein atRBX1 (RING BOX PROTEIN1), the knockdown of which causes severe developmental phenotypes such as poorly developed leaves and loss of apical

dominance (Lechner et al., 2002), is part of a multimeric E3 ligase. RBX1 is the E2-binding subunit of SCF (SKP1-CULLIN-F-BOX), CUL3-BTB/POZ (CULLIN-3 – BRIC-A-BRAC, TRAMTRACK and BROAD COMPLEX/POX VIRUS and ZINC FINGER), and CUL4-DDB1 (UV-DAMAGED DNA-BINDING PROTEIN1) E3 ligases; henceforth termed the cullin-ring ligases (CRLs) (Mazzucotelli et al., 2006). All E3 ligases, except HECT E3s, coordinate the ligation of the E2-conjugated ubiquitin to the substrate, without themselves covalently binding the ubiquitin. HECT E3 ligases, however, form a thioester intermediate with the ubiquitin molecule before transfer of the ubiquitin moiety, by ligation, to the substrate (Hershko and Ciechanover, 1998).

The modular nature of multimeric E3 ligases and the diversity of their subunits generates a large number of substrate specificities. Indeed, the most abundant E3 subgroup in Arabidopsis, with 724 members, is that of the F-BOX proteins (Mazzucotelli et al., 2006). F-BOX proteins are the substrate binding modules of the SCF-type E3 ligases, which determine the target specificity of the multimeric E3s. They have been identified to play a role in many developmental processes in Arabidopsis. For example, the F-BOX protein UNUSUAL FLORAL ORGANS (UFO) is a regulator of floral development and meristem identity (Levin and Meyerowitz, 1995); and SLEEPY1 (SLY1) is a positive regulator of gibberellin signalling (Dill et al., 2004, McGinnis et al., 2003).

5.1.2 – Regulation of E3 ligase activity

Ubiquitination of a target protein often leads to its irreversible destruction by targeting to the proteasome (Glickman and Ciechanover, 2002, Hochstrasser, 1996). In the cell cycle for example, ubiquitin-mediated protein destruction ensures unidirectional cell-cycle progression. Examples of this include the APC (anaphase promoting complex) mediated ubiquitination of A- and B-type cyclins and the SCF-mediated ubiquitination of D-type cyclins (Dewitte and Murray, 2003). To enable these cellular decisions to be executed quickly and completely, pools of E3 ligase enzymes are often pre-existing and tightly regulated (Peters, 2006). For this reason E3 ligases are subject to a large amount of regulatory post-translational modification.

The activity and specificity of multimeric E3 ligases is dependent on the presence of all required subunits, and mechanisms that interfere with, or enhance subunit assembly can act as regulators of E3 ligase activity. In humans, the inhibitory CAND1 (CULLIN-ASSOCIATED AND NEDDYLATION-DISSASSOCIATED) protein competes with the substrate recognition module (e.g. DDB1) for the binding of the E2-binding module (CUL1/RBX), thus preventing complex formation and repressing E3 function (Zheng et al., 2002). Conversely, there is also evidence

that the dimerisation of CRL subunits can result in an increased concentration of E2 and substrate, and thereby increase E3 activity (Merlet et al., 2009).

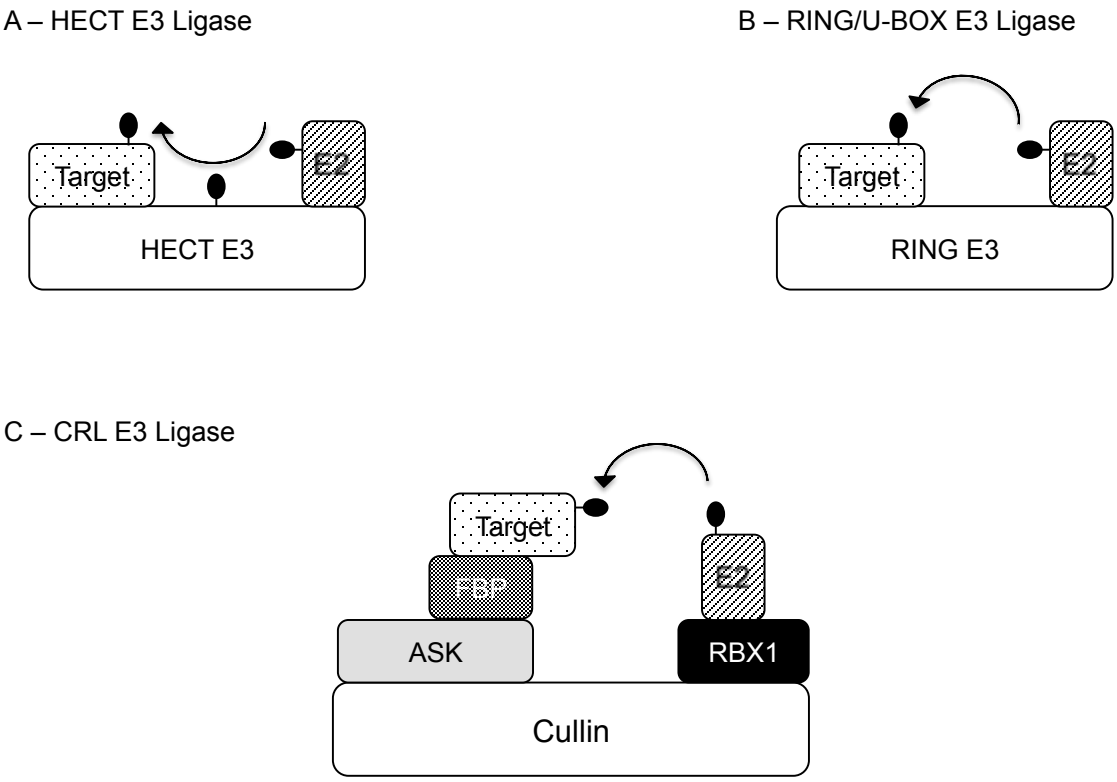

Figure 5.1 – Three different classes of E3 ligases

(A-C) A simplified classification of E3 ligases into three key classes. (A) HECT E3 ligases are monomeric and form a thioester intermediate with the ubiquitin molecule (black ellipse) prior to ligation. (B) The RING/U-BOX family of E3 ligases can also be monomeric, but do not form a thioester intermediate with ubiquitin during the ligation reaction. (C) CRL E3 ligases are multimeric protein complexes, with specific E2-binding and substrate-binding modules. CRL E3 ligases do not directly interact with ubiquitin during the ligation reaction.

In addition to regulating subunit availability, post-translational manipulation of protein structure can also affect CRL activity. The ligation of the small ubiquitin related peptides NEDD8 (in mammals) and RUB (in plants) to the CUL backbone of CRLs has been shown to be sufficient to modify CUL tertiary structure and thereby alter its binding affinity to RBX1 (Duda et al., 2008, Biedermann and Hellmann, 2011). This results in a more flexible E2-binding module, reducing the distance from E2 to substrate, and enhancing E3 activity through the facilitation of multiple catalytic geometries (Duda et al., 2008, Merlet et al., 2009).

Similarly to CRLs, monomeric E3s are also regulated by a combination of post-translational modification and the availability of cognate substrate-binding adaptor proteins. For example, and perhaps comparable to the neddylation of CRLs, poly-ubiquitination of monomeric E3s, such as the auto-ubiquitination of the human BRCA1/BARD1 complex, has been shown to stimulate E3 activity (Mallery et al., 2002). In contrast, poly-ubiquitination of the human RING E3, MDM2 is a repressive signal, and the activity of this enzyme is regulated by the antagonism of its auto-ubiquitination by the de-ubiquitinating activity of its cognate DUB; USP2a (Fang et al., 2000, Stevenson et al., 2007). It has also been shown that post-translational modification of the Human E3 ligase, PARKIN is sufficient to de-repress the enzyme and alter its specificity. PARKIN exists in an auto-inhibitory state that can be released *in vitro* by the addition of N-terminal epitope tags (Burchell et al., 2012), and can be converted from a mono-ubiquitin ligase to a poly-ubiquitin ligase by an N-terminal truncation *in vitro* (Chew et al., 2012). Together these data suggest that E3 ligases can contain auto-inhibitory domains, which may be removed through cleavage of, or steric interference with the inhibitory region.

In addition to the steric activation of E3 ligases, there is also evidence that proteolytic processing of E3s can cause their activation by re-localisation. The membrane localised Human PA-TM-RING E3 ligase, RNF13, is cleaved at its trans-membrane domain, which releases the C-terminal RING-containing domain to the cytoplasm (Bocock et al., 2010). This re-localisation may be required to bring it into contact with its substrate, and therefore may be essential to *activate* the enzyme.

For monomeric E3s, the availability of adaptor proteins also provides an additional level of regulatory control. An extreme example of this is the human HECT E3 ligase, SMURF2, a regulator of TGF-β endocytosis. Its cognate adaptor, SMAD7, acts as an additional E2 binding site, increasing the affinity for the E2 and thereby enhancing its ligase activity (Ogunjimi et al., 2005). Also, and comparable to the dependence on the availability of substrate-binding modules in modular E3s, the yeast E3 ligase RSP5 requires an adaptor protein complex for

target specificity (Léon and Haguenauer-Tsapis, 2009). In this example three proteins – BSD2, TRE1 and TRE2 – interact to target RSP5 to its substrate; SMF1 (Stimpson et al., 2006, Hettema et al., 2004). Finally, highlighting the diverse regulatory roles carried out by adaptors, SMAD7's interaction with SMURF2 also causes the re-localisation of the E3 ligase from the nucleus to the cytoplasm and plasma membrane (Kavsak et al., 2000), and disrupts its native autoinhibitory conformation (Wiesner et al., 2007).

5.1.3 – Ubiquitin chains: a diversity of signalling modifications

Ubiquitin modifications occur in a variety of forms ranging from mono-ubiquitination to long-chain poly-ubiquitination (Pickart and Fushman, 2004, Ikeda and Dikic, 2008, Kerscher et al., 2006). Mono-ubiquitination is chiefly used as a reversible post-translational modification similar to that of phosphorylation, and its role in coupled mono-ubiquitination is discussed in more detail in section 3.1.1. This section will focus on the diversity in structure and function of poly-ubiquitin chains.

Poly-ubiquitin chains are formed through the creation of an isopeptide linkage between the C-terminal glycine of ubiquitin (Gly76) and a lysine residue on the preceding ubiquitin molecule (Pickart and Fushman, 2004). There are seven lysines in ubiquitin - K6, K11, K27, K29, K33, K48 and K63 – allowing for seven possible ubiquitin chain 'architectures'. Five out of the seven architectures have been detected in Arabidopsis in the following order of abundance: K48 >> K63 > K11 >> K33 > K29 (Saracco et al., 2009). In yeast, all seven linkages have been detected in the order of abundance: K48 > K63 & K11 >> K33, K27, K6 & (K29); with K29 linkages only being detected on proteins also ubiquitinated at K33 (Peng et al., 2003). The identification of all seven linkages *in vivo* suggests that all architectures are genuine signalling modifications. Linear poly-ubiquitin chains – where a peptide linkage forms between the α-amino group of Met1 of one ubiquitin and the α-carboxyl group of the C-terminal Gly76 of another (Rieser et al., 2013) – have also been identified in animal systems. These chains are formed through the linear ubiquitin chain assembly complex (LUBAC) (Kirisako et al., 2006), and are thought to be non-degradative signals involved in the regulation of proteins such as TUMOUR NECROSIS FACTOR RECEPTOR1 (TNFR1) (Rieser et al., 2013).

K48-linked poly-ubiquitin chains are generally accepted to be necessary for targeting proteins to the proteasome-mediated degradation pathway (Hershko and Ciechanover, 1998, Jacobson et al., 2009, Thrower et al., 2000), whereas other linkages are assumed to have non-degradative signalling functions. K63 linked ubiquitin has been shown to be non-degradative and necessary to regulate human pattern recognition receptor signalling (Kawai and Akira,

2010), as well as the activation of the CHK1 checkpoint kinase (Cheng et al., 2013b). The biological function of the other ubiquitin linkages is less well understood, although there is evidence that K29- and K33-linked ubiquitin are negative regulators of the human kinases NUAK1 and MARK1 (Al-Hakim et al., 2010). Interestingly, K29-linked ubiquitin has also been shown to play a significant role, alongside K48-linked ubiquitin chains, in signalling the proteasome-mediated destruction of DELLA proteins (Wang et al., 2009).

5.1.4 – EOD1/BB and DA2 are RING E3 ligases

EOD1/BB and DA2 are both RING-finger proteins that negatively influence the duration of proliferative growth in Arabidopsis (Disch et al., 2006, Xia, 2013). Original research demonstrated that EOD1 is an active E3 ligase *in vitro* and that it interacts with the E2 conjugating enzyme UBC10 (Disch et al., 2006).

eod1 null mutants have enlarged petals and sepals, and thicker stems than the wild-type; leaf size is not increased in these null mutants, but is decreased in overexpression lines, indicating that it acts as a negative regulator of growth (Disch et al., 2006). In the *eod1* loss of function mutant, the enlarged organs consist of an increased number of wild-type sized cells, which is a consequence of a prolonged duration of cell proliferation (Disch et al., 2006). *eod1* null mutants also have enlarged gynoecia, which occasionally form multiple carpels (Disch et al., 2006); they also have enlarged floral meristems, which sometimes results in the initiation of an additional petal (Yunhai Li, personal communication). These phenotypes are strikingly similar to those seen for *da1-1*. Moreover, in addition to sharing petal size, sepal size and stem thickness phenotypes, both mutants negatively influence organ growth through the same developmental mechanism- a reduction in the duration of cell proliferation.

da2-1 leaves and petals are also enlarged relative to the wild-type, with the enlarged organs consisting of an increased number of normally-sized cells (Xia, 2013). *da2-1* seeds are heavier that wild-type seeds, and have a size distribution that is different to the wild-type (more larger seeds and fewer smaller seeds) (Xia, 2013). Interestingly, the increase in seed size is maternally controlled and is a consequence of an increased duration of proliferation in the integuments (Xia, 2013). This is analogous to the large-seed phenotype of *da1-1* plants, which is also maternally inherited. Collectively these data demonstrate that *DA1*, *DA2* and *EOD1* negatively influence the duration of cell proliferation during organ growth. This is consistent with their high expression levels in proliferating tissues (Xia, 2013, Li et al., 2008, Disch et al., 2006).

eod1-2 and da2-1 do not genetically interact with each other to control organ and seed size, but they both have been shown to interact synergistically with *da1-1* to influence organ

growth (Li et al., 2008, Xia, 2013). Taken together, the biochemical, cell-biological and developmental similarities shared between DA1, and EOD1 and DA2 suggest that DA1 may influence the activities of both E3 ligases to regulate organ growth. Due to the initial characterisation being carried out with the *da1-1* allele only, it is not possible to determine whether the observed genetic interactions are with *DA1* specifically, or whether they are with the multimeric complex of DA1 family members with which the *da1-1* mutation is predicted to interfere. In order to elucidate this, it was important to initially determine genetic interactions between *da2-1* and *eod1-2* , and the *da1ko1* single loss of function mutant.

5.2 – DA1 interacts with EOD1 and DA2

DA1, *DA2* and *EOD1* are all negative regulators of growth as shown by the increased organ size of loss of function mutations (Li et al., 2008, Xia, 2013, Disch et al., 2006). *DA1* interacts synergistically with both *EOD1* and *DA2* to further negatively influence growth (Li et al., 2008, Xia, 2013), suggesting that they may work in a common mechanism in which one may enhance the function of the other. The ability of DA1 to bind ubiquitin (section 3.3), and the fact that EOD1 and DA2 encode E3 ligases, suggests that these synergic genetic interactions may result from the respective proteins functioning together in a complex.

5.2.1 – *DA1* genetically interacts with *EOD1* and *DA2* to influence seed and petal size

The original work that identified a genetic interaction between *DA1* and the DA1-interacting E3 ligases, EOD1 and DA2 (termed DIEs) was performed with the dominant negative *da1-1* mutant (Xia, 2013, Li et al., 2008). Work in section 3.2.2 identified that the dominant negative-interfering effect of this allele is likely to be due to the physical interaction of DA1 and DAR1 in an active complex. As such, it is possible that the DIEs interact with either DA1, DAR1 or both. In order to investigate whether the genetic interaction is with *DA1* specifically, a genetic analysis of *eod1-2* and *da2-1* with *da1ko1* (rather than with *da1-1*) was carried out.

5.2.1.1 – da1ko1 seeds and petals are significantly larger that Col-0

Seed and petal areas were measured using a high-resolution scanner and subsequent ImageJ analysis (see section 2.3.5.1 for details).

For each genotype, 20 petals were collected and placed – intact – on transparent adhesive tape and attached to a clean polished black background. Petal area was recorded using a high-resolution scanner following a protocol adapted from (Herridge et al., 2011). Images were

scanned, and areas were calculated using the ImageJ image analysis software (http://rsbweb.nih.gov/ij/links.html).

Seed areas were calculated using a similar method. However, due to their smaller size (relative to the fixed resolution of the scanner) the number of seeds in the sample was increased to n>100, and instead of adhering to tape, the seeds were scattered in a petri dish prior to scanning.

This method permitted extremely accurate measurements and was much more precise than previous seed-size analysis methods, which assessed differences in seed size through the *distribution* of seed size (Li et al., 2008, Xia, 2013). Instead of looking at the percentages of seeds in three or four different size categories, this method directly measured the area of individual seeds. It was also automated and therefore allowed the high throughput analysis of large datasets.

For these reasons, this analysis has revealed hitherto undetected phenotypes for *da1ko1* single knockout seeds and petals. Fig. 5.2 shows that *da1ko1* seeds (Student's T-test, p=0.043) and petals (Student's T-test, p=0.019) are significantly larger than Col-0. This result demonstrates that *DA1* is not 100% redundant with *DAR1*, and suggests that some DA1 function is independent of DAR1. Taken with evidence from section 3.2.2 confirming that DA1 can homo- and hetero-oligomerise, these data suggest that in some aspects of seed and petal size regulation, DA1 might function as a homo-oligomer.

5.2.1.2 – DA1 genetically interacts with EOD1 and DA2 to influence seed and petal size

In agreement with observations from Dish et al (2006) and Xia et al (in press), Fig. 5.2b shows that *eod1-2* and *da2-1* petals are significantly larger than Col-0 (Student's T-test, P<0.005). The data also show that *da1ko1/eod1-2* and *dako1/da2-1* petals are significantly larger than petals of *eod1-2* and *da2-1* plants (Student's T-test, P<0.001). Importantly, the increase in petal area (relative to Col-0) in *da1ko1/eod1-2* and *dako1/da2-1* plants is significantly larger than that of their constituent single mutations (Student's T-test, p<0.002) (Fig. 5.2e). This shows that there is a synergistic interaction between *da1ko1* and *eod1-2,* and between *da1ko1* and *da2-1*. This data builds on earlier observations that the DIEs synergistically interact with the *da1-1* allele, and demonstrates that they interact with *DA1* directly to set petal size.

eod1-2 was crossed with *dar1* and *da1ko1/dar1* plants in order to investigate whether *EOD1* also genetically interacts with DAR1. The data displayed in Fig. 5.2c confirm that in addition to

interacting with *da1ko1*, *eod1*-2 interacts with the *da1ko1/dar1* genotype. However, the data also reveal that there is no synergistic interaction between *dar1* and *eod1-2.* This shows that *EOD1* interacts specifically with DA1 to set petal size, and that the observed interaction with *da1-1* (Li et al., 2008) and *da1ko1/dar1* is dependent on the presence of a *da1* null allele.

Analysis of seed size phenotypes (Fig. 5.2) reveals that *EOD1* and *DA2* differentially regulate the setting of seed and petal size. Unlike for petals, *eod1-2* and *da2-1* have no effect on seed area. Interestingly, despite this lack of phenotype, the *da1ko1*/*eod1-2* and *da1ko1*/*da2-1* double mutants both have significantly larger seeds than the *da1ko1* single knockouts. Although not by definition a synergistic interaction, these data do appear to show that *eod1-2* and *da2-1* enhance the *da1ko1* seed area phenotype.

One reason for the different influence of *eod1-2* and *da2-1* on seed and petal growth may be the dramatically different development of these organs. In particular, compared to petals, seeds contain multiple tissue types and are developmentally influenced by two genotypes (see Box. 1.1). This developmental difference is supported by observations in Fig. 5e, which show crosses of *eod1-2* with *dar1* and *da1ko1/dar1* plants. These lines showed weak genetic interactions between *da1ko1* and *eod1-2,* and *dar1* and *eod1-2*, and a much stronger interaction between *eod1-2* and the *da1ko1/dar1* double-knockout genotype. This contrasted with the petal data, which showed that almost all of the increase in petal area in the *da1ko1/dar1/eod1-2* triple mutant was due to the *da1ko1/eod1-2* genotype. These observations suggest that while *EOD1* interacts specifically with *DA1* to set petal size, it interacts with both *DA1 and DAR1* to set seed size. Based on observations that DA1 and DAR1 can homo- and hetero-oligomerise *in vitro* (section 3.2.2), it is possible that *EOD1* interacts with a *DA1* homo-complex to influence petal growth, and a *DA1-DAR1* hetero-complex to influence seed growth.

These data show that *DA1* interacts synergistically with both *EOD1* and *DA2* in the setting of petal size. The absence of epistasis indicates that although in the same overall petal-size regulating pathway, the genes are not in a linear relationship, but rather they act together on a common target or in a common pathway. Importantly, the observed synergism also reveals that the interacting partners influence each other in a positive manner, suggesting that DA1 might enhance EOD1 and DA2 function, and *vice versa* (see Fig. 5.11).

There are two ways of explaining this synergistic, enhancing phenotype. Firstly, it is possible that DA1 and the DIEs function in 'parallel' pathways acting on a common target and do not

themselves physically interact. In this model, the observed genetic interaction would result from the downstream convergence of the two pathways, and the enhancing effect would be a consequence of the interaction of downstream proteins. An alternative model involves DA1 and the DIEs operating at the same step in a pathway through a physical interaction that enhances their collective function. These models were tested by determining if there were physical interactions between DA1 the DIEs.

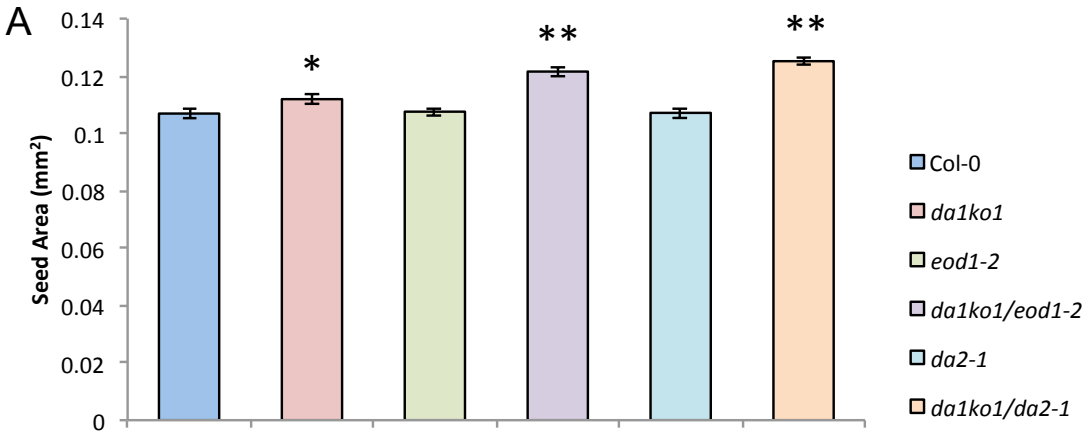
A
Seed Area (mm²)
0.14
0.12
0.1
0.08
0.06
0.04
0.02
0
*
**
**
Col-0
da1ko1
eod1-2
da1ko1/eod1-2
da2-1
da1ko1/da2-1

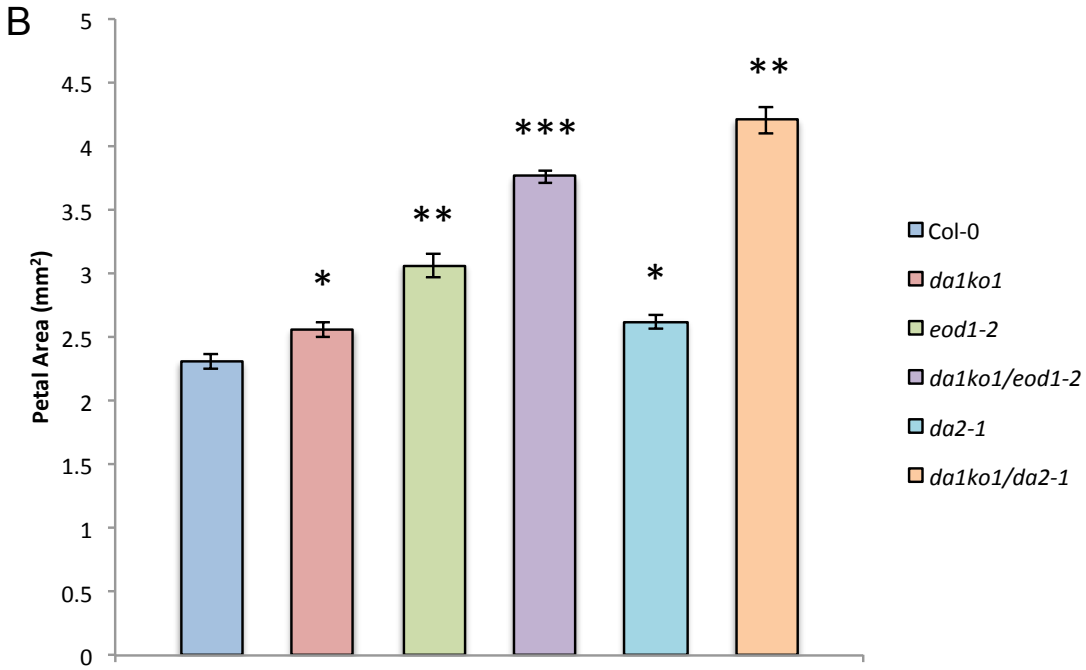
B
Petal Area (mm²)
5
4.5
4
3.5
3
2.5
2
1.5
1
0.5
0
*
**
***
*
**
Col-0
da1ko1
eod1-2
da1ko1/eod1-2
da2-1
da1ko1/da2-1

C

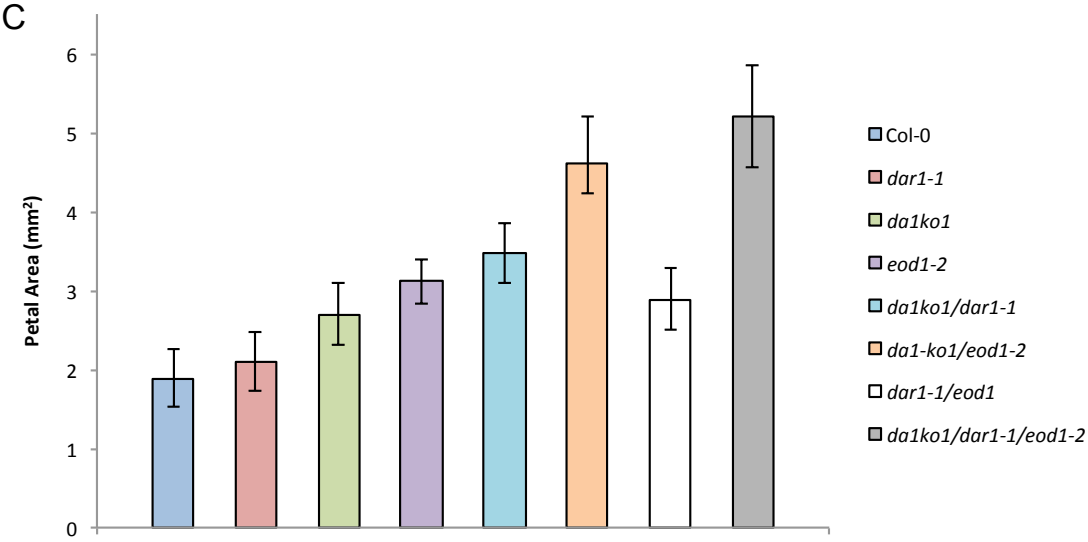
Petal Area (mm²)
0
1
2
3
4
5
6
Col-0
dar1-1
da1ko1
eod1-2
da1ko1/dar1-1
da1-ko1/eod1-2
dar1-1/eod1
da1ko1/dar1-1/eod1-2

D

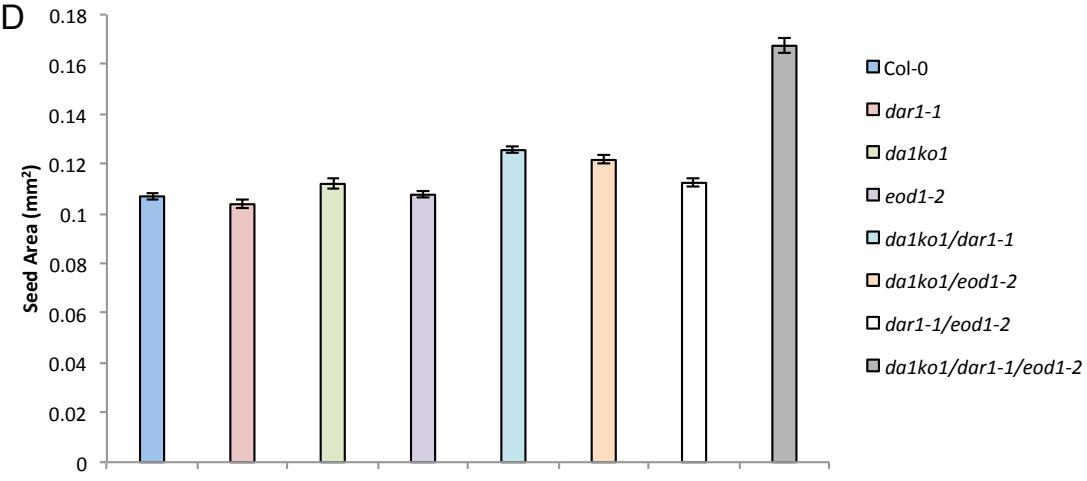
Seed Area (mm²)
0
0.02
0.04
0.06
0.08
0.1
0.12
0.14
0.16
0.18
Col-0
dar1-1
da1ko1
eod1-2
da1ko1/dar1-1
da1ko1/eod1-2
dar1-1/eod1-2
da1ko1/dar1-1/eod1-2

E

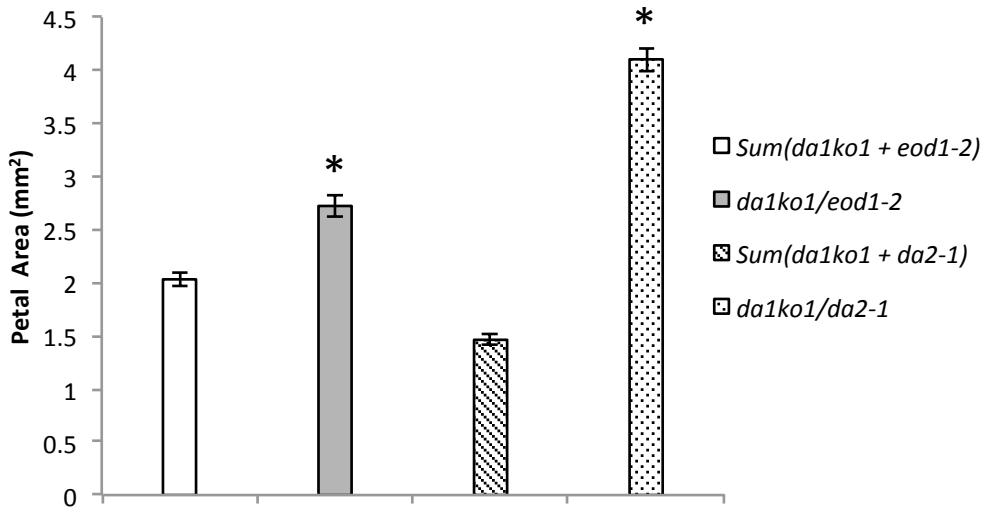

Figure 5.2 – Genetic interactions between *DA1*, *EOD1* and *DA2*

(A-B) *da1ko1* interacts with *eod1-2* and *da2-1* to regulate final seed (A) and petal (B) area. (A-E) Data are presented as means ± SE and significant values are according to Student's T-test ($p<0.05$). (A) *da1ko1* seeds are significantly larger than Col-0 (marked with '*'), and, while *eod1-2* and *da2-1* single mutants are not significantly different from *da1ko1*, *da1ko1/eod1-2* and *da1ko1/da2-1* seeds are significantly larger than *da1ko1* (marked with '**'). (B) *da1ko1* and *da2-1* petals are significantly larger than Col-0 (marked with '*'), but not significantly different from one another. *eod1-2* petals are significantly larger than *da1ko1* petals (marked with '**') and *da1ko1/eod1-2* petals are significantly larger than those of the *eod1-2* single knockout (marked with '***'). *da1ko1/da2-1* petals are significantly larger that *da1ko1* petals. (C) *eod1-2* interacts with *da1ko1* specifically, in the regulation of petal size. *da1ko1/eod1-2* petals are significantly larger that *eod1-2*, whereas *dar1-1/eod1-2* petals are smaller that eod1-2. While *da1ko1/dar1-1/eod1-2* petals are significantly larger than da1ko1/eod1-2 petals, their overall size is similar. (D) *da1ko1*, *dar1-1* and *da1ko1/dar-1* all interact with *eod1-2* to regulate seed area, however *da1ko1/dar1-1/eod1-2* seeds are considerably larger than *da1ko1/eod1-2* and *dar1-1/eod1-2* seeds. (E) The increase in petal area (relative to Col-0) in the double mutants *da1ko1/eod1-2* and *dako1/da2-1*, is significantly larger than the combined increases of the respective single mutants.

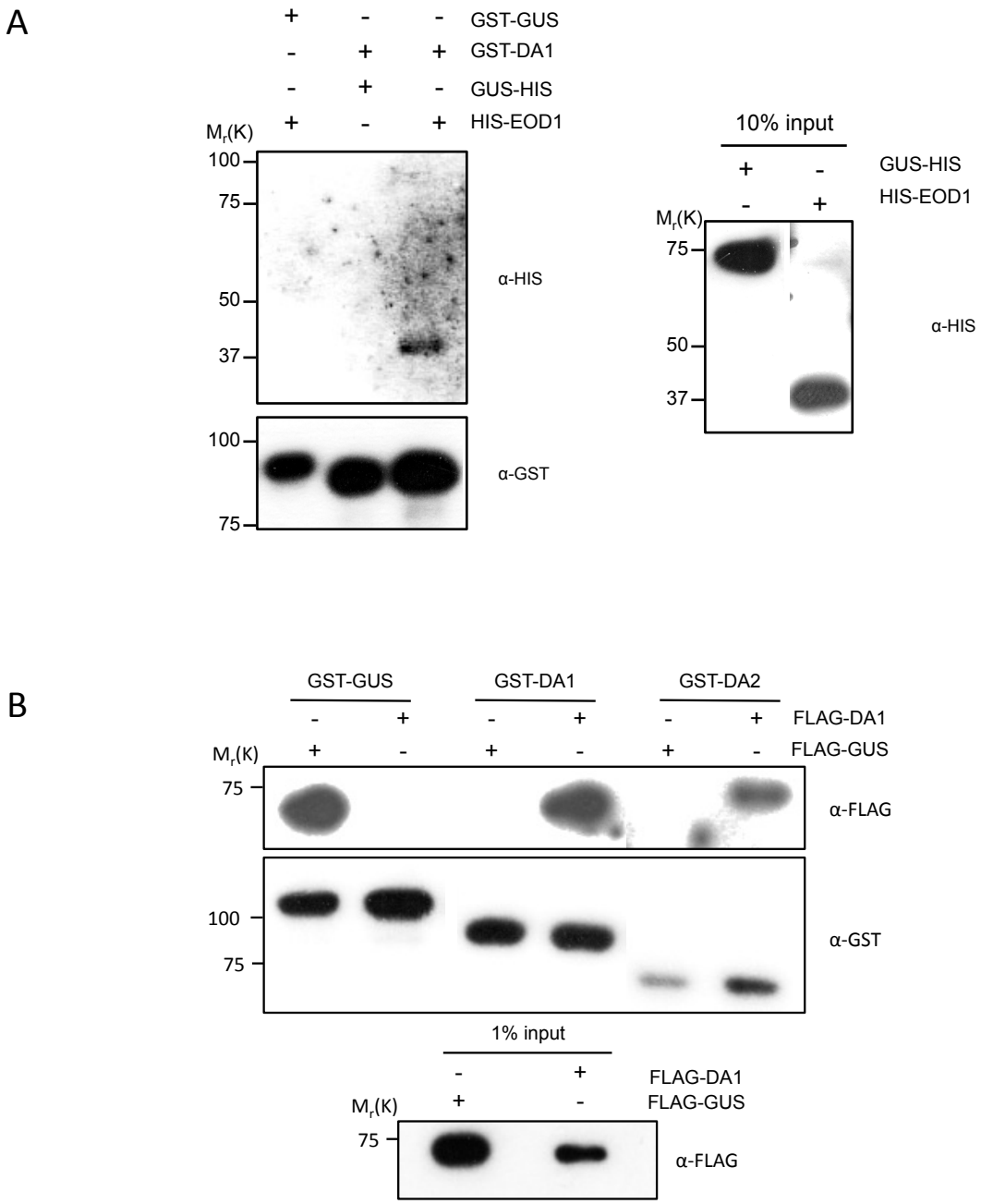

Figure 5.3 – DA1 interacts with EOD1 and DA2 *in vitro*

(A) *E. coli* expressed GST-tagged bait proteins were incubated with *E. coli* expressed HIS-tagged prey proteins before purification on glutathione sepharose beads and immunoblotting for GST and HIS. HIS-EOD1 co-purified with GST-DA1 (lane 3) but not GST-GUS (lane 1). (B) *E. coli* expressed GST-tagged bait proteins were incubated with *E. coli* expressed FLAG-tagged prey proteins before purification on glutathione sepharose beads and immunoblotting for GST and FLAG. FLAG-DA1 co-purified with GST-DA2 (lane 6), whereas FLAG-GUS did not (lane 5).

5.2.2 – DA1 physically interacts with EOD1 and DA2

The synergistic interactions between *DA1* and both DIEs suggested that DA1 and each E3 ligase function together to influence seed and petal growth. Because DA1 has a functioning UIM domain (section 3.3), and both DA2 and EOD1 are E3 ligases, a potential physical interaction based on this tentative biochemical association, was tested.

5.2.2.1 – DA1 interacts with EOD1 and DA2 in vitro

To test a possible physical interaction, an *in vitro* co-immunoprecipitation (co-IP) was carried out using *E. coli* expressed recombinant proteins. To assess a DA1 - EOD1 interaction, GST-DA1 was incubated with HIS-EOD1, before purification on glutathione sepharose beads and immunoblotting. As negative controls, GST-GUS was incubated with HIS-EOD1, and GST-DA1 with HIS-GUS. Fig. 5.3a shows that while there was no interaction between DA1 and GUS, or GUS and EOD1, GST-DA1 was able to pull down HIS-EOD1.

To assess a possible DA1 - DA2 interaction, GST-DA2 was incubated with FLAG-DA1. As negative controls, GST-GUS was incubated with FLAG-DA1, and GST-DA2 with FLAG-GUS. In addition, the homo-oligomerisation of DA1 and GUS was used to design two positive controls: GST-DA1 interacting with FLAG-DA1, and GST-GUS interacting with FLAG-GUS. Fig. 5.3b showed that, together with the GUS - GUS and DA1 - DA1 positive controls, the only positive interaction shown by pull-down was between GST-DA2 and FLAG-DA1.

These data demonstrated that DA1 interacts with both EOD1 and DA2 *in vitro*.

5.2.2.2 – DA1 interacts with EOD1 and DA2 in vivo

The *in vitro* data demonstrated a direct physical interaction between DA1 and both DIEs (see Box 3.1). To increase the biological significance of these observations, an *in vivo* assessment of the interaction was carried out. Due to the rapid turnover of DA1 and EOD1 in stable transgenic lines (Lena Stransfeld and Michael Lenhard, personal communication), a transient expression method using protoplasts and split-YFP bi-molecular fluorescence complementation was devised (see Box 3.1). In this experimental system, N-terminal and C-terminal fragments of YFP (YFPn and YFPc respectively) were fused to bait and prey proteins, which were co-transfected into protoplasts. When bait and prey proteins exist in close contact within the cell, the two fragments of YFP are able to re-form the functional protein and fluoresce. YFPn was fused to the N-terminus of DA1 and YFPc to the N-terminus of EOD1 and

DA2. YFPc was also fused to the N-terminus of ACLA2 (ATP-CITRATE LYASE2), which was used as a negative control for DA1 interactions.

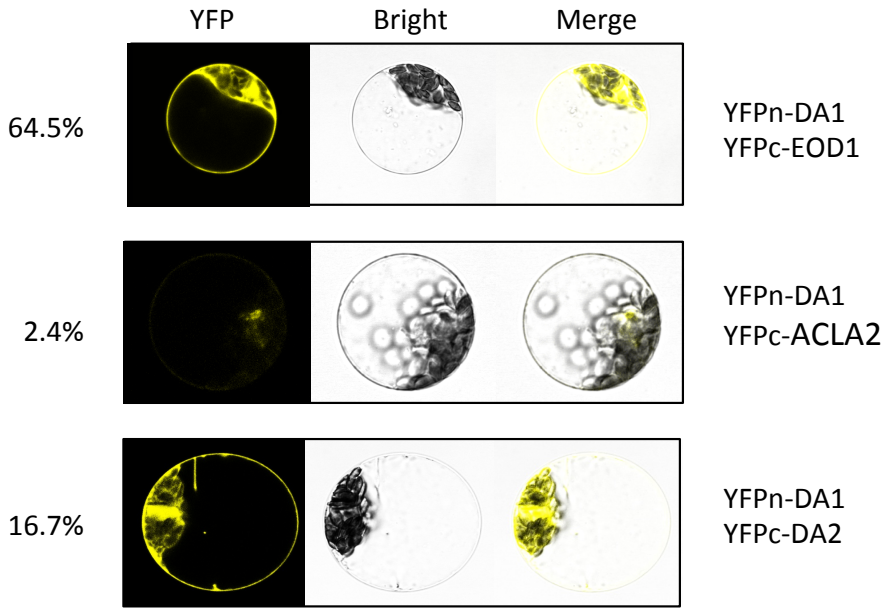

Figure 5.4 – DA1 interacts with EOD1 and DA2 *in vivo*

A protoplast split-YFP bi-molecular fluorescence complementation assay demonstrating DA1 interacts with EOD1 and DA2 *in vivo*. Protoplasts were co-transformed with bait (YFPn-tagged) and prey (YFPc-tagged) constructs. Strong YFP fluorescence can be seen in YFPn-DA1:YFPc-EOD1 and YFPn-DA1:YFPc-DA2 treatments, whereas only a weak background fluorescence was observed for the negative control (YFPn-DA1:YFPc-ACLA2). Percentage values correspond to the percentage of protoplasts fluorescing to level represented in the figure.

Fig. 5.4 showed that although there is a weak background interaction between DA1 and ACLA2, there is considerably stronger YFP fluorescence from the DA1-EOD1 and DA1-DA2 treatments. This demonstrates that in an *in vivo* system, DA1 is in sufficiently close contact with EOD1 and DA2 for the YFP fragments to create a functional protein. Although this did not prove that DA1 and the DIEs could form direct contacts, *in vitro* evidence in section 5.2.2.1 suggested that this was highly likely.

Additional support for these interactions comes from recent transient co-IP studies in *Nicotiana benthamiana* by Yunhai Li at the Chinese Academy of Sciences. These data show an interaction between DA1 and DA2 (Xia, 2013), and between DA1 and EOD1 (personal

communication). Taken together with the protoplast split-YFP studies and the *in vitro* physical interaction data, there is strong evidence that DA1 and DA2, and DA1 and EOD1 are *bona fide* physically interacting partners.

This physical interaction between DA1 and the DIEs reveals that the synergistic genetic interaction seen in section 5.2.1.2 may be a consequence of the direct physical interaction between DA1 and the E3s. This suggests that the enhancing phenotype measured in section 5.2.1.2 might be due to DA1 *directly* enhancing EOD1 and DA2 function and/or *vice versa*. Evidence that DA1 UIM2 binds mono-ubiquitin (section 3.3) and evidence that EOD1 and DA2 are both E3 ligases (Disch et al., 2006, Song et al., 2007) further suggest that this enhancing effect may involve ubiquitin-mediated mechanisms. In humans, the UIM-containing endocytic adaptor protein EPS15 is regulated by coupled mono-ubiquitination (van Delft et al., 1997, Woelk et al., 2006) and therefore it is possible that DA1 may be regulated by a similar ubiquitination event involving its cognate E3 ligases; EOD1 and DA2. Moreover, as DA1 contains a peptidase domain, it is possible that it is the putative peptidase activity that is regulated by EOD1 and DA2. Furthermore, and perhaps revealing a mutually enhancing interaction, it may be that DA1 enhances EOD1 and DA2 in a peptidase-dependent manner. To test these hypotheses, DA1 peptidase activity and its potential regulation by ubiquitination were tested.

5.3 –DA1 cleaves EOD1 and DA2 in a ubiquitin dependent manner

In vitro experimental evidence has shown that EOD1 is an active E3 ligase (Disch et al., 2006), and that DA1 non-covalently interacts with ubiquitin via its UIMs (section 3.3). These established links to the ubiquitin system provide a starting point for exploring and defining the mechanisms by which DA1 and EOD1, and DA1 and DA2 mutually enhance their activities as growth repressors. The *DA2* rice ortholog, *GW2* (*GRAIN WEIGHT2*), has been shown to be active as an E3 ligase *in vitro* (Song et al., 2007), but there was no evidence for the E3 activity of Arabidopsis DA2. In order to infer a mechanistic link between DA1 and DA2 it was important to first assay the activity of DA2 *in vitro*.

5.3.1 – DA2 is an active E3 ligase *in vitro*

Ubiquitination assays were carried out in a minimal *in* vitro system using only E1, E2, E3 and ubiquitin (see section 2.5.4), in which - as is typical for these assays - the ability of an E3 ligase to auto-ubiquitinate was considered to be evidence of its activity (Disch et al., 2006, Song et al., 2007, Zhang et al., 2005). Commercial E1 activating enzyme (Human UBE1) and ubiquitin (Human recombinant) were used in these assays. Based on its interaction and activity with

EOD1 (Disch et al., 2006), bacterially expressed Arabidopsis UBC10 (construct kindly provided by Michael Lenhard) was used as the E2-conjugating enzyme in these reactions. The three enzymatic components of the ubiquitin system were incubated with ubiquitin and ATP before an aliquot of the reaction was subjected to SDS-PAGE and immunoblot analysis.

Fig. 5.5 shows that in the presence of E1, E2 and ubiquitin, high molecular weight (80-140kDa) DA2 species are generated in a canonical 'ubiquitin smear'. These high molecular weight species are poly-ubiquitinated DA2, confirming that DA2 is able to auto-poly-ubiquitinate. The data in this figure are consistent with those from GW2 (Song et al., 2007), and confirm that Arabidopsis DA2 is an active E3 ligase *in vitro*.

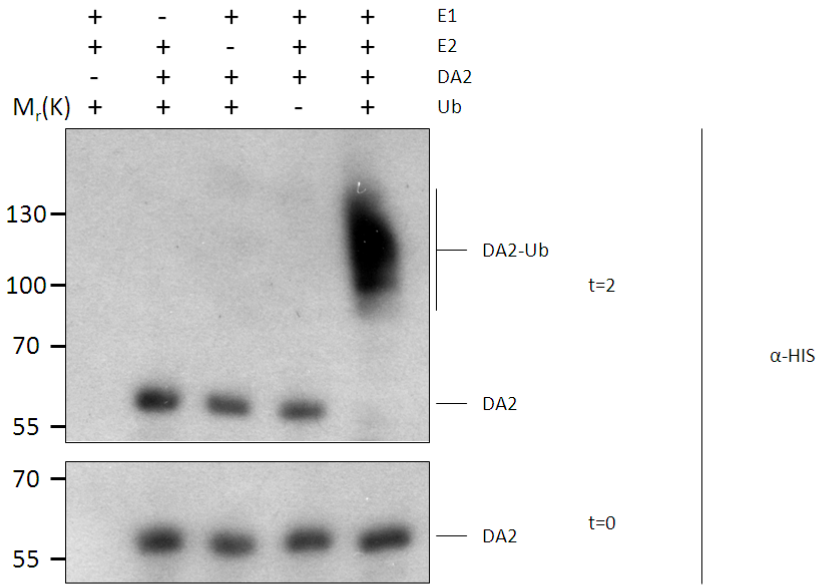

Figure 5.5 – Arabidopsis DA2 is an active E3 ligase *in vitro*

An *in vitro* ubiquitination assay Arabidopsis with DA2 as the E3 ligase. In the presence of E1 (human UBE1), E2 (GST-UBC10) and ubiquitin, DA2-HIS catalyses the formation of high molecular weight poly-ubiquitin chains (this figure was produced by Andrei Kamenski, a visiting undergraduate student).

5.3.2 – DA1 cleaves EOD1 in a ubiquitin-dependent manner

To determine whether DA1 cleaved EOD1, an ubiquitination assay was performed (as described in section 5.3.1) with the addition of purified bacterially-expressed FLAG-DA1. As with the ubiquitination assay in section 5.3.1, after the reaction was terminated, an aliquot was run on SDS-PAGE and subjected to immunoblot analysis. Consistent with earlier

observations (Disch et al., 2006) in the presence of E1, E2 and ubiquitin, HIS-EOD1 auto-ubiquitinated (Fig. 5.6a , lane 1). This Figure also shows that in the absence of ubiquitin (lanes 2 and 4) HIS-EOD1 remained stable (it was not degraded), even in the presence of DA1 (lane 4). However, in the presence of ubiquitin *and* DA1 (lane 3) HIS-EOD1 was no longer observed on the blot. Surprisingly, intermediate molecular-weight products, indicating degradation, were not visible in western blot experiments that used anti-HIS antibodies (to detect HIS-EOD1). As the EOD1 construct used in this assay had an N-terminal HIS tag, the disappearance of a HIS signal from the blot indicated that either the entire protein was being rapidly proteolytically digested, or that there was a single N-terminal cleavage event adjacent to the HIS tag (creating a small peptide that ran off the gel). In order to investigate this possibility, a new EOD1-HIS construct was generated with a HIS tag at the C-terminus.

With both DA1 and ubiquitin present in this assay (Fig. 5.6b lane 3), a lower molecular weight EOD1 species was visible, which had lost approximately 10kDa from its N-terminus. This showed that a 10kDa fragment was cleaved from the N-terminus of EOD1 by the action of DA1 and ubiquitin. The EOD1 vector used in this assay (pETnT (Fig. S1)) had an N-terminal HA-FLAG-tag as well as a C-terminal HIS-tag. Interestingly, anti-FLAG blots did not detect the expected 10kDa fragment (data not shown). This may have been due to either the instability of the cleaved fragment, or the possibility of it adopting a new conformation that interfered with the presentation of the N-terminal epitope tag.

The relatively poor size resolution of SDS-PAGE electrophoresis of proteins, and the observation that EOD1 electrophoresed at a larger molecular weight than predicted (which is not unusual (Bocock et al., 2010)), meant that the location of the DA1-mediated cleavage site could not be precisely estimated using the resolution of SDS-PAGE. In order to identify the precise location of the cleavage site, a proteomics approach was taken. At the time of writing, Edman sequencing of purified DA1-cleaved EOD1 has identified a putative cleavage site at aa60. This is consistent with the size of the cleavage product on SDS PAGE (Fu-Hao Lu, unpublished work).

A

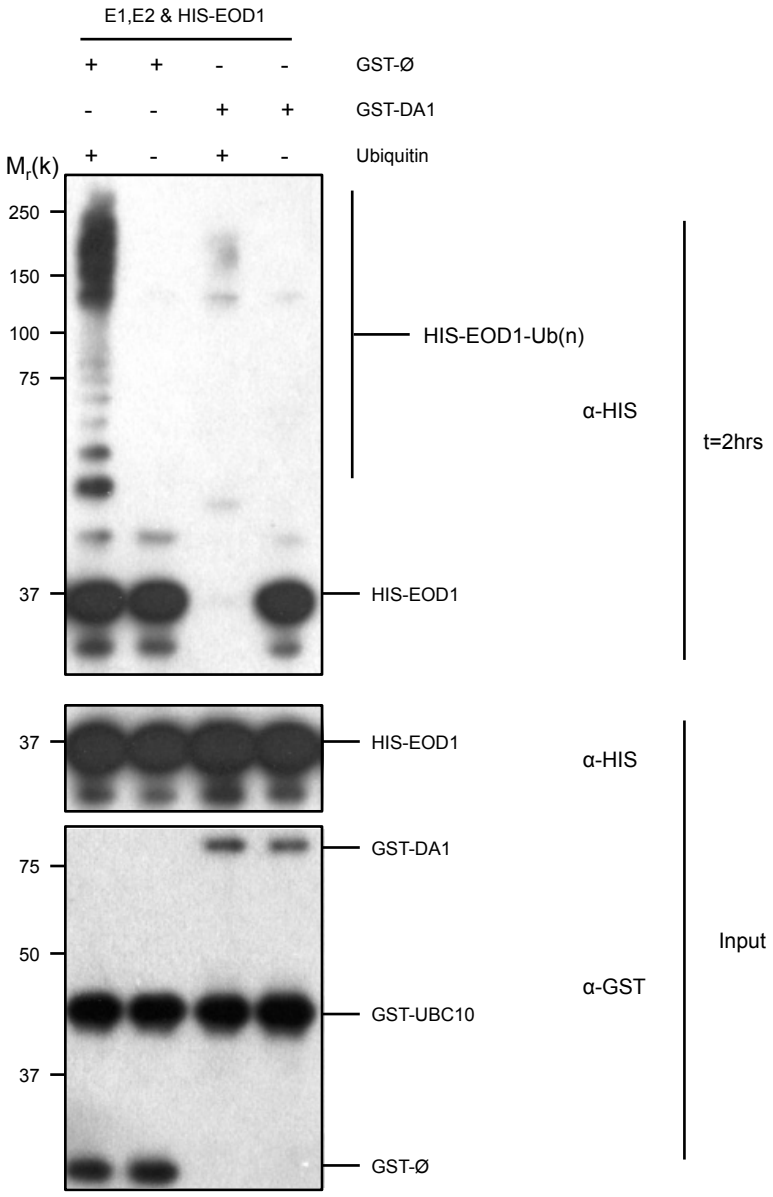
E1,E2 & HIS-EOD1
+ + - - GST-Ø
- - + + GST-DA1
+ - + - Ubiquitin
Mr(k)
250
150
100
75
37
HIS-EOD1-Ub(n)
HIS-EOD1
α-HIS
t=2hrs
37
HIS-EOD1
α-HIS
75
50
37
GST-DA1
GST-UBC10
GST-Ø
α-GST
Input

B

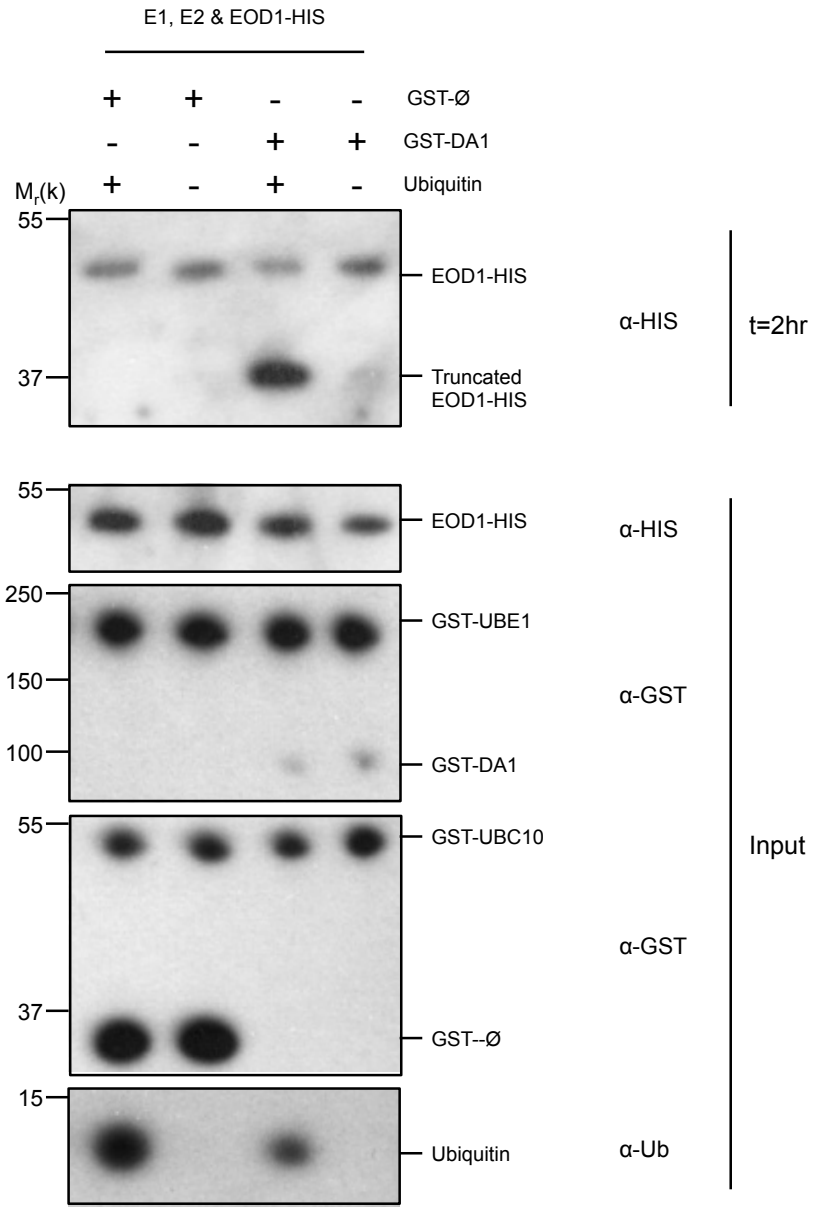

Figure 5.6 – DA1 cleaves EOD1 in an ubiquitin-dependent manner

In vitro ubiquitination assays with DA1 and either HIS-EOD1 (A) or EOD1-HIS (B). All assays include E1 (GST-UBE1 (human)), E2 (GST-UBC10) and ubiquitin. (A) High molecular-weight species of HIS-EOD1 (lane 1) reveal that HIS-EOD1 is poly-ubiquitinated in ubiquitin treatments. HIS-EOD1 is stable when GST-DA1 is added in the absence of ubiquitin (lane 4), however when ubiquitin and GST-DA1 are both included in the reaction (lane 3) HIS-EOD1 is no longer visible on the blot. (B) High molecular-weight species of EOD1-HIS are not visible upon ubiquitin treatment (lane 1), indicating that HIS-EOD1 is unable to auto-ubiquitinate. When ubiquitin and GST-DA1 are included in the reaction a lower molecular-weight species of EOD1-HIS appears on the blot; this truncated EOD1-HIS is approximately 10kDa shorter than full-length EOD1.

As discussed in section 5.2, the synergistic (enhancing) genetic interactions between *DA1* and *EOD1* predicted that DA1 may enhance the function of EOD1. It is therefore possible that the DA1- and Ubiquitin-mediated cleavage of EOD1 may increase the activity of EOD1 as a negative regulator of growth. Current work is defining the specific cleavage site and the activities of cleaved EOD1. Interestingly, there are some highly relevant examples of how the activities of E3 ligases are controlled by protein cleavage. In the human RING E3 ligase PARKIN, there is an auto-repressive N-terminal region that can be removed through cleavage (Burchell et al., 2012, Chew et al., 2012). An alternative model involves proteolytic cleavage revealing or removing a signal peptide, resulting in the spatial re-localisation of the protein in a mechanism similar to that seen in the human PA-TM-RING E3 ligase RNF13 (Bocock et al., 2010) (see section 5.1.2 for a detailed review of these examples).

Although HIS-EOD1 is an active E3 ligase, characterised by its ability to auto-ubiquitinate (Fig. 5.6a), FLAG-EOD1-HIS does not auto-ubiquitinate (Fig. 5.6b). While surprising, this observation is similar to that of Burchell et al (2012) in their study of the E3 ligase PARKIN. They showed that large N-terminal tags (FLAG, HA etc…) were sufficient to de-repress PARKIN auto-ubiquitination, whereas the smaller HIS tag was unable to do so. In the case of EOD1, it appears that either the converse is true (small N-terminal HIS tags permit E3 auto-ubiquitination and large N-terminal FLAG-tags inhibit E3 auto-ubiquitination activity), or the addition of a C-terminal HIS tag is sufficient to inhibit E3 auto-ubiquitination. To clarify this issue, two new constructs (FLAG-EOD1 and EOD1-HIS) could be tested for auto-ubiquitination. However, in the absence of this data, the observations from Fig. 5.6 are sufficient to provide evidence that epitope-tags can *alter* EOD1 activity; perhaps through interfering with auto-regulatory protein conformations. This would suggest that EOD1, in a similar way to PARKIN (Burchell et al., 2012), may have an inhibitory protein conformation that is relieved by DA1-mediated cleavage. The experiments reported here strongly support a role for peptidase-mediated cleavage of EOD1 by DA1 as a mechanism for controlling its activity. A key question is whether DA1-mediated cleavage increases its activity towards other substrates, and/or changes substrate specificity.

Having established a promising mechanism by which DA1 and ubiquitin may modulate EOD1 activity, the genetic analysis in section 5.2.1 predicts an enhancing interaction in which the E3 ligases EOD1 and DA2 may also activate or enhance DA1 function. The observation that DA1 cleaved EOD1 in an ubiquitin-dependent manner suggested that DA1 may be activated by EOD1-mediated ubiquitination. Therefore, the activity of the EOD1 and DA2 E3 ligases towards DA1 was tested *in vitro*.

5.3.3 – EOD1 and DA2 (but not BBR) ubiquitinate DA1 *in vitro*

To test the hypothesis that the interactions of EOD1 and DA2 with DA1 may lead to DA1 ubiquitination, ubiquitination assays incorporating E1, E2, the E3 ligases HIS-EOD1 or DA2-HIS, and FLAG-DA1 were performed. Aliquots of the reactions were subjected to SDS-PAGE and immunoblot analysis to detect DA1 modifications. To test the specificity of DA1-E3 ligase reactions, the E3 ligase BBR (BIG BROTHER RELATED, AT3G19910) was used as a negative control. BBR is the most similar E3 ligase to EOD1 based on protein sequence (Fig. S4b), and is an active E3 ligase *in vitro* (Fig. S4a).

Fig. 5.7 shows that in the presence of EOD1 and DA2 (lanes 5 and 6), DA1 is ubiquitinated. It also clearly shows that BBR (lane 7) does not cause DA1 ubiquitination. This demonstrates that DA1 is ubiquitinated by EOD1 and DA2 specifically, and that DA1 is not a non-specific target for E3 ligases. Interestingly, the ubiquitination patterns catalysed by EOD1 and DA2 are noticeably dissimilar. EOD1 catalyses the addition of approximately 3 to 6 ubiquitin molecules on DA1, whereas DA2 catalyses the addition of only 1 to 3 ubiquitin molecules on DA1. It is unclear whether these modifications are functionally distinct. The ubiquitin modifications could be short chains linked to a single lysine residue, or could be single ubiquitin molecules linked to several different DA1 lysine residues. The latter modifications are typical of ubiquitination events that regulate protein activities (Woelk et al., 2006, Hoeller et al., 2006)).

Combined with the ubiquitin dependence of DA1 function seen in section 5.3.2, these data suggest that DA1 cleavage of EOD1 could be activated by ubiquitination. To test this prediction it was important to confirm that as well as being *necessary* for activation, DA1 ubiquitination was *sufficient* to stimulate the activity of the peptidase. To do this, ubiquitinated DA1 was purified and assayed for its activity in cleaving EOD1 and DA2.

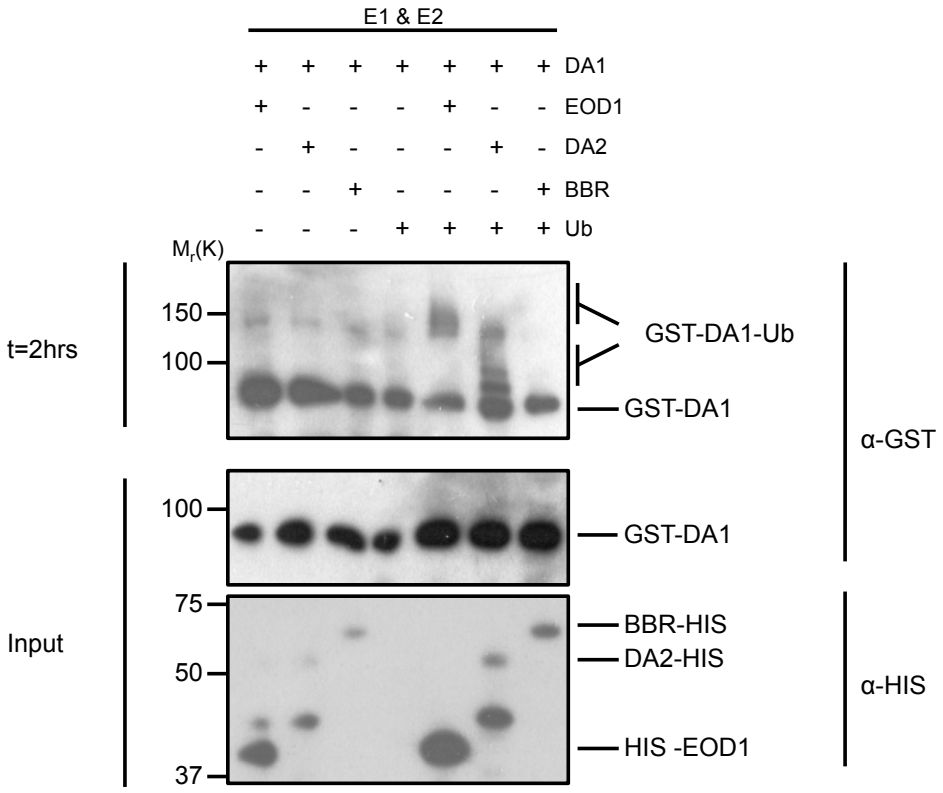

Figure 5.7 – EOD1 and DA2 ubiquitinate DA1 *in vitro*

Ubiquitination reactions were run with E1 (UBE), E2 (UbcH5b), ubiquitin, GST-DA1 and either HIS-EOD1, DA2-HIS or BBR-HIS. Following EOD1 and DA2 treatments, high molecular-weight species of GST-DA1 are visible on the blot, revealing that GST-DA1 is ubiquitinated. Treatment with BRR does not result in ubiquitination of GST-DA1. This indicates that DA1 is not a general target of E3 ligase activity. A lower molecular weight band that co-purifies from *E. coli* with DA2-HIS can be seen in lanes 2 and 6. This is thought to be due to an ectopic translational event from an intragenic ATG (see section 5.3.4.1 for further discussion).

5.3.4 – Ubiquitinated DA1 is sufficient to specifically cleave EOD1 and DA2

5.3.4.1 – Ubiquitinated DA1 is sufficient to specifically cleave EOD1 and DA2 in vitro

To test the activity of ubiquitinated DA1 (DA1-ub) in cleaving EOD1 or DA2, DA1-ub was purified and added to a reaction containing only EOD1 or DA2 E3 ligase. In order to synthesise DA1-ub, an ubiquitination reaction containing E1, E2, HIS-EOD1 and FLAG-DA1 was carried out, followed by immunopurification of DA1 using α-FLAG beads. This method also co-purifies non-ubiquitinated DA1 (see Fig. 5.7), but due to the high activity of DA1-ub, this did not alter the interpretation of data. The experimental set-up was designed to compare the activities of DA1-ub and non-ubiquitinated DA1. In addition, it tested a possible role for the DA1 peptidase domain in the cleavage of EOD1 and DA2. This was done by mutating the conserved zinc-coordinating histidines (to alanines) in the peptidase active site (see section 3.1.3). These changes resulted in the conversion of the conserved HEMMH domain to AEMMA, and were predicted to abrogate peptidase function (McGwire and Chang, 1996, Zhang et al., 2001). The resulting mutant version of FLAG-DA1 was termed $DA1^{pep}$ and was ubiquitinated and purified as described above. Finally, to test the specificity of DA1 function on EOD1 and DA2, a negative control of BBR was included in the assay.

Fig. 5.8 shows that purified FLAG-DA1-ub was sufficient to cleave EOD1 and DA2 (lanes 1 and 2), whereas, neither DA1 nor $DA1^{pep}$-ub was able to do so (lanes 4,5,7 and 8). DA2 was cleaved resulting in an approximately 17kDa DA2-HIS product. The lack of activity of DA1-ub towards BBR (lane 3) suggested that DA1-ub is specifically active towards the EOD1 and DA2 RING E3 ligases.

In Fig. 5.7 and Fig. 5.8 , *E.coli* expressed DA2 has a lower molecular-weight band (35kDa) that co-purifies with DA2 (Fig. 5.8 lanes 2,5 and 8). This band cross-reacts with α-HIS and is likely to be an ectopic translational event from an intragenic ATG. In order to remove this band and to further confirm the validity of $DA1^{ub}$-mediated cleavage activities, this assay was also carried out in an *in vivo* system.

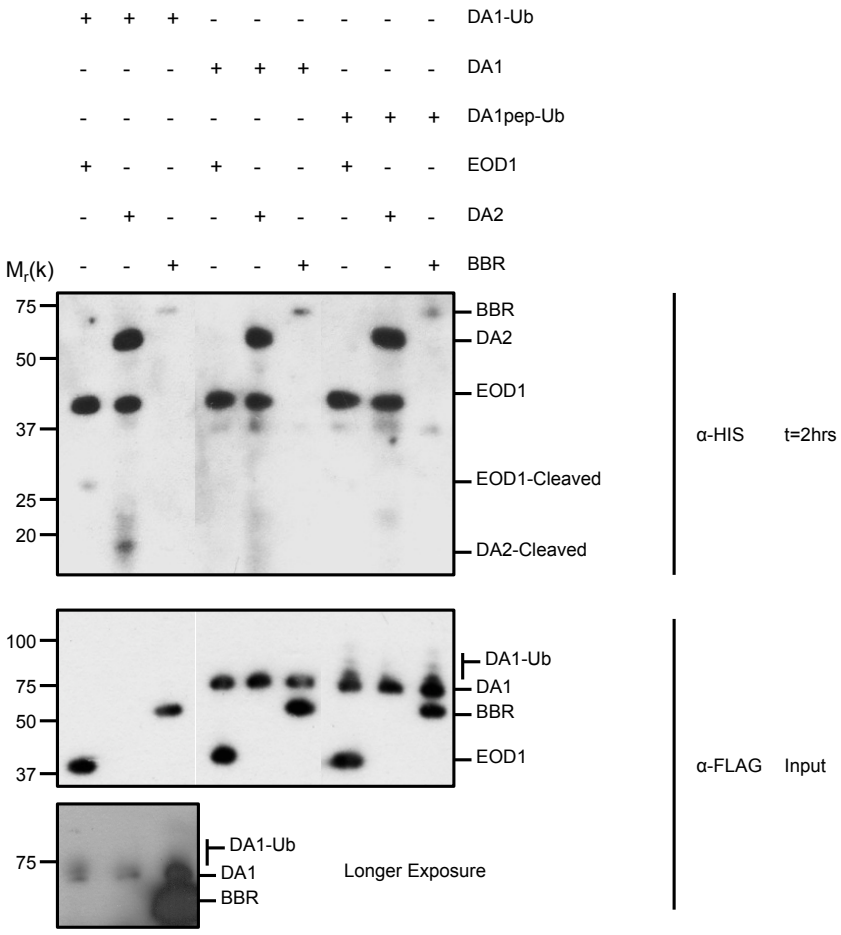

Figure 5.8 – Ubiquitinated DA1 is sufficient to cleave EOD1 and DA2 *in vitro*

Purified FLAG-DA1, FLAG-DA1-ub (ubiquitinated DA1) and FLAG-DA1pep-ub (ubiquitinated DA1 peptidase mutant) was added to a reaction containing EOD1, DA2, or BBR. Only DA1-ub was sufficient to cleave EOD1 (lane 1) and DA2 (lane 2), and no treatments resulted in the cleavage of BBR. A lower molecular weight band that co-purifies from *E. coli* with DA2-HIS can be seen in lanes 2,5 and 8. This is thought to be due to an ectopic translational event from an intragenic ATG (see section 5.3.4.1 for further discussion). More complete cleavage of EOD1 and DA2 by DA1-Ub is presented in Fig S5.

5.3.4.2 – DA1 specifically cleaves EOD1 and DA2 in Arabidopsis protoplasts

Due to the instability of EOD1 in stable transgenic systems (Lena Stransfeld, personal communication), transient expression systems were used for the *in vivo* investigation. Guided by the success of expressing EOD1-YFP and DA2-YFP fusions in Arabidopsis mesophyll protoplasts for BiFC analysis (section 5.2.2.2), a protoplast system was used to assess DA1-dependent cleavage of EOD1 and DA2 *in vivo*.

To ensure that any observed cleavage of EOD1 and DA2 was dependent on added DA1 proteins, *da1ko1/dar1* protoplasts that lacked DA1 and DAR1 protein were used in the PEG-mediated co-transfection experiments. Protoplasts were transfected with HA-DA1 or HA-DA1^{pep}, and with C-terminal FLAG-tagged E3 ligases EOD1, DA2 or BBR. BBR was included as a negative control to test the specificity of DA1 towards EOD1 and DA2. Fig. 5.10 shows that in HA-DA1 transfected protoplasts, lower-molecular weight cleavage products of EOD1 (lane 1) and DA2 (lane 3) are produced (as in *in vitro* experiments (Figure 5.8)). In contrast, these cleavage products were not seen in DA1^{pep} treatments (lanes 2 and 4). Fig. 5.10 also showed that BBR was not cleaved by DA1 (lane 5), confirming that DA1 has specificity towards EOD1 and DA2.

In this experiment, all the E3 ligases were tagged with a C-terminal FLAG tag. Analysis of Fig. 5.10 reveals that, in contrast to the N-terminal cleavage of EOD1, DA2 was cleaved approximately 20kDa from its C-terminus. The FLAG epitope tag is approximately 3kDa suggesting that DA2 was cleaved approximately 17kDa from its C-terminus. However, as DA2 has an N-terminal RING domain and EOD1 has a C-terminal RING domain, both cleavage events create proteins that contain an intact RING domain.

Taken together, the *in vitro* and *in vivo* data confirmed that DA1 is a functional peptidase that is activated by ubiquitination mediated by the E3 ligases, EOD1 and DA2. Interestingly, the E3 ligases required for the activation of DA1 were those that are the targets of the peptidase. This mutual dependence suggests a model in which EOD1 and DA2 activate the DA1 peptidase through ubiquitination. This peptidase then cleaves the E3 ligases to create new truncated proteins (Fig. 5.12). The observed synergistic genetic interactions (section 5.2.1) suggest that these truncated E3 ligases have new or increased activities with respect to inhibiting cell proliferation during organ formation (Disch et al., 2006, Xia, 2013, Song et al., 2007). Such a novel feed-forward mechanism, whereby E3 ligases stimulate their activation through ubiquitination of a cognate peptidase, is a previously un-described regulatory mechanism that

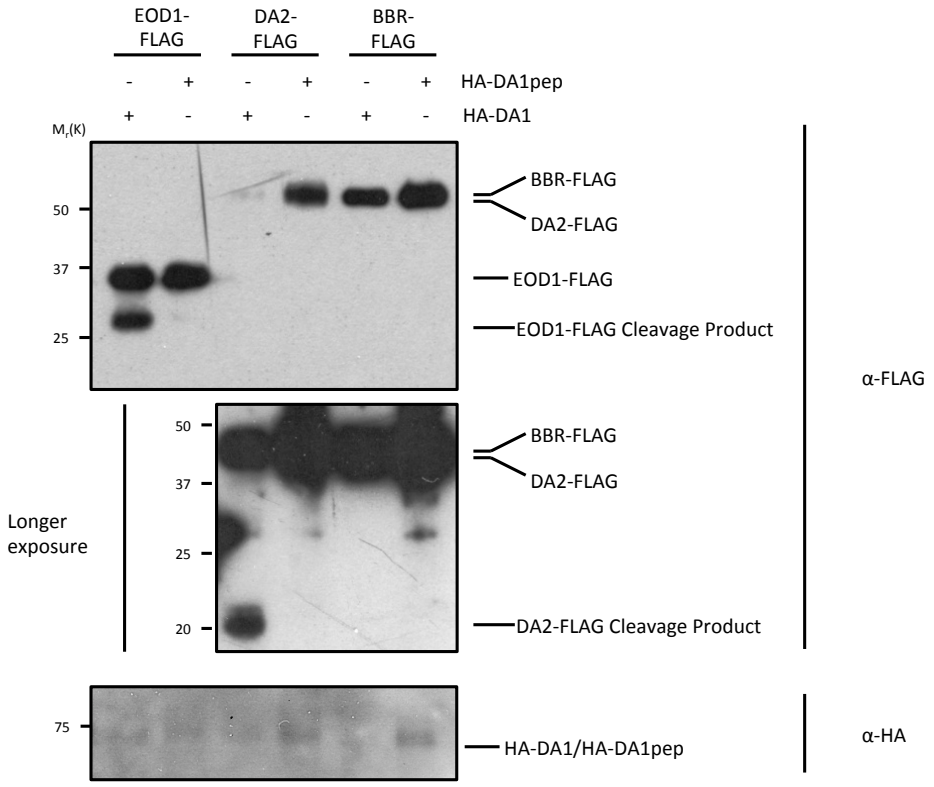

Figure 5.9 –DA1 cleaves EOD1 and DA2 *in vivo*

Western blot from *da1ko1/dar1-1* protoplasts co-transfected with either EOD1-FLAG, DA2-FLAG or BBR-FLAG, and one of either HA-DA1pep or HA-DA1. In HA-DA1 treatments EOD1-FLAG and DA2-FLAG are cleaved to reveal their truncated species (lanes 1 and 3, respectively). Longer exposure was required to visualise truncated DA2-FLAG. HA-DA1 treatments were not sufficient to cleave BBR-FLAG, suggesting specificity towards EOD1 and DA2. HA-DA1pep treatments were not sufficient to cleave EOD1-FLAG and DA2-FLAG, revealing that the DA1 peptidase is essential for their cleavage.

may have a more widespread role than just controlling E3 ligase activity in the regulation of cell proliferation in Arabidopsis. Given that the activity of the Human E3 ligase PARKIN is influenced by an N-terminal cleavage event (Chew et al., 2012), it is also possible that such a mechanism may also be relevant for the control of E3 ligase activity in other organisms.

A peptidase-mediated activation of an E3 ligases would probably be an irreversible modification, leading to increased and/or different activities of the E3. It is possible that the observed auto-ubiquitination of the E3 ligases (Fig. 5.5 & 5.6) may also be an additional mechanism for regulating E3 ligase activities. For example, this could be K48 linked poly-ubiquitination leading to proteasome- mediated degradation. The short half-lives of EOD1 and DA2 in plant cells suggests a rapid turnover consistent with ubiquitin-directed proteasome-mediated degradation. In order to investigate this, an *in vitro* study of EOD1 and DA2 auto-ubiquitination was undertaken.

5.4 – EOD1 and DA2 are ubiquitinated differently

Understanding poly-ubiquitin chain architecture can reveal whether the chain is likely to be a signal for proteasome-mediated destruction or to provide another function. The two most common poly-ubiquitin chain linkage types are K48 and K63 (Saracco et al., 2009); K48 –linked ubiquitin chains have a well-established role in targeting proteins for proteasome- mediated destruction (Hershko and Ciechanover, 1998, Jacobson et al., 2009, Thrower et al., 2000). Conversely, there is no consensus as to the role of K63-linked ubiquitin chains, however there is evidence that they are involved in enzyme activation (Cheng et al., 2013b) and receptor signalling (Kawai and Akira, 2010).To identify the types of ubiquitin linkages created by DA2 and EOD1 auto-ubiquitination, ubiquitination assays (see section 5.3.1) were performed using recombinant ubiquitin molecules with these K48 or K63 residues mutated to arginine.

Fig. 5.10a shows that in ubiquitination assays using wild-type and K63R ubiquitin (UbK63), auto-ubiquitination of EOD1 resulted in a typical 'ubiquitin smear' (lanes 8 and 10). In contrast, the use of K48R ubiquitin (UbK48) created only three EOD1-ubiquitin bands (lane 9). These likely represent either a single triple-ubiquitin chain or three mono-ubiquitination events. To distinguish between these possibilities, ubiquitination assays were performed using methylated ubiquitin (Ub-Me), which has all lysine residues methylated and as a consequence is unable to form ubiquitin polymers. Fig. 11b shows that when Ub-Me is used (lane 6), only mono-ubiquitinated EOD1 is generated; revealing that EOD1 is ubiquitinated at one site only. This indicated that the three ubiquitinated species of EOD1 in the UbK48 treatment in Fig. 11a probably represented a single chain of three ubiquitin molecules.

A

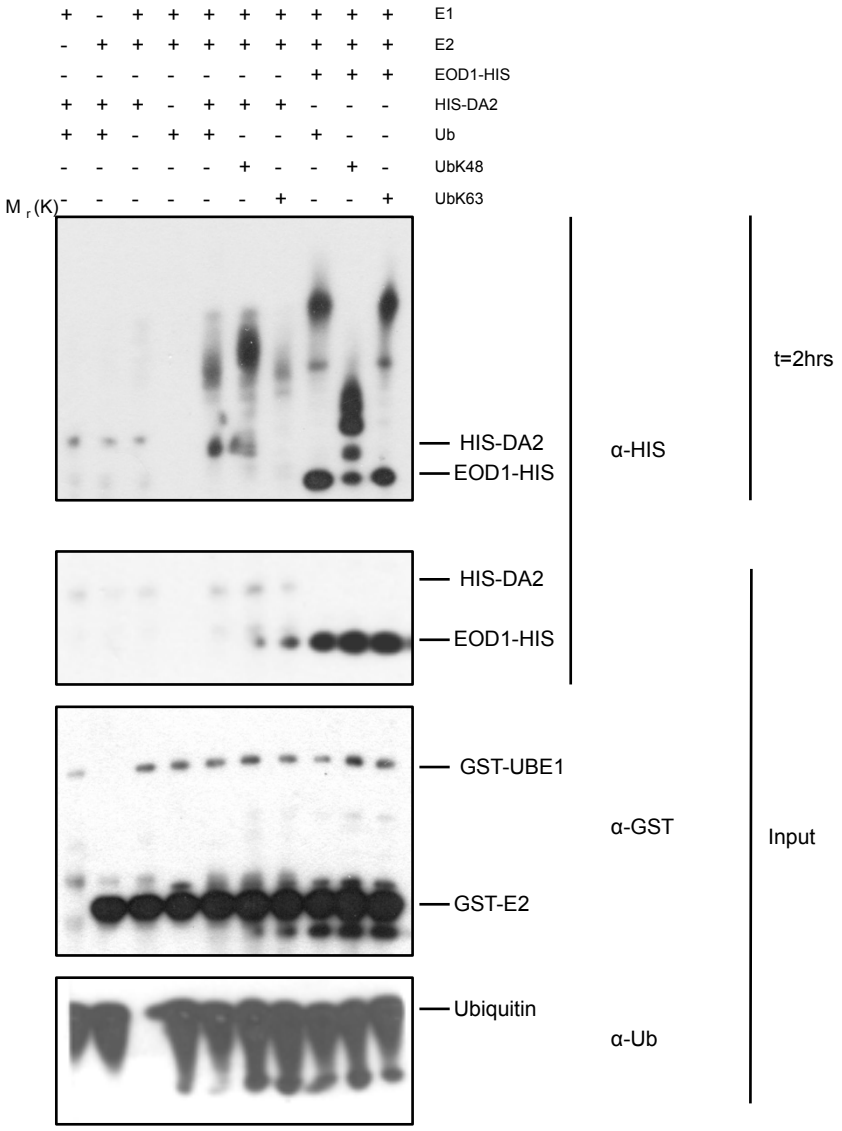
+ - + + + + + + + + E1
- + + + + + + + + + E2
- - - - - - - + + + EOD1-HIS
+ + + - + + + - - - HIS-DA2
+ + - + + - - + - - Ub
- - - - - + - - + - UbK48
- - - - - - + - - + UbK63
M r (K)
HIS-DA2
EOD1-HIS
α-HIS
t=2hrs
HIS-DA2
EOD1-HIS
GST-UBE1
α-GST
Input
GST-E2
Ubiquitin
α-Ub

B

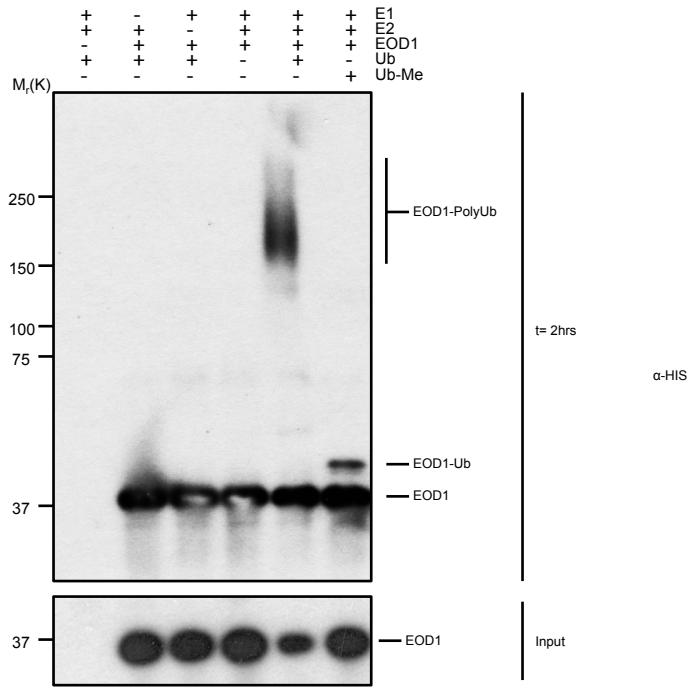

Figure 5.10 –EOD1 and DA2 auto-ubiquitination patterns

Ubiquitination reactions were run with E1 (UBE (human)), E2 (GST-UBC10), and either HIS-EOD1 or DA2-HIS. The reactions included either wild-type ubiquitin (Ub), ubiquitin mutated at lysine 48 (UbK48), ubiquitin mutated at lysine 63 (UbK63) or methylated ubiquitin (Ub-Me). (A) When UbK48 is used in the reaction, EOD1 is unable to auto-ligate more than three ubiquitin molecules (lane 9), suggesting that the majority of EOD1 auto-poly-ubiquitin is linked through lysine 48. When UbK63 is used in the reaction, the intensity of DA2-HIS auto-ubiquitination is reduced (lane 7), suggesting that DA2 may be capable of forming K63-linked auto-poly-ubiquitin. (B) When Ub-Me is used in a reaction with HIS-EOD1, EOD1 is only able to auto-mono-ubiquitinate, suggesting that EOD1 is ubiquitinated at one residue only.

These data showed that EOD1 auto-ubiquitination involves the formation of a K48-linked ubiquitin chain that may target EOD1 for proteasome-mediated destruction (Thrower et al., 2000). The analyses also showed that although the majority of the poly-ubiquitin chain is K48 linked, a short tri-ubiquitin chain is able to be formed through an alternative linkage. Currently the significance of this observation is not known, however, the auto-ubiquitination of EOD1 with K48-linked poly-ubiquitin suggests a mechanism in which it promotes its own instability. It is intriguing to speculate that DA1-mediated cleavage of EOD1 may influence its stability by altering its auto-ubiquitination. This could be tested by investigating the nature of the auto-poly-ubiquitin ligated by the cleaved version of EOD1.

In contrast to the data for EOD1 ubiquitination described above, UbK48 had no effect on DA2 auto-ubiquitination (Fig. 5.10 lane 6). This showed that unlike EOD1, DA2 does not auto-catalyse K48-linked poly-ubiquitin chains. The assay also showed that UbK63 reduced the degree of auto-ubiquitination (lane 7), suggesting that DA2 poly-ubiquitin chains can be part K63-linked and part an alternative linkage. These observations imply that the suggested model for EOD1 'stabilisation' through interference with K48 chain formation, is not applicable to DA2. It also suggests that, if DA1 is assumed to regulate both E3 ligases in the same fashion, the model for activation of EOD1 through stabilisation (with regards to proteasome degradation) is also unlikely to be valid.

The observation that EOD1 promotes its own instability through auto-ubiquitination suggests that its abundance and functions are tightly regulated. This indicates that it may be involved in regulating rapid, or time-bound cellular processes, and that its activity may be damaging if it is not tightly controlled. This is consistent with the model of DA1-mediated protein cleavage of EOD1, which is a one-way switch that drives the coordinated formation of EOD1 and DA2 E3 ligases that may have altered behaviours. Identifying putative targets of EOD1- and DA2-mediated ubiquitination, in addition to DA1, is therefore a high priority.

5.6 – Discussion

Research in this chapter has defined a novel mutually enhancing regulatory relationship between two RING E3 ligases that control growth through independent pathways, and a cognate specific peptidase that is predicted to alter their activity in a coordinated and uni-directional manner. This is predicted to enhance and/or alter the activity of the E3s towards unknown substrates that mediate cell proliferation and set final organ size. Fig. 5.12 is a schematic representation of this regulatory system, where EOD1/DA2 activation of DA1 results in their peptidase-mediated cleavage and the possible modification of their activity. The 'feed-

forward' aspect of this model implies that upon initiation (i.e. activation of DA1 peptidase activity) the process is irreversible. This suggests that DA1 functions as a 'molecular ratchet' that ensures rapid and unidirectional decision-making in a similar way to checkpoint decision-making in the cell cycle (reviewed in Elledge (1996)).

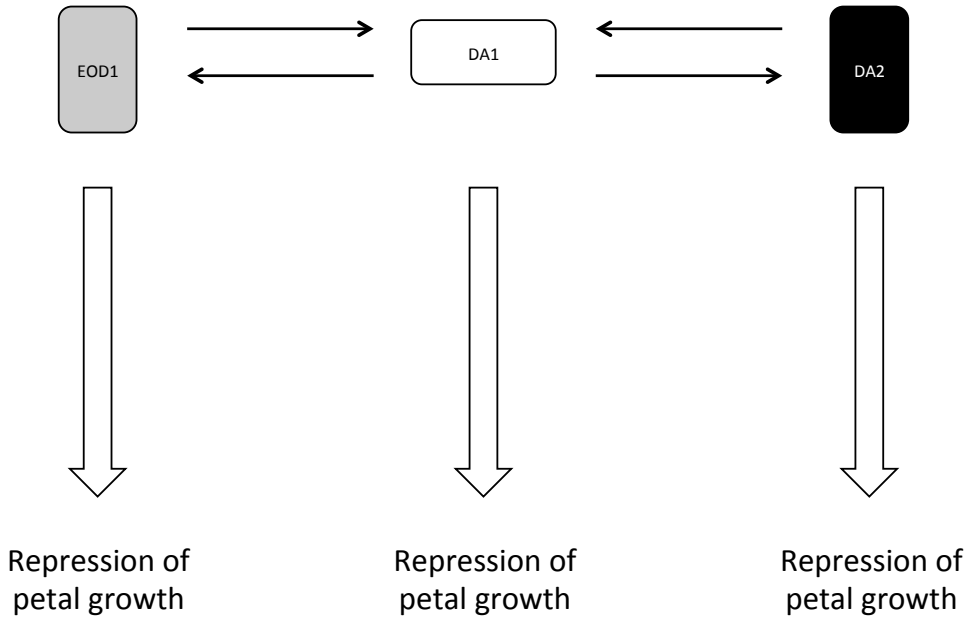

Figure 5.11 – Together, DA1 and EOD1 and DA2 collectively enhance their effect as growth repressors

Model illustrating the enhancing relationship between DA1 and the E3 ligases, EOD1 and DA2. All three proteins are negative regulators of the duration of cell proliferation in the developing organ. Genetic analysis predicts that when DA1 and EOD1 (or DA2) are both present, their collective role in growth repression is enhanced.

5.6.1 – DA1 peptidase activity is activated by ubiquitination

Genetic analysis in section 5.2.1 predicted that EOD1 and DA2 act to enhance DA1 function. This was confirmed by observations that ubiquitination of DA1 by EOD1 is sufficient to activate the DA1 peptidase (section 5.3). The mechanism of activation is unclear, however the presence of an active UIM domain in DA1 (section 3.3) suggests that it may be through a mechanism similar to that of coupled mono-ubiquitination, such as in EPS15. The ubiquitination of EPS15 is dependent on the interaction of the EPS15-UIM with a ubiquitinated E3 ligase (Woelk et al., 2006). This suggests that ubiquitination of DA1 may involve the UIM targeting DA1 to the auto-ubiquitinated EOD1/DA2.

The observation that non-ubiquitinated DA1 does not exhibit peptidase activity - at least towards EOD1 and DA2 - suggested that the non-ubiquitinated form of DA1 exists in an auto-repressive state. Studies of coupled mono-ubiquitination have led to the suggestion that UIM binding to ubiquitin in *cis* can lead to major conformational changes (Hicke et al., 2005), which could in turn alter the activity of the protein. It is therefore possible to speculate that UIM interactions with *cis*-ubiquitin would be sufficient to activate the peptidase. Both EOD1 and DA2 undergo long chain auto-poly-ubiquitination (Fig. 5.3.1-2), but they also coordinate the ligation of short ubiquitin chains onto DA1. It is possible that this is due to geometric constraints of the EOD1/DA2-UBC10 complex, but it is also feasible that the DA1 UIM competes with the E3-E2 complex for binding of ubiquitin molecules on DA1, thereby preventing chain elongation. Recent work in yeast has shown that the ubiquitin-binding domain of VPS23 competes with the RSP5 E3 ligase for the binding of the mono-ubiquitin present on the arrestin-related protein RIM8 (Herrador et al., 2013). The *trans*-interaction of UBD and ubiquitin in this example is thought to be sufficient to repress poly-ubiquitination, and presents the possibility that the short chains present on DA1 are a consequence of a *cis*-interaction of UIM and ubiquitin.

Another potential *cis*-regulatory mechanism involves the DA1 LIM domain, which is present in all members of the DA1 family, and in the same position relative to the conserved peptidase domain. The LIM domain of LIM kinase-1 is proposed to have a *cis*-inhibitory activity towards its kinase domain (Nagata et al., 1999), leading to the speculation that the

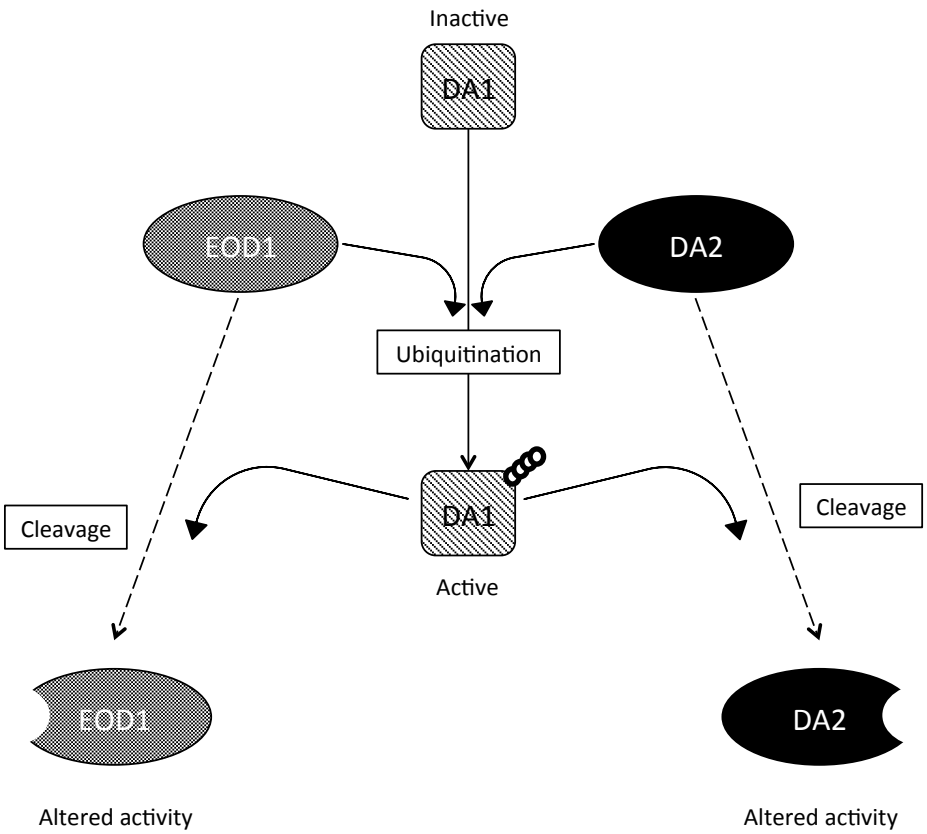

Figure 5.12 – DA1 may exist in a reciprocally enhancing feed-forward loop with EOD1 and DA2.

A model explaining the observed genetic, physical and biochemical interactions between DA1, and EOD1 and DA2. First, EOD1 and DA2 activate DA1 through an ubiquitination step. This is then followed by the peptidase-mediated cleavage of EOD1 and DA2 by ubiquitinated DA1, and the subsequent cleavage-dependent activation of the E3 ligases.

DA1 LIM (or LIM-like) domain has an analogous role with respect to its peptidase domain. It may be that this inhibitory LIM-peptidase interaction is modulated by UIM interactions with ubiquitin in *cis*. This is supported by evidence from section 3.2.3 that revealed that the LIM domain is not involved in DA1-DA1 oligomerisation, and is therefore a good candidate for interacting with the peptidase.

To test the sufficiency of $DA1^{ub}$ to cleave EOD1 and DA2 (section 5.3.4), DA1-ub was incubated with EOD1 and DA2. DA1-ub was generated in an ubiquitination reaction using EOD1 only. Therefore, despite the fact that EOD1 and DA2 have both been identified as *bona fide* targets of the DA1 peptidase, it remains unclear whether DA2 can activate DA1 peptidase activity by ubiquitination as well. The fact that DA2 can ubiquitinate DA1 and that BBR cannot (section 5.3.3), and that ubiquitination activates DA1, suggests that DA2 is indeed able to activate DA1.

5.6.2 – EOD1 and DA2 are modified by peptide cleavage

Based on the genetic analysis in section 5.2, it was predicted that DA1 might also enhance the activities of EOD1 and DA2 (Fig. 5.12). Research described in Section 5.3 demonstrated that DA1 specifically cleaves EOD1 and DA2, and therefore it is predicted that this cleavage enhances the activities of these two DIEs. The mechanism by which DA1-ub-mediated cleavage enhances E3 activity is currently not known. But some interesting examples of E3 ligase regulation may be relevant. Studies of the human E3 ligase PARKIN have shown that the *in vitro* removal of an inhibitory N-terminal fragment was sufficient to activate the auto-poly-ubiquitination activity of PARKIN (Chew et al., 2012). Moreover, the addition of large N-terminal epitope tags to PARKIN interfered with this inhibitory domain and de-repressed its auto-ubiquitination activity (Burchell et al., 2012). Interestingly, the addition of a large N-terminal epitope tag to EOD1, (together with a small C-terminal tag) appeared to repress E3 activity (Fig. 5.6b), suggesting that modification of EOD1 tertiary structure may also influence EOD1 activity.

The observation that EOD1 and DA2 are able to auto-ubiquitinate and ubiquitinate DA1 prior to their cleavage, suggested that DA1-mediated cleavage may alter their *specificity* rather than their *activity*. This distinction can be illustrated by the neddylation and rubylation of CRL E3 ligases (see section 5.1.2), an event that changes CRL quaternary structure to create novel catalytic geometries, which alter the specificity of the enzymes (Duda et al., 2008, Merlet et al., 2009). EOD1 and DA2 are both cleaved at the opposite end of the protein to the RING domain, and, as the RING domain mediates E2-binding, it is possible that the RING-distal 'domain' is that which determines substrate specificity. Therefore it is conceivable that DA1-mediated

cleavage substantially alters the substrate-binding domain such that new catalytic geometries are created. This modification could enhance E3 activity in the same way that neddylation increases the activity of $SCF^{\beta TRCP}$ towards Ikbα (Read et al., 2000), and the activity of SCF^{skp2} towards $p27^{kip1}$ (Morimoto et al., 2000, Podust et al., 2000). Alternatively, it could affect the ubiquitin chain specificity of the E2-E3 complex, allowing it to alter the architecture of the ligated chains in a similar way to the truncation of PARKIN that enables it to form poly-ubiquitin chains (Chew et al., 2012).

An alternative explanation for the predicted enhancing/activating effects of DA1-ub mediated cleavage of EOD1 and DA2 may be the disruption or revelation of a signal peptide that determines the location of the E3 enzymes. For example, cleavage of the membrane integral E3 ligase RNF13 revealed a putative nuclear localisation signal (Bocock et al., 2010) thought to be responsible for previously observed nuclear localisation (Tranque et al., 1996). If RNF13 substrates are in the nucleus, a relocation event might lead to greater E3 activity without modifying the enzyme biochemistry.

5.6.3 – DA1 cooperates with EOD1 and DA2 to influence final organ size

The experiments described in this chapter demonstrated genetic, physical and biochemical interactions between DA1, EOD1 and DA2 in the regulation organ growth. They identified a novel feed-forward loop involving the ubiquitin-activated, peptidase-mediated modification of E3 ligases by a cognate peptidase.

Analysis of the growth responses of individual and combined mutants (see section 5.2.1) provided clear evidence that in addition to their mechanistic interactions, DA1, EOD1 and DA2 also have functions that appear to be independent of each other. In *da1ko1* plants, where DA1-mediated controls do not function, EOD1 and DA2 were still able to partially supress the double knockout petal phenotypes (*da1ko1/eod1-2* or *da1ko1/da2-1* respectively). This suggests that they have also a DA1-independent role in setting organ size. This could be through a basal activity of the full-length RING E3 ligases, or through modifications by other activating peptidases. Similarly, in *eod1-2* and *da2-1* lines, the presence of DA1 was sufficient to partially supress the large double knockout petal phenotypes; revealing that, despite the absence of EOD1 and DA2, DA1 still influences growth, perhaps through activation by another as-yet-unidentified ubiquitin ligase.

Taken together, these experiments and interpretations suggested that DA1, EOD1 and DA2 do not function in simple linear pathways that converge to influence growth (Fig. 5.14a). A more

realistic model involves the coordinated activation of DA1 by a set of E3 ligases that control linked cellular activities during cell proliferation (Fig. 5.14b). The identification of these DA1-regulated E3 ligases, and other proteins, will be facilitated by identifying and assessing the DA1 cleavage site using bioinformatics and biochemistry.

Chapter 6 - Genetic linkage and association screens for regulators of petal and seed growth

6.1 – General introduction

This chapter was initiated as a complementary project to run alongside the DA1 functional characterisation reported in Chapters 3 to 5. It was designed to identify novel genes involved in the setting of seed and petal size, and through doing so, to develop our understanding of the processes involved in organ growth and development, and their contribution to natural variation in organ size in populations of Arabidopsis.

Mutant screens, such as those used to identify *DA1* and *EOD1* (Li et al., 2008, Disch et al., 2006), are powerful tools for identifying genes of interest. However they use heavy doses of mutagens that cause a narrow range of severe effects, such as the complete loss of gene function. Natural genetic variation includes a wide variety of different alleles that have been selected over millions of generations and provide both a different spectrum of mutants and evidence for the biological role of the genetic variation in fitness and adaptation at the population level. Such analyses can identify key regulatory nodes and genes that have been selected by evolution. Therefore to complement and extend the analyses of induced mutations, an investigation of natural variation in organ-size was undertaken. Natural variation allows you to exploit a larger pool of variation not available in common laboratory strains. Because the lines are genotyped and inbred you can also phenotype them repeatedly to see how the environment interacts with your trait.

Two different strategies for investigating complex-traits such as final organ size exist in Arabidopsis: population-based association studies, and family-based QTL mapping studies (Mitchell-Olds, 2010). Population-based association studies take advantage of genetic variation amongst natural populations of Arabidopsis, seeking out associations between phenotypes of interest and genomic markers (Atwell et al., 2010). Alternatively, family-based linkage-mapping studies look for genotype-phenotype associations amongst artificial inbred populations originating from a small number of founding parent lines. Both strategies search for statistically significant associations between phenotypes of interest and SNP genomic markers.

Both techniques seek to uncover the genetic elements that underlie natural phenotypic variation. This is done through the identification of statistical associations between a phenotype of interest and an array of genomic SNP markers. The most highly associated markers are then used to identify the causal genes based on their genetic linkage to the marker. As such, the predictive power of these techniques is dependent on the linkage disequilibrium (LD) within each mapping population. LD is the phenomenon that certain alleles are non-randomly associated due to limited recombination events occurring between their loci (Jorde, 2000). At linked loci, instead of finding a random combination of the constituent alleles, there are linked "haplotype blocks" (Weigel, 2012). The amount of linkage disequilibrium in the population – the length of these haplotype blocks – defines the maximal resolution of the association analysis. If linkage disequilibrium is large, e.g. 10 Mb, then one can only be confident that the causal variation is within 10 Mb of the associated marker SNP, whereas if linkage disequilibrium is only 10Kb, then there is confidence that the causal variation is within one of two genes of the marker SNP. Amongst other factors, linkage disequilibrium is affected by the rate of recombination, and therefore the degree of intermixing within a population will determine the resolution of an association analysis (Jorde, 2000).

Population-based association studies utilise highly recombined natural populations, and the resulting short LD allows the identification of high-resolution QTLs (Mitchell-Olds, 2010, Bergelson and Roux, 2010, Weigel, 2012, Kover and Mott, 2012). This is in contrast to family-based mapping studies, which are often carried out with F5 or F6 progeny and therefore often result in much broader QTLs (Mitchell-Olds, 2010, Bergelson and Roux, 2010, Kover et al., 2009). Nonetheless, despite the greater mapping resolution achievable in population-based studies, their predictive power can be reduced by population structure effects (Mitchell-Olds, 2010, Bergelson and Roux, 2010, Weigel, 2012, Kover and Mott, 2012). In this context, population structure refers to genomic variation that is immortalised in accessions and yet has no true linkage to the phenotypic variation being investigated (Mitchell-Olds, 2010). For example - distantly related, phenotypically divergent accessions will have significant genotypic differences in many genomic locations; only some of which will contribute to the phenotype of interest. This means that association analyses are likely to identify multiple false-positives. Different strategies have been developed to reduce the effect of population structure; including using mixed-model analyses (Kang et al., 2008) and the use of less-structured, geographically confined population samples (Filiault and Maloof, 2012) that are likely to have a limited number of founder types. Importantly, these corrective methods trade-off with the power of the association study; with mixed-model analysis increasing the rate of false-

negatives (Mitchell-Olds, 2010), and the use of geographically confined populations reducing the amount of genetic variation included in the study.

Despite this, population-based studies typically contain significantly more genotypic variation than artificial mapping families, whose diversity is limited by the relatively small gene pool held by the founding parental lines. Nonetheless, the genetic diversity found in artificial mapping families can vary significantly depending on the number and diversity of parents (Bergelson and Roux, 2010). Conventional bi-parental RIL populations, such as that which recently identified *ERECTA* as a regulator of petal growth (Abraham et al., 2013), contain only the genetic variation present in the two founding parents. In contrast, the multi-parental RIL-type MAGIC population incorporates the genetic variation of 19 parent lines (Kover et al., 2009).

The complementary strengths and weaknesses of both population- and family- based mapping approaches enables powerful analyses to be achieved through a combinational approach; as evidenced by recent work identifying regulators of flowering time (Brachi et al., 2010). Following from these data, and in light of the general consensus that a combinational approach is superior (Mitchell-Olds, 2010, Kover and Mott, 2012, Bergelson and Roux, 2010, Weigel, 2012), studies described in this thesis have taken a dual approach to search for regulators of seed and petal growth: a Genome Wide Association Study (GWAS), and a QTL analysis of the MAGIC RIL-type population. Both strategies used large populations of Arabidopsis (272 lines for the GWAS, 443 lines for the MAGIC analysis). The two test populations did not overlap, and the study did not expect to find the same causal variation in both populations. Instead, it aimed to maximise gene discovery through a combinatorial approach, and to look for functional similarities amongst candidate genes from both screens. This chapter describes the genes that have been identified as candidate regulators of organ size. The details of the individual genetic analyses will be discussed in section 6.3 and 6.4 respectively.

6.2 – Seed and petal phenotypes were investigated

In line with the overall direction of this thesis, rather than focusing on any one specific organ type, this chapter is interested in elucidating the mechanisms governing organ growth *in general*. As a consequence, the genetic analyses described in this section are focused on two key phenotypic areas: petal growth and seed growth.

Significant developmental differences between petals and seeds (reviewed in detail in Chapter 1) mean that many aspects of their development are regulated through independent pathways. An extreme example of this is the maternal regulation of seed size through the *ttg2* (*transparent testa glabra2*) mutation (see section 1.4), which relies on the interaction of the integument and endosperm, tissues that are specific to seeds (Garcia et al., 2005). In addition to these organ-specific growth pathways, genes that regulate core growth functions, such as cell proliferation and cell expansion, are often involved in the setting the size of both organ types. For example, *DA1* and *KLUH* influence seed and petal growth, through manipulating the duration of cell proliferation (Li et al., 2008, Adamski et al., 2009, Anastasiou et al., 2007). This study uses two organ-types in order to broaden its scope; exploiting two distinct developmental systems to maximise the identification of common *and* organ-specific regulators.

The following sections describe the logic behind the selection of, and the methods used to record the phenotypes chosen for this study.

6.2.1 – Petal and seed area

The manipulation of core developmental processes that drive organ growth, such as cell proliferation and cell expansion (see section 1.3), will often result in organs of a wild-type morphology, but an altered overall size. For example, regulators of cell proliferation – *DA1, KLU* and *EOD1* – all affect overall petal area without altering the shape of the organ (Anastasiou et al., 2007, Disch et al., 2006, Li et al., 2008, Adamski et al., 2009). In addition, an increase in organ size can be achieved in concert with significant morphological changes. This is illustrated by the larger and rounder leaves found on *da1-1* plants (Li et al., 2008), and the larger more serrated leaves found in the *rpt2a* mutant, which has increased cell expansion (Sonoda et al., 2009). In order to identify elements in core developmental pathways, involved in the manipulation of *overall* organ size, plants were phenotyped for mean petal area and mean seed area.

For each line, ten petals were collected from 5 individual plants (two per plant). The petals were harvested from the first flowers per plant, to ensure developmental equivalence; once harvested they were placed intact, on transparent adhesive tape and attached to a clean black background. Petal area was recorded using a high-resolution scanning method following a protocol adapted from (Herridge et al., 2011). Images were scanned, and areas were calculated using the ImageJ image analysis software (see section 2.3.5.1), which allowed for a high-throughput data input pipeline. To identify general growth regulators and cell-cycle genes

(instead of only petal-specific genes) petal area was not normalised to sepal area (Abraham et al., 2013).

Seed areas were calculated using a similar method. Due to their smaller size (relative to the fixed resolution of the scanner), the number of seeds in the sample were increased to n>60, and instead of adhering to tape, the seeds were scattered in a petri dish prior to scanning.

For seed analysis, the ImageJ software was set to exclude aggregations of seed in the petri-dish; such that only individual seed areas were recorded. As a fail-safe, and to ensure the accuracy of the data, after each ImageJ measurement, a manual check of the scans was made to ensure no seed aggregates had been measured.

6.2.2 – Petal shape

Organ *size* is intricately linked to organ *shape* (see section 1.2.2), and an increasing number of genes, primarily characterised in *Antirrhinum* and Arabidopsis, have been identified that play a significant role in influencing organ shape. Prolonged cell division in leaf meristemoid cells of the Arabidopsis *PEAPOD* (*PPD*) mutant (White, 2006), and mis-regulation of the cell-cycle arrest front in the Antirrhinum *CINCINNATA* (*CIN*) mutant (2003), both result in an increase in leaf size *and* curvature; illustrating the intimate relationship between size and shape. Despite this inter-relatedness, many genes appear to coordinate organ shape without affecting the overall organ area. For example, although *tcp14* and *tcp15* mutants do not affect overall leaf size, principle component analysis reveals that they cause significant changes to leaf shape and aspect ratio (Kieffer et al., 2011).

Cell proliferation and cell expansion are the driving forces behind organ growth, however it is the spatial coordination of these forces that determines final organ shape. Many factors are thought to be involved in the setting of shape, including mobile morphogens such as the proposed *KLUH*-dependent mobile growth factor (Adamski et al., 2009, Eriksson et al., 2010, Kazama et al., 2010) and genes that exert biophysical constraints on the developing organ. For example, *ttg2* biophysically constrains the developing endosperm through the seed-coat (Garcia et al., 2005), and *angustifolia* (*an*) mutants have a long and narrow leaf phenotype as a result of altered cortical microtubule arrangements, which promote cell-expansion in the apical-basal axis (Kim et al., 2002). These topics are reviewed in detail in Chapter 1.

This genetic analysis of petal shape is designed to identify any genes involved in the *coordination* of petal growth.

In this analysis, three petal shape parameters were recorded: petal length, petal width and petal shape (length/width). The primary measurements (length and width) were recorded using the ImageJ software directly from the high-resolution petal scans described in section 6.2.1. Petal shape was calculated as a secondary measurement from the ratio of length/width according to recent published work (Abraham et al., 2013).

6.2.3 – Variation in seed and petal size

Despite the indeterminate nature of vegetative plant growth, organs such as seeds, petals and leaves display determinate growth (see section 1.2.1). The uniformity of final organ size and morphology within species, compared to between species, demonstrates a high level of developmental regulation. This regulation can be seen clearly in the 'compensation' mechanism that ensures uniformity in organ size in spite of changes in cell proliferation and expansion (Dewitte et al., 2007, Ferjani et al., 2007, Jones et al., 1998). This not only implies that the developing organ possesses an intrinsic knowledge of its pre-determined final size, but that there are regulatory networks in place to buffer against aberrations in development. Variation in the degree of uniformity of final organ size is likely to reflect differences in these 'buffering' regulatory networks, and in order to identify genes in these 'buffering' networks, a genetic analysis of the variation in final organ size was carried out.

The phenotype used for these analyses was the standard error (SE) of the mean organ area (for petal and seed respectively).

6.3 – MAGIC analysis of seed size

This MAGIC analysis was designed to investigate the regulation of seed and petal growth in Arabidopsis. The project was initiated late on in my research schedule as a means to screen for, and identify novel regulators of organ growth that could be subjected to further functional study akin to that described for DA1 in Chapters 3-5. As a consequence of the late start, at the time of writing only the seed data have been analysed.

NASC Stock Number	Accession	Origin
N6643	Bur-0	Ireland
N6660	Can-0	Canada
N6673	Col-0	USA
N6674	Ct-1	Italy
N6688	Edi-0	Scotland
N6736	Hi-0	Netherlands
N6762	Kn-0	Lithuania
NW20	Ler-0	Germany
N1380	Mt-0	Libya
N6805	No-0	Germany
N6824	Oy-0	Norway
N6839	Po-0	Germany
N6850	Rsch-4	Russia
N6857	Sf-2	Spain
N6874	Tsu-0	Japan
N6889	Wil-2	Russia
N6891	Ws-0	Russia
N6897	Wu-0	Germany
N6902	Zu-0	Germany

Table 6.1 – MAGIC parent lines

List of the parental accessions used to generate the MAGIC lines (table adapted from NASC, http://arabidopsis.info/CollectionInfo?id=112).

This section describes the MAGIC mapping population and how it has been used to identify *a priori* and novel candidate genes predicted to be involved in the regulation of seed area. It documents the identification of eight QTL for mean seed area, short-lists *a priori* and novel candidate gene-lists for each QTL, and briefly interrogates the sequence of selected candidate genes to screen for possible causative genetic variation. Importantly, this section aims to develop a platform for identifying the causative variation underlying the identified QTL, *not* to prove the causality of individual genes; a step that is beyond the scope of this work.

The mapping population used in this study was The Multiparent Advanced Generation Inter-Cross (MAGIC) lines; a collection of 527 RILs generated from inter-mating 19 natural accessions

(Kover et al., 2009), kindly provided by Phil Wigge at the Sainsbury Laboratory Cambridge University, Cambridge. The 19 parents (Table 6.1) had been intercrossed for four generations before being immortalised by six generations of backcrossing. This has resulted in 527 stable homozygous lines, of which 452 were available for this study. Compared to conventional bi-parental RIL populations, the presence of 19 parents incorporates increased allelic diversity into the mapping population (Kover et al., 2009). In addition, the increased number of recombination steps involved, improves the mapping resolution of the MAGIC population to as little as 300Kb (Kover et al., 2009).

The final immortalised lines are unique mosaics of the 19 founder genomes, formed of a series of haplotype blocks, each descended from one of the 19 parents. The location and ancestral origin of these haplotype blocks can be mapped using genotype data available for each line (Kover et al., 2009). The ability to probabilistically infer the mosaic structure of each ML allows the prediction of parental contribution to each QTL. In addition, all 19 parental lines have publicly available genome sequences (Gan et al., 2011), which allows the targeted interrogation of parent-specific genome sequence data at predicted QTL loci.

The MAGIC analysis was performed in collaboration Mathew Box at the Sainsbury Laboratory Cambridge University, Cambridge. The QTLs were identified using HAPPY: 'a software package for multipoint QTL mapping in genetically heterogeneous animals' (Mott, 2000, Mott et al., 2000). Using the collected phenotype values and pre-existing genotype data, this method reconstructs ancestral haplotypes for each ML and subsequently tests for QTLs using linear regression analysis (Mott et al., 2000). For this investigation, the genotype information used in the HAPPY analysis was from 1250 SNPs, spaced roughly 100Kb apart (Kover et al., 2009, Mott et al., 2011).

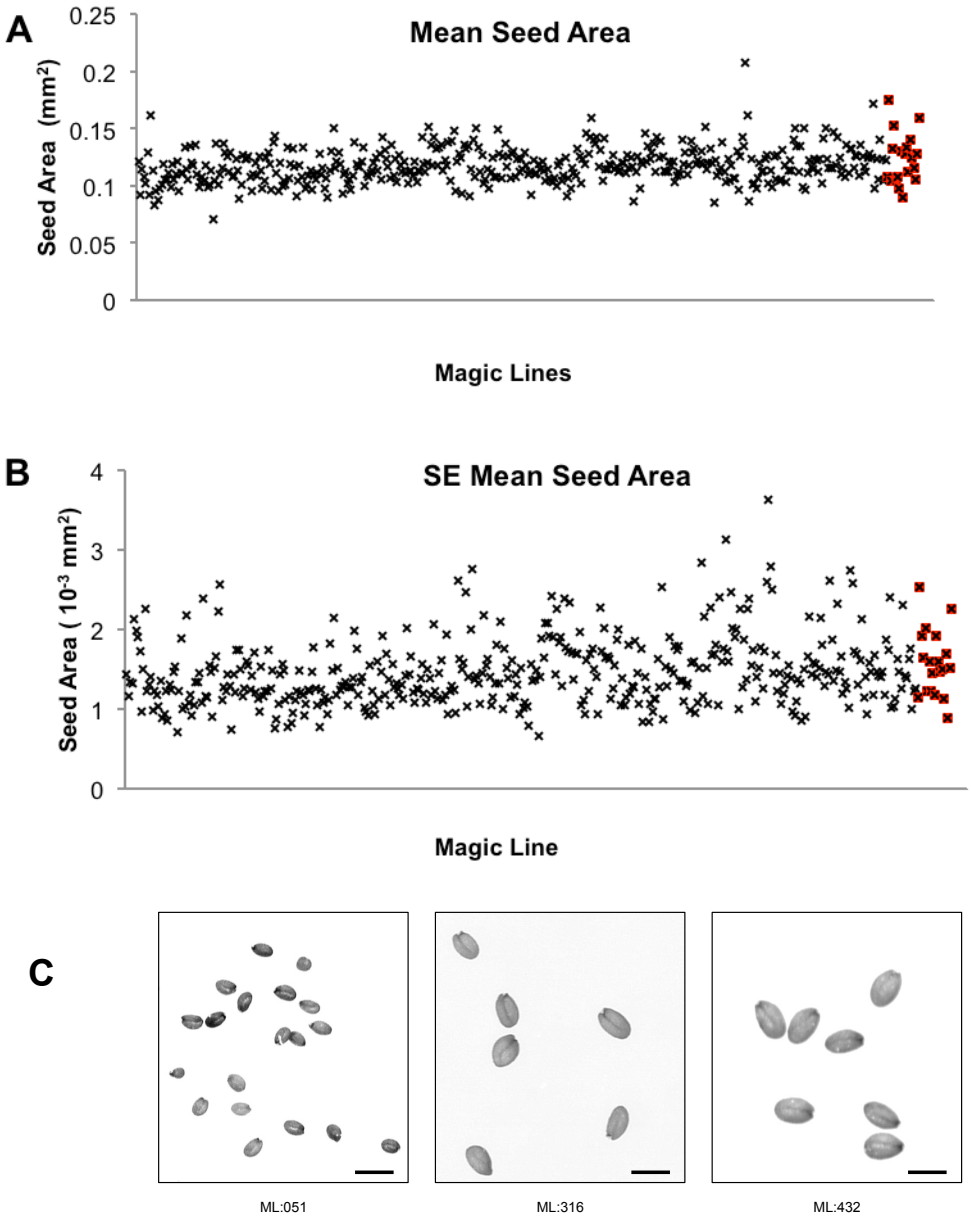

Figure 6.1 – Variation in seed area in the MAGIC population

(A) The distribution of seed area within the MAGIC population, data is presented as means (n=64). (B) The distribution of SE mean seed area (data presented as SE mean (n=64)) representing the amount of variation within each line of the mapping population. (A-B) Black crosses represent MAGIC descendant lines and black crosses with red backgrounds represent MAGIC parental lines. (C) Scans of seed from three different MAGIC lines; scale bar = 600µm.

6.3.1. – Transgressive segregation of seed size in the MAGIC lines

There was considerable variation in both the mean and standard error seed area within the MAGIC mapping population. Fig. 6.1 shows that ML seeds varied from an average of 0.071mm^2 (line 51) to 0.208mm^2 (line 432); an increase of 291%. Seeds from the lines with the most extreme seed area values (lines 51 and 432), and an intermediate line (line 316) are shown in Fig. 6.1c, illustrating the variation within the population. Interestingly, Fig. 6.1a also shows that the range of mean seed-size amongst ML descendants (0.071mm^2 to 0.208 mm^2) is greater than that of the MAGIC parental lines (0.090mm^2 to 175mm^2); revealing seed area is a transgressive phenotype amongst the MAGIC population.

A transgressive phenotype, where hybrid lineages display more extreme phenotypes than their parental lines is also seen for the SE mean seed area data (Fig. 6.1a,b). For this data set, ML hybrids range from 1.1x10^{-3} mm^2 (line 216) to 4.5x10^{-3} mm^2 (line 432), whereas parental SEs vary from 1.3x10^{-3} mm^2 to 3.2x10^{-3} mm^2.

Transgressive segregation occurs when alleles at multiple loci in parental lines recombine in the hybrids. This results from the interactions of some alleles that act to 'increase' the phenotype and others that 'reduce' it, and while some hybrid combinations will cancel each other out, others will complement each other and generate an extreme effect (Bell and Travis, 2005). Such extreme phenotypic values may be a consequence of novel combinations of epistatic or additive parental alleles (Dittrich-Reed and Fitzpatrick, 2012), or they may result from synergistic interactions that arise genes from working in a common mechanism, similar to that seen for the *da1-1* and *eod1-2* alleles (Li et al., 2008).

This transgressive segregation of the seed area phenotype confirms that the phenotype is both complex and quantitative. It supports observations in the literature that multiple genes combine to regulate seed growth, and, as is demonstrated by *KLUH* and *DA1*, that these genes have antagonistic roles (Li et al., 2008, Adamski et al., 2009, Anastasiou et al., 2007). This reveals that within the parental MAGIC population variation is likely to be polygenic with alleles that vary in strength both positively and negatively. Through the hybridisation of these ancestral lines, and the subsequent disruption of this network, the QTL analysis described in sections 6.3.2 and 6.3.3 can be used to identify constituent regulatory genes.

6.3.2 – No significant QTLs were identified for SE seed area

Despite the large degree of variation in the SE mean seed area dataset, no QTLs were identified in this MAGIC analysis. Fig. 6.2 shows the QTL scan, and, although there are several moderate peaks in chromosome one and chromosome four, none is sufficiently significant.

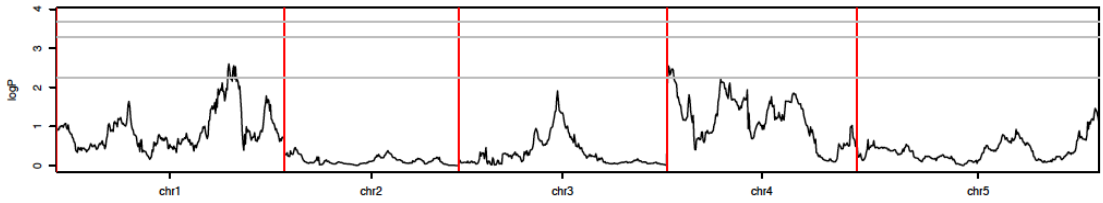

Figure 6.2 – No QTL for SE mean seed area in the MAGIC population

Associations of SE mean seed area with genome position. The x-axis represents the full genome length of Arabidopsis, with the vertical bars denoting boundaries between chromosomes. The y-axis displays the associations of genotype markers at different positions on the genome with the phenotype. Associations are presented as logP values and grey bars represent genome-wide significance thresholds for p=0.5, p=0.1 and p=0.05. Significant associations are marked with gold stars. This genome scan reveals that there are no significant associations between genotype markers and the SE mean seed area phenotype.

6.3.3 – 8 QTLs identified for mean seed area

HAPPY analysis (Mott, 2000, Mott et al., 2000) of mean seed area in the MAGIC mapping population revealed eight QTL for seed area, which had peaks that were significantly associated with the phenotype to the 95% significance level. There is one QTL in chromosome 1, one QTL in chromosome 2 and six smaller QTL in chromosome 4 (Fig. 6.3). Table 6.2 shows that QTL 1 and 2 (on chromosome 1 and chromosome 2 respectively) are considerably broader that the remaining QTL; with QTL1 being ~5.3Mb and QTL8 only ~22Kb.

This difference in QTL size is reflected in the number of candidate genes underlying each QTL. QTL1 and QTL2 (~5.3Mb and ~3.0Mb) cover 1410 and 742 genes respectively, and the 300Kb either side of the peak SNP (Kover et al., 2009) for each QTL covers 172 and 150 genes respectively. In contrast, the entirety of QTL8 covers only 4 genes. Although the large size of QTL1 and QTL2 is not abnormal (Abraham et al., 2013, Kover et al., 2009), the considerably narrower resolution of QTL 4,5,7 and 8 may be an artefact of a fragmented larger QTL.

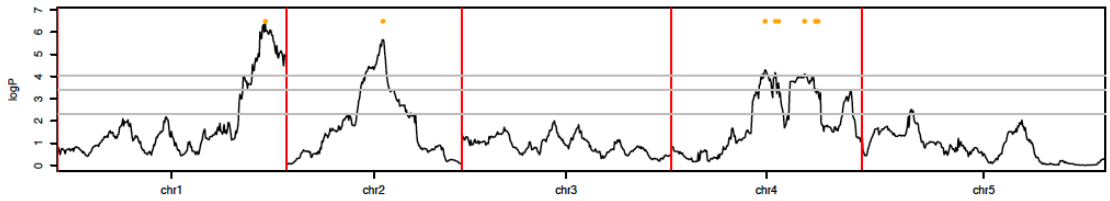

Figure 6.3 – Eight QTL for mean seed area in the MAGIC population

Associations of mean seed area with genome position. The x-axis represents the full genome length of Arabidopsis, with the vertical bars denoting boundaries between chromosomes. The y-axis displays the associations of genotype markers at different positions on the genome with the phenotype. Associations are presented as logP values and grey bars represent genome-wide significance thresholds for p=0.5, p=0.1 and p=0.05. Significant associations (those with a genome-wide p-value of p<0.05) are marked with gold stars. This genome scan reveals that there are eight significant associations between genotype markers and the mean seed area phenotype. The peak SNPs of each association are located at: Chr1-28136775, Chr2-12428271, Chr4-10045141, Chr4-11326180, Chr4-11579827, Chr4-13576430, Chr4-14533009 and Chr4-14658631.

QTL	Chr	QTL start (bp)	QTL end (bp)	Size (Mb)	QTL Peak	Peak SNP	LogP	Genome-wide p-value
1	Chr1	25027501	30348203	5.320702	28136775	MASC00850	6.493990919	0.003
2	Chr2	10242327	13258513	3.016186	12428271	MN2_12435349	5.656010097	0.011
3	Chr4	9364976	10777260	1.412284	10045141	PHYE_1561	4.299730069	0.035
4	Chr4	11001770	11470264	0.468494	11326180	NMSNP4_11326190	4.176744435	0.043
5	Chr4	11488346	11579827	0.091481	11579827	MN4_11579839	3.709603639	0.077
6	Chr4	12654216	14379731	1.725515	13576430	MN4_13576438	4.103519746	0.047
7	Chr4	14379870	14533009	0.153139	14533009	MN4_14533015	3.451684135	0.096
8	Chr4	14635799	14658631	0.022832	14658631	MASC03154	3.423096522	0.097

Table 6.2 – Details of eight QTL for mean seed area

The table provides details of the location of each QTL (Chr=chromosome), including the chromosome position of the start, the end and the peak of the QTL. The table also provides the ID of the peak SNPs and their genome-wide p-values.

6.3.4 – 21 *a priori* candidate genes identified in QTLs

Four of the eight QTL intervals (QTL 1,2,3 and 6) overlapped with genes known to be involved in the regulation of organ growth. The presence of such *a priori* candidates in the QTL intervals presents the possibility that these genes are responsible for the phenotypic variation observed in the mapping population.

The *a priori* gene list (Table S1) is populated with genes that have published organ-growth phenotypes, and is designed to be used as a tool for explaining observed phenotypic variation with previously characterised genes. 21 members from this list are present in four of the QTL intervals identified for seed area (Table 6.3), including six *TCP* transcription factors (*TCPs 1,2,10,12,15 and 22)*, three *CLAVATA* related genes (*CLV1*, *CLE8*, *CLE26*) and the E3 ligase *DA2*. Represented in these QTL are *a priori* genes involved in both core aspects of cell growth; including DA2, a negative regulator of cell *proliferation* (Xia, 2013), and RPT2a, the negative regulator of cell *expansion* (Sonoda et al., 2009).

The QTL intervals include characterised seed-specific growth regulators, such as *SHB1* (*SHORT HYPOCOTYL UNDER BLUE1*), which interacts with *MINISEED3* and *HAIKU2* to control seed development (Zhou et al., 2009). However, they also include genes that only have characterised phenotypes in leaves and petals, including the homeobox transcription factor, *ZHD5* (*ZINC-FINGER HOMEODOMAIN 5*), over-expression of which has been shown to increase leaf area as a consequence of increased cell size (Hong et al., 2011). In addition, the regulator of petal size and shape, *ERECTA,* is present in QTL2 (Abraham et al., 2013, Shpak et al., 2003).

The QTL intervals also include genes involved in phytohormone signalling, including the ethylene response factor *ERF6* (*ETHYLENE ELEMENT BINDING FACTOR6*), which is a negative regulator of leaf growth (Dubois et al., 2013) and a positive regulator of jasmonate and ethylene mediated pathogen defence (Moffat et al., 2012). Additionally, a member of the gibberellin-signalling pathway, the gibberellic acid oxidase, *GA20OX1*, is present in QTL6.

QTL	GENE ID	GENE NAME
QTL1	AT1G67260	TCP1
QTL1	AT1G67775	CLE8
QTL1	AT1G68480	JAG
QTL1	AT1G68800	TCP12
QTL1	AT1G69690	TCP15
QTL1	AT1G69970	CLE26
QTL1	AT1G72010	TCP22
QTL1	AT1G75240	ZHD5 (ZINC FINGER HOMEODOMAIN5)
QTL1	AT1G75820	CLV1 (CLAVATA 1)
QTL1	AT1G76420	CUC3
QTL1	AT1G78300	GRF2
QTL1	AT1G78420	DA2
QTL2	AT2G26330	ERECTA
QTL2	AT2G31070	TCP10
QTL3	AT4G17490	ETHYLENE RESPONSE FACTOR 6
QTL3	AT4G18390	TCP2
QTL6	AT4G24900	TTL
QTL6	AT4G25350	SHB1 (SHORT HYPOCOTYL UNDER BLUE 1)
QTL6	AT4G25420	GA20OX1 (GIBBERELLIN 20-OXIDASE)
QTL6	AT4G28840	TIE
QTL6	AT4G29040	RPT2A (REGULATORY PARTICLE AAA-ATPASE 2A

Table 6.3 – The QTL for mean seed area include 21 *a priori* regulators of organ growth

The table provides the details of 21 *a priori* regulators of organ growth and development that are present within the eight QTL identified for mean seed area. Genes listed are a subset of those presented in Table S1.

The observed QTL overlap with *a priori* genes involved in all aspects of organ development, and with characterised responses to many of the major plant hormones, is encouraging; although it must be reiterated that said *a priori* genes are only *candidates* and not necessarily causal. Further investigation – which is beyond the scope of this study – is underway to identify causality (see section 6.3.7).

Of particular interest to this thesis is the presence of *DA2*, *TCP15* and *TCP22* in QTL1. Although it is impossible to confirm causality at this stage, data from Chapters 4 and 5 strongly support a role for these genes in regulating seed area. Section 5.2.1.2 and recent work with our collaborators at the Chinese Academy of Sciences (Xia, 2013), demonstrates that DA2 – in certain genetic backgrounds – has a significant negative influence on seed area. Although

section 5.2.1.2 indicates that a *da1* null allele is required for *da2-1* to influence seed area, it is possible that the genetic background of the MAGIC population is conducive to *da2* acting independently of a *da1* null allele.

In addition, Chapter 4 has described in detail the role of *TCP15* in growth and development, and it is therefore particularly interesting to identify this gene in QTL1. However, *TCP22* is also of interest due recent work which has shown that, based on sequence analysis of the TCP domain, TCP22 (and TCP14) are the most closely related family members to TCP15 (Aggarwal et al., 2010). And as Fig. S3 documents, previous studies in the lab have characterised *TCP22* as a regulator of organ growth and development.

6.3.5 – Bur-0 haplotype predicted to contribute to increase in seed area

Fig. 6.4 shows boxplots of each parental line, representing the estimated contribution of their haplotype to each QTL phenotype and the predicted direction of their contribution. One particular parental haplotype – Bur-0 – is predicted contribute the largest increase in seed area across all eight QTL. In some instances, such as QTL2 (Fig. 6.4b), other parental lines including Edi-0, Kn-0 and Oy-0 also have a strong predicted contribution. However, for others, such as QTL6 (Fig. 6.4f), the estimated Bur-0 haplotype influence is considerably larger than all other parental lines.

Inspection of the variation in seed area amongst the parental lines (Fig. 6.7) reveals that Bur-0 has the largest seed of all parents. This strengthens the predictions in Fig. 6.4 that the Bur-0 haplotype is responsible for all eight QTL and suggests that the interrogation of the Bur-0 genotype at these intervals may yield insights as to the true causative variation. This genotype interrogation is made possible by the sequencing of all parental lines (Gan et al., 2011) and the availability of the sequence data through the Rätsch lab GBrowse (http://gbrowse.cbio.mskcc.org/gb/gbrowse/thaliana-19magic/).

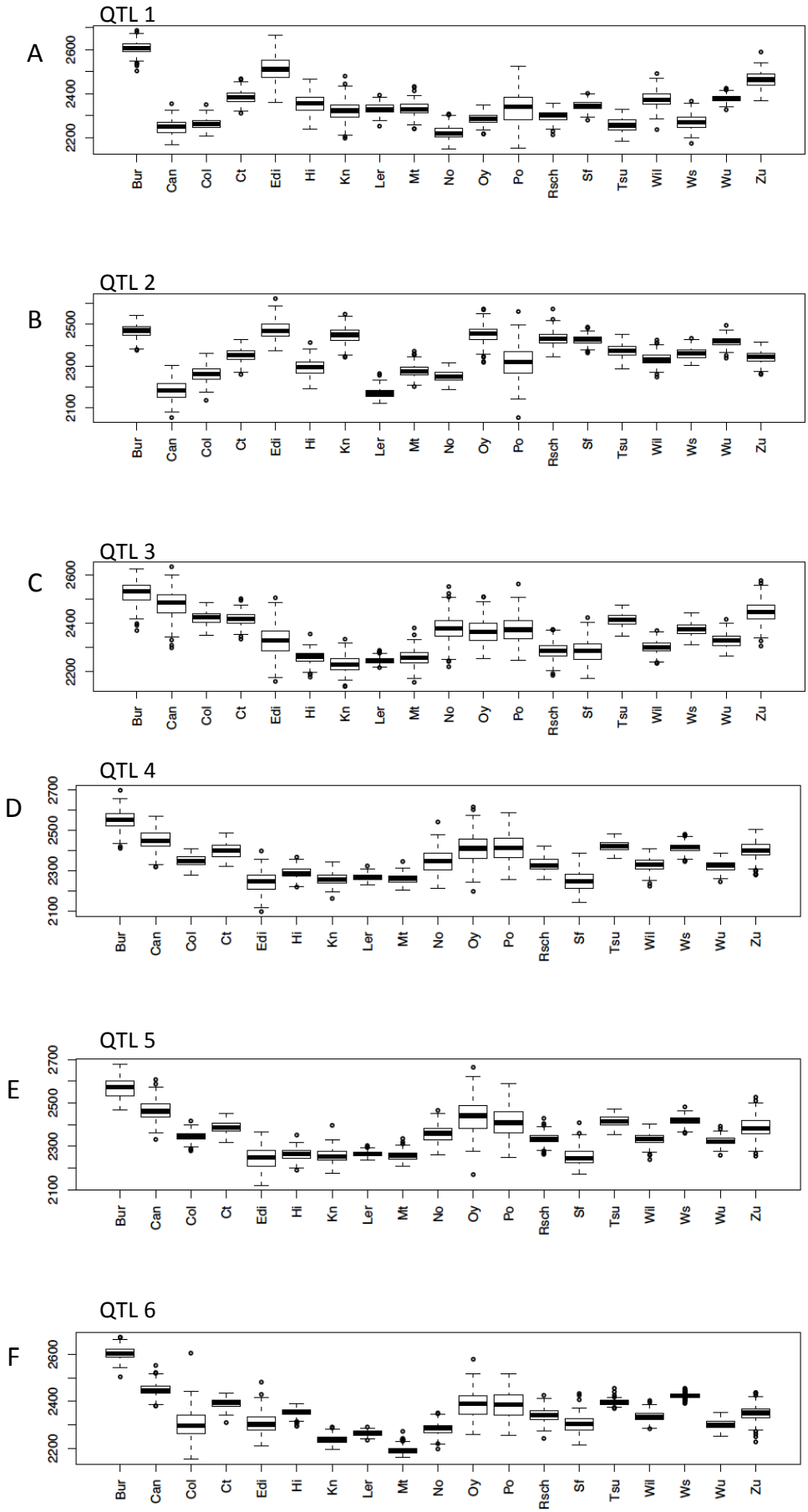
A
QTL 1
2200
2400
2600
Bur
Can
Col
Ct
Edi
Hi
Kn
Ler
Mt
No
Oy
Po
Rsch
Sf
Tsu
Wil
Ws
Wu
Zu
B
QTL 2
2100
2300
2500
C
QTL 3
D
QTL 4
2700
E
QTL 5
F
QTL 6

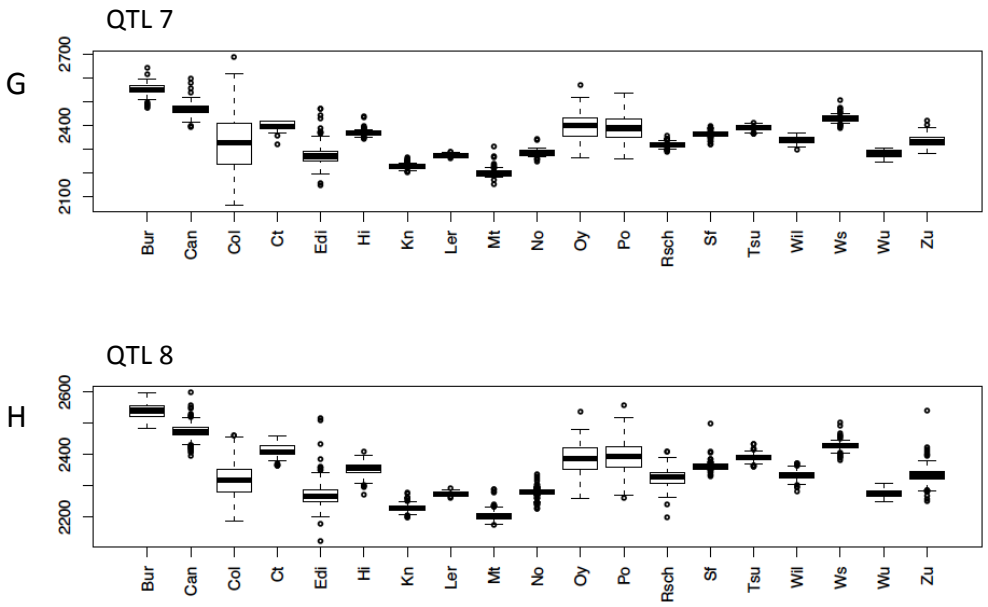

Figure 6.4 – The predicted contribution of ML parents to the eight observed QTL

(A-H) The predicted contribution of ML parental lines to the eight observed QTL; figures A-H represent QTL 1-8 respectively. The x-axis shows the identities of the 19 parent lines from the MAGIC population. The y-axis is a prediction of the parental influence on phenotype using pixels as units (1 pixel = $5x10^{-5}$ mm^2); in all QTL a Bur-0 allele is predicted to positively influence seed area.

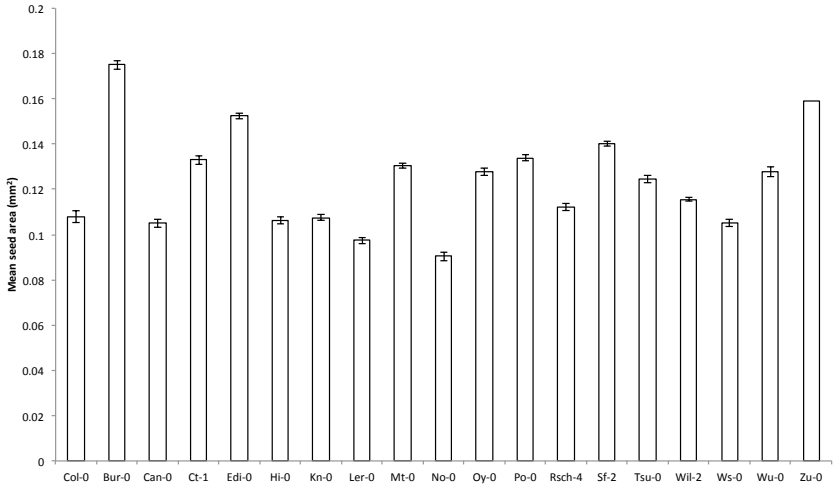

Figure 6.5 – Variation in petal area amongst the 19 MAGIC parent lines

The x-axis shows the identities of the 19 parent lines of the MAGIC population and the y-axis plots the mean seed area ± SE. Bur-0 has the largest seed area in the parental population.

Fig. 6.6 shows the location of Bur-0 specific polymorphisms in a selection of candidate genes. Fig. 6.6a reveals that there are a considerable number of Bur-0 specific SNPs in the promoter region of *TCP15*. The promoter of *TCP15* is considered to begin 1.92 Kb upstream of the 5' UTR (Kieffer et al., 2011), and as illustrated in Fig. 6.6a, a region of ~500bp extending to up to 2Kb from the 5'UTR is populated with SNPs unique to Bur-0. Given the published *TCP15* developmental phenotypes (Kieffer et al., 2011), and the seed size phenotypes documented in section 4.3.3, it is plausible that this promoter variation may be that which underpins QTL1.

Other genes of interest include *ERECTA,* an LRR-RLK involved in the regulation of organ shape (Shpak et al., 2003, Torii et al., 1996), which was recently identified in a bi-parental RIL mapping population as a regulator of petal shape (Abraham et al., 2013). There were two Bur-0 specific amino acid transitions in the *ERECTA* coding sequence, four Bur-0 specific insertion/deletion events in the promoter region and a two amino-acid deletion in the 5' UTR (Fig. 6.6e). The two amino acid transitions ($P^{155}L$ and $T^{225}A$) are both in the *ERECTA* N-terminal leucine rich repeat domains - LRR4 and LRR7 respectively. Interestingly, another single amino acid transition in LRR9 (*er-103,* $M^{282}I$) has been shown to be sufficient to cause a reduction in plant height, silique length and width, and pedicel length (Torii et al., 1996). Suggesting that the observed Bur-0 specific transitions in LRR4 and LRR7 may indeed be sufficient to cause similar developmental phenotypes. Unfortunately the publication describing the *er-103* mutation (Torii et al., 1996) does not document a seed size phenotype. However, due to the intimate interaction between maternal tissue and the developing seed, it is possible that such severe silique phenotypes may affect seed size. This phenomenon is illustrated by the barley *seg1, 3, 6 & 7* mutants, which have a reduced seed size due maternal impairment of seed nutrition (Felker et al., 1985), and the *ttg2* mutation that represses seed development through an integument-mediated mechanism (Garcia et al., 2005).

Finally, investigation of the polymorphism environment of *SHB1* – the only seed-specific *a priori* candidate present in the QTL intervals – reveals the presence of a Bur-0 specific SNP in the 3' end of the coding sequence (Fig. 6.6b). This SNP, a $T^{1944}G$ substitution, results in a Ser-Arg transition at position 648, which is located in the EXS domain (InterPro:IPR004342); a region rich in trans-membrane helices with a possible role in endomembrane sorting (Wang et al., 2004). The exact location of the $Ser^{648}Arg$ transition is in an extracellular inter-transmembrane region. The role of the EXS domain is not clear, however it has been demonstrated that over expression of this domain phenocopies the *shb1* null mutant and generates a short hypocotyl phenotype (Zhou and Ni, 2010, Kang et al., 2013). The sufficiency

of the EXS domain to cause the short hypocotyl phenotype, suggests that it may also be intimately involved in the generation of the seed size phenotype reported in Zhou et al (2009). If this is the case then it is possible that the Ser^{648}Arg transition could influence the seed size.

These observations are not yet sufficient to establish the identity of genes causal to the QTL, however they strengthen the arguments for the involvement of these genes, and allow the formulation of hypotheses that can be tested to develop our understanding further. For example, the identification of significant Bur-0 polymorphisms in the promoter of *TCP15* and coding sequence of *SHB1* allows the initiation of quantitative complementation experiments. A strategy that involves crossing the allele of interest into a knock-out background and assaying its ability to complement the knock-out. This is then compared to the effect of the crossing the allele of interest into the wild type background, to control for the genome-wide heterozygosity of the F1.

This section has discussed the identification of *a priori* candidate genes in QTL intervals, and subsequent interrogation of their parent-specific genotypes. However, in addition to *known* regulators of seed size, the MAGIC analysis has the potential to identify *novel* regulators.

6.3.6 – Candidate novel regulators of organ size

In order to identify novel regulators of seed size from all eight QTL, a short-list of genes was created by mining all genes mapping to QTLs for the keywords: *expansion*, *proliferation*, *cell-cycle*, *embryo*, and *endosperm*, as well as manual analysis of all the published gene descriptions. The resulting list of candidate genes is shown in Table S5 and includes many cell-cycle genes including *APC6* (*ANAPHASE PROMOTING COMPLEX 6*), *CYCLIN A1;2*, *CYCLIN B2;4* and *CDKB2;1*. It also identified members of the brassinosteroid signalling pathway: *BZR1* (*BRASSINAZOLE-RESISTANT 1*) and *BIN2* (*BRASSINOSTEROID INSENSITIVE 2*), both of which are involved in regulating the brassinosteroid growth response (He et al., 2005, He et al., 2002).

The list also identified many apparent seed-specific candidates; in all QTL there were 30 *EMB* genes, a subset of which are displayed in Table S5 and all of which are shown to be defective in embryo development (Tzafrir et al., 2004). Of these, *EMB1417* and *EMB1989* both sit within 41Kb of the peaks of QTL 4 and 5 respectively; and *EMB1417* - a pentatricopeptide repeat-containing protein - has a Bur-0 specific amino-acid transition (L^{68}Q) in its N-terminal region. In addition, in QTL 6 there is a cluster of four *SEED STORAGE ALBUMIN* genes (*SESA1-4)* that encode members of one of the three major seed storage protein families (Shewry et al., 1995). Interestingly, analysis of the sequence data from the MAGIC parent lines reveals the presence

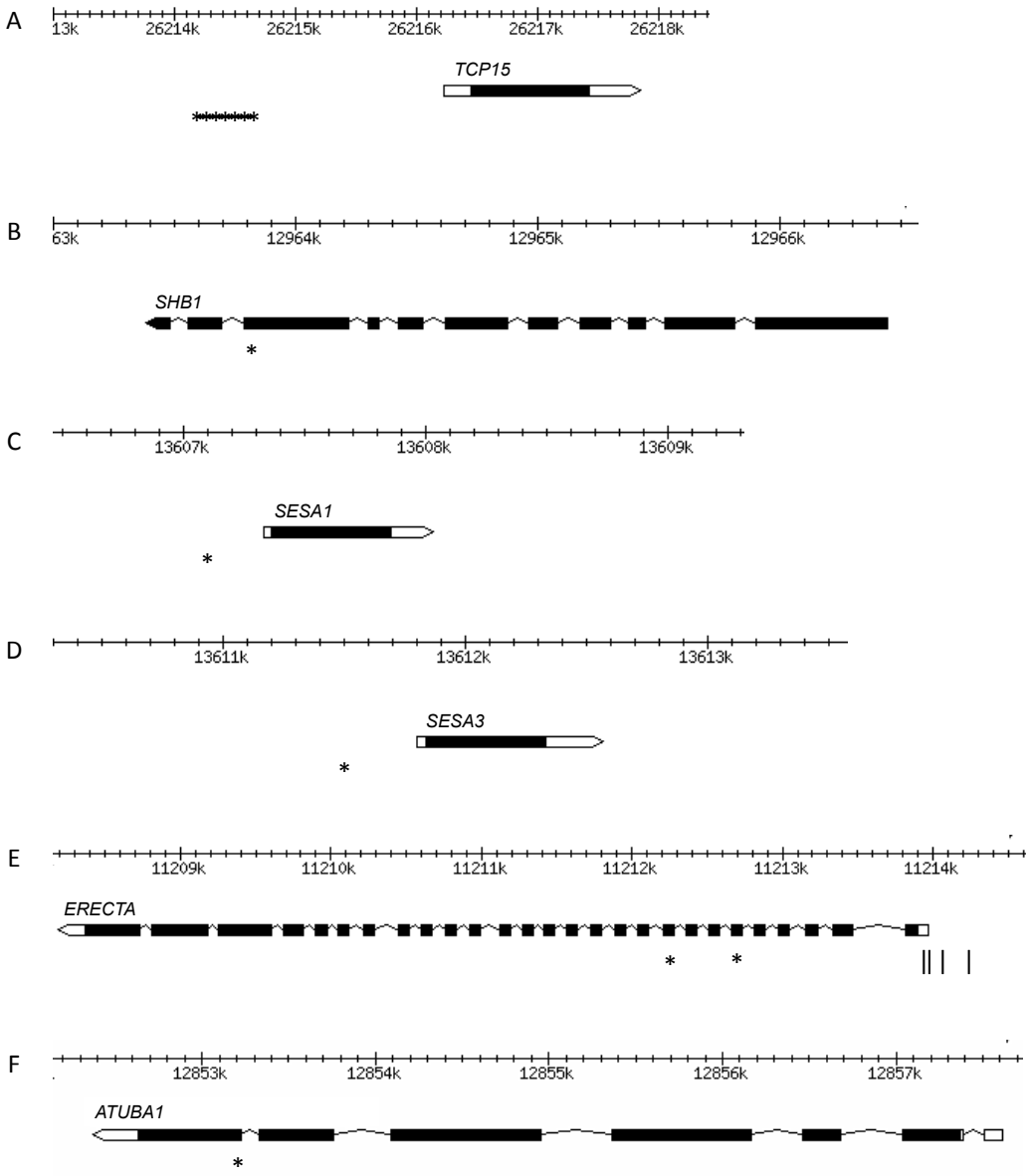

Figure 6.6 – Bur-0 specific polymorphisms in candidate genes

(A-F) Bur-0 specific SNPs ('*') and insertion/deletion events ('|') in *a priori* candidate genes for the eight identified seed area QTL. The figure highlights only mis-sense polymorphisms in transcribed sequence and polymorphisms in promoter regions. (A) *TCP15* has a large amount of Bur-0 specific polymorphisms in a 500bp region of its promoter; these polymorphisms include SNPs and insertion/deletion events. (B) *SHB1* has a single T-G transition in the ninth exon. (C,D) *SESA1* and SESA3 both have SNPs in their promoter regions (<400bp from their ATG). (E) *ERECTA* has two SNPs in its coding sequence: a C-T transition in exon 6 and a T-C transition in exon 9. (F) *ATUBA1* has a single A-G transition in exon 6. SNP locations were identified using, and images were adapted from the Rätsch lab GBrowse (http://gbrowse.cbio.mskcc.org/gb/gbrowse/thaliana-19magic/).

of single Bur-0 specific SNPs in the promoter regions of *SESA1* and *SESA3* (Fig. 6.6c,d), which are 31.25Kb and 35.75Kb from the peak SNP in QTL 6 respectively.

An ubiquitin pathway gene with a direct link to DA1 is also present in this list of potential novel regulators. *ATUBA1*, one of the two Arabidopsis E1 activating enzymes, and a Y2H interactor with DA1 (Chapter 4), is present in QTL2. This gene has been shown to play a role in plant innate immunity and to have an organ size phenotype in certain genetic backgrounds (Goritschnig et al., 2007). *ATUBA1* has one Bur-0 specific SNP in the coding sequence, an $A^{2656}G$ substitution, which results in a $T^{886}A$ transition in C-terminal region of the protein (Fig. 6.6f). Interestingly, this amino-acid transition is within the ATUBA1 C-terminal fragment that was pulled out by DA1 in the Y2H described in Chapter 4, and is 146 amino acids from the deletion responsible for the *mos5* phenotype described in (Goritschnig et al., 2007). Furthermore, the transition is in position eight of the second ubiquitin-activating enzyme repeat (Interpro: IPR000127, Pfam: PF02134), suggesting that the mutation could alter catalytic activity. Modification of *ATUBA1* function, as shown in the *mos5* deletion, can have relatively specific phenotypic effects. In the case of *mos5*, the mutation appears to effect only plant innate immunity (including a growth response); suggesting a specific relationship with a subset of Arabidopsis E2s. If this is indeed the case, then the Bur-0 specific $T^{886}A$ transition may also specifically affect growth and development pathways, and is therefore a good candidate for the causative genetic variation in QTL2.

6.3.7 – Future work

As discussed in section 6.3, this work was initiated with the intention of identifying shortlists of *a priori* and *de novo* candidate genes, which could be tested in the future to determine their role in the identified QTL. The MAGIC analysis has successfully identified a list of 21 *a priori* candidates and 75 *de novo* candidates. Interrogation of the sequence of these genes in the parental haplotypes predicted to underlie each QTL, has offered additional insight into the likelihood of these genes being causal.

This not only provides a rich resource of candidate genes for further investigation, but the SNP interrogation of parental haplotypes, and subsequent focus on genes with Bur-0 specific polymorphisms allows the further refining of the candidate list. Unfortunately, due to time constraints, and the nature of this work as a side-project, complete SNP interrogation of all candidate genes has not been completed and an ultimate short-list of candidates has not yet been populated. Nonetheless, sections 6.3.4 to 6.3.6 provide good support for the further study of genes including: *DA2*, *TCP15*, *TCP22*, *ERECTA*, *ATUBA1*, *SESA1*, *SESA3* and *EMB1417*.

Knockout lines will be acquired for these genes, and if knockout phenotypes exist, a strategy of quantitative complementation will be undertaken to determine their role in their respective QTL.

6.4 – Genome wide association analysis of petal and seed growth

This genome wide association (GWA) analysis was designed to investigate the regulation of seed and petal growth in Arabidopsis. As with the MAGIC analysis, this project was initiated late on in my research schedule as a means to screen for and identify novel regulators of organ growth that could be subjected to further functional study. At the time of writing, the mapping population had been genotyped, the genotype-phenotype associations had been analysed and candidate genes had been identified. This chapter focuses on two putative associations only, one for mean petal length and one for SE mean petal area (see section 6.2.3 for explanation). It briefly documents the identification of these loci and the candidate genes therein, but does not investigate the associations any further. Work to prove the causality of these candidate genes is on-going and is not reported in this chapter.

The mapping population used in this investigation was made up of a subset of the 1001 genomes project (Weigel and Mott, 2009) consisting of 272 Swedish accessions kindly provided by Caroline Dean at the John Innes Centre, Norwich (Table S2). This population was being used at the John Innes Centre by Caroline Dean and Mathew Box to map genes involved in the vernalisation response. During this work, variation in petal size was observed within the population and therefore it was selected for this study of organ growth. Due to its confined geographical distribution, this population is thought to have reduced population structure effects and, as a consequence, a reduced frequency of false positives (Filiault and Maloof, 2012). Despite this mitigating measure, genetic diversity in Eurasian accessions of Arabidopsis has been shown to follow a broad trend of "isolation by distance" (Platt et al., 2010). In order to determine whether this isolation by distance might lead to population-structure effects within this Swedish population, the effect of latitude on phenotype was investigated (Filiault and Maloof, 2012). Figure 6.7 shows that there were negative correlations between latitude and both mean petal area and mean petal length (Pearson's r, $p=0.006$ and $p=0.044$, respectively), and a positive correlation between latitude and mean seed area (Pearson's r, $p<0.0001$). For these reasons it was decided that a further corrective approach would be used in this analysis (Cheng et al., unpublished).

The genome wide association analysis was kindly performed in collaboration with Caroline Dean at the John Innes Centre, Norwich; Mathew Box at the Sainsbury Laboratory Cambridge

University, Cambridge; and Justin Borevitz and Riyan Cheng at the Australian National University, Canberra, Australia. The analysis was carried out using the QTLRel package (Cheng et al., 2011) and call_method_75_ TAIR9 SNP data (Horton et al., 2012). Alleles with a frequency of less than 0.05 were excluded from the analysis.

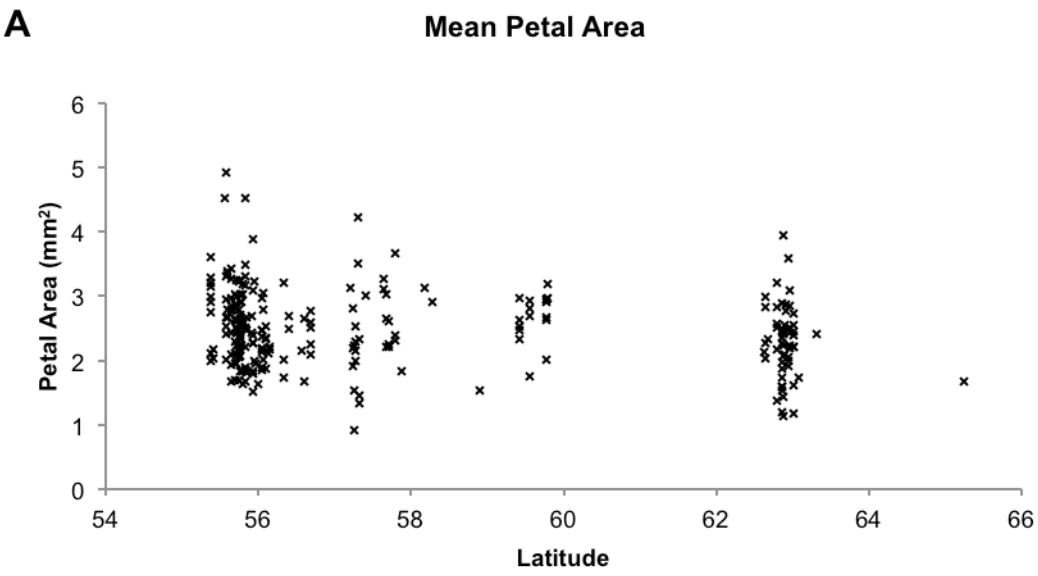
A
Mean Petal Area
Petal Area (mm²)
0
1
2
3
4
5
6
54
56
58
60
62
64
66
Latitude

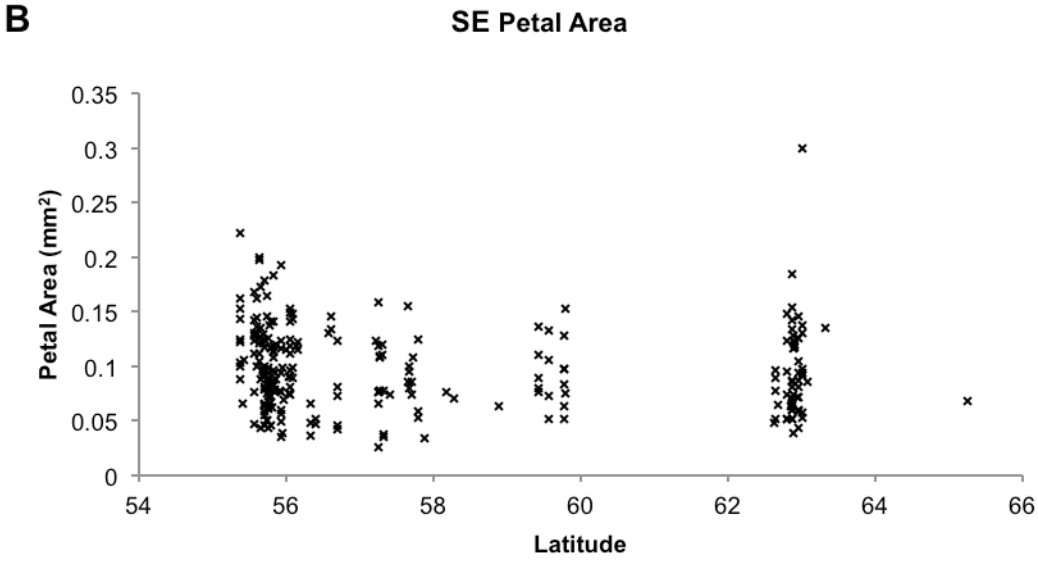
B
SE Petal Area
Petal Area (mm²)
0
0.05
0.1
0.15
0.2
0.25
0.3
0.35
54
56
58
60
62
64
66
Latitude

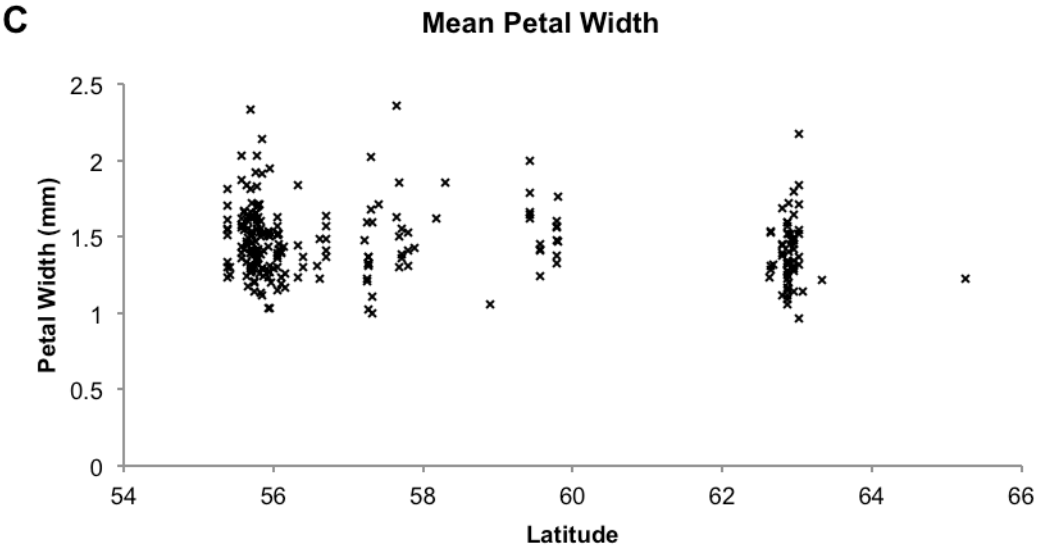
C
Mean Petal Width
Petal Width (mm)
0
0.5
1
1.5
2
2.5
54
56
58
60
62
64
66
Latitude

D

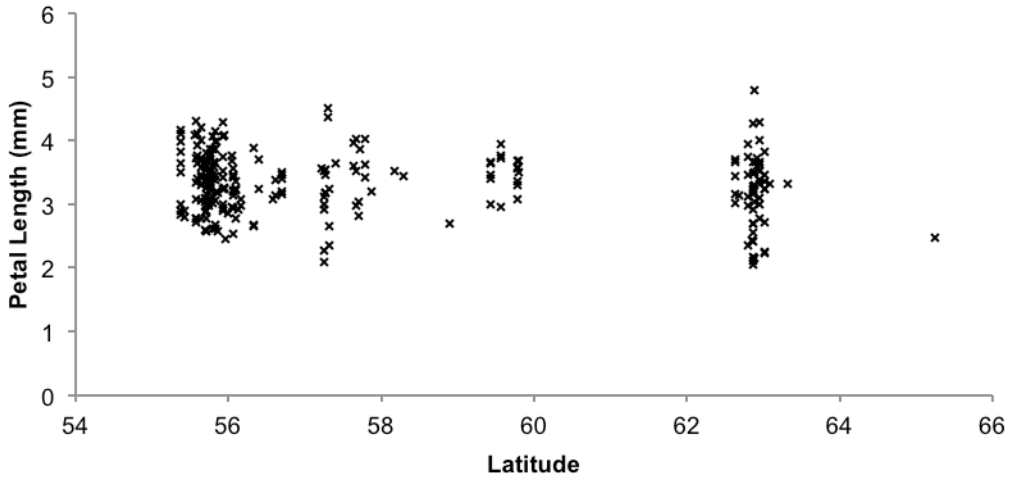
Mean Petal Length
Petal Length (mm)
0
1
2
3
4
5
6
54
56
58
60
62
64
66
Latitude

E

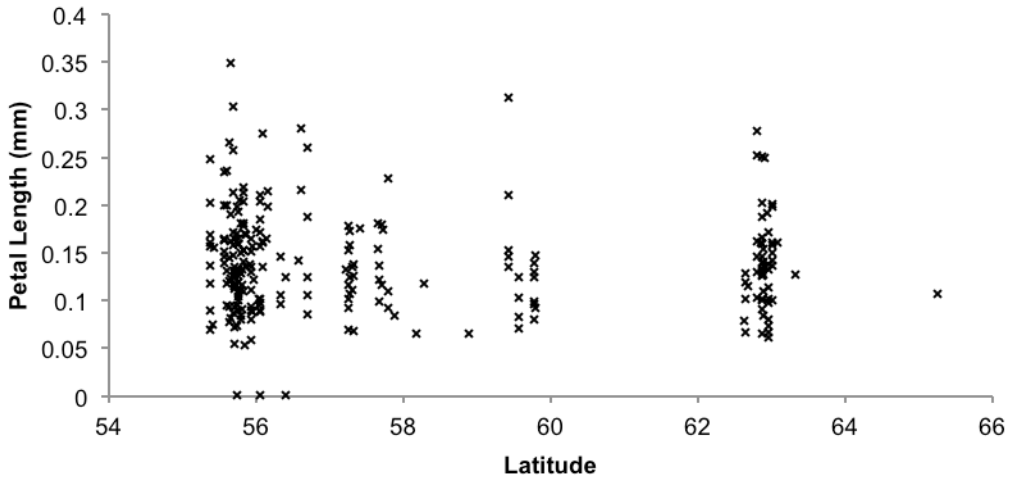
SE Petal Length
Petal Length (mm)
0
0.05
0.1
0.15
0.2
0.25
0.3
0.35
0.4
54
56
58
60
62
64
66
Latitude

F

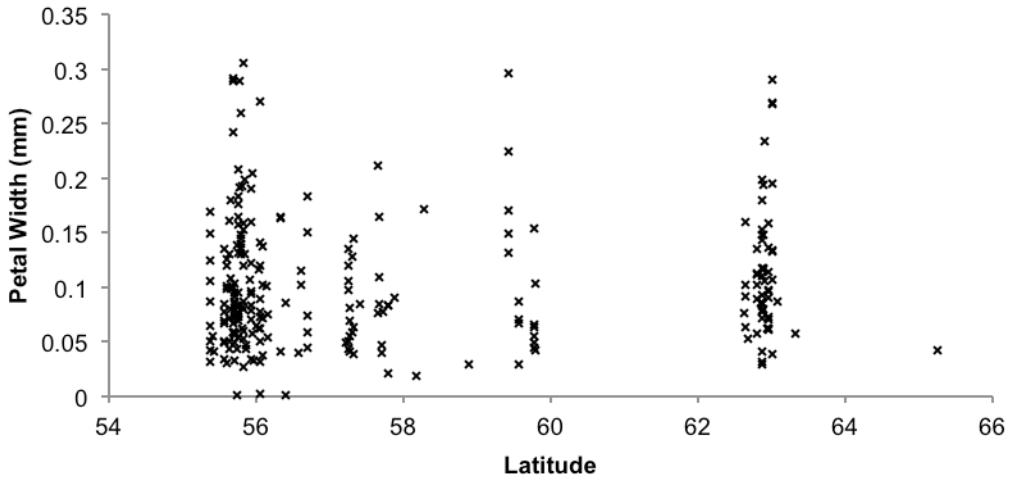
SE Petal Width
Petal Width (mm)
0
0.05
0.1
0.15
0.2
0.25
0.3
0.35
54
56
58
60
62
64
66
Latitude

G

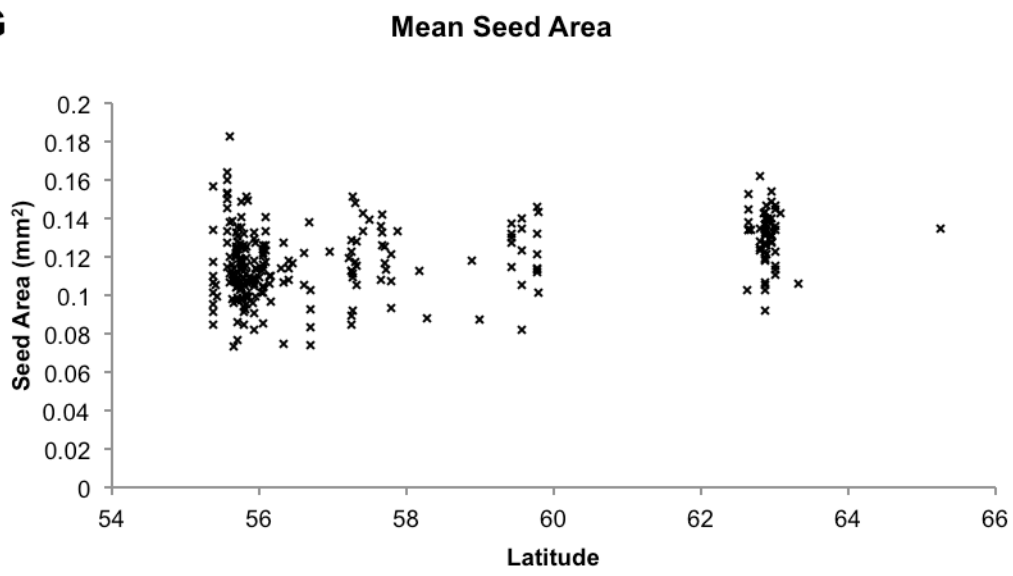
Mean Seed Area
Seed Area (mm²)
0.2
0.18
0.16
0.14
0.12
0.1
0.08
0.06
0.04
0.02
0
54
56
58
60
62
64
66
Latitude

H

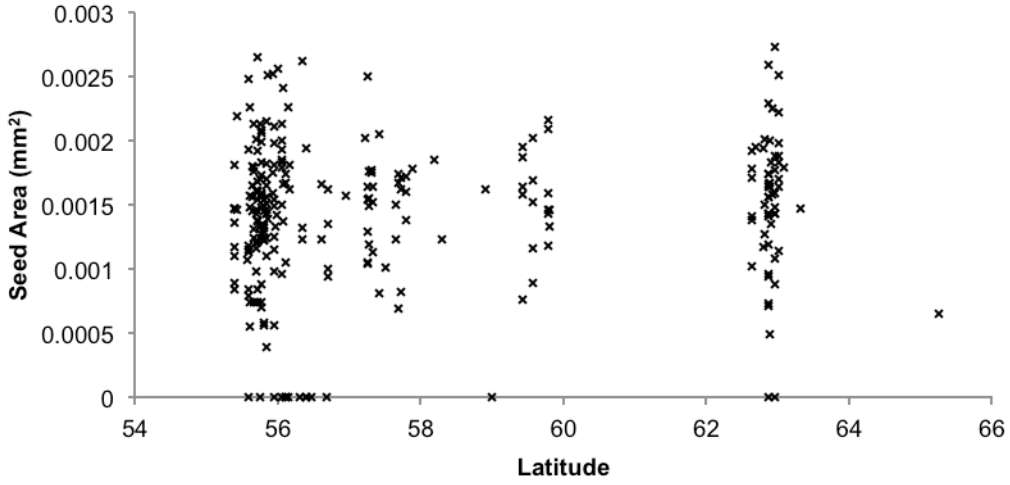
SE seed Area
Seed Area (mm²)
0.003
0.0025
0.002
0.0015
0.001
0.0005
0
54
56
58
60
62
64
66
Latitude

I

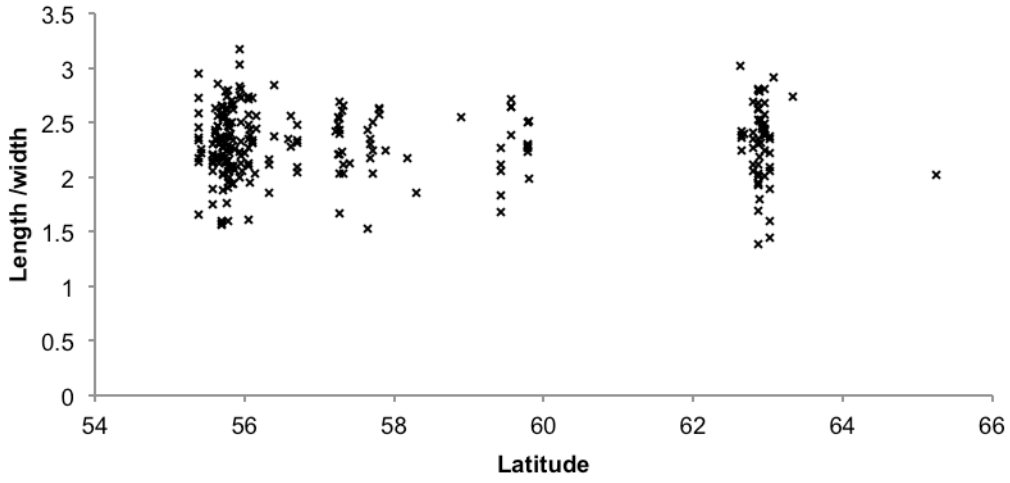
Petal Shape
Length /width
3.5
3
2.5
2
1.5
1
0.5
0
54
56
58
60
62
64
66
Latitude

J

Phenotype	Pearson's r	t-statistic	p-value
Mean Petal Area	-0.17486	2.79682	**0.00557**
SE Petal Area	-0.10869	1.72183	0.08635
Mean Petal Width	-0.12408	1.96931	0.05003
SE Petal Width	0.07125	1.12489	0.26172
Mean Petal Length	-0.12750	2.02435	**0.04401**
SE Petal Length	-0.04855	0.76553	0.44469
Mean Seed Area	0.33643	5.78264	**<0.0001**
SE Mean Seed Area	0.09716	1.58018	0.11527
Petal Shape	-0.00646	0.10170	0.91908

Figure 6.7 – Phenotype-latitude correlations

(A-I) Scatterplots display mean values for the phenotypes used in the GWA, plotted against the latitude at which the accessions were collected. (J) A table displaying the significance of the phenotype-latitude correlations. Mean petal area, mean petal length and mean seed area correlate with latitude with a significance of $p<0.05$. Correlation was calculated using Pearson's r.

A

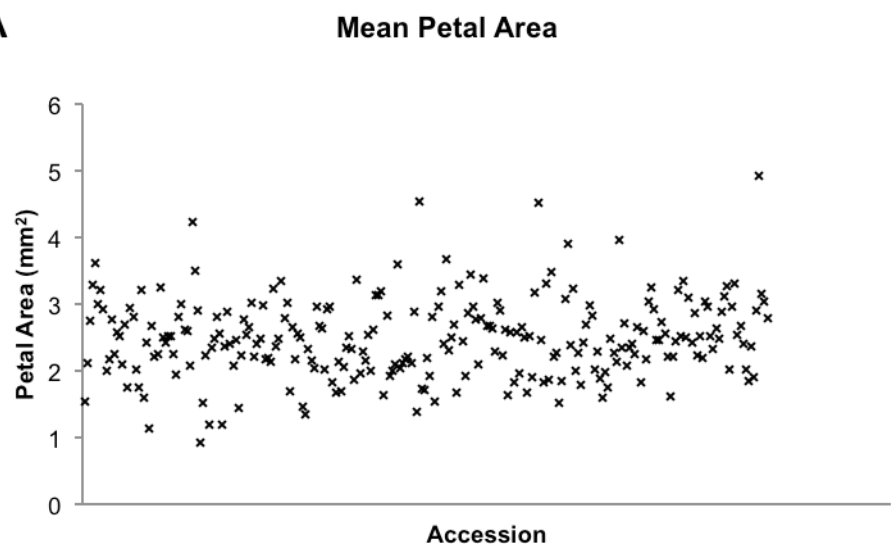
Mean Petal Area
Petal Area (mm²)
0
1
2
3
4
5
6
Accession

B

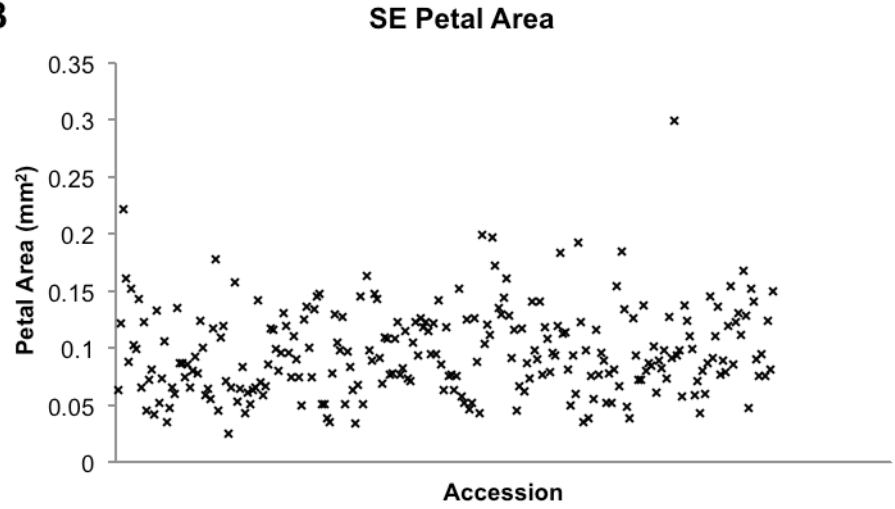
SE Petal Area
Petal Area (mm²)
0
0.05
0.1
0.15
0.2
0.25
0.3
0.35
Accession

C

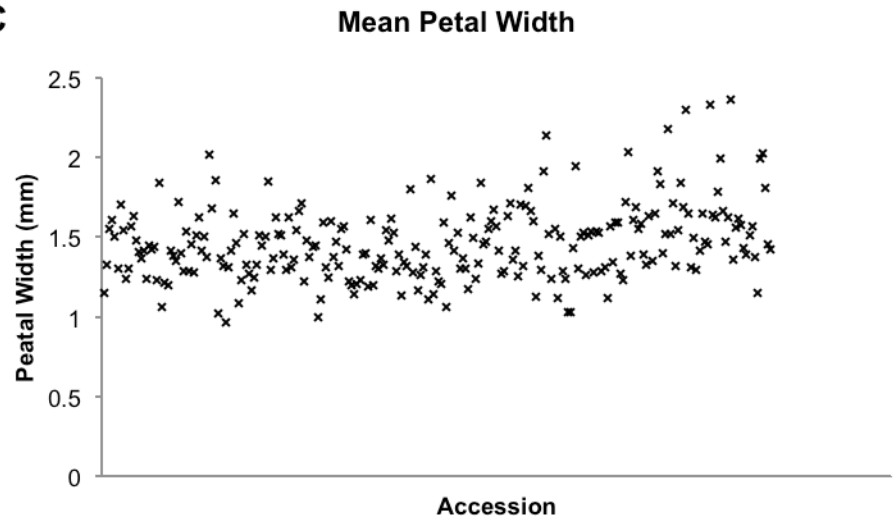
Mean Petal Width
Peatal Width (mm)
0
0.5
1
1.5
2
2.5
Accession

D

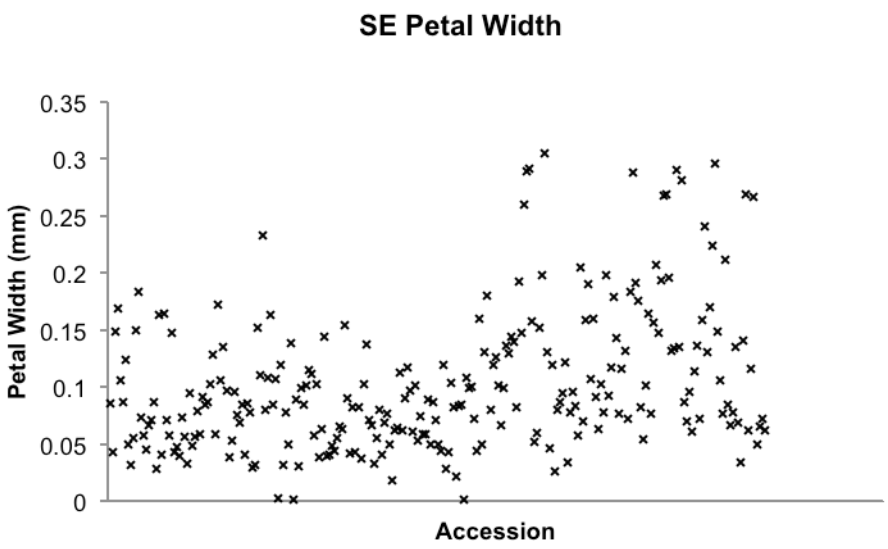
SE Petal Width
Petal Width (mm)
0.35
0.3
0.25
0.2
0.15
0.1
0.05
0
Accession

E

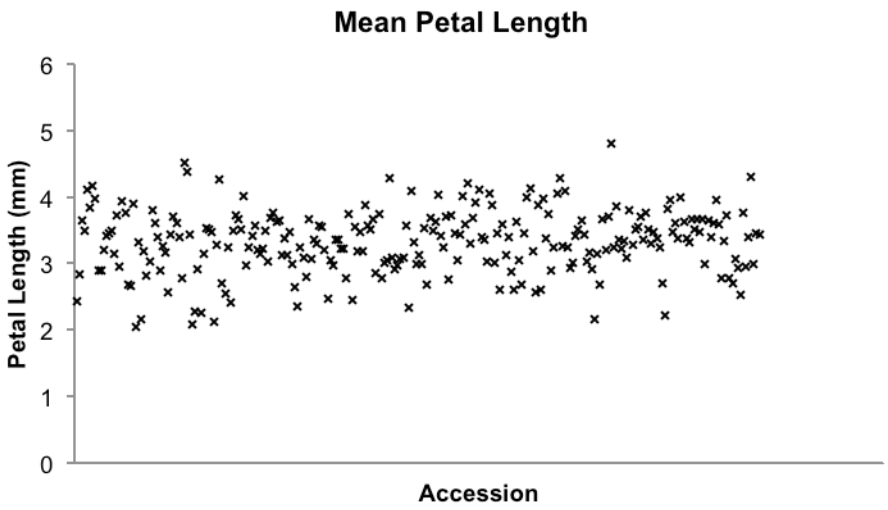
Mean Petal Length
Petal Length (mm)
6
5
4
3
2
1
0
Accession

F

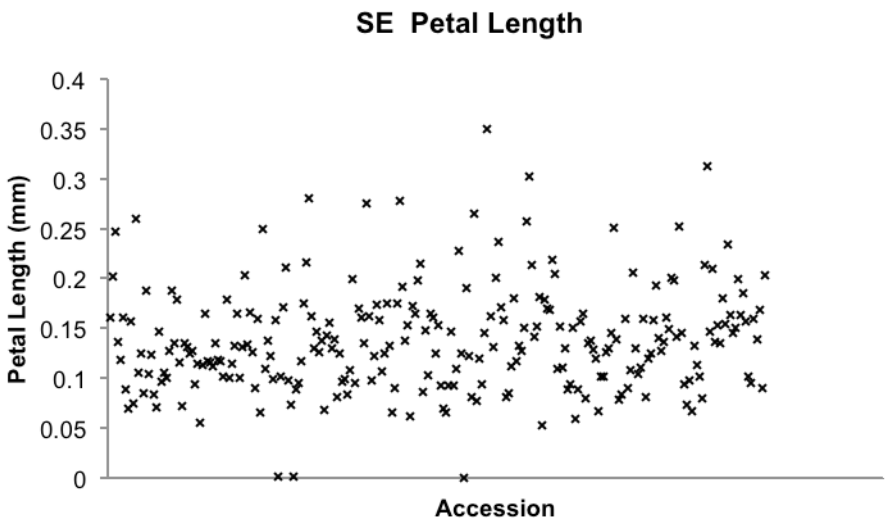
SE Petal Length
Petal Length (mm)
0.4
0.35
0.3
0.25
0.2
0.15
0.1
0.05
0
Accession

G

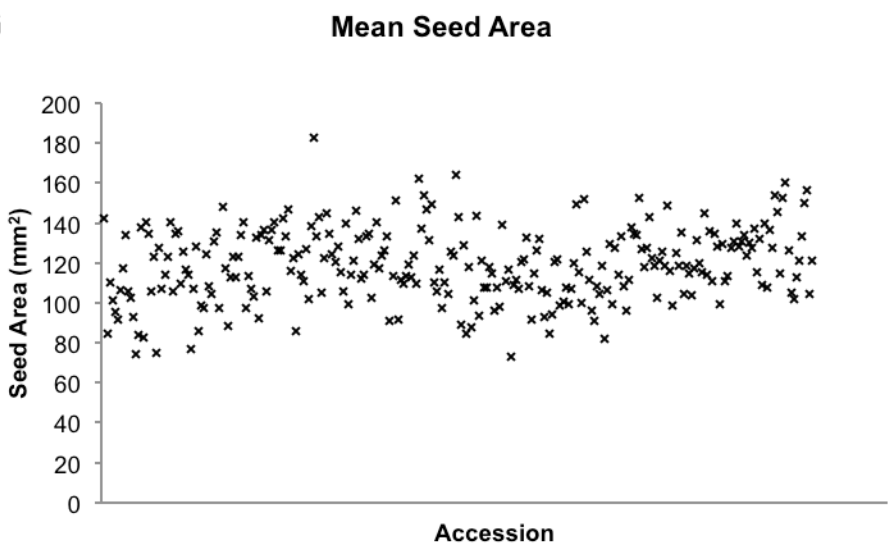
Mean Seed Area
Seed Area (mm²)
200
180
160
140
120
100
80
60
40
20
0
Accession

H

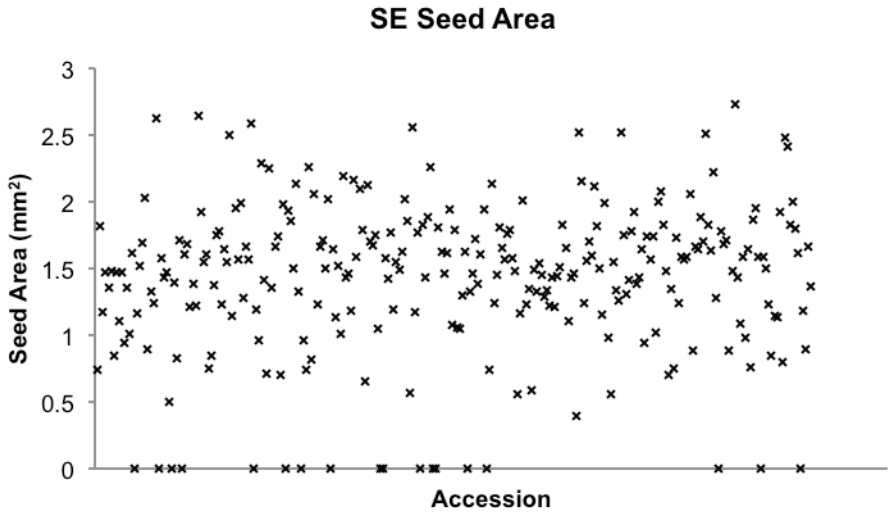
SE Seed Area
Seed Area (mm²)
3
2.5
2
1.5
1
0.5
0
Accession

I

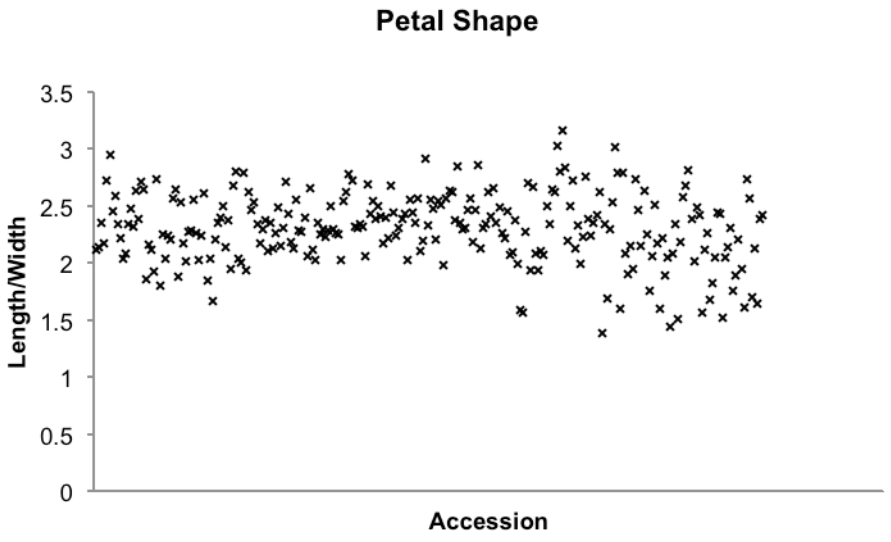
Petal Shape
Length/Width
3.5
3
2.5
2
1.5
1
0.5
0
Accession

Figure 6.8 – Phenotype distributions in the GWA mapping population

Mean values for petal area (A), petal length (C), petal width (E) and seed area (G); and SE of the mean values for petal area (B), petal length (D), petal width (F) and seed area (H). (I) Aspect ratio plotted as (mean petal length / mean petal width). (Petal data, n=10; seed data n=100)

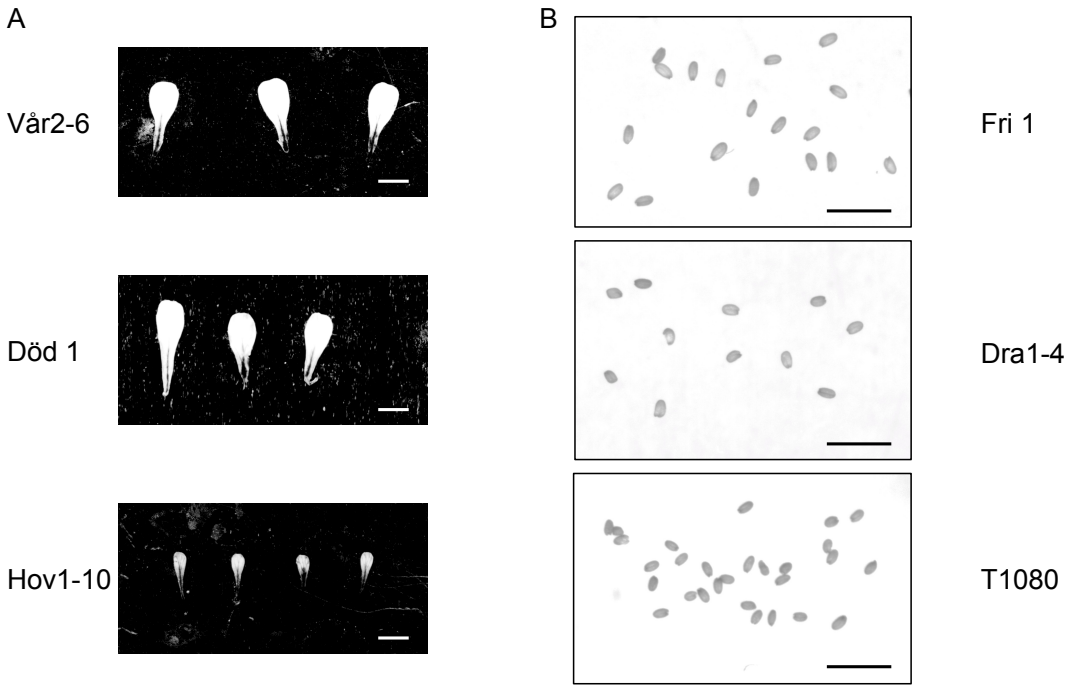

Figure 6.9 – Petal and seed phenotypes

Scanned images of petals (A) and seeds (B) for imageJ analysis (scale bar = 2mm)

6.4.1 – Natural variation in seed and petal phenotypes

Phenotypic analysis revealed that petal area, petal length, petal width and seed area phenotypes varied widely within the sample population. Petals varied in mean area from 0.915 mm^2 (Död 1) to 4.92mm^2 (Vår2-6), an increase of 537%. Seed area varied from 0.073mm^2 (T1080) to 0.183mm^2 (Fri 2), an increase of 250%. Fig. 6.11a shows petals from Död 1, Vår2-6 and an intermediate petal, Hov1-10; Fig. 6.11b shows seeds from T1080, Fri 1 and in intermediate seed, Rev-3.

The results of the GWA analysis are presented as whole-genome Manhattan plots, with genomic position plotted against association significance (Fig. 6.10). Associations were presented as LOD scores and thresholds were estimated by the permutation test (2500 permutations)(Cheng and Palmer, 2013). SNPs with LOD scores greater than the respective genome-wide significance thresholds were considered for further analysis.

The trade-off between stringency and call rate has resulted in the somewhat nominal setting of significance thresholds in GWAs studies (McCarthy et al., 2008, Atwell et al., 2010). For this reason, the significance threshold in this study is used as a mechanism to guide the discovery of causal variation. SNPs that fall above the significance threshold will be followed with the aim of identifying *de novo* regulatory genes. However, non-significant SNPs close to the significance threshold and adjacent to *a priori* candidates may also be of interest to this study.

A

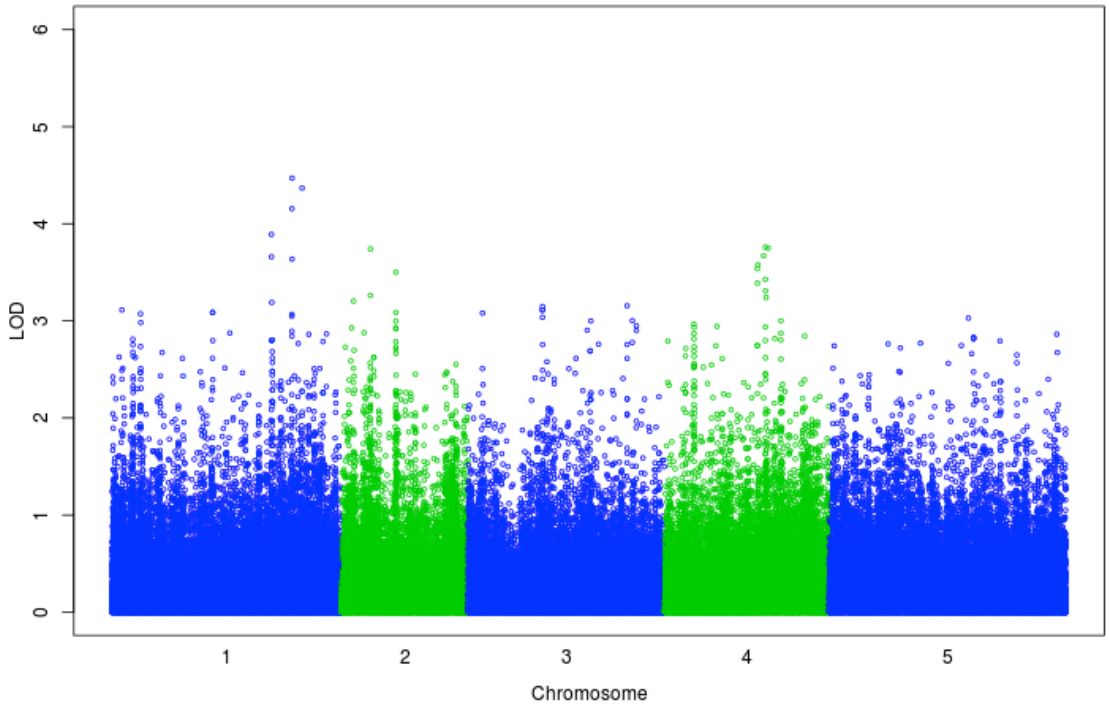
Mean Petal Area
LOD
0
1
2
3
4
5
6
1
2
3
4
5
Chromosome

B

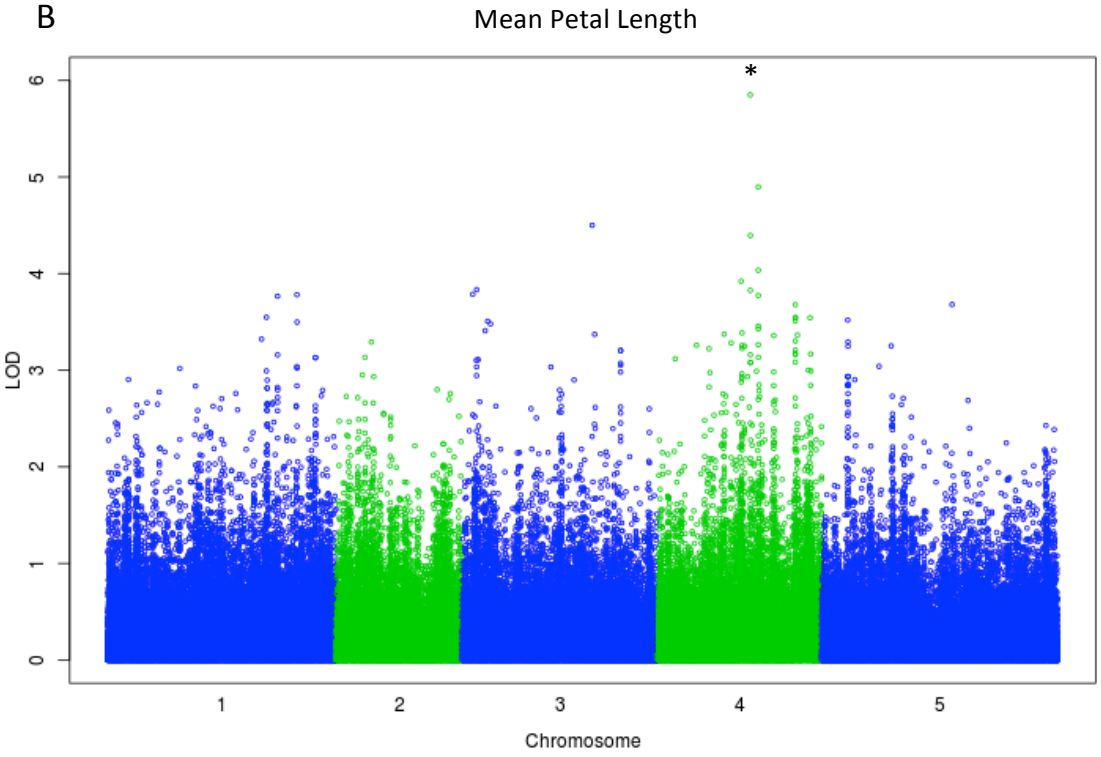
Mean Petal Length
*
LOD
0
1
2
3
4
5
6
1
2
3
4
5
Chromosome

C

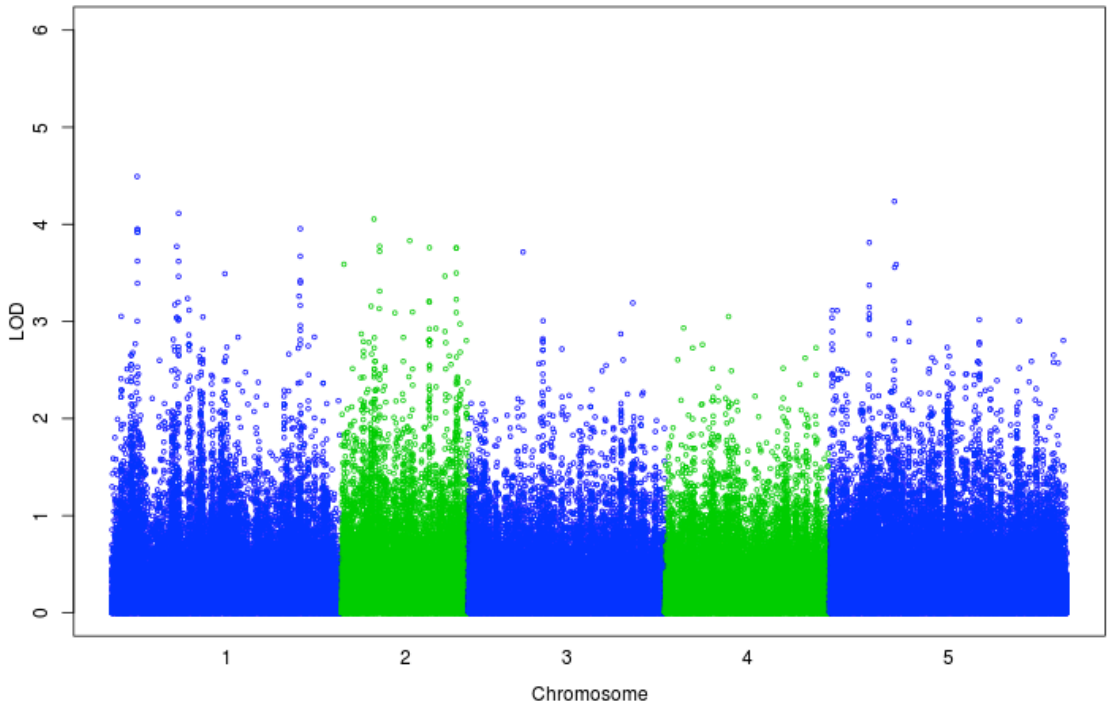
Mean Petal Width
LOD
0
1
2
3
4
5
6
1
2
3
4
5
Chromosome

D

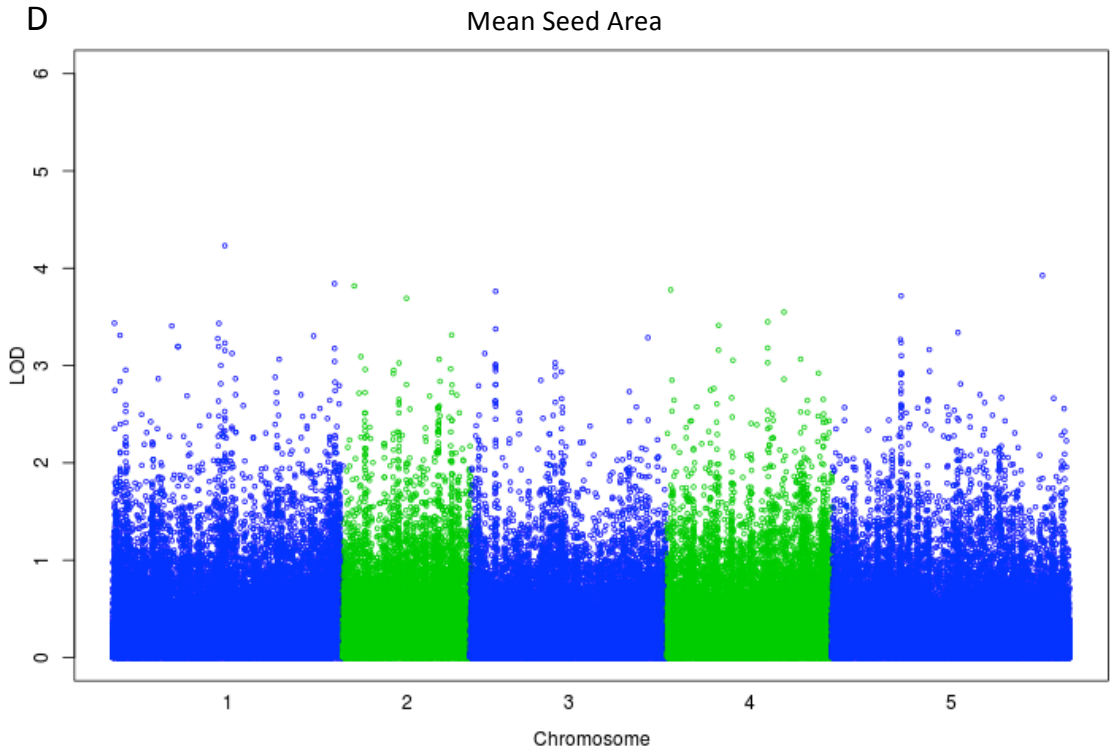
Mean Seed Area
LOD
0
1
2
3
4
5
6
1
2
3
4
5
Chromosome

E

Petal Shape

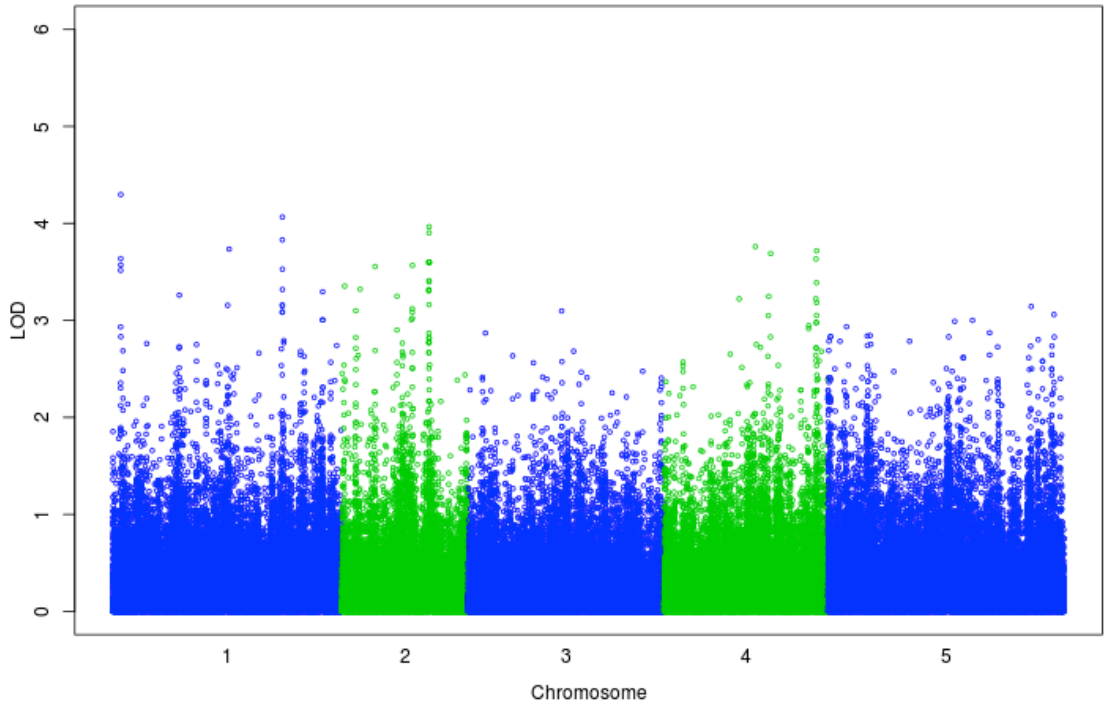

F

SE Mean Petal Area

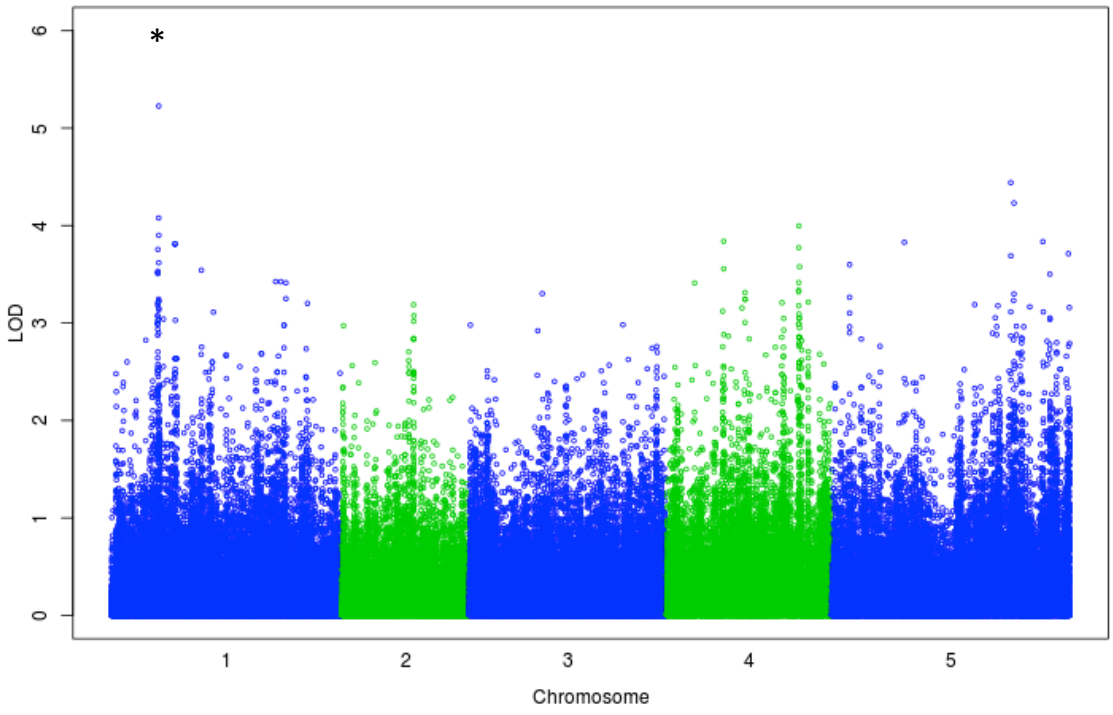

G

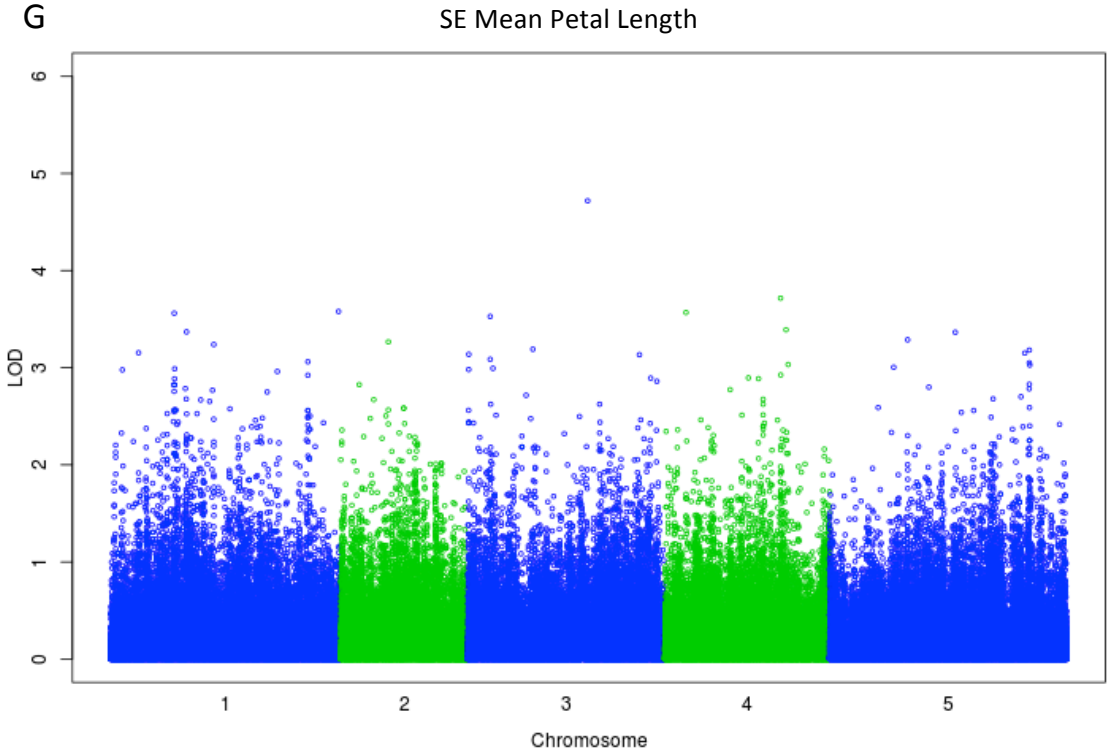
SE Mean Petal Length
LOD
0
1
2
3
4
5
6
1
2
3
4
5
Chromosome

H

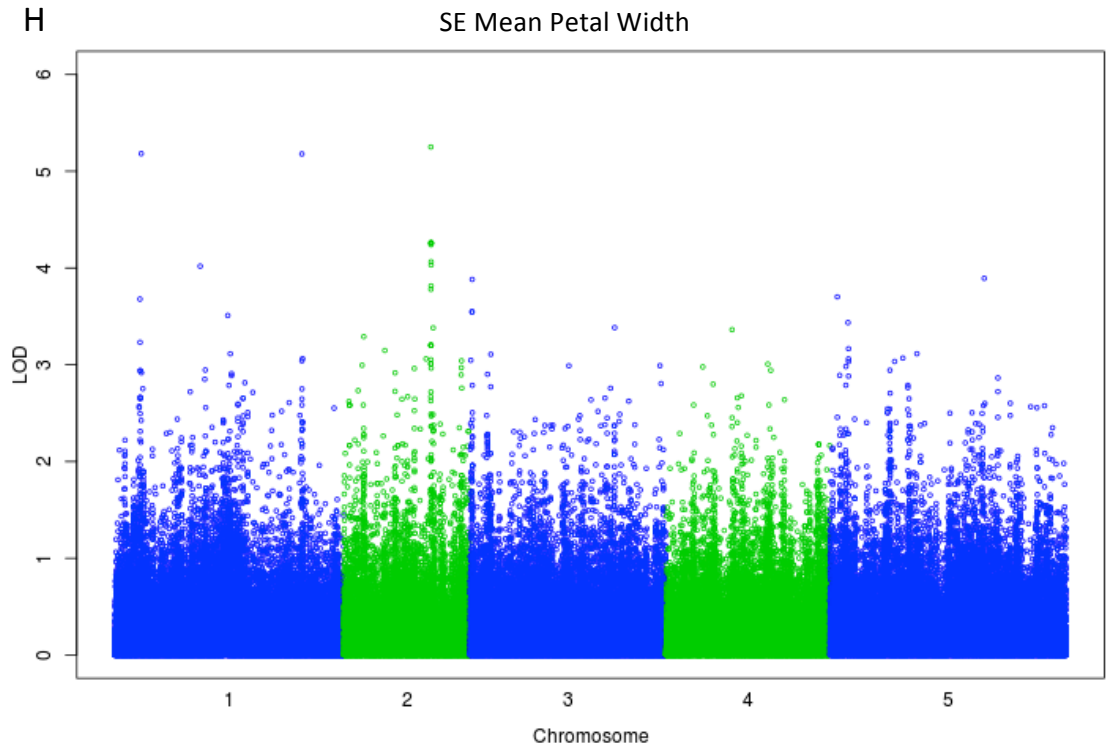
SE Mean Petal Width
LOD
0
1
2
3
4
5
6
1
2
3
4
5
Chromosome

H

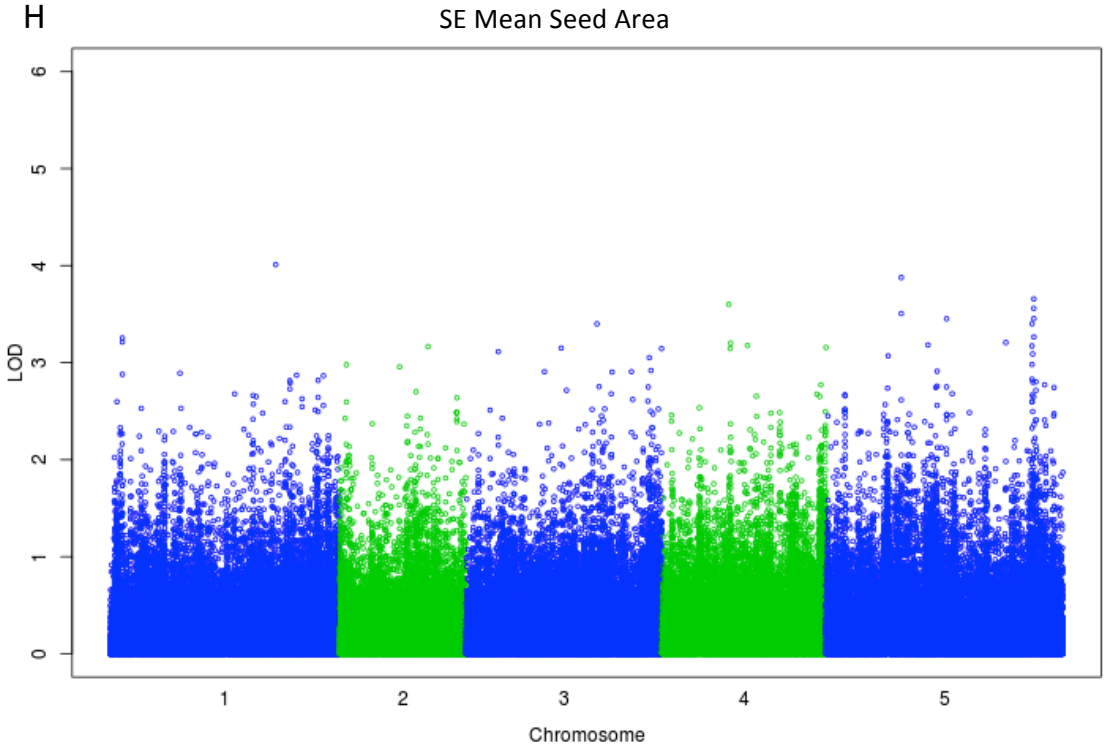

I

Phenotype	Significance	Chr1	Chr2	Chr3	Chr4	Chr5	Genome
Mean Petal Area	0.1	4.76632	4.43997	4.67473	4.60904	4.68857	5.38634
Mean Petal Area	0.05	5.06718	4.78796	5.01636	5.03478	5.10523	5.78109
Mean Petal Area	0.01	5.82572	5.52993	5.84721	5.81530	6.00708	6.45741
Mean Petal Width	0.1	4.85770	4.55815	4.77427	4.70212	4.82212	5.49773
Mean Petal Width	0.05	5.25696	4.94375	5.11562	5.09641	5.16713	5.91964
Mean Petal Width	0.01	6.08508	5.82206	5.86884	5.99104	6.06160	6.64984
Mean Petal Length	0.1	4.67971	4.34684	4.59511	4.52073	4.62106	5.27263
Mean Petal Length	0.05	4.99840	4.64120	4.91601	4.82940	4.98345	5.57528
Mean Petal Length	0.01	5.67693	5.29947	5.75778	5.55072	5.81650	6.31547
Mean Seed Area	0.1	4.61988	4.39584	4.55730	4.46356	4.65790	5.21451
Mean Seed Area	0.05	4.92639	4.69700	4.84001	4.79474	5.02598	5.75572
Mean Seed Area	0.01	5.76458	5.44659	5.52112	5.41619	5.81205	6.31792

Figure 6.10 – Genome-wide association of phenotype with SNP markers

(A-G) Manhattan plots of genotype-phenotype associations. The x-axis represents the full genome length of Arabidopsis; different colours denote the boundaries between chromosomes. The y-axis displays the associations of genotype markers at different positions on the genome (with the respective phenotype). Associations are presented as LOD scores. (I) Table of significance thresholds; for each of four phenotypes (mean petal area, mean petal length, mean petal width and mean seed area). LOD scores for p<0.1, 0.05 and 0.01 significance thresholds are given as per-chromosome (Chr = chromosome) and per-genome values. SNPs with LOD scores greater than these thresholds are considered to be significantly associated with the phenotype to the confidence level expressed by the respective p-value. (B,C) The '*' marks the position of strongly associated SNPs of particular interest to this study.

6.4.2 – A SNP at Ch4-9471419 associates with mean petal length

As Fig. 6.10b reveals, the SNPs; Ch4-9471419 and Chr4-10183417 associate with the mean petal length phenotype, with LOD scores of 5.85 and 4.89 respectively (SNP position indicated by '*') . The per-genome and per-chromosome p<0.1 significance thresholds are LOD=5.27 and LOD=4.60 respectively revealing that both SNPs are significant using the p<0.1 per-chromosome threshold. Moreover, the per-chromosome p<0.01 significance threshold for chromosome 4 is LOD= 5.55, revealing that the association of the peak SNP (Ch4-9471419) is significant to p<0.01. This SNP alone is predicted to contribute a 0.26% decrease in petal length. However, at the time of writing, the contribution of the underlying haplotype was still being calculated.

The association interval for a significant SNP is determined by the LD of the region of the genome in which the SNP is located. Due to the preliminary state of this analysis, at the time of writing the specific LD for this region of had not been calculated. However, based on genome-wide analysis of LD in Arabidopsis, this investigation assumes a genome-wide average LD of 10Kb, (Kim et al., 2007). Table 6.4 shows the genes present within 20Kb of the peak SNP (Ch4-9471419) and highlights those within 10Kb. The peak SNP for this association is located in the third intron of AT4G16830, a Hyaluronan / mRNA binding family gene, which has no known organ size phenotypes.

Within the preliminary 10Kb association interval is the *REDUCED VERNALIZATION RESPONSE 2* (*VRN2*) gene, encoding a zinc finger protein with similarity to the Polycomb group (PcG) of proteins (Gendall et al., 2001). *VRN2* is characterised as being part of polycomb repressive complex 2 (PRC2), involved in the epigenetic regulation of the vernalisation response, and in particular in the maintenance of *FLC* (*FLOWERING LOCUS C*) repression after cold treatment (Gendall et al., 2001, De Lucia et al., 2008). In addition to VRN2, the PRC2 includes two PHD-finger proteins VERNALIZATION 5 (VRN5) and *VERNALIZATION INSENSITIVE 3* (VIN3) (Greb et al., 2007, De Lucia et al., 2008, Wood et al., 2006). Whereas VRN2 is constitutively associated with the *FLC* locus, VRN5 associates (in a *VIN3*-dependent manner) with intron 1 of *FLC* upon cold-treatment, before re-distributing to a more *FLC*-wide pattern after a return to warm conditions (De Lucia et al., 2008).

Interestingly, *VRN5* has been reported to be involved in leaf, petal and silique development, with *vrn5* mutants shown to have curled leaves, an increase in petal number and distorted siliques (Greb et al., 2007). It has also been reported that *vrn2* plants exhibit increased petal

area and an increase in petal number compared to the wild-type (Caroline Dean, personal communication). Both VRN2 and VRN5 are members of a polycomb group complex involved in the epigenetic regulation of gene expression (Wood et al., 2006, Gendall et al., 2001, De Lucia et al., 2008), and it is therefore possible that their influence on gene expression extends to genes involved in petal development.

Gene	Distance from Peak SNP (Kb)	Gene Name
AT4G16780	-21491	ARABIDOPSIS THALIANA HOMEOBOX PROTEIN 2, ATHB-2
AT4G16790	-19000	Hydroxyproline-rich glycoprotein family protein
AT4G16800	-15492	ATP-dependent caseinolytic (Clp) protease/crotonase family protein
AT4G16807	-13064	Unknown protein
AT4G16810	**-10358**	**VEFS-Box of polycomb protein**
AT4G16820	**-3080**	**PHOSPHOLIPASE A I BETA 2, PLA-I{BETA]2**
AT4G16830	**70**	**Hyaluronan / mRNA binding family protein**
AT4G16835	**2364**	**Tetratricopeptide repeat (TPR)-like superfamily protein**
AT4G16840	**3785**	**Unknown protein**
AT4G16845	**6591**	**REDUCED VERNALIZATION RESPONSE 2, VRN2**
AT4G16850	**9488**	**Unknown protein**
AT4G16855	**11019**	**Unknown protein**
AT4G16860	20722	RECOGNITION OF PERONOSPORA PARASITICA 4, RPP4

Table 6.4– Association interval around Chr4-9471419

List of genes within 20Kb of peak SNP Chr4-9471419; genes within 10Kb are in bold. Distances are calculated from middle of gene to peak SNP

In addition to regulating the vernalisation response, PcG proteins have been shown be involved in seed development. They are known to play a role in the repression of genes involved in promoting precocious endosperm proliferation and genes involved in the promotion of proliferation of the embryo and endosperm after fertilisation (Bemer and

Grossniklaus, 2012, Köhler and Makarevich, 2006, Grossniklaus et al., 2001). The PcG complex involved in regulating seed growth consists of at least four proteins: MEDEA (MEA), FERTILIZATION INDEPENDENT ENDOSPERM 2 (FIE), FERTILIZATION SEEDS 2 (FIS2) and MULTICOPY SUPPRESSOR OF IRA 1-5 (MSI1-5) (Bemer and Grossniklaus, 2012, Köhler and Makarevich, 2006, Luo et al., 1999, Ohad et al., 1999, Grossniklaus et al., 1998, Köhler et al., 2003); with MEA and FIS2 also serving as subunits in the VRN2-PRC2 complex (Bemer and Grossniklaus, 2012). In addition, MEA and FIS2 also form part of a PcG complex with CURLY-LEAF (CLF)/SWINGER (SWN) and EMBRYONIC FLOWER 2 (EMF2) (Katz et al., 2004, Bemer and Grossniklaus, 2012, Chanvivattana et al., 2004). Interestingly, *CLF* promotes the rates of cell proliferation and cell expansion in in the developing leaf, with *clf* mutants exhibiting a curled-leaf phenotype and a reduction in petal size in the second whorl (Kim et al., 1998a, Krizek et al., 2006). *CLF* is also involved in the *AGAMOUS*-dependent repression of *WUSCHEL* (*WUS*) (Liu et al., 2011), suggesting that it may be involved in the regulation of meristem size (Schoof et al., 2000, Bleckmann et al., 2010), and as a consequence floral organ number (Schoof et al., 2000). Interestingly, yeast-2-hybrid data reveals a physical interaction between the C5 domain of CLF and the VEFS domain of VRN2 (Chanvivattana et al., 2004), suggesting that the *VRN2* may be able to influence petal number and size via interactions with *CLF*.

Further than 10Kb from the peak SNP (Ch4-9471419) are additional genes that have links to organ growth and development, including *ARABIDOPSIS THALIANA HOMEOBOX PROTEIN 2* (*ATHB2*), a Class II homeodomain-leucine zipper gene that is regulated by far-red light (Carabelli et al., 1993, Morelli and Ruberti, 2002). Over-expression of *ATHB2* results in longer hypocotyls, smaller cotyledons and fewer, smaller leaves (Steindler et al., 1999, Schena et al., 1993). The reduced cotyledon size is due to a reduction in cell expansion, whereas the elongation of hypocotyls is due to increased cell expansion (Steindler et al., 1999). ATHB2 also negatively regulates cell proliferation in the root (Steindler et al., 1999), revealing that it can influence both cell expansion and cell proliferation. More recently, *ATHB2* has been shown to influence adaxial-abaxial polarity in the developing leaf (Bou-Torrent et al., 2012, Turchi et al., 2013). Taken together, these data show that ATHB2 controls the development of leaves and the setting of final leaf size in Arabidopsis. Due to the similarities that exist between leaf and petal development (see Chapter 1), it is possible that ATHB2 may also influence petal size and therefore be causal for the variation observed in this GWAs for petal length.

Additional candidate genes include the *RPP5* (*RECOGNITION OF PERONOSPORA PARASITICA 5*) cluster of seven (Toll Interleukin1 receptor-nucleotide binding-Leucine-rich-repeat) TIR-NBS-

LRR class resistance (R) genes (Yi and Richards, 2007) that are located 20Kb downstream of the peak SNP. The closest of these genes to the peak SNP is *RPP4*, which like its ortholog, RPP5, is essential for resistance to *Peronospora* parasitica (Van Der Biezen et al., 2002, Parker et al., 1993). Also in the RPP5 cluster and within 30Kb of Ch4-9471419 is *SUPRESSOR OF NPR1-1* (*SNC1*), a TIR-NBS-LRR R gene that promotes the expression of pathogenesis-related genes and whose gain of function mutant has a dwarfed phenotype (Li et al., 2001, Zhang et al., 2003).

6.4.3 – A SNP at Chr1:6666179 associates with SE mean petal area.

The following section briefly describes data that suggest that an allele of DA1 might associate with the phenotype – SE mean petal area. This section of the GWA study is still on-going, therefore these data must be considered preliminary. Nonetheless, the data appear to confirm predictions made in Chapter 1 that genetic variation at the DA1 locus might be involved in a size-sensing mechanism during petal growth.

Fig. 6.10f shows a large peak in chromosome 1 (indicated by '*' and the second largest peak in the whole study), indicating a strong association between a region of chromosome 1 and the SE mean petal area phenotype. The peak SNP (Chr1:6666179) has a LOD score of 5.23. At the time of writing, the significance thresholds had not been calculated for this phenotype, however the average per-chromosome $p<0.10$ and $p<0.05$ significance thresholds for chromosome 1 for the four tested phenotypes are LOD=4.73 and LOD=5.06 respectively. These values are encouraging as they suggest that the peak SNP (Chr1:6666179) associates with the SE mean petal area phenotype with a significance of $p<0.05$. Currently, the influence of the associating haplotype on this phenotype is unknown.

The peak SNP (Chr1:6666179) is located 150bp downstream of the 3' UTR of *DA1*. Genes within 20Kb of this SNP are shown in Table 6.5. Within 10Kb of the peak SNP are two genes of interest: *DA1* and *ATGATL1* (*GALACTURONOSYLTRANSFERASE-LIKE 1*). *AGATL1* is located 5Kb from the peak SNP and encodes a galacturonosyltransferase involved in carbohydrate metabolism (Shao et al., 2004). Loss of function of *ATGATL1* results in a dwarfed phenotype with smaller leaves and smaller floral organs, which is thought to be a consequence of cell wall defects influencing cell expansion rates (Shao et al., 2004).

Gene	Distance from Peak SNP (Kb)	Gene Name
AT1G19230	-19474	Riboflavin synthase-like superfamily protein
AT1G19240	-16348	Unknown protein
AT1G19250	-14376	FLAVIN-DEPENDENT MONOOXYGENASE 1, FMO1
AT1G19260	**-7765**	**TTF-type zinc finger protein**
At1G19270	**-1915**	**DA1**
At1g19290	**1427**	**Pentatricopeptide repeat (PPR) superfamily protein**
AT1G19300	**5716**	**ATGATL1, GALACTURONOSYLTRANSFERASE-LIKE 1**
AT1G19310	**10775**	**RING/U-box superfamily protein**
AT1G19320	13588	Pathogenesis-related thaumatin superfamily protein
AT1G19330	15869	unknown protein;
AT1G19340	19755	Methyltransferase MT-A70 family protein;

Table 6.5 – Association interval around Chr1-6666179

List of genes within 20Kb of peak SNP Chr1-6666179; genes within 10Kb are in bold. Distances are calculated from middle of gene to peak SNP

The SE phenotypes included in this assay were intended to map genes with roles in 'buffering' the variation in organ size (see section 6.2.3), such that altered function would lead to altered variation in organ size. Screening for mean organ size is likely to identify genes involved in all aspects of growth control, including genes involved in sensing mechanisms and genes involved in core growth processes, such as cell division and cell expansion. Conversely, screening for genes involved in determining the regularity of organ size could tend to identify genes that play a role in sensing organ size. The phenotypes of the *da1-1* and *da1ko1* mutants have been well described in this thesis as well as in recent publications (Xia, 2013, Li et al., 2008), confirming that knockout of the *DA1* gene is sufficient to interfere with organ development and the setting of organ size. It is also possible to speculate that, because *da1-1* and *da1ko1/dar1-1* mutations are unable to be compensated (Li et al., 2008), *DA1* is involved in some way in a size sensing pathway in developing organs (discussed in section 1.5.4). The data

described in this section, which suggest that DA1 might be involved in controlling the regularity of organ size in natural populations of Arabidopsis, supports these predictions.

Moreover, if indeed a *DA1* allele is casual in this association, interrogation of the genomes of the relevant accessions may uncover novel allelic variation in *DA1*. Such variation would permit further genetic and biochemical investigation of DA1, and potentially yield new insights into DA1 enzymology and interactomics. For these reasons, pursuing this line of research is a priority.

6.4.4 – Future work

So far, this chapter documents the growth and phenotyping of a mapping population, the investigation of phenotype-genotype associations, the identification of associations, and the subsequent identification of possible candidate genes. This work will be immediately followed by the analysis of knock-out mutations in candidate genes, as well as quantitative complementation crosses of these alleles. Candidate genes include VRN2.

6.5 – Future perspectives

As set out in section 6.1, this chapter is a parallel, complementary project to the DA1 functional analysis reported in Chapters 3-5. The work in this chapter was commenced later during my research programme and consequently some analyses are still underway. As discussed in sections 6.3 and 6.4, the MAGIC and GWA analyses have generated several promising leads around which future research efforts can be built.

The MAGIC analysis of seed phenotypes has identified 8 QTL for mean seed area, identifying a list of candidate genes which include *a priori* growth regulators including *DA2* and *TCP15;* both of which are of wider relevance to this thesis (Chapters 4 and 5 respectively). The QTL also include potential *de novo* candidates involved in many aspects of organ size control, including the brassinosteroid response, the cell cycle and the regulation of seed development.

The GWA analysis has identified a genomic region in chromosome 4 that associates with phenotypic variation in petal length and a region of chromosome 1 that associates with SE petal area. The former region includes pathogen response and shade avoidance response genes, both with links to the regulation of growth and development. Of particular interest is the identification of *VRN2* as a promising candidate and the observation that mutations in other members of PRC2 can result in petal and seed growth phenotypes (Greb et al., 2007, Chanvivattana et al., 2004, Kim et al., 1998a, Katz et al., 2004). The region of chromosome 1 that associates with SE petal area includes two genes with organ size phenotypes, *AGATL1*

(Shao et al., 2004) and DA1 (Li et al., 2008). The inability of cell expansion rates to compensate for an increased duration of cell proliferation during organ growth in *da1-1* mutants suggests that *DA1* may be involved in a size sensing mechanism in the developing organ. The identification of *DA1* as a candidate in the association with SE petal area, suggests that natural variation at the DA1 locus has a role in regulating the uniformity of organ size in Arabidopsis populations.

Future work will involve, as outlined in sections 6.3 and 6.4, determining the genotype contribution to the phenotypic variation, which will help to understand the relative influence of the variation at that particular locus. Future work will also test the influence of the identified candidate genes (and their constituent SNPs) on the phenotypes in question. Currently, work is underway to perform quantitative complementation crosses with the candidate genes identified in this thesis.

The work in this chapter has established a platform for future gene discovery and provides lists of candidate genes that may be important regulators of seed or petal development.

Chapter 7 - General Discussion

The work documented in this thesis has shed light on two key areas of DA1 biology. Firstly, a biochemical study of the DA1 protein has demonstrated that it is an ubiquitin-dependent metallopeptidase, with a potentially enhancing activity towards the two E3 ligases, EOD1 and DA2. Secondly, an investigation of DA1 interacting partners has revealed that DA1 has the potential to function in several growth control pathways, which overlap both organ development and pathogen response.

The biochemical analyses have revealed a novel regulatory feed-forward loop between two RING E3 ligases and an interacting peptidase. This would be the first time that an ubiquitin-activated peptidase has been shown to regulate the activity of an E3 ligase, and presents a novel regulatory mechanism whose significance may extend as far as the field of human cancer biology. In terms of higher plants however, the interactomic analysis in Chapter 4 suggests that peptidase-mediated regulation by members of the DA1 family may play a role in both pathogen-related and developmental growth regulation.

Finally, the identification of *DA1* in a genome wide association analysis for variation in seed and organ size has demonstrated that natural allelic variation in *DA1* may contribute to fitness and adaptation of populations in the natural landscape.

7.1 – DA1, EOD1 and DA2: molecular characterisation

7.1.1 – DA1: a ubiquitin activated peptidase

The biochemical analyses documented in Chapter 5 revealed that the predicted metallopeptidase domain in DA1 is active towards EOD1 and DA2. Importantly, it also demonstrates that its activity is dependent on the ubiquitination of DA1. This suggests that native, full-length DA1 exists in an auto-repressive state, which is disrupted by the addition of a short ubiquitin chain or several mono-ubiquitin molecules (Fig. 7.1).

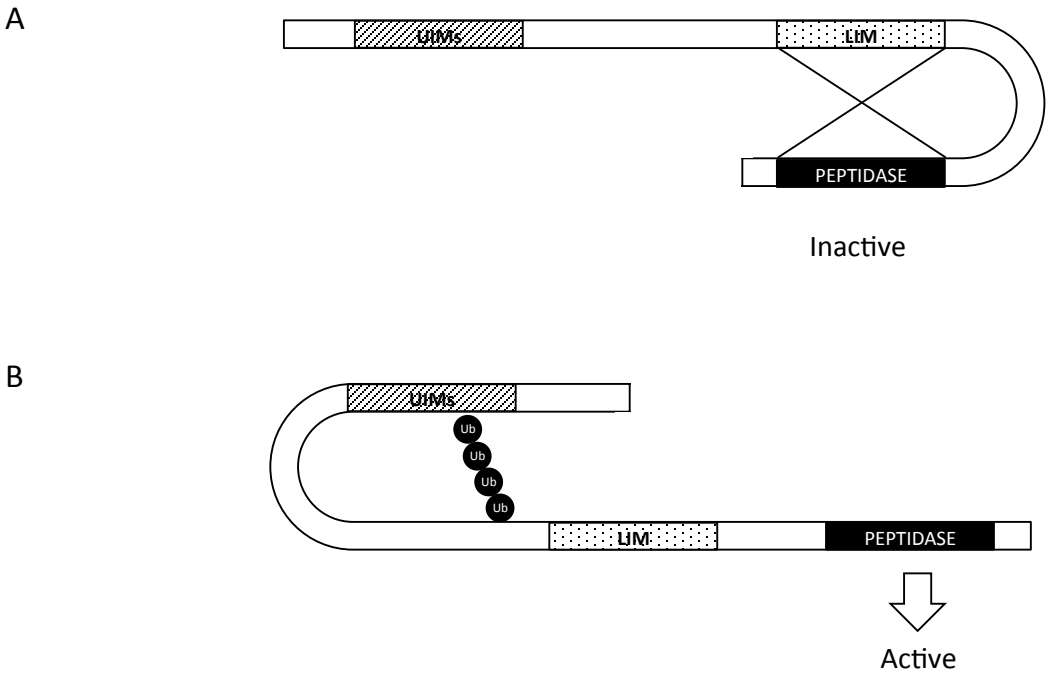

Figure 7.1 – A model for the activation of the DA1 peptidase by coupled ubiquitination

Native DA1 exists in an auto-inhibited conformation (A), possibly due to an interaction between the LIM domain and the C-terminal peptidase. Ligation of a short ubiquitin chain to an as yet unknown region of the protein might cause an interaction between the DA1 UIM domains and this cis-ubiquitin chain (B). This interaction might result in a conformational change that releases the peptidase from auto-inhibition.

Evidence that DA1 UIM2 binds mono-ubiquitin *in vitro* suggests that the ubiquitin-dependent activation of DA1 could occur through interaction between the DA1 UIMs and cis-ubiquitin, in a mechanism similar to that observed for coupled mono-ubiquitination (Woelk et al., 2006, Haglund and Stenmark, 2006, Hoeller et al., 2006). Indeed, ubiquitination of the mammalian UBD-containing proteins, STS1, STS2, EPS15 and HRS results in UBD-cis-ubiquitin interactions, which generate a change in protein confirmation (Hoeller et al., 2006). Based on this observation, it is reasonable to suggest that the ubiquitination of DA1 might trigger an interaction between the DA1 UIMs and cis-ubiquitin, the result of which would cause a DA1 conformational change and thereby de-repress metallopeptidase activity.

In support of this is the observation that the UIM of the yeast transcription factor MET4 interacts with cis-ubiquitin, such that the interaction limits the cis-ubiquitin chain to only four

ubiquitin molecules (Flick et al., 2006). Thus the observation that EOD1 and DA2 are only able to ligate short chains onto DA1, in spite of their ability to auto-*poly*-ubiquitinate, suggests that the DA1 UIM may interact with, and cap cis-ubiquitin chain elongation.

Interestingly, in some proteins the presence of a UBD has been shown to be necessary *and* sufficient for their coupled mono-ubiquitination (Woelk et al., 2006). In addition to interacting with cis-ubiquitin, the UIM of EPS15 interacts with an ubiquitin molecule on its cognate E3 ligase; an event that is necessary for EPS15 ubiquitination (Woelk et al., 2006). This is thought to represent EPS15 recruiting its cognate E3 ligase such that an interaction can occur (Woelk et al., 2006). It is therefore possible that as well as acting as a cis-regulatory domain, the UIM in DA1 may act to mediate the interaction between DA1 and its cognate E3 ligases.

Although the UIM domain is a good candidate for regulating DA1 peptidase activity through a coupled mono-ubiquitination-like mechanism, the LIM domain is a good candidate for a putative peptidase interaction domain. Although LIM domains have been characterised as general protein-protein interacting interfaces (Maul et al., 2003, Shirasaki and Pfaff, 2002, Moes et al., 2012), it is possible that the DA1 LIM domain regulates peptidase activity through a similar mechanism to that of the LIM domain of LIM KINASE-1 (LIMK-1) (Nagata et al., 1999). LIMK-1 auto-regulates its kinase activity through a direct interaction between its LIM domain and its kinase domain (Nagata et al., 1999). The identification of a LIM-like domain in DA1 family members (section 3.2.5) presents the possibility that the LIM-like domain may also regulate peptidase activity. Evidence for this comes from the observation that mutation of the DAR4/CHS3 LIM-like domain is sufficient to constitutively 'activate' the resistance responses (Bi et al., 2011). DAR4/CHS3 is involved in disease responses, and a single mutation in a conserved cysteine residue in its LIM-like domain is sufficient to constitutively activate immune responses (Bi et al., 2011). Assuming that (as with DA1) the DAR4 peptidase domain is functional and responsible for the activation of defence responses, then constitutive activation of an immune response may be a consequence of its constitutive peptidase activity. It follows therefore that mutation of the LIM-like domain may be sufficient to de-repress the peptidase. These observations suggest a model that explains the regulation of DA1 peptidase activity through the coupled-mono-ubiquitination mediated de-repression of LIM-mediated repression of peptidase activity (figure 7.1).

The model in Fig. 7.1 also predicts how the da1-1 $R^{358}K$ mutation could abrogate peptidase function. This amino acid change is within the highly conserved C-terminal region 60 amino acids upstream of the peptidase active site (Li et al., 2008). *In vitro* and *in vivo* data from

Chapter 5 revealed that mutation of the peptidase active site is sufficient to abolish DA1 peptidase activity towards EOD1 and DA2. It is therefore possible that the da1-1 mutation may also reduce peptidase function. This can be readily tested by incorporating the da1-1 protein into the *in vitro* and *in vivo* peptidase activity assays described in section 5.3.

The model also predicts that abrogation of LIM or LIM-like function may be sufficient to constitutively activate the DA1 peptidase, and abrogation of UIM function may be able to constitutively inactivate the peptidase. This could be directly tested using the *in vitro* and *in vivo* peptidase activity assays (section 5.3) using the DA1uim12 mutant (full length DA1, with both UIMs mutated) and the DA1lim8 mutant proteins. An alternate but not exclusive function for the UIMs may be to recognise ubiquitinated E2 or EOD1, or both.

The demonstration that DA1 is an ubiquitin-dependent peptidase is important for understanding the functions of other members of the DA1 family. It is also one of the first examples of a well-characterised regulatory peptidase in plants and emphasises the significant broader roles of peptidases in regulating diverse plant processes, such as the role of SOL1 (a Zn-carboxypeptidase) in the regulation of meristem development (Casamitjana-Martınez et al., 2003). All DA1 family members contain a LIM domain and a highly conserved C-terminal region with a metallopeptidase active site (Fig. 3.1), with the LIM domain providing a postulated auto-regulatory function. Regardless of the involvement of the LIM domain in peptidase regulation, the demonstration in this thesis that the DA1 peptidase is active, suggests that all other DA1 family members might function through their peptidase domains. So far DAR1 has been characterised as a regulator of organ size (Li et al., 2008), DAR2 as a regulator of root meristem size (Peng et al., 2013), and DAR4 as an R-protein and regulator of freezing tolerance (Yang et al., 2010, Bi et al., 2011). Whether or not these proteins interact with their own E3 ligases, the insight developed in this thesis is likely to accelerate the understanding of the molecular basis of their phenotypes and provide further information on a novel regulatory mechanism.

Taking DAR4/CHS3 as an example, recent work concluded that the LIM domain may act as an intra-molecular repressor of DAR4/CHS3 R-protein activity (Bi et al., 2011, Yang et al., 2010). However, the lack of information regarding C-terminal peptidase function led to the hypothesis that the LIM domain interacts with, and represses some aspect of N-terminal protein function (Bi et al., 2011). Although this may indeed be the case, the identification of an active peptidase in the C-terminus of DA1 leads to the prediction that the DAR4 peptidase is

also active and therefore may be a target of LIM-repression. This is directly testable using the biochemical assays developed in this thesis.

This thesis presents, to the best of my knowledge, the first example of ubiquitin-dependent peptidase activation. Due to the essentially irreversible nature of protein cleavage, peptidase activity must be very stringently regulated. For example, caspases, proteases involved in apoptosis in animal systems (Thornberry and Lazebnik, 1998), are proteolytically activated (Mason and Joyce, 2011) as well as being targets of phosphorylation-mediated regulation (Cardone et al., 1998). In plants, proteolysis and phosphorylation are also utilised as mechanisms to regulate peptidase activity. For example, the activity of the 26S proteasome is regulated by phosphorylation (Kurepa and Smalle, 2008, Lee et al., 2003, Umeda et al., 1997), and the Arabidopsis CARBOXYPEPTIDASE Y (AtCPY) is activated through cleavage by the cysteine protease VPEγ (VACUOLAR PROCESSING ENZYME-γ) (Rojo et al., 2004, Rojo et al., 2003). These examples highlight the existence of both phosphorylation- and peptidase-mediated regulation of peptidase enzymes, however until this study there has been no evidence of ubiquitin-mediated regulation of peptidases. Nevertheless, the concept of ubiquitin-regulated enzyme activity is not new; for example poly-ubiquitin activation of the E3 ligase BRCA1 (Mallery et al., 2002), the K29/K33-linked ubiquitin-mediated regulation of the NUAK1 kinase (Ikeda and Dikic, 2008, Al-Hakim et al., 2008) and the mono-ubiquitin modification of the endocytic protein EPS15 (Woelk et al., 2006, Hoeller et al., 2006) have all been reported.

7.1.2 – EOD1 and DA2 are peptidase-regulated E3 ubiquitin ligases

Genetic data presented in Chapter 5, revealing that DA1 synergistically interacts with EOD1 and DA2 to influence petal and seed size, shows an enhancing interaction, which suggests that DA1 activity might enhance both EOD1 and DA2 functions. Biochemical data in Chapter 5 also revealed that DA1 peptidase activity cleaves EOD1 and DA2. Taken together, these data suggest that DA1 might increase the growth-repressive activities of these two E3 ligases through a peptidase-mediated cleavage.

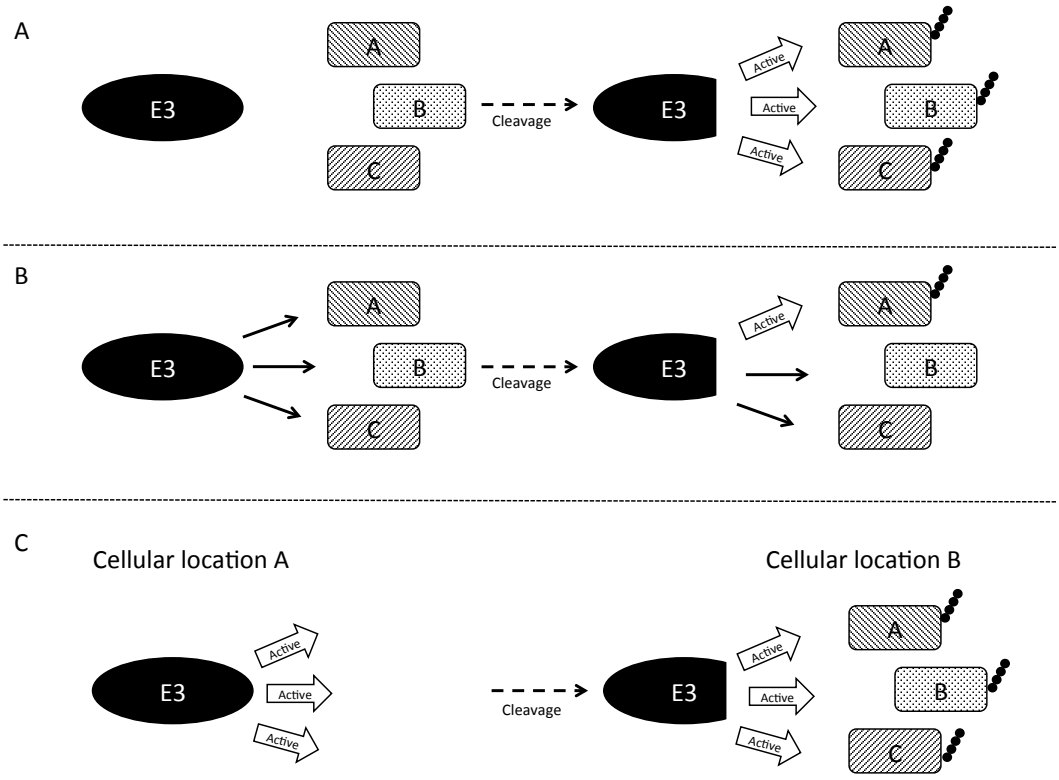

Figure 7.2 – Models for the peptidase-mediated activation of EOD1 and DA2

(A) The E3 ligase exists in a native inactive state and peptidase mediated cleavage *catalytically* activates the E3, such that its activity towards all targets (shaded squares) is increased. (B) The native E3 is catalytically active but has weak substrate binding affinities. Peptidase-mediated cleavage enhances specific substrate binding affinities, and thereby enhances its activity to specific substrates. (C) The native E3 ligase is active, but present in a different subcellular location to its substrates. Peptidase-mediated cleavage results in translocation of the E3 to the same subcellular location as its substrates, thereby spatially activating the E3.

The substrates of EOD1 and DA2 E3 ligase activity (other that DA1) are not yet known, and therefore the biochemical consequences of their cleavage are currently difficult to predict. I propose three potential models to guide experiments to determine how DA1 might enhance EOD1 and DA2 function: through a general increase in E3 catalytic activity, through an increase in catalytic activity towards a specific set of substrate proteins, and through a sub-cellular re-localisation event that spatially enhances enzyme activity.

The importance of accurate spatial activation of enzymes can be seen with the BIN2 (BRASSINOSTEROID INSENSITIVE 2) serine/threonine kinase, which mediates the brassinosteroid response through the phosphorylation of the brassinosteroid responsive transcription factors, BZR1 (BRASSINAZOLE RESISTANT 1) and BES1 (BRI1 EMS 1) (Belkhadir and Chory, 2006, Vert and Chory, 2006, He et al., 2002). BIN2 is expressed throughout the cell, but because BES1 is constitutively localised to the nucleus, the *activity* of BIN2 is dependent on its nuclear localisation (Vert and Chory, 2006).There is only weak, indirect evidence to suggest that E3 ubiquitin ligases are regulated in a similar way. This is evidence that the membrane localised RING E3 ligase RNF13 undergoes cleavage that then releases the RING domain into the cytoplasm and nucleus (Tranque et al., 1996, Bocock et al., 2010). Despite this observation, it is unclear whether the cleavage event affects the *activity* of RNF13. Interestingly DA1-mediated cleavage of EOD1 and DA2 leaves an intact RING domain.

Although spatial activation EOD1 and DA2 remains a possibility (Fig. 7.2c), evidence presented in Chapter 5 suggests that post-translational modification of EOD1 can affect its catalytic behaviour, thereby favouring other models of activation. In particular, tentative evidence that EOD1 activity is influenced by the addition of a small epitope-tag to its N terminus (section 5.3.2) reveals a potential role for post-translational modification in the regulation of EOD1 activity. This is similar to observations of the human E3 ligase PARKIN, whose catalytic activity and chain specificity can be altered through the addition of N-terminal epitope tags and N-terminal truncations (Burchell et al., 2012, Chew et al., 2012).

Interestingly, as in PARKIN, native EOD1 and DA2 are able to auto-poly-ubiquitinate (Chew et al., 2012, Xia, 2013, Disch et al., 2006), suggesting that cleavage may not be necessary for E3 activity, but that it might required to alter their catalytic properties. In the case of PARKIN, N-terminal truncation alters the enzyme's preference for mono-ubiquitin and poly-ubiquitin chains (Chew et al., 2012). This likely reflects a change in catalytic geometries resulting from

the modification of the N-terminal substrate-binding domain. Both PARKIN and EOD1 have C-terminal RING-domains (E2-binding domains), indicating that

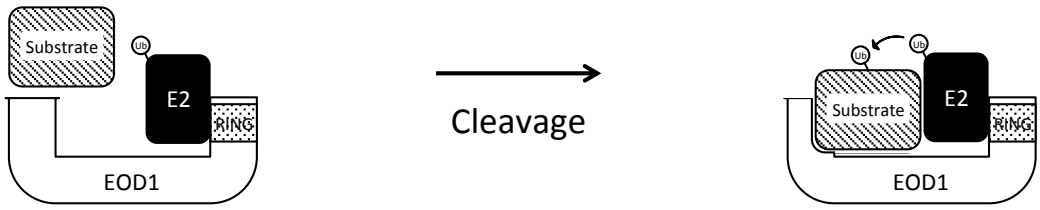

Figure 7.3 – A Model for the peptidase-mediated modification of EOD1 substrate specificity

It is possible that in EOD1's native state, the C-terminal E2-binding RING domain is functional but the N-terminal substrate-binding domain is not. It is possible that peptidase-mediated cleavage of the N-terminus of EOD1 alters the substrate-binding domain such that the substrate can be accommodated. This would enable the E2 and the substrate to interact, and subsequently permit the ligation of the E2-conjugated ubiquitin to the substrate protein.

their N-terminal regions may be involved in substrate binding. Consequently, the cleavage of EOD1 might trigger changes to the catalytic geometry of its active site and alter substrate or chain *specificity* (Fig. 7.2b). Therefore it may be that DA1-mediated cleavage of EOD1 and DA2 alters their catalytic specificity (either substrate of chain-type) and not their general catalytic activity (Fig. 7.3).

The observations that E3 ligases can be regulated by post-translational modification – including this study – have implications across the field of biology and in particular in the study of cancer biology. Many tumour suppressors and oncogenes are E3 ligases. These include the RING E3, MDM2, which is a negative regulator of the central tumour suppressor gene p53 (Fang et al., 2000, Gottlieb and Oren, 1998), and the RING E3, BRCA1, which is involved in DNA damage repair (Gowen et al., 1998) and is a key marker of ovarian and breast cancer (Futreal et al., 1994, Miki et al., 1994). Other examples include the IAP (INHIBITOR OF APOPTOSIS) protein, which is involved in the ubiquitin-dependent degradation of caspases (Scott et al., 2005) as well as various components of the SCF complex, such as SKP2 and FBW7, which have

been implicated in lung cancer, and ovarian cancer, breast cancer, lymphoma and colorectal cancer respectively (Nakayama and Nakayama, 2006).

Such is the prevalence of E3 ligases in the development of cancers, that various E3s have been suggested as therapeutic targets of anti-cancer drugs (Sun, 2006, Sun, 2003). Identification of a novel mechanism for the regulation of E3 ligases in plants may guide the discovery of a similar mechanism in animal systems, and will ensure that all opportunities for manipulating E3 ligase activity are understood.

7.1.3 – DA1, EOD1 and DA2: a novel enhancing regulatory loop

Together, these data reveal a novel enhancing regulatory loop involving the regulation of an E3 ligase through its interaction with an interacting peptidase enzyme. If both the E3 ligase and peptidase components of this module activate one-another, then once initiated, the reciprocal activation of peptidase and E3 would be likely to progress in an irreversible manner. This is a novel switching mechanism that may act as a molecular ratchet that drives the unidirectional, irreversible amplification of a signal (Fig. 5.13).

Similar peptidase-mediated reciprocally-activating enzyme loops, such as those proposed for the DA1-EOD1 and DA1-DA2 examples described in this work, have been described in studies of apoptosis in animal systems. Caspase-9, a member of the caspase family of cysteine proteases involved in the apoptotic pathway, is involved in an activating feed-forward loop with its sister caspase, caspase-3 (Budihardjo et al., 1999). Once cleaved from its inactive procaspase state, caspase-9 cleaves procaspase-3, which, once active, cleaves more procaspase-9 (Budihardjo et al., 1999). This cycle feeds forward to activate the entire pool of caspase-9 and caspase-3, thereby irreversibly committing the animal cell towards apoptosis (Budihardjo et al., 1999, Thornberry and Lazebnik, 1998). It is possible that the auto-activating DA1-EOD1 module acts in a similar way to the capsase-9-caspase-3 module. This would predict that under conditions that result in the interaction of EOD1 and DA1, an irreversible EOD1- and DA1-dependent signalling cascade is initiated.

More specifically, this work reveals a novel mechanism for the regulation of E3 ligases. Previous work has revealed the regulation of E3 activity through a variety of mechanisms including ubiquitination (Stevenson et al., 2007, Mallery et al., 2002), neddylation and rubylation (Duda et al., 2008, Biedermann and Hellmann, 2011), binding-site competition (Zheng et al., 2002), dimerization (Merlet et al., 2009) and artificial truncation (Chew et al., 2012). To date, to my knowledge no one has demonstrated the *in vivo* cleavage of an E3 ligase by a cognate peptidase enzyme.

In addition to the novelty of this regulatory mechanism, as well as its implications for other studies in biology, this thesis has advanced our understanding of the role of EOD1, DA2 and DA1 at the level of the developing organ (see section 7.2). Furthermore it has created significant new insight into detailed molecular mechanisms that themselves provide a way to investigate the wider cellular consequences of EOD1-, DA2- and DA1- mediated regulation. The ability to constitutively activate EOD1 and DA2 enables one to screen for E3 substrate proteins using a method similar to that used in (Emanuele et al., 2011). A promising approach to identify substrates of E3 ligases by converting them to neddylating proteins (Zhuang et al., 2012) could also be used. Furthermore, on-going work (Grant BB/K017225/1) to identify the sequence specificity of DA1 cleavage has the potential to allow *in silico* screening for novel DA1 targets.

Breakthroughs in understanding of the molecular relationship between DA1 and EOD1 (and DA2) will also enable strategies for the improvement of yield in commercial crop varieties. The knowledge that DA1 acts synergistically with both EOD1 and DA2 in the regulation of organ size suggests that a combination of mutations will increase seed size and crop yield. As part of this project a patent application was recently filed for the protection of DA1-DA2 technologies.

7.2 – DA1: regulating organ growth and development

7.2.1 – DA1: A role in organ growth and pathogen response pathways?

Recent work is beginning to reveal considerable overlap between the regulation of plant growth and development and pathogen responses. A reduction in plant growth is a stereotypical response to pathogen challenge, and many investigations of plant PAMP (pathogen associated molecular patterns) responses utilise seedling growth response assays (Gómez‐Gómez et al., 1999, Gómez-Gómez and Boller, 2000, Zipfel et al., 2006). Indeed the challenge of Arabidopsis seedlings with the PAMPs, flg22 (flagellin), and elf18 (EF-Tu), results in an inhibition of growth (Gómez‐Gómez et al., 1999, Gómez-Gómez and Boller, 2000, Zipfel et al., 2006).

Further cross-talk between these two biological processes have been revealed by mutations in pathogen-response related genes that have significantly altered growth and development phenotypes. For example, the gain-of-function mutation in the plant resistance gene *SNC1* (*SUPRESSOR OF NPR1-1*), which results in constitutive expression of pathogenesis-related (PR) genes, also has a dwarfed phenotype (Li et al., 2001, Zhang et al., 2003). This overlap of growth responses and innate immunity is further highlighted by the involvement of BAK1 (BRI1-

ASSOCIATED RECEPTOR KINASE 1) in both the brassinosteroid response and the FLS2 PAMP response. *bak1* knockout mutants have a reduced sensitivity to brassinosteroids and flg22 treatment, and have a semi-dwarfed phenotype (Chinchilla et al., 2007b, Li et al., 2002a). BAK1 has been shown to interact with both BRI1 (BRASSINOSTEROID INSESNITIVE 1) and FLS2 and thereby facilitate brassinosteroid- and flg22-responsive signalling respectively (Chinchilla et al., 2007b, Li et al., 2002a, Nam and Li, 2002).

Whereas BAK1 provides an example of a gene involved in transducing both growth-related and pathogen-related signals, the TCP family of transcription factors may be a common component of growth and pathogen signalling pathways. As described in Chapter 4, members of the large TCP family of transcription factors are well characterised regulators of growth and development (Martín-Trillo and Cubas, 2010), with evidence that Class I TCPs bind directly to the promoters of cell cycle genes (Li et al., 2012). However, a recent interactomic study also identified TCP14 as a hub in response to *Pseudomonas syringae* and *Hyaloperonospora arabidopsidis* infection (Mukhtar et al., 2011). In addition, the partial correlation analysis of transcriptome data (Maclean, unpublished) documented in Fig. S2 identified *DA1* as a hub in a network of interactions in response to flg22, with *TCP15* being a downstream target of *DA1*.

7.2.2 – DA1 and LRR-RLKs: regulation by internalisation?

Data from a partial correlation analysis (Maclean, unpublished) that accurately predicted an interaction between *DA1* and *TCP15* (section 4.3) have implicated DA1 in the FLS2-mediated PAMP response. Although there is no direct evidence yet of an interaction between *DA1* and *FLS2*, this thesis presents evidence of a link between DA1 and two LRR-RLKs, both of which have connections to growth regulation *and* FLS2.

First, section 4.4.1.2 revealed that *da1-1* seedlings have a reduced sensitivity to epibrassinolide; partially phenocopying *bak1* knockout seedlings. *bak1* plants have a semi-dwarfed phenotype and over-expression of *BAK1* has been shown to increase leaf elongation (Li et al., 2002a, Song et al., 2009), which demonstrates a role in the regulation of final organ size. Various brassinosteroid-related genes have been implicated in the regulation of organ growth, and in particular, in the mis-regulation of cell expansion (Azpiroz et al., 1998, Clouse et al., 1996, Nakaya et al., 2002, Hu et al., 2006) and indeed the large leaf phenotype of *BAK1* overexpressing plants is a consequence of enhanced cell expansion (Li et al., 2002a, Song et al., 2009). While the bulk of these brassinosteroid-related organ-size changes are largely driven by altered expansion rates (Azpiroz et al., 1998, Clouse et al., 1996, Li et al., 2002a, Song et al., 2009), it has been reported that there are also concurrent changes in cell proliferation (Nakaya

et al., 2002). These data make it difficult to see a direct developmental link between the *da1-1* phenotype and the brassinosteroid response because, whereas *DA1* influences the timing of the switch from cell-proliferation to cell-expansion (Li et al., 2008), brassinosteroids appear to predominantly increase cell expansion (Kim and Wang, 2010, Johnson and Lenhard, 2011). However, as discussed in Chapter 1, there are likely to be many signals acting simultaneously on cells of the developing leaf, and their respective influences and effects on growth will depend heavily on other signals at that precise time during organ formation. It is relevant to note that CYCD3, considered to be a negative regulator of the switch from cell-proliferation to cell-expansion (Dewitte et al., 2007), is also up-regulated in endoreduplicating expanding tomato cells (Joubes and Chevalier, 2000).

DA1 has also been shown to physically interact with the cytoplasmic domain of the LRR-RLK, TMK4 in a yeast-2-hybrid and an *in vitro* system. TMK4 was recently identified as a positive regulator of growth and development, as it promotes cell expansion in the developing root and cell proliferation in the developing leaf (Dai et al., 2013). It has also been shown to enrich with FLS2 in lipid rafts after cell cultures were stimulated with flg22 (Keinath et al., 2011); possibly reflecting a direct or indirect response to flg22. In addition to this tentative link with flg22-responses, mutations in TMK4 have been shown to reduce sensitivity to auxin perception (Dai et al., 2013). This is reminiscent of the reduced sensitivity of *bak1* and *da1-1* plants to brassinosteroids (Li et al., 2002a), and of *bak1* plants to flg22 (Chinchilla et al., 2007b).

7.2.2.1 – Models for DA1-dependent LRR-RLK regulation

In animal systems, it is well documented that RTKs (receptor tyrosine kinases) such as EGFR (EPIDERMAL GROWTH FACTOR RECEPTOR) are ubiquitinated upon ligand binding, and that this ubiquitination is sufficient for receptor internalisation and degradation (Haglund et al., 2003). In plants, there is good evidence that FLS2, and tentative evidence that BRI1, BAK1 and EFR (EF-Tu RECEPTOR) are ubiquitinated (Lu et al., 2011, Göhre et al., 2008). The ubiquitination of FLS2 appears to negatively influence its stability (Göhre et al., 2008, Lu et al., 2011), but it is unclear whether the ubiquitin 'smears' presented in Göhre et al (2008) and Lu et al (2011) represent poly-ubiquitin chains or multiple mono-ubiquitination events, as was observed in human EGFR (Haglund et al., 2003). If FLS2 is mono-ubiquitinated, it is possible that, as with EGFR, the ubiquitination event serves to promote internalisation and either recycling to the plasma membrane or degradation in the lysosome. In contrast, poly-ubiquitination suggests ubiquitin-directed proteasome-mediated degradation. There is evidence that internalisation of the BRI1-BAK1 complex is essential for signal propagation (Geldner et al., 2007, Karlova and de

Vries, 2006), and therefore it is possible that endocytosis of FLS2 leads to signal propagation, as well as degradation (Robatzek et al., 2006).

The purported regulated internalisation of ubiquitinated, membrane-bound animal RTKs by UIM-containing adaptor proteins is referred to as the UIM-cycle (Marmor and Yarden, 2004), and it is possible that DA1 is involved in a similar cycle with plant LRR-RLKs (Fig. 7.4). The UIM-cycle predicts that UIM-containing adaptor proteins bind to ubiquitinated RLKs resulting in their internalisation and degradation or recycling to the plasma membrane (Marmor and Yarden, 2004). Evidence that DA1 physically interacts with the cytoplasmic domain of TMK4 suggests that DA1 might act as an ubiquitin dependent adaptor protein, regulating this internalisation and degradation/recycling of TMK4.

An alternative model incorporates the observed synergistic/enhancing interaction of DA1 with EOD1 and DA2 (Fig. 7.5). This models predicts that DA1 promotes the EOD1- or DA2-mediated ubiquitination of TMK4, thereby triggering its internalisation and degradation, and the subsequent attenuation of its signalling. In this model (Fig. 7.5) there are several potential roles for the DA1 UIM domains. First, as with the UIM-cycle, the DA1 UIMs may recruit DA1 to a pre-existing ubiquitin moiety on the RLK, thereby recruiting its cognate E3s to ligate a further ubiquitin signal (Fig. 7.5a). This would be similar to the recruitment of BRCA1 to sites of DNA damage by the UIM-containing protein RAP80, which binds pre-existing ubiquitin chains at sites of DNA damage (Guzzo et al., 2012, Sobhian et al., 2007, Wang et al., 2007). Alternatively, the UIMs may be involved in a coupled mono-ubiquitination-like mechanism, whereby the UIMs recruit the cognate E3 to DA1, and also regulate peptidase activity via interactions with cis-ubiquitin (Fig. 7.5b). A variation on this model is that, instead of ubiquitination of TMK4, the function of the TMK4-DA1-EOD1 interaction is the peptidase-mediated processing of TMK4 by DA1 (Fig. 7.6). This could be similar to the peptidase-mediated cleavage of the membrane-anchored mammalian

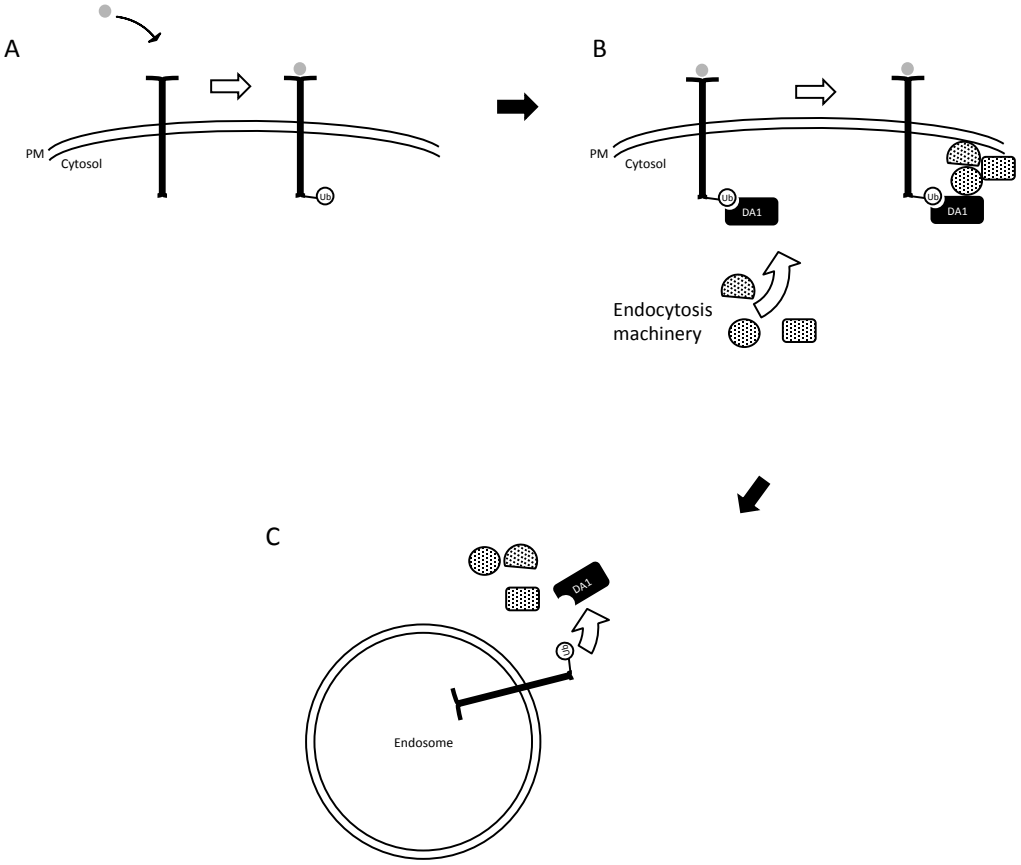

Figure 7.4 – The UIM-cycle

A purported regulatory cycle in which UIM-containing proteins regulate the internalisation and endocytosis of membrane localised receptor molecules. (A) Upon binding of the ligand (grey circle) a receptor-like kinase (black 'T') is ubiquitinated in its cytoplasmic domain. (B) The ubiquitin moiety recruits DA1 (through its UIM domain), DA1 then recruits the endocytotic machinery, which results in receptor internalisation. (C) Once internalised, DA1 is released along with the associated endcytotic machinery. Figure based on Marmoor and Yarden (2004).

heparin-binding EGF-like growth factor (HB-EGFR) (Nanba et al., 2003). This cleavage event results in the translocation of the HB-EGFR C-terminal fragment to the nucleus and the subsequent export of the transcriptional repressor PZLF (promyelocytic leukaemia zinc finger), which is a negative regulator of the cell cycle (Nanba et al., 2003).

This model also incorporates the observation that DA1 physically interacts with TMK4 as well as DA2 and EOD1, which suggests that DA1 may be responsible for mediating an RLK – E3 interaction, leading to RLK ubiquitination by the E3 ligase, cleavage by DA1, or both. If EOD1 and DA2 are required to ubiquitinate TMK4, then DA1-mediated co-localisation of RLK and the E3 ligases would activate the E3s only when directly bound to their substrate by DA1. In animal systems there are examples of E3 *activating* enzymes, which localise to the targets of their respective E3s in a similar manner. The RING E3, MDM2, which ubiquitinates and negatively regulates the tumour suppressor p53, is stabilised (activated) by the de-ubiquitinating enzyme HAUSP, which itself interacts with p53 (Stevenson et al., 2007, Li et al., 2002b). In a similar system, SMAD7 both activates the human HECT E3 ligase, SMURF2, and relocates it from the nucleus to the plasma membrane, which is the location of the SMURF2 target protein, TGF-β (Wiesner et al., 2007, Ogunjimi et al., 2005, Kavsak et al., 2000).

The requirement for the suggested reciprocal activation in the DA1-E3 ligase module would ensure that neither component could be active without interaction with each other. This would safeguard against premature receptor internalisation and limit the signalling response to tissues and developmental stages where both proteins are expressed. Furthermore, the feed-forward nature of such a DA1-E3 module would suggest that subsequent E3 activity would be all or nothing; preventing partial ubiquitination and ensuring complete receptor internalisation. Experiments to test this model of DA1 function are possible using DA1-interacting proteins identified by Y2H in Chapter 4. These experiments would include *in vitro* assays for cleavage and ubiquitination.

7.2.2.2 – The developmental significance of a DA1-RLK interaction

Both models discussed in section 7.2.2.1 are supported by preliminary data that show that DA1 and TMK4 antagonistically influence leaf growth. Whereas TMK4 has been shown to increase leaf size through a promotion of cell proliferation (Dai et al., 2013), DA1 is known to negatively influence the duration of this proliferative phase (Li et al., 2008). It is possible therefore that DA1 is involved in the attenuation of TMK4 dependent growth promotion, suggesting that *da1-1/tmk1/tmk4* triple mutant leaves would phenocopy the *da1-1* leaf.

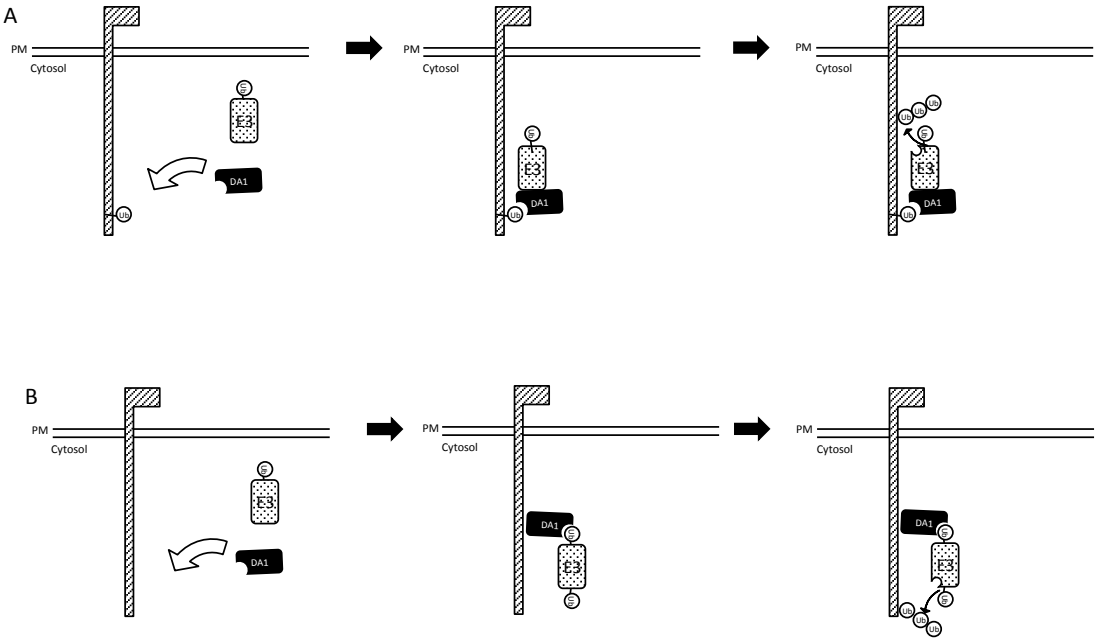

Figure 7.5 – Two possible models for the DA1-E3 regulated ubiquitin-directed internalisation of RLKs

(A,B) Models that explore the possible role of DA1 as an adaptor protein, localising E3 ligases to the cytosolic domain of RLKs, such that the RLKs are ubiquitinated. (A) DA1 might interact with an ubiquitin moiety on the RLK through its UIMs, and interact with its cognate E3 ligase through another domain. This interaction could result in the recruitment of the E3 to the RLK and the subsequent activation of the E3. (B) DA1 could interact with the RLK through an unknown domain, and bind E3-isopetide-linked ubiquitin through its UIM domain. This interaction could result in the recruitment of the E3 to the RLK and the subsequent activation of the E3.

Interestingly, as discussed in Chapter 1, the fact that the *da1-1* large organ phenotype is not complemented by a reduction in cell size suggests that DA1 may be part of a mechanism involved in perception of a hypothetical diffusible growth signal (section 1.5.5). LRR-RLKs are well characterised as signal receptor molecules and have been shown to transduce both steroid (Clouse et al., 1996, Kinoshita et al., 2005) and peptide signals (Chinchilla et al., 2006, Zipfel et al., 2006). The direct interaction of DA1 with TMK4, and its possible indirect links to BAK1 and FLS2, suggest that DA1 may regulate the activity of an LRR-RLK involved in sensing such a diffusible signal. Furthermore, proliferating cells in *da1-1* organs appear have a reduced sensitivity to the signals promoting the switch from proliferation to expansion. This is supported by data presented in section 4.4.1.2, which show that both *da1-1* and *bak1-4* seedlings have reduced sensitivity to brassinosteroid perception. This is particularly interesting considering BAK1 phosphorylation of PUB12/13 has been shown to be essential for an FLS2-PUB13/14 interaction (Lu et al., 2011). In the flg22 response at least, this is consistent with *da1-1* phenocopying a knockout in a gene shown to be responsible for promoting the ubiquitination of an LRR-RLK.

7.2.3 – From DA1 to the cell cycle: linking via TCP transcription factors

The *da1-1* large organ phenotype is a consequence of a delayed exit from the mitotic cell-cycle, suggesting that either directly or indirectly, DA1 may regulate cell-cycle progression. Prior to the work documented in this thesis, the link between DA1 and the cell-cycle was unknown. However, the interaction between DA1 and TCP15 (section 4.3) provides a potential link from the *da1-1* phenotype to the regulation of cell-cycle components via *TCP14* and *TCP15*, which are involved in regulating cell proliferation and cell expansion in developing tissues (Kieffer et al., 2011, Li et al., 2012, Uberti-Manassero et al., 2012). However, the precise role of TCP15 in the regulation of cell proliferation and expansion remains unclear, possibly due to its apparent tissue-specific effects and the coupled nature of cell proliferation and cell expansion. Nonetheless, the observation that organ growth is affected via a mis-regulation of proliferation and expansion, suggests that, developmentally, TCP15 may work in the same pathway as DA1 (Kieffer et al., 2011, Li et al., 2012, Uberti-Manassero et al., 2012). Indeed, genetic interactions presented in sections 4.3.3.1 and 4.3.3.2 suggest that *DA1* and *TCP14/15* operate in the same pathway to regulate stem height and petal size.

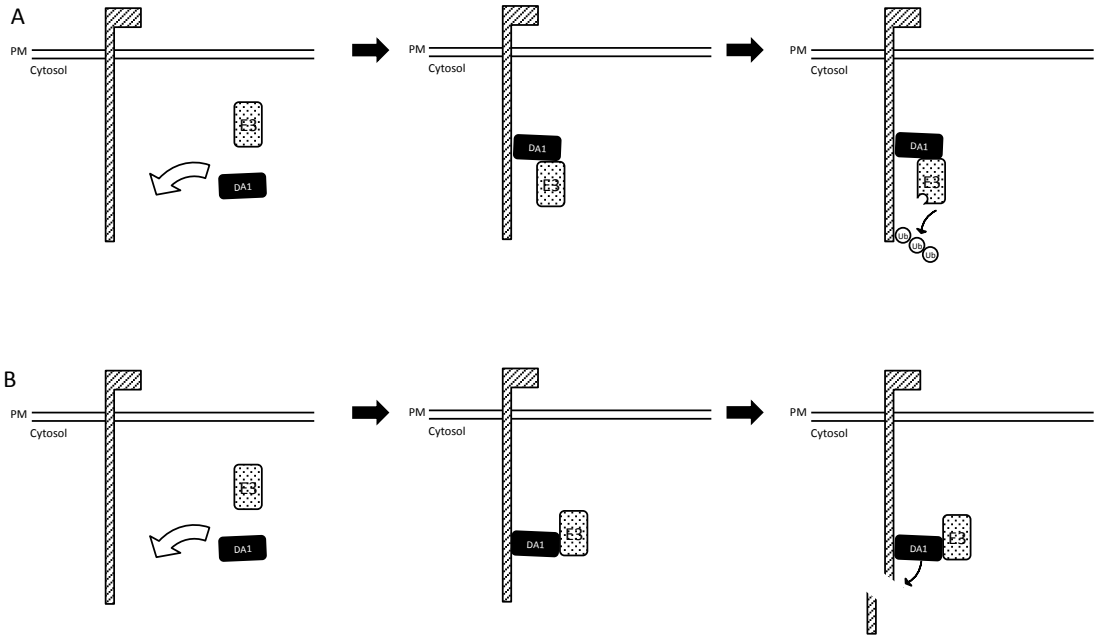

Figure 7.6 – Possible models for the ubiquitin- and peptidase- mediated regulation of RLKs by a DA1-E3 module

It is conceivable that the DA1-E3 module might regulate RLKs through an ubiquitin or peptidase-mediated mechanism. In both of these models DA1 would behave as an adaptor protein, targeting the E3 to the RLK, and upon interaction with the E3, DA1 and the E3 would reciprocally activate. (A) DA1 recruits the E3 to the RLK cytoplasmic domain. The E3-DA1 module reciprocally activates (not shown) and the active E3 ligase then ubiquitinates the cytoplasmic domain of the RLK. (B) DA1 recruits the E3 to the RLK cytoplasmic domain. The E3 activates the DA1 peptidase and the activated DA1 then cleaves the cytoplasmic domain of the RLK.

Recent work has also revealed several direct links between *TCP15* and the cell cycle (Kieffer et al., 2011, Li et al., 2012). It has been reported that TCP15 binds directly to the promoter of the S-phase cyclin, CYCA2;3; as well as to the promoter of RBR1, which is a regulator of the transition between proliferation and endocycling (Li et al., 2012, Magyar et al., 2012). In addition, Li et al (2012) and Kieffer et al (2011) list a total of 12 cell-cycle regulators that are differentially regulated in either knockout, overexpressing or –EAR domain fused *TCP* backgrounds. Taken together with the physical and genetic interactions of DA1 and TCP15, these data indicate the DA1 may function closely with the cell cycle machinery to regulate exit from the mitotic cell-cycle.

Work in this thesis, as well as in three recent publications (Kieffer et al., 2011, Li et al., 2012, Uberti-Manassero et al., 2012) has demonstrated that the effect of *TCP15* on organ growth is highly tissue specific, leading to apparently contradictory results and interpretations. This is highlighted by data from Kieffer et al (2011), who show that while *TCP14* and *TCP15* promote cell proliferation in the leaf, they both repress proliferation in the stem. For this reason it is not easy to establish a specific developmental role for TCP15, and it is therefore difficult to predict a directional mechanistic relationship between DA1 and TCP15. What is clear however is that DA1 and TCP15 both affect the balance between cell proliferation and cell expansion, and that TCP15 appears to directly regulate cell-cycle regulators. It is therefore reasonable to predict that one of the routes by which DA1 influences the persistence of the mitotic cell-cycle may be through the direct regulation of TCP15 activity. As is discussed in section 7.2.3.1, this may be through a peptidase or ubiquitin-mediated mechanism, which can be directly tested.

7.2.3.1 – Unifying observations on the role of DA1 in organ growth

The biochemical and genetic analyses described in this thesis have described a novel mechanism mediated by DA1 peptidase function that may regulate the activities of two E3 ubiquitin ligases involved in organ growth and seed size control. How DA1-mediated regulation of E3 ligase activity influences organ growth has been explored using examples of two DA1-interacting proteins, both of which have established roles in growth control. There is preliminary data that DA1 also interacts with several other proteins (see Table 4.1) that have established roles in growth and development. DA1-mediated E3 ligase activity may also influence the activity of these proteins, perhaps suggesting a broad role for DA1 in orchestrating leaf growth.

The identification of interactions between DA1 and four transcription factors known to regulate organ development (*LBD41*, *ASL1*, *TCP15* and *ATHB8* (Prigge et al., 2005, Chalfun-

Junior et al., 2005, Uberti-Manassero et al., 2012, Li et al., 2012, Kieffer et al., 2011, Meng et al., 2010)) suggests that DA1 influences organ growth through the regulation of a broad range of transcription factors.

As discussed in section 5.6.3, DA1 appears to have an EOD1- and DA2- independent activity, which suggests that the DA1 peptidase might be active towards some substrates in its native state, or alternatively it could be activated by other E3 ligases. PUB12/13/14 are candidate E3 ligases for this role. PUB12 and PUB13 are the E3 ligases responsible for ubiquitination of FSL2 (Lu et al., 2011) and are involved influencing the sensitivity of flg22 perception (Marino et al., 2012, Lu et al., 2011). Because there are indirect links between *DA1* and the flg22 PAMP response (discussed in section 4.4), as well as evidence that *DA1* influences the sensitivity of brassinosteroid perception, and because both flg22 and brassinosteroids are perceived (in part) by BAK1 (Chinchilla et al., 2006, Chinchilla et al., 2007a, Gómez-Gómez and Boller, 2000, Li et al., 2002a, Nam and Li, 2002), it is possible that PUB12 and PUB13, and BAK1 and DA1 function together to regulate flg22 and brassinosteroid perception. PUB14 may also be a candidate DA1-activating E3 ligase due to its documented Y2H interaction with TCP15 (Dreze et al., 2011).

It is currently an exciting time in the field of plant developmental biology, with the detailed functional characterisation of known growth regulators occurring alongside the discovery of new regulatory genes. The linkage and association screens reported in Chapter 6 aim to continue this progress of gene discovery and, as described, have so far identified over 90 candidate genes for further study and characterisation.

In addition to identifying novel regulators of organ growth and development, these screens may also have identified potentially novel allelic variation in *a priori* growth regulators, which may be related to fitness and adaptation to growth in different environments. Of particular interest to this work is the identification of *DA1* as a candidate gene in a GWA study of natural variation in SE mean petal area. It is hoped that continued investigation in this area may yield insight into novel *DA1* alleles, which in turn may feed into new functional analyses such as those described in this thesis.

Supplementary Information

S1 – Supplementary Figures

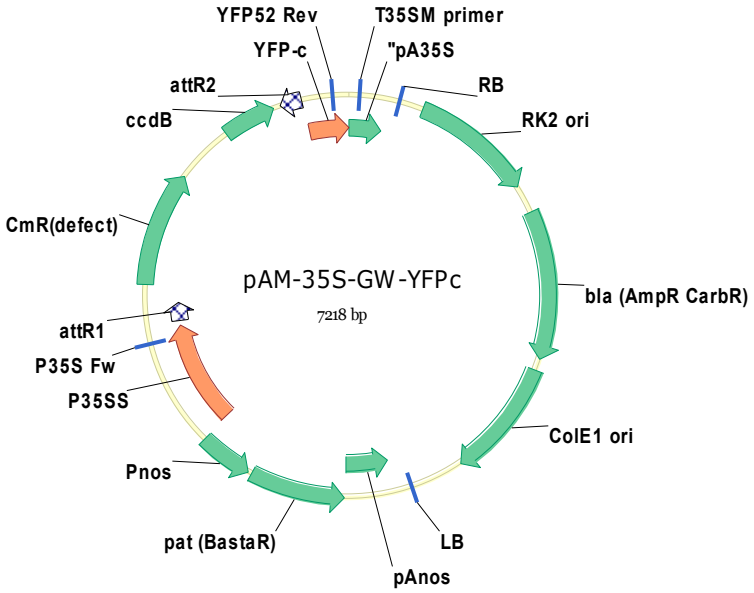

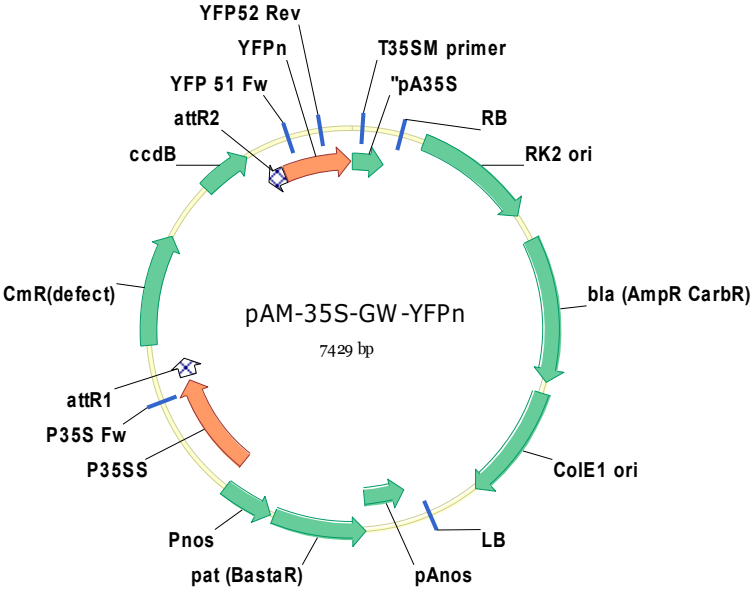

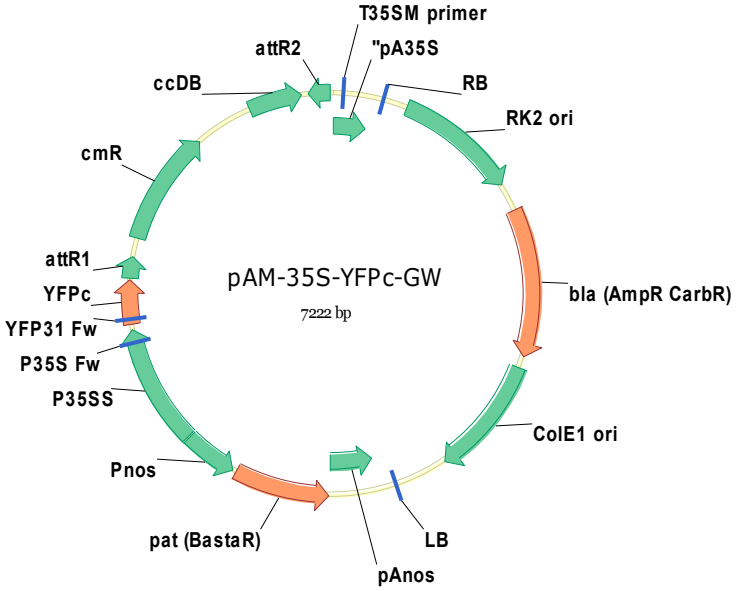
T35SM primer
attR2
"pA35S
ccDB
RB
RK2 ori
cmR
attR1
pAM-35S-YFPc-GW
7222 bp
bla (AmpR CarbR)
YFPc
YFP31 Fw
P35S Fw
P35SS
ColE1 ori
Pnos
pat (BastaR)
LB
pAnos

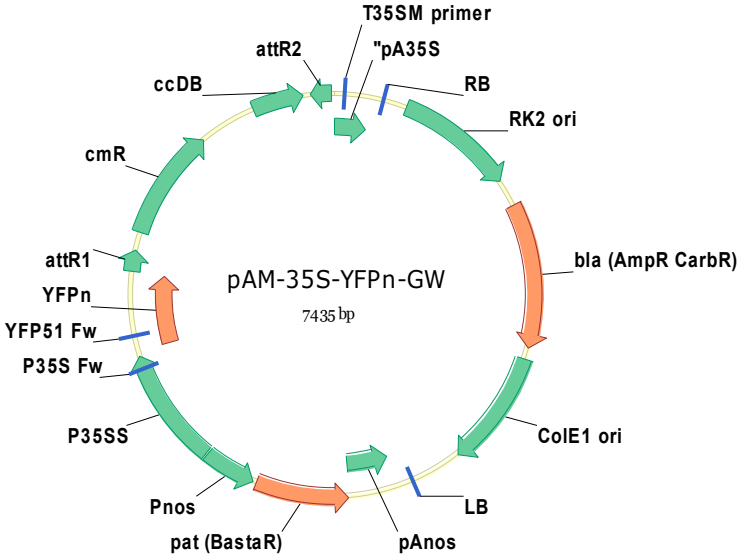
T35SM primer
attR2
"pA35S
ccDB
RB
RK2 ori
cmR
attR1
pAM-35S-YFPn-GW
7435 bp
bla (AmpR CarbR)
YFPn
YFP51 Fw
P35S Fw
P35SS
ColE1 ori
Pnos
LB
pat (BastaR)
pAnos

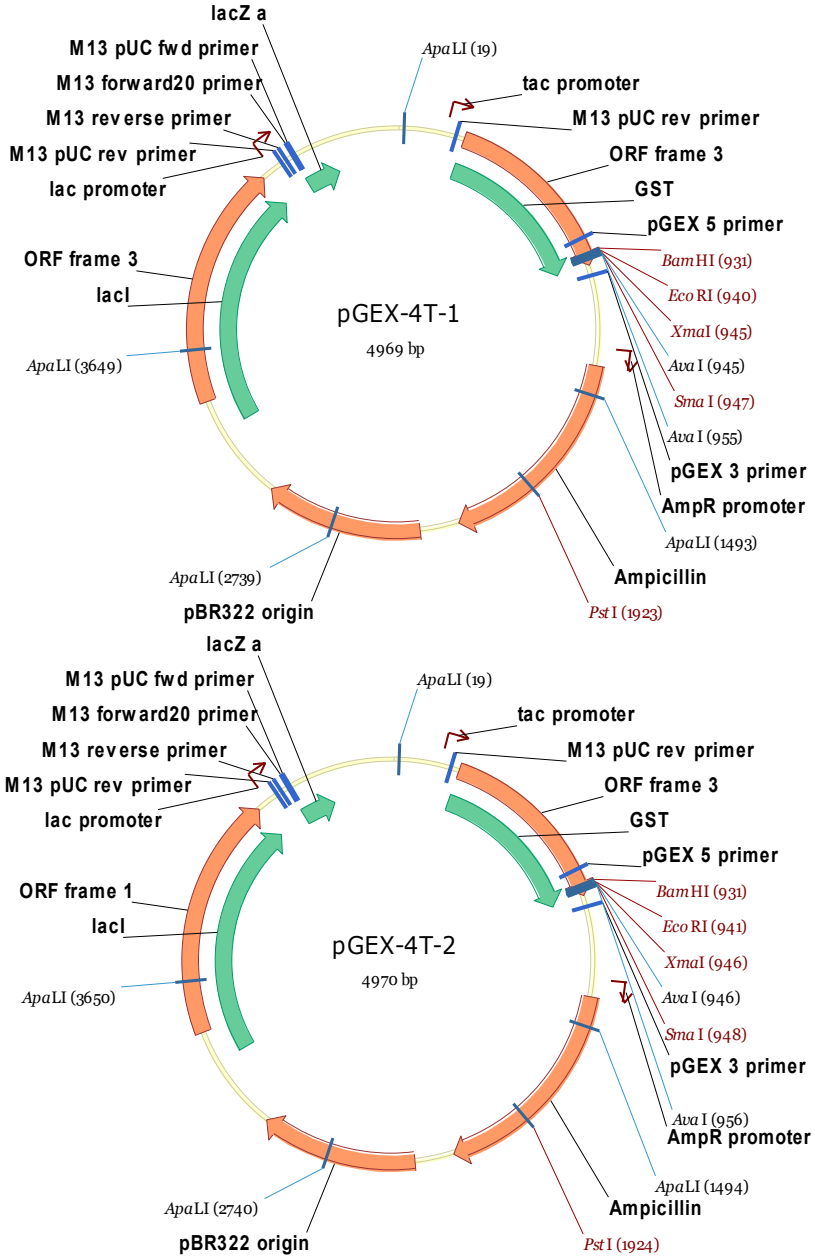
lacZ a
M13 pUC fwd primer
M13 forward20 primer
M13 reverse primer
M13 pUC rev primer
lac promoter
ApaLI (19)
tac promoter
M13 pUC rev primer
ORF frame 3
GST
pGEX 5 primer
BamHI (931)
EcoRI (940)
XmaI (945)
AvaI (945)
SmaI (947)
AvaI (955)
pGEX 3 primer
AmpR promoter
ApaLI (1493)
Ampicillin
PstI (1923)
ORF frame 3
lacI
ApaLI (3649)
pGEX-4T-1
4969 bp
ApaLI (2739)
pBR322 origin
lacZ a
M13 pUC fwd primer
M13 forward20 primer
M13 reverse primer
M13 pUC rev primer
lac promoter
ApaLI (19)
tac promoter
M13 pUC rev primer
ORF frame 3
GST
pGEX 5 primer
BamHI (931)
EcoRI (941)
XmaI (946)
AvaI (946)
SmaI (948)
pGEX 3 primer
AvaI (956)
AmpR promoter
ApaLI (1494)
Ampicillin
PstI (1924)
ORF frame 1
lacI
ApaLI (3650)
pGEX-4T-2
4970 bp
ApaLI (2740)
pBR322 origin

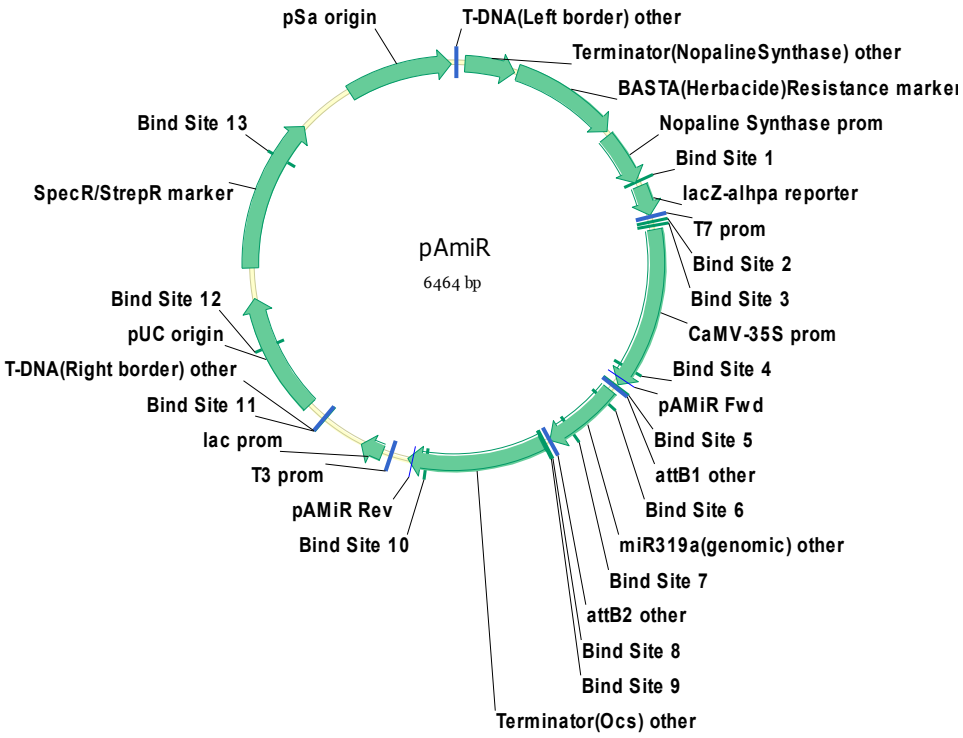
pAmiR
6464 bp
pSa origin
T-DNA(Left border) other
Terminator(NopalineSynthase) other
BASTA(Herbacide)Resistance marker
Nopaline Synthase prom
Bind Site 1
lacZ-alhpa reporter
T7 prom
Bind Site 2
Bind Site 3
CaMV-35S prom
Bind Site 4
pAMiR Fwd
Bind Site 5
attB1 other
Bind Site 6
miR319a(genomic) other
Bind Site 7
attB2 other
Bind Site 8
Bind Site 9
Terminator(Ocs) other
Bind Site 10
pAMiR Rev
T3 prom
lac prom
Bind Site 11
T-DNA(Right border) other
pUC origin
Bind Site 12
SpecR/StrepR marker
Bind Site 13

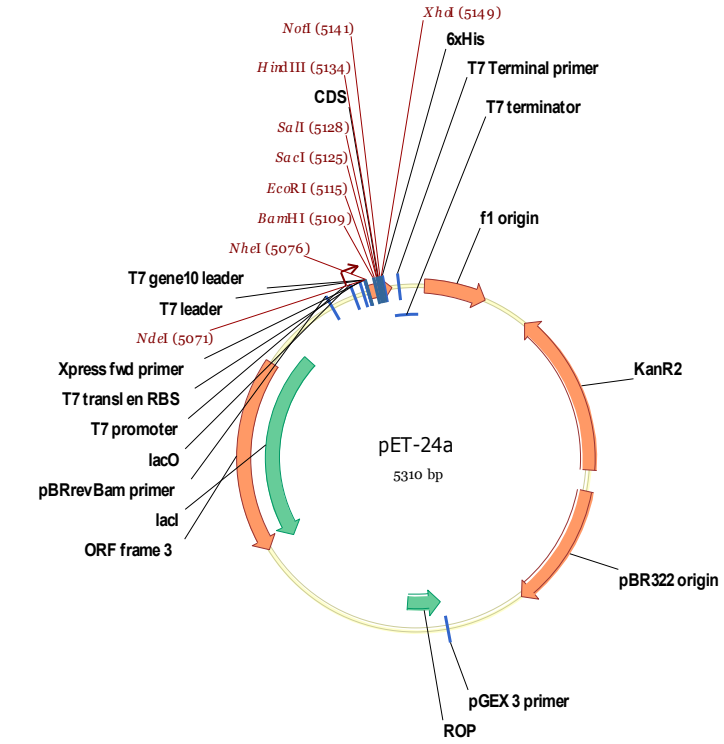
NotI (5141)
XhoI (5149)
6xHis
T7 Terminal primer
HindIII (5134)
CDS
T7 terminator
SalI (5128)
SacI (5125)
EcoRI (5115)
f1 origin
BamHI (5109)
NheI (5076)
T7 gene10 leader
T7 leader
NdeI (5071)
KanR2
Xpress fwd primer
T7 transl en RBS
T7 promoter
pET-24a
5310 bp
lacO
pBRrevBam primer
lacI
pBR322 origin
ORF frame 3
pGEX 3 primer
ROP

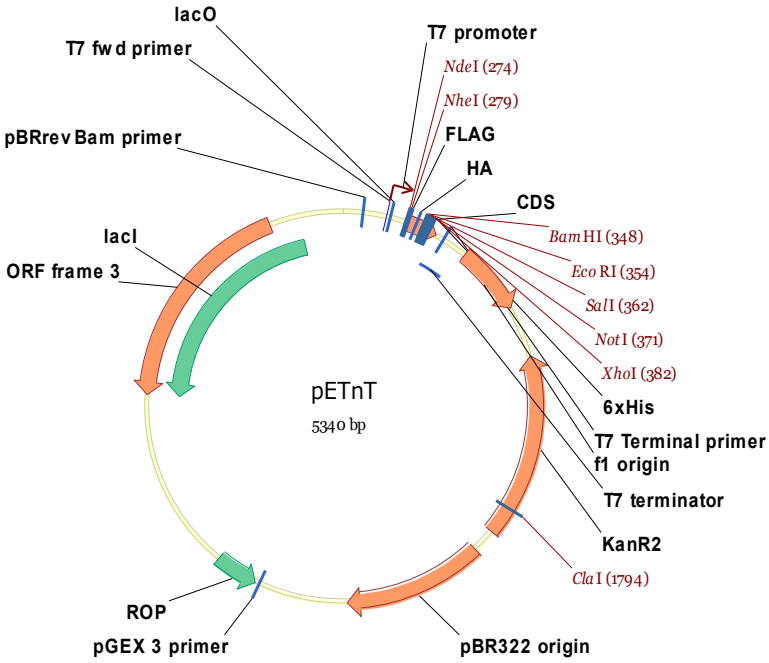
lacO
T7 promoter
T7 fwd primer
NdeI (274)
NheI (279)
pBRrev Bam primer
FLAG
HA
CDS
lacI
BamHI (348)
ORF frame 3
EcoRI (354)
SalI (362)
NotI (371)
XhoI (382)
pETnT
5340 bp
6xHis
T7 Terminal primer
f1 origin
T7 terminator
KanR2
ClaI (1794)
ROP
pGEX 3 primer
pBR322 origin

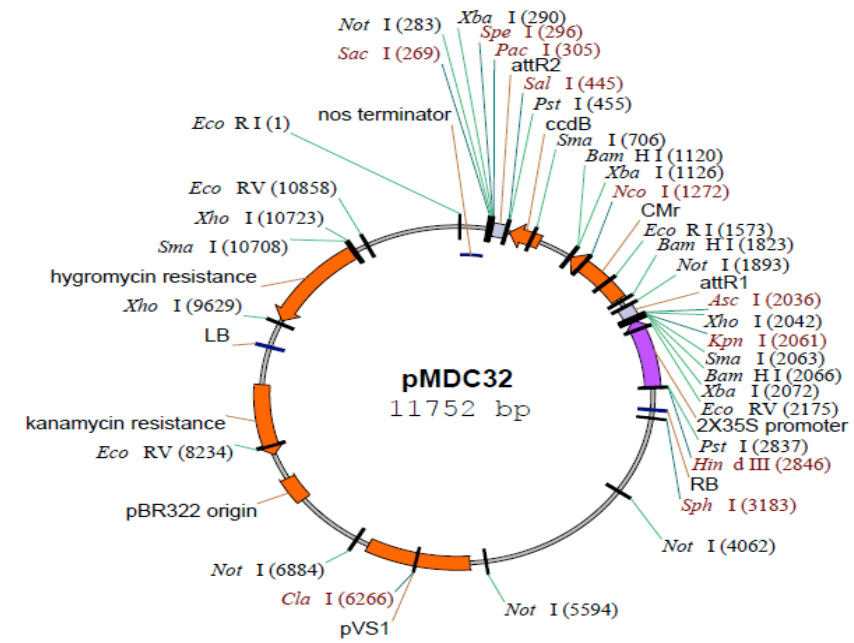
Not I (283)
Xba I (290)
Spe I (296)
Sac I (269)
Pac I (305)
attR2
Sal I (445)
Pst I (455)
Eco R I (1)
nos terminator
ccdB
Sma I (706)
Bam H I (1120)
Xba I (1126)
Eco RV (10858)
Nco I (1272)
Xho I (10723)
CMr
Sma I (10708)
Eco R I (1573)
Bam H I (1823)
hygromycin resistance
Not I (1893)
attR1
Xho I (9629)
Asc I (2036)
LB
Xho I (2042)
Kpn I (2061)
Sma I (2063)
pMDC32
Bam H I (2066)
11752 bp
Xba I (2072)
Eco RV (2175)
kanamycin resistance
2X35S promoter
Eco RV (8234)
Pst I (2837)
Hin d III (2846)
RB
pBR322 origin
Sph I (3183)
Not I (4062)
Not I (6884)
Cla I (6266)
Not I (5594)
pVS1

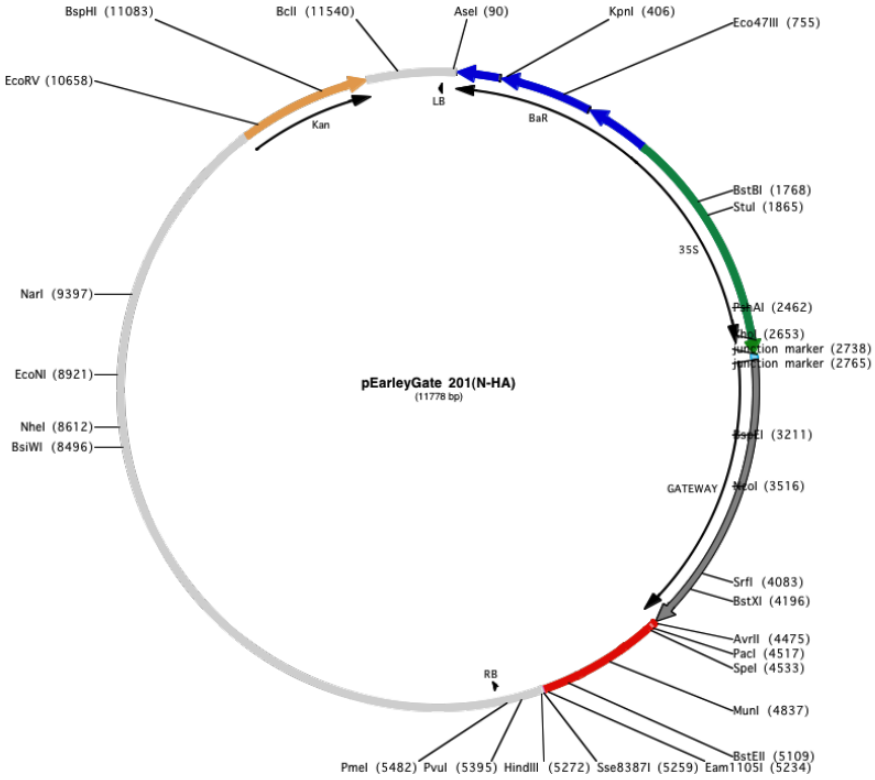
BspHI (11083)
BclI (11540)
AseI (90)
KpnI (406)
Eco47III (755)
EcoRV (10658)
LB
Kan
BaR
BstBI (1768)
StuI (1865)
35S
NarI (9397)
EcoNI (8921)
pEarleyGate 201(N-HA)
(11778 bp)
NheI (8612)
BsiWI (8496)
GATEWAY
SrfI (4083)
BstXI (4196)
AvrII (4475)
PacI (4517)
SpeI (4533)
RB
MunI (4837)
BstEII (5109)
PmeI (5482)
PvuI (5395)
HindIII (5272)
Sse8387I (5259)
Eam1105I (5234)

Figure S1 – Vector maps

Maps of all vectors used in this thesis, with the exception of pw1211, which does not have an annotated map. Maps display key coding regions and vector identities are located in the centre of each map. All maps were generated in Vector NTI (Invitrogen) with the exception of the maps for pMDC32 and pEarleyGate201, which are adapted from http://botserv1.uzh.ch/home/grossnik/curtisvector/pMDC32.pdf and http://sites.bio.indiana.edu/~pikaardlab/pEarleyGate%20plasmid%20vectors%20copy/plasmid%20circular%20maps/pEarleyGate%20201(N-HA).pdf respectively.

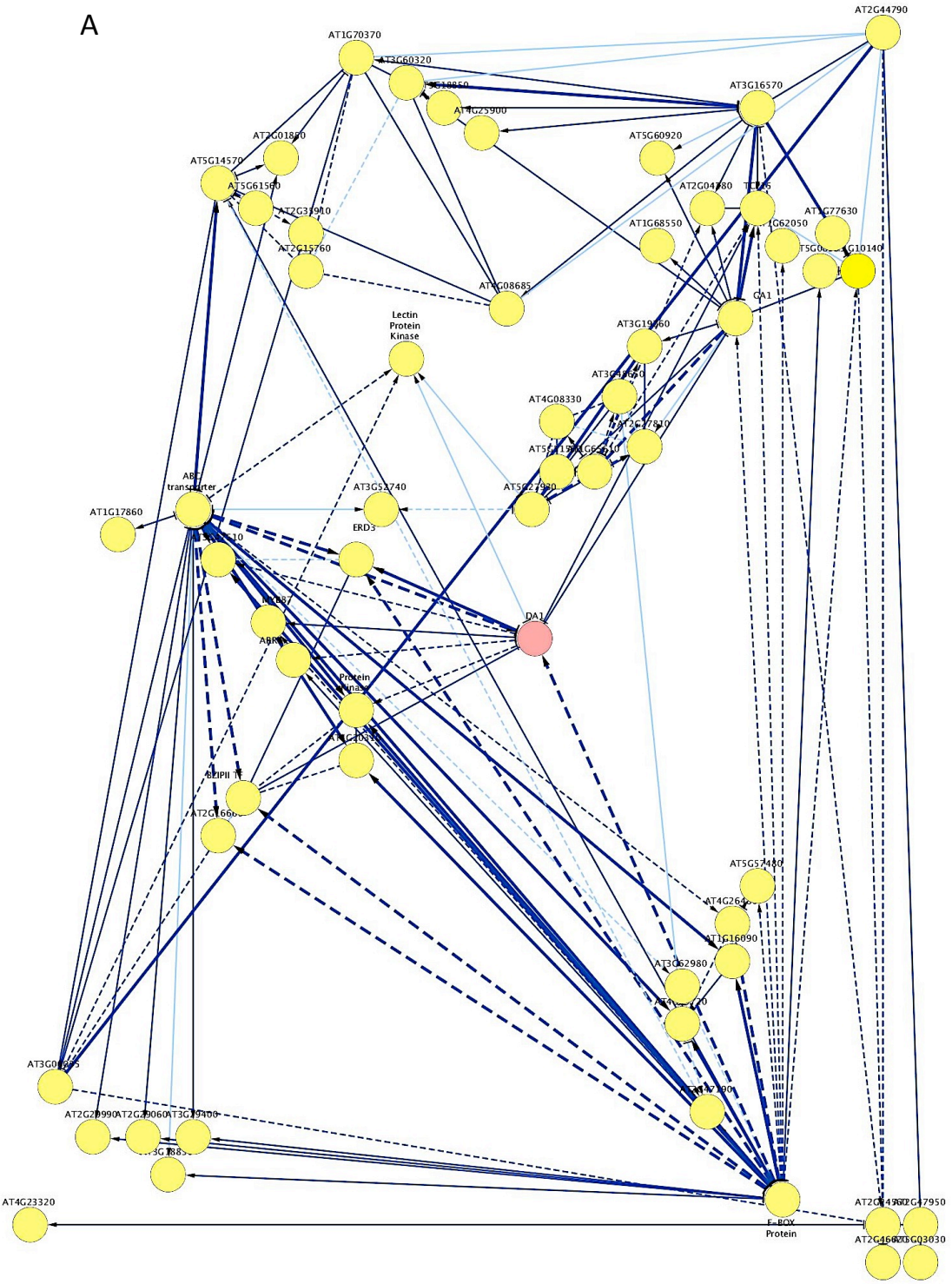
A
AT2G44790
AT1G70370
AT3G60320
AT3G16570
AT4G25900
AT2G01850
AT5G60920
AT5G14570
AT5G61560
AT2G04780
AT2G31910
AT1G77630
AT1G68550
AT2G15760
AT2G08685
CA1
Lectin
Protein
Kinase
AT3G19260
AT4G08330
AT1G17860
AT3G52740
ERD3
DA1
AT5G57480
AT1G16090
AT3G62980
AT4G23320
AT2G20990
AT2G29060
AT3G19400
E-BOX
Protein

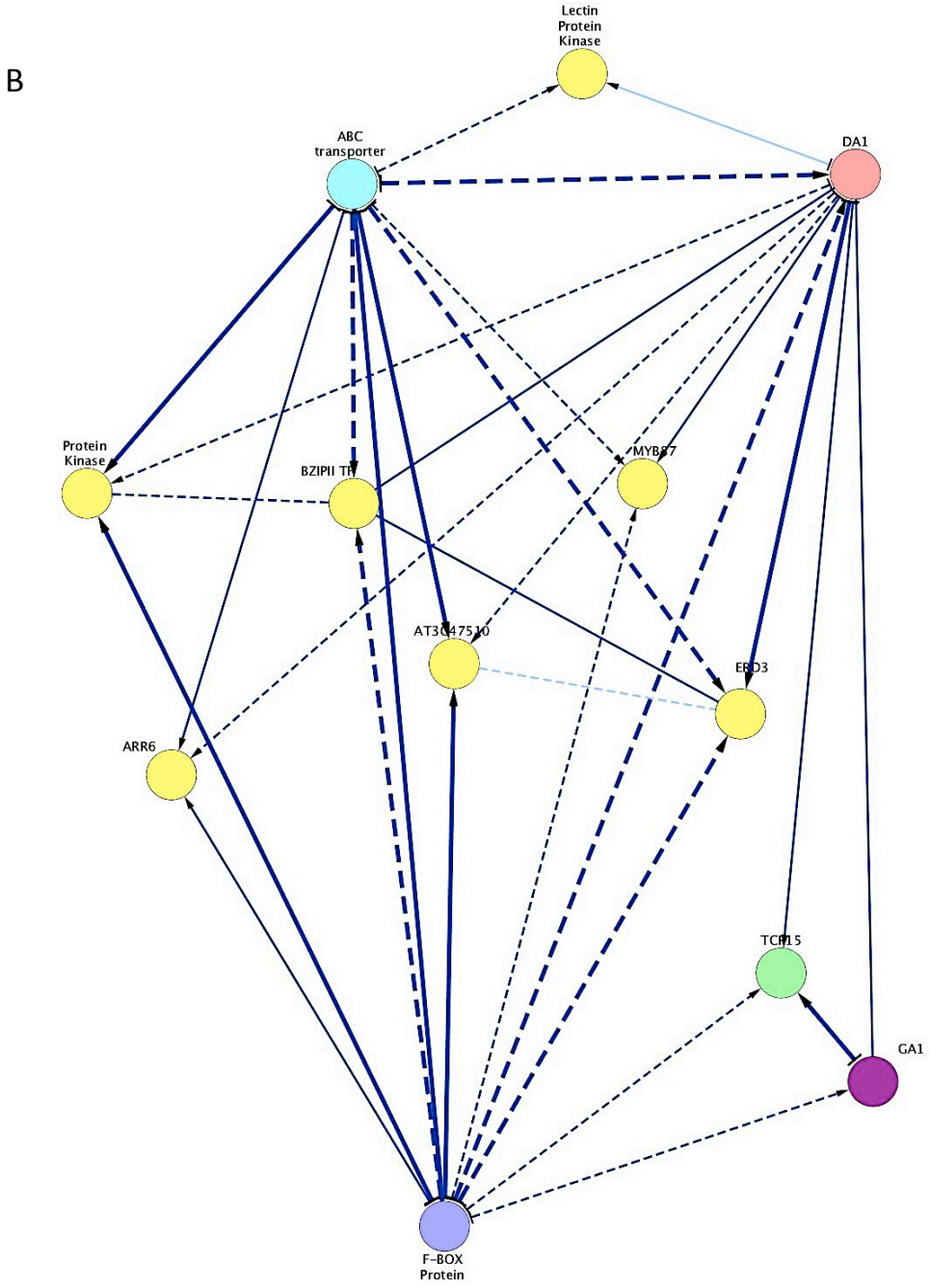

Figure S2 – Partial correlation analysis (Dan Maclean, unpublished)

A partial correlation analysis of expression data from 5-week old Arabidopsis leaves treated with flg22. Circles represent genes, lines represent predicted interactions between genes, the weight of the lines corresponds to the strength of the predicted interaction, and the arrows denote the direction of the predicted interaction. (A) The complete network, (B) the nearest-neighbour network for DA1.

A

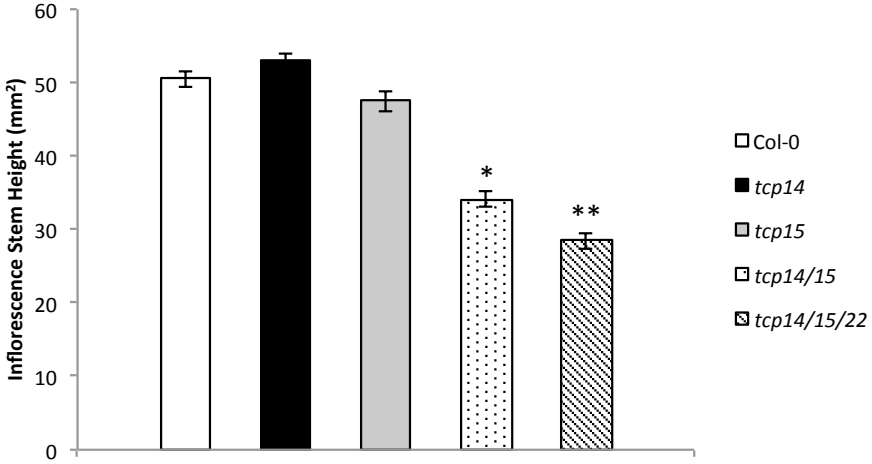
Inflorescence Stem Height (mm²)
60
50
40
30
20
10
0
*
**
Col-0
tcp14
tcp15
tcp14/15
tcp14/15/22

B

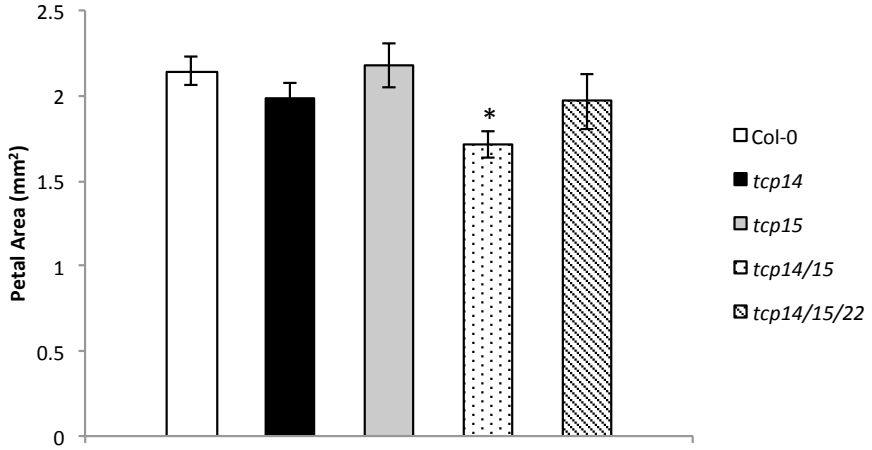
Petal Area (mm²)
2.5
2
1.5
1
0.5
0
*
Col-0
tcp14
tcp15
tcp14/15
tcp14/15/22

C

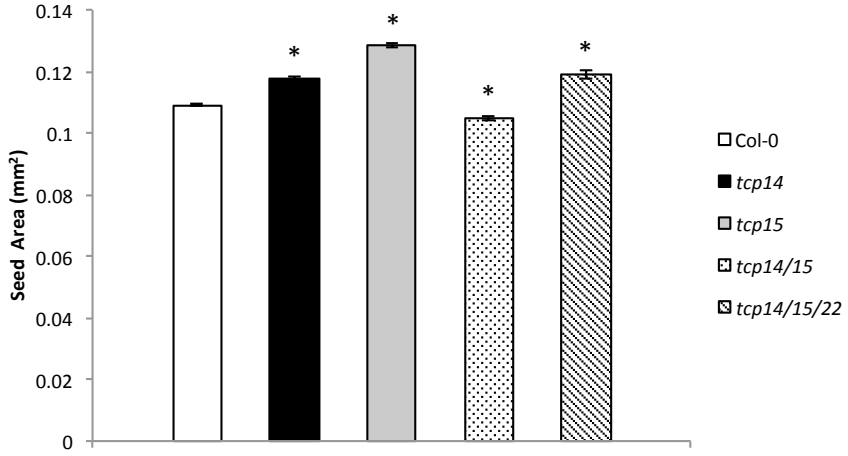
Seed Area (mm²)
0.14
0.12
0.1
0.08
0.06
0.04
0.02
0
*
*
*
*
Col-0
tcp14
tcp15
tcp14/15
tcp14/15/22

Figure S3 – *TCP22* influences organ growth

The effect of the *tcp22* mutation on inflorescence stem height (n=6), petal area (n=10) and seed area (n=600) was investigating by crossing the *tcp14/tcp15* double mutant with *tcp22*. Data is presented as means ± SE. Phenotypes that were significantly different from Col-0 (Student's T-test, $p<0.05$) are marked with '*', and phenotypes that were significantly different from *tcp14/tcp15* were marked with '**'. (A) The stems of *tcp14/tcp15/tcp22* plants are significantly shorter than those of the *tcp14/tcp15* double mutant, indicating that the *tcp22* allele acts to enhance the *tcp14/tcp15* phenotype. (B) Petals of *tcp14/tcp15/tcp22* plants are not different from Col-0, whereas *tcp14/tcp15* petals are smaller, suggesting that the *tcp22* allele antagonises the *tcp14/tcp15* allele and that TCP22 may be a negative regulator of petal growth. (C) Seeds of *tcp14/tcp15/tcp22* plants are larger than Col-0, whereas *tcp14/tcp15* seeds are smaller; suggesting that the *tcp22* allele antagonises the *tcp14/tcp15* allele and that TCP22 may be a negative regulator of seed growth.

A

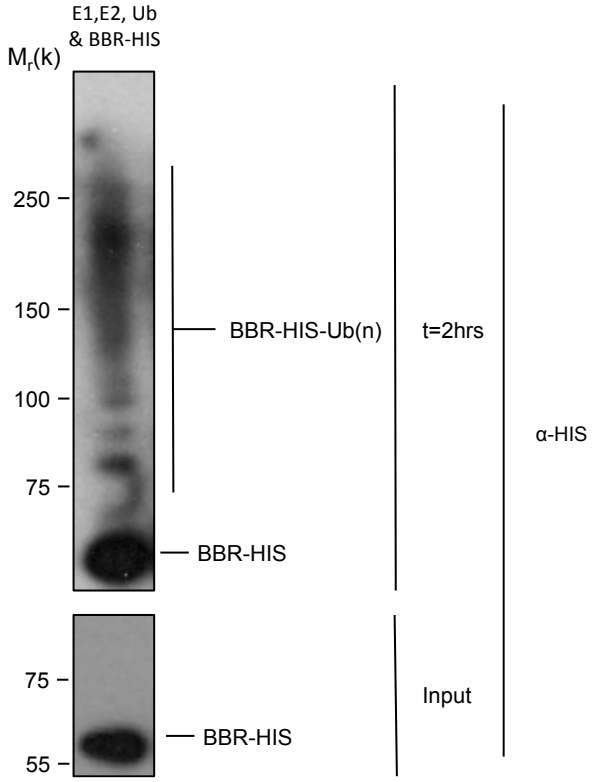

B

```
EOD1      --MNGDNR---------------------------------------------------- 6
BBR       MPMENDNGPHVGNVVVTAEQATKINETDGRLPENRQTGVVSDTGSGSERGEQGVGESAVA 60
            *:.**

EOD1      ---PVEDAHYTETG-FPYAATGSYMDFYGGAAQGPLNYDHAATMHPQDNLYWTMNTNAYK 62
BBR       VAVPVEESGSISVGELPAPRSSSARVPFTNLSQIDADLALARTLQEQERAYMMLTMNSEI 120
             ***::   ..* :* . :.*    : . :*   :   * *:: *:. *  :. *:

EOD1      FGFSGSDNASFYGSYDMNDHLSRMSIGRTNWDYHP------------------------- 97
BBR       SDYGSWETGSYVYDEDEFDDPENEDEDDDEDEYETDDDPQEDGLDVNVHANEDDQEDDGN 180
           .:.. :..*:  . *  *. .. . .  : :*..

EOD1      --MVNVADDPENTVARSVQIGDTDEHSE--------AEECIANEHDPDSPQVSWQDDIDP 147
BBR       SDIEEVAYTDDEAYARALQEAEERDMAARLSALSGLANRVVEDLEDESHTSQDAWDEMDP 240
            : :**   ::: **::* .:  : :         *:. : : .* . .. .  *::**

EOD1      DTMTYEELVELGEAVGTESRGLSQELIETLPTKKYKFGSIFSRKRAGERCVICQLKYKIG 207
BBR       DELSYEELLALGDIVGTESRGLSADTIASLPSKRYKEG--DNQNGTNESCVICRLDYEDD 298
          * ::****: **: ********* : * :**:*:** *   .:: :.* ****:*.*: .

EOD1      ERQMNLPCKHVYHSECISKWLSINKVCPVCNSEVFGEPSIH------------------- 248
BBR       EDLILLPCKHSYHSECINNWLKINKVCPVCSAEVSTSTSGQS------------------ 340
          *  : ***** ******.:**.********.:**  ..* :
```

Figure S4 – The E3 ligase BIG BROTHER-RELATED (BBR) (At3g19910) is similar to EOD1

(A) ClustalW alignment of EOD1 and BBR protein sequence (Goujon et al., 2010, Larkin et al., 2007), see Table S3 for key to colour codes. (B) BBR is an active E3 ligase *in vitro*. An *in vitro* ubiquitination assay with BBR as the E3 ligase. In the presence of E1 (human UBE1), E2 (GST-UBC10) and ubiquitin, BBR-HIS catalyses the formation of high molecular weight poly-ubiquitin chains.

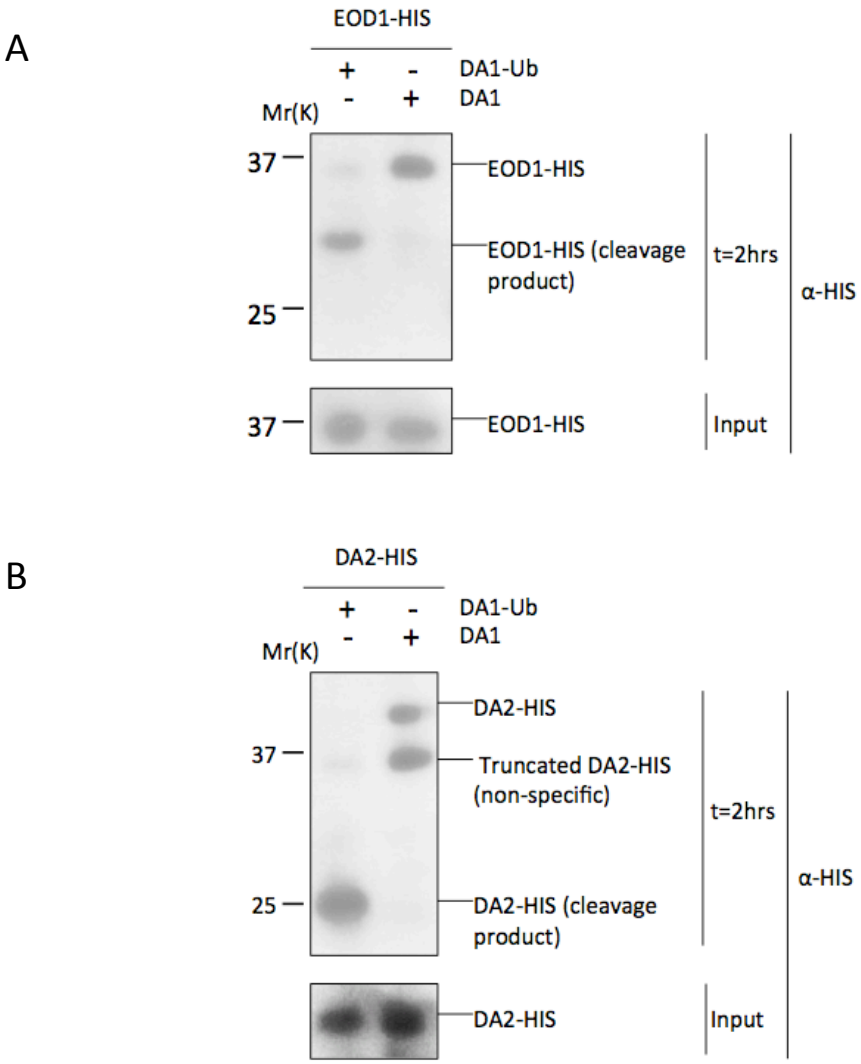

Figure S5 – Ubiquitinated DA1 is sufficient to cleave EOD1 and DA2 *in vitro*

(A,B) Purified FLAG-DA1 and FLAG-DA1-ub (ubiquitinated DA1) was added to a reaction containing EOD1 (A) or DA2 (B). Only DA1-ub was sufficient to cleave EOD1 (A; lane 1) and DA2 (B; lane 1). (B) A lower molecular weight band that co-purifies from *E. coli* with DA2-HIS can be seen in lane 2. This is thought to be due to an ectopic translational event from an intragenic ATG (see section 5.3.4.1 for further discussion).

S2 - Supplementary Tables

Gene name	Gene ID	Reference
ABAP1 (ARMADILLO BTB PROTEIN1)	AT5G13060	(Masuda et al., 2008)
ABA2 (ABA DEFICIENT2)	AT1G52340	(Horiguchi et al., 2006b)
ABA3 (ABA DEFICIENT3)	AT1G16540	(Horiguchi et al., 2006b)
ABP1 (AUXIN BINDING PROTEIN1)	AT4G02980	(Chen et al., 2001)
ACD6 (ACCELERATED CELL DEATH6)	AT4G14400	(Lu et al., 2009)
AGG3 (ARABIDOPSIS G PROTEIN GAMMA SUBUNIT3)	AT5G20635	(Chakravorty et al., 2011)
AHK1 (ARABIDOPSIS THALIANA HISTIDINE KINASE1)	AT2G17820	(Nishimura et al., 2004)
AHK2 (ARABIDOPSIS THALIANA HISTIDINE KINASE2)	AT5G35750	(Nishimura et al., 2004)
AHK3 (ARABIDOPSIS THALIANA HISTIDINE KINASE3)	AT1G27320	(Nishimura et al., 2004)
ANT (AINTEGUMENTA)	AT4G37750	(Mizukami and Fischer, 2000)
AN (ANGUSTOFOLIA)	AT1G01510	(Kim et al., 2002)
AP2 (APETALA 2)	AT4G36920	(Bowman et al., 1991)
APC10 (ANAPHASE PROMOTING FACTOR10)	AT2G18290	(Eloy et al., 2011)
ARF2 (AUXIN RESPONSE FACTOR2)	AT5G62000	(Okushima et al., 2005)
GRF8 (GROWTH-REGULATING FACTOR 8)	AT5G37020	(Okushima et al., 2005)
ARF7 (AUXIN RESPONSE FACTOR7)	AT5G20730	(Wilmoth et al., 2005)
ARF8 (AUXIN RESPONSE FACTOR8)	AT1G1920	(Wilmoth et al., 2005)
ARGOS	AT3G59900	(Hu et al., 2003)
ARL (ARGOS-LIKE)	AT2G44080	(Hu et al., 2006)
ATAF2	AT5G08790	(Delessert et al., 2005)
ATHB16 (ARABIDOPSIS THALIANA HOMEOBOX PROTEIN 16)	AT4G40060	(Wang et al., 2003b)
AVP1 (ARABIDOPSIS THALIANA V-PPASE)	AT1G15690	(Li et al., 2005b)
AXR1 (AUXIN RESISTANT1)	AT1G05180	(Horiguchi et al., 2006b)
AXR3 (AUXIN RESISTANT3)	AT1G04250	(Pérez-Pérez et al., 2010)
BB/EOD1 (BIG BROTHER/ENHANCER OF DA1 1)	AT3G63530	(Disch et al., 2006)
BEN1	AT2G45400	(Yuan et al., 2007)
BIG	AT3G02260	(Guo et al., 2013)
BPEp (BIG PETAL P)	AT1G59640	(Szécsi et al., 2006)
BRI1 (BRASSINOSTEROID INSENSITIVE1)	AT4G39400	(Clouse et al., 1996)
CDC27A	AT3G16320	(Rojas et al., 2009).
CKX3 (CYTOKININ OXIDASE3)	AT2G41510	(Bartrina et al., 2011)
CKX5(CYTOKININ OXIDASE5)	AT1G75450	(Bartrina et al., 2011)
CLE26 (CLAVATA3/ESR-RELATED 26)	AT1G69970	(Strabala et al., 2006)
CLE8 (CLAVATA3/ESR-RELATED 8)	AT1G67775	(Fiume and Fletcher, 2012)
CLV1 (CLAVATA1)	AT1G75820	(Clark et al., 1997)
CTR1 (CONSTITUTIVE TRIPLE RESPONSE)	AT5G03730	(Kieber et al., 1993)
CUC1 (CUP-SHAPED COTELYDON1)	AT5G53950	(Aida et al., 1997)
CUC2 (CUP-SHAPED COTELYDON2)	AT5G53950	(Hibara et al., 2006)

Table S1

CUC3 (CUP-SHAPED COTELYDON3)	AT1G76420	(Hibara et al., 2006)
CYCLIND3;1	AT4G34160	(Dewitte et al., 2007)
CYCLIND3;2	AT5G67260	(Dewitte et al., 2007)
CYCLIND3;3	AT3G50070	(Dewitte et al., 2007)
DA1	AT1G19270	(Li et al., 2008)
DA2	AT1G78420	(Xia, 2013)
DAR1 (DA1-RELATED1)	AT4G36860	(Li et al., 2008)
DHS (DEOXYHYPUSINE SYNTHASE)	AT5G05920	(Wang et al., 2003a)
DWF4 (DWARF4)	AT3G50660	(Choe et al., 2001)
E2F3 (E2F TRANSCRIPTION FACTOR3)	AT2G36010	(Magyar et al., 2012)
EBP1 (ERBB-3 BINDING PROTEIN1)	AT3G51800	(Horvath et al., 2006)
EIN2 (ETHYLENE-INSENSITIVE2)	AT5G03280	(Alonso et al., 1999),
EIN3 (ETHYLENE-INSENSITIVE3)	AT3G20770	(Horiguchi et al., 2006b)
EOD3 (ENHANCER OF DA1 3)	AT2G46660	(Fang et al., 2012)
ER (ERECTA)	AT2G26330	(Shpak et al., 2003)
ERF6 (ETHYLENE RESPONSIVE ELEMENT BINDING FACTOR 6)	AT4G17490	(Dubois et al., 2013)
ETO1 (ETHYLENE-OVERPRODUCTION1)	AT3G51770	(Ecker, 1995)
EIN1 (ETHYLENE-INSENSITIVE1)	AT1G66340	(Horiguchi et al., 2006b)
EXO (EXORDIUM)	AT4G08950	(Coll-Garcia et al., 2004)
EXP10 (EXPANSIN10)	AT1G26770	(Cho and Cosgrove, 2000)
EXP3 (EXPANSIN3)	AT2G37640	(Kwon et al., 2008)
FIE (FERTILISATION INDEPENDNENT ENDOSPERM)	AT3G20740	(Ohad et al., 1999)
FRL1 (FRILL1)	AT1G20330	(Hase et al., 2000)
FUS3 (FUSCA 3)	AT3G26790	(Raz et al., 2001)
FUGU2	AT1G65470	(Ferjani et al., 2007)
FZR2 (FIZZY-RELATED2)	AT4G22910	(Larson-Rabin et al., 2009)
GA1 (GA REQUIRING1)	AT4G02780	(Ubeda-Tomás et al., 2009)
GA20OX1 (GIBBERELLIN 20-OXIDASE)	AT4G25420	(Huang et al., 1998)
GASA14 (G A-STIMULATED IN ARABIDOPSIS14)	AT5G14920	(Sun et al., 2013)
GIF1 (GRF-INTERACTING FACTOR1)	AT5G28640	(Lee et al., 2009)
GIF2 (GRF-INTERACTING FACTOR2)	AT1G01160	(Lee et al., 2009)
GIF3 (GRF-INTERACTING FACTOR3)	AT4G00850	(Lee et al., 2009)
GOA (GORDITA)	AT1G31140	(Prasad et al., 2010)
GRF1 (GROWTH REGULATING FACTOR1)	AT2G22840	(Kim et al., 2003)
GRF2 (GROWTH REGULATING FACTOR2)	AT1G78300	(Kim et al., 2003)
GRF5 (GROWTH REGULATING FACTOR5)	AT3G13960	(Horiguchi et al., 2005)
HOG1 (HOMOLOGY-DEPENDENT GENE SILENCING1)	AT4G13940	(Godge et al., 2008)
HRC1 (HERCULES1)	AT1G45233	(Century et al., 2008, Jiang, 2004)
JAR1 (JASMONATE RESISTANT1)	AT2G46370	(Horiguchi et al., 2006b)
KRP1 (KIP-RELATED PROTEIN1)	AT2G23430	(Malinowski et al., 2011)
KRP7 (KIP-RELATED PROTEIN7)	AT1G49620	(Cheng et al., 2013a)
KRP4 (KIP-RELATED PROTEIN4)	AT2G32710	(Cheng et al., 2013a)

Table S1

IKU (HAIKU)	AT2G35230	(Zhou et al., 2009)
INO (INNER NO OUTER)	AT1G23420	(Villanueva et al., 1999)
JAG (JAGGED)	AT1G68480	(Ohno et al., 2004)
KAT2 (3-KETOACYL-COA THIOLASE2)	AT2G33150	(Footitt et al., 2007)
KLU (KLUH)	AT1G13710	(Anastasiou et al., 2007)
KRP2 (KIP-RELATED PROTEIN2)	AT3G50630	(Cheng et al., 2013a)
KRP3 (KIP-RELATED PROTEIN3)	AT5G48820	(Cheng et al., 2013a)
LUG (LEUNIG)	AT4G32551	(Liu and Meyerowitz, 1995)
LOB (LATERAL ORGAN BOUNDARIES)	AT5G63090	(Lin et al., 2003)
MED25 (MEDIATOR SUBUNIT 25)	AT1G25540	(Xu and Li, 2011)
MED8 (MEDIATOR SUBUNIT 8)	AT2G03070	(Xu and Li, 2012)
MINI3 (MINISEED 3)	AT1G55600	(Zhou et al., 2009)
miR319a	AT4G23713	(Palatnik et al., 2003)
miR396a	AT2G10606	(Rodriguez et al., 2010)
miR396b	AT5G35407	(Rodriguez et al., 2010)
MSI1 (MULTICPOY SUPPRESSOR OF IRA1)	AT5G58230	(Köhler et al., 2003)
NAC1 (NAC DOMAIN CONTAINING PROTEIN1)	AT1G56010	(Xie et al., 2000)
NGA1 (NGATHA1)	At2G46870	(Alvarez et al., 2009)
NUB (NUBBIN)	AT1G13400	(Dinneny et al., 2006)
OBP2	AT1G07640	(Skirycz et al., 2006)
ORS1 (ORGAN SIZE RELATED1)	AT2G41230	(Feng et al., 2011)
PPD (PEAPOD)	AT4G14713	(White, 2006)
RBR1 (RETINOBLASTOMA-RELATED1)	AT3G12280	(Magyar et al., 2012)
ROT3 (ROTUNDIFOLIA3)	AT4G36380	(Kim et al., 1998b)
ROXY1	AT3G02000	(Xing et al., 2005)
ROXY2	AT5G14070	(Xing and Zachgo, 2008)
RPT2A (REGULATORY PARTICLE AAA-ATPASE 2a)	AT4G29040	(Sonoda et al., 2009)
RSW1 (RADIAL SWELLING 1)	AT4G32410	(Hématy et al., 2007)
SHB1 (SHORT HYPOCOTYL UNDER BLUE1)	AT4G25350	(Zhou et al., 2009)
SHR (SHORT-ROOT)	AT4G37650	(Nakajima et al., 2001)
SLY1 (SLEEPY1)	AT4G24210	(Dill et al., 2004)
SPT (SPATULA)	AT4G36930	(Ichihashi et al., 2010)
SRF4 (STRUBBELIG-RECEPTOR FAMILY4)	AT3G13065	(Eyüboglu et al., 2007)
STY1 (STYLISH1)	AT3G51060	(Sohlberg et al., 2006)
SWP (STUWWELPETER)	AT3G04740	(Autran et al., 2002)
TCP1	At1G67260	(Koyama et al., 2010b))
TCP10	At2G31070	(Palatnik et al., 2003)
TCP12	At1G68800	(Aguilar-Martínez et al., 2007)
TCP13	At3G02150	(Koyama et al., 2007)
TCP14	At3G47620	(Kieffer et al., 2011)
TCP15	At1G69690	(Kieffer et al., 2011)
TCP17	At5G08070	(Koyama et al., 2007)

Table S1

TCP2	At4G18390	(Palatnik et al., 2003)
TCP20	At3G27010	(Li et al., 2005a)
TCP11	At5G08330	(Viola et al., 2011)
TCP22	At1G72010	See Fig. S3
TCP23	At1G35560	(Balsemão-Pires et al., 2013)
TCP24	At1G30210	(Palatnik et al., 2003)
TCP3	At1G53230	(Palatnik et al., 2003)
TCP4	At3G15030	(Palatnik et al., 2003)
TCP5	At5G60970	(Koyama et al., 2007)
TCP8	At1G58100	(Patel, 2012)
TCP9	At2G45680	(Balsemão-Pires et al., 2013)
TIE (TCP INTERACTOR CONTAINING EAR MOTIF PROTEIN)	AT4G28840	(Tao et al., 2013)
TOR (TARGET OF RAPAMYCIN)	AT1G50030	(Deprost et al., 2007)
TTG2 (TRANSPARENT TESTA GLABRA2)	AT2G37260	(Garcia et al., 2005)
TTL (TITAN-LIKE)	AT4G24900	(Nam and Li, 2004)
UBP15 (UBIQUITIN-SPECIFIC PROTEASE15)	AT1G17110	(Horiguchi et al., 2006a)
ZHD5 (ZINC FINGER HOMEODOMAIN5)	AT1G75240	(Hong et al., 2011)

Table S1 – List of *a priori* growth regulators

The table lists genes that have been characterized as regulators of leaf growth, petal growth and seed growth. It is based on tables from Gonzalez et al (2008) and Breuninger & Lenhard (2010).

AccessionName	AccessionID
T910	6143
Ådal 3	9323
Öde 2	9434
Öde 3	9435
Ale1-2	5829
AleA 1	9325
Aledal-11-63	1163
Aledal-1-34	1153
Aledal-14-73	1166
Aledal-17-82	1169
Aledal-6-49	1158
Ale-Ster-41-1	991
Ale-Ster-44-4	992
Ale-Ster-50-11	996
Ale-Ster-56-14	997
Ale-Ster-57-16	998
Ale-Ster-59-18	999
Ale-Ster-64-24	1002
Ale-Ster-77-31	1006
ÖMö1-7	6073
Ängsö-12-402	1303
Ängsö-57-419	1312
Ängsö-59-422	1313
Ängsö-74-430	1317
Ängsö-80-432	1318
App1-12	5830
App1-14	5831
App1-16	5832
Bag 1	9330
Bar 1	9332
Bil-3	5835
Bön 1	9336
Boo2-3	5836
Böt 1	9339
Böt 4	9342
Brösarp-11-135	1061
Brösarp-11-138	1062
Brösarp-21-140	1063
Brösarp-25-142	1064
Brösarp-34-145	1066
Brösarp-37-149	1068
Brösarp-43-152	1069
Brösarp-45-153	1070
Brösarp-51-157	1072
Brösarp-53-159	1073
Brösarp-61-162	1074
Brösarp-63-163	1075
Dja 1	9343
Dja 2	9344

AccessionName	AccessionID
Död 1	9351
Djk 3	9349
Död 2	9352
Död 3	9353
Dör-10	5856
Dra1-4	5865
Dra2-1	5867
Dra-3	5860
Dra3-9	5870
Eden 15	9354
Eden 16	9355
Eden 17	9356
Eden-1	6009
Eden-4	8218
Eden-5	6010
Eden-6	6011
Eden-7	6012
Eden-9	6013
EdJ 2	9363
Eds-9	6017
EkN 3	9367
EkS 2	9369
EkS 3	9370
FäL 1	9371
Fjä1-2	6019
Fjä1-5	6020
Fjä2-4	6021
Fjä2-6	6022
Fly2-1	6023
FlyA 3	9380
Fri 1	9381
Fri 2	9382
Fri 3	9383
Frö 1	9384
Frö 3	9385
Gårdby-17-198	1132
Gårdby-22-213	1137
Gro-3	6025
Grön 12	9386
Grön 14	9388
Grön-5	6030
Had 1	9390
Had 2	9391
Had 3	9392
Hag 2	9394
Hal 1	9395
Ham 1	9399
Ham-10-239	1366
Ham-13-241	1367

Table S2

AccessionName	AccessionID
Ham-2-2	1360
Ham-27-256	1374
Ham-6-232	1362
Ham-7-233	1363
Hel 3	9402
Hen-16-268	1585
HolA1 1	9404
HolA1 2	9405
HolA2 2	9407
Hov1-10	6035
Hov1-7	6034
Hov3-2	6036
Hov3-5	6038
Kal 2	9408
Kia 1	9409
Kor 1	9410
Kor 2	9411
Kor 3	9412
Kor 4	9413
Kru 3	9416
Kva 2	9418
Lag 1	9419
Lan 1	9421
Lis-3	6041
Löv-1	6043
Näs 2	9427
Nyl 13	9433
Nyl-7	6069
Omn-1	6070
Omn-5	6071
Ost-0	8351
Puk 1	9436
Puk 2	9437
Rev-2	6076
Rev-3	6077
Röd-17-319	1435
Sim 1	9442
Sku-30	1552
Sparta-1	6085
Spro 1	9450
Spro 2	9451
Spro 3	9452
Sr:3	6086
Stabby-13	1391
Stabby-26	1404
Ste 2	9453
Ste 3	9454
Ste 4	9455
Stu-2	6087
T1000	6090
T1010	6091
T1020	6092
T1030	6093
T1040	6094
T1050	6095
T1060	6096
T1070	6097
T1080	6098
T1090	6099
T1110	6100
T1120	6101
T1130	6102
T1150	6103
T1160	6104
T450	6105
T460	6106
T470	6107
T480	6108
T510	6109
T520	6110
T530	6111
T540	6112
T550	6113
T570	6114
T580	6115
T590	6116
T610	6118
T620	6119
T630	6120
T640	6121
T670	6122
T680	6123
T690	6124
T710	6125
T720	6126
T730	6127
T740	6128
T750	6129
T760	8225
T780	6131
T790	6132
T800	6133
T810	6134
T840	6136
T850	6137
T860	6138
T880	6140
T890	6141
T900	6142
T920	6144
T930	6145
T940	6146

Table S2

AccessionName	AccessionID
T950	6147
T960	6148
T970	6149
T980	6150
T990	6151
TÄL 07	6180
TÅD 01	6169
TÅD 02	6170
TÅD 03	6171
TÅD 04	6172
TÅD 05	6173
TÅD 06	6174
TAA 03	6153
TAA 04	6154
TAA 14	6163
TAA 17	6166
TBÖ 01	6184
TDr-1	6188
TDr-11	6197
TDr-13	6198
TDr-14	6199
TDr-15	6200
TDr-16	6201
TDr-17	6202
TDr-18	6203
TDr-2	6189
TDr-22	6207
TDr-3	6190
TDr-4	6191
TDr-5	6192
TDr-7	6193
TDr-8	6194
TDr-9	6195
TEDEN 02	6209
TEDEN 03	6210
TFÄ 04	6214
TFÄ 02	6212
TFÄ 05	6215
TFÄ 06	6216
TFÄ 07	6217
TFÄ 08	6218
TGR 01	6220
TGR 02	6221
THÖ 03	8227
THÖ 08	6226
TNY 04	6231
TOM 01	6235
TOM 02	6236
TOM 03	6237
TOM 04	6238
TOM 06	6240
TOM 07	6241
Tomegap-2	6242
Tos-31-374	1247
Tos-75-384	1252
Tos-82-387	1254
Tos-93-391	1256
Tos-95-393	1257
TRÄ 01	6244
Tur 3	9469
Tur 4	9470
TV-10	6258
TV-22	6268
TV-30	6276
TV-38	6284
TV-4	6252
TV-7	6255
UII2-13	8427
UII3-4	6413
UIIA 1	9471
UIIA 2	9472
UII2-5	6974
Vår2-6	7517
VårA 1	9476
Yst 1	9481
Yst 2	9482
Fly2-2	6024
Stu1-1	6088
Vår2-1	7516
Hovdala-2	6039
TGR 02	6221
Hovdala-6	8307
Bå1-2	8256
ÖMö2-1	7518
Brö1-6	8231
St-0	8387
Eden-2	6913
Ör-1	6074
Fjä1-1	8422
Algutstrum	8230
Gul1-2	8234
Tottarp-2	6243

Table S2

Table S2 – List of accessions used in GWA studies

Accession names and accession IDs for the Arabidopsis lines used in the GWA analysis of organ size (Chapter 6). All accessions are from Sweden and are a subset of the 1001 genomes project (Weigel and Mott, 2009). The accessions were kindly provided by Caroline Dean at the John Innes Centre, Norwich.

Residue	Colour	Property
AVFPMILW	RED	Small (small+ hydrophobic (incl.aromatic -Y))
DE	BLUE	Acidic
RK	MAGENTA	Basic - H
STYHCNGQ	GREEN	Hydroxyl + sulfhydryl + amine + G
Others	Grey	Unusual amino/imino acids etc

Table S3 – ClustalW colour codes

Explanation of colour codes used for ClustalW alignments from http://www.ebi.ac.uk/Tools/msa/clustalw2 (Goujon et al., 2010, Larkin et al., 2007).

Group name	Amino acids	Displayed as
Default	X	.
Single	X	-
Alanine	A	A
Cysteine	C	C
Aspartic Acid	D	D
Glutamic Acid	E	E
Phenylalanine	F	F
Glycine	G	G
Histidine	H	H
Isoleucine	I	I
Lysine	K	K
Leucine	L	L
Methionine	M	M
Asparagine	N	N
Proline	P	P
Glutamine	Q	Q
Arginine	R	R
Serine	S	S
Threonine	T	T
Valine	V	V
Tryptophan	W	W
Tyrosine	Y	Y
Negative	D,E	-
Ser/Thr	S,T	*
Aliphatic	I,L,V	l
Positive	H,K,R	+
Tiny	A,G,S	t
Aromatic	F,H,W,Y	a
Charged	D,E,H,K,R	c
Small	A,C,D,G,N,P,S,T,V	s
Polar	C,D,E,H,K,N,Q,R,S,T	p
Big	E,F,H,I,K,L,M,Q,R,W,Y	b
Hydrophobic	A,C,F,G,H,I,L,M,T,V,W,Y	h

Table S4 – Chroma colour codes

Explanation of CHROMA colour codes used for protein alignments (http://smart.embl-heidelberg.de/help/chroma.shtml).

QTL	Gene	Distance from Peak (Kb)	Gene Names
1	AT1G80370	-2078.508	CYCA2;4, CYCLIN A2;4
1	AT1G79840	-1902.423	GL2, GLABRA 2
1	AT1G79350	-1712.248	EMB1135, EMBRYO DEFECTIVE 1135
1	AT1G78770	-1482.408	ANAPHASE PROMOTING COMPLEX 6, APC6
1	AT1G77390	-946.319	CYCA1, CYCA1;2, CYCLIN A1,
1	AT1G76540	-584.649	CDKB2;1, CYCLIN-DEPENDENT KINASE B2;1
1	AT1G76310	-492.445	CYCB2;4, CYCLIN B2;4
1	AT1G75500	-202.238	WALLS ARE THIN 1, WAT1
1	AT1G75080	-49.682	BRASSINAZOLE-RESISTANT 1, BZR1
1	AT1G73965	320.643	CLAVATA3/ESR-RELATED 13, CLE13
1	AT1G73165	627.938	CLAVATA3/ESR-RELATED 1, CLE1
1	AT1G72980	680.317	LBD7, LOB DOMAIN-CONTAINING PROTEIN 7
1	AT1G72970	682.41	EDA17, EMBRYO SAC DEVELOPMENT ARREST 17
1	AT1G72300	917.475	PSY1 RECEPTOR, PSY1R
1	AT1G71440	1214.052	TFC E, TUBULIN-FOLDING COFACTOR E
1	AT1G71220	1290.001	EBS1, EMS-MUTAGENIZED BRI1 SUPPRESSOR 1,
1	AT1G71190	1302.556	SAG18, SENESCENCE ASSOCIATED GENE 18
1	AT1G70910	1402.378	DEP, DESPIERTO
1	AT1G70540	1542.475	EDA24, EMBRYO SAC DEVELOPMENT ARREST 24
1	AT1G70520	1550.701	ALTERED SEED GERMINATION 6, ASG6,
1	AT1G70490	1571.908	ARFA1D, ATARFA1D
1	AT1G70210	1695.429	ATCYCD1;1, CYCD1;1, CYCLIN D1;1
1	AT1G69588	1958.292	CLAVATA3/ESR-RELATED 45, CLE45
1	AT1G69270	2095.08	RECEPTOR-LIKE PROTEIN KINASE 1, RPK1
1	AT1G69230	2109.745	SP1L2, SPIRAL1-LIKE2
1	AT1G68840	2255.744	EDF2, ETHYLENE RESPONSE DNA BINDING FACTOR 2
1	AT1G68795	2295.522	CLAVATA3/ESR-RELATED 12, CLE12
1	AT1G68510	2429.207	LBD42, LOB DOMAIN-CONTAINING PROTEIN 42
1	AT1G68310	2536.298	AE7, AS1/2 ENHANCER7
1	AT1G67775	2725.271	CLAVATA3/ESR-RELATED 8, CLE8
1	AT1G67100	3082.485	LBD40, LOB DOMAIN-CONTAINING PROTEIN 40
2	AT2G25660	1506.475	EMB2410, EMBRYO DEFECTIVE 2410
2	AT2G26760	1025.893	CYCB1;4, CYCLIN B1;4
2	AT2G26830	982.905	EMB1187, EMBRYO DEFECTIVE 1187
2	AT2G27170	814.993	TITAN7, TTN7
2	AT2G27250	762.894	ATCLV3, CLAVATA3, CLV3
2	AT2G27960	517.067	CKS1, CYCLIN-DEPENDENT KINASE-SUBUNIT 1
2	AT2G27970	515.517	CDK-SUBUNIT 2, CKS2
2	AT2G28830	59.555	ATPUB12, PLANT U-BOX 12, PUB12
2	AT2G29680	-262.955	ATCDC6, CDC6, CELL DIVISION CONTROL 6
2	AT2G30110	-426.723	ATUBA1, UBIQUITIN-ACTIVATING ENZYME 1
2	AT2G30410	-531.778	KIESEL, KIS, TFCA, TUBULIN FOLDING FACTOR A
2	AT2G31060	-787.641	EMB2785, EMBRYO DEFECTIVE 2785

Table S5

2	AT2G31081	-810.052	CLAVATA3/ESR-RELATED 4, CLE4
2	AT2G31082	-813.299	CLAVATA3/ESR-RELATED 7, CLE7
2	AT2G31083	-824.221	ATCLE5, CLAVATA3/ESR-RELATED 5, CLE5
2	AT2G31085	-826.171	ATCLE6, CLAVATA3/ESR-RELATED 6, CLE6
3	AT4G17300	361.884	ATNS1, NS1, OVA8, OVULE ABORTION 8
3	AT4G17695	195.773	KAN3, KANADI 3
3	AT4G18510	-167.004	CLAVATA3/ESR-RELATED 2, CLE2
3	AT4G18710	-252.676	BIN2, BRASSINOSTEROID-INSENSITIVE 2,
3	AT4G19350	-517.749	EMB3006, EMBRYO DEFECTIVE 3006
3	AT4G19560	-617.931	CYCT1;2
3	AT4G19600	-629.609	CYCT1;4
3	AT4G16780	595.213	ARABIDOPSIS THALIANA HOMEOBOX PROTEIN 2, ATHB-2,
4	AT4G20740	198.938	EMB3131, EMBRYO DEFECTIVE 3131
4	AT4G21070	75.779	BREAST CANCER SUSCEPTIBILITY1, ATBRCA1,
4	AT4G21130	50.883	EMB2271, EMBRYO DEFECTIVE 2271
4	AT4G21190	33.08	EMB1417, EMBRYO DEFECTIVE 1417
5	AT4G21800	5.86	QQT2, QUATRE-QUART2
5	AT4G21710	40.931	EMB1989, EMBRYO DEFECTIVE 1989, NRPB2, RPB2
6	AT4G24560	894.356	UBIQUITIN-SPECIFIC PROTEASE 16, UBP16
6	AT4G24680	840.066	MODIFIER OF SNC1, MOS1
6	AT4G25640	498.684	ATDTX35, DETOXIFYING EFFLUX CARRIER 35,
6	AT4G26080	355.308	ABA INSENSITIVE 1, ABI1, ATABI1
6	AT4G26300	265.887	EMB1027, EMBRYO DEFECTIVE 1027
6	AT4G26330	254.496	ATSBT3.18, UNE17, UNFERTILIZED EMBRYO SAC 17
6	AT4G26420	224.748	GAMT1
6	AT4G27140	-31.25	AT2S1, SEED STORAGE ALBUMIN 1, SESA1
6	AT4G27150	-33.278	AT2S3, SEED STORAGE ALBUMIN 3, SESA2
6	AT4G27160	-35.749	AT2S3, SEED STORAGE ALBUMIN 3, SESA3
6	AT4G27170	-37.509	AT2S4, SEED STORAGE ALBUMIN 4, SESA4
6	AT4G28110	-392.276	ATMYB41, MYB DOMAIN PROTEIN 41, MYB41
6	AT4G28210	-414.917	EMB1923, EMBRYO DEFECTIVE 1923
6	AT4G28980	-713.139	CDKF;1, CYCLIN-DEPENDENT KINASE F;1
6	AT4G29060	-742.981	EMB2726, EMBRYO DEFECTIVE 2726

Table S5 – *De novo* candidate gene list for MAGIC analysis

Names and IDs of genes identified from the 8 MAGIC QTL for seed area. Genes were identified from the QTL gene list by mining the list for the keywords: *expansion*, *proliferation*, *cell-cycle*, *embryo*, and *endosperm*, as well as manual analysis of all the published gene descriptions. Distance from peak SNP values are given from the midpoint of the respective genes.

Abbreviations

3’	3 prime
5’	5 prime
ATP	adenoside triphosphate
BSA	bovine serum albumin
cDNA	complementary deoxyribonucleic acid
dATP	deoxyadenosine triphosphate
dCTP	deoxycytidine triphosphate
dGTP	deoxyguanosine triphosphate
DNA	deoxyribonucleic acid
dNTP	deoxyribonucleotide triphosphate
DO	drop out
dpi	dots per inch
DTT	dithiothreitol
dTTP	thymidine triphosphate
EDTA	ethylenediaminetetraacetic acid
EGTA	ethylene glycol-bis(2-aminoethylether)-N,N,N’,N’-tetraacetic acid
GST	glutatione S-transferase
HEPES	4-(2-hydroxyethyl)piperazine-1-ethanesulfonic acid
HIS	histidine
HRP	horseradish peroxidase
IPTG	isopropyl β-D-1-thiogalactopyranoside
LB	Luria broth
LiAc	lithium acetate
MES	2-(N-morpholino)ethanesulfonic acid
Ø	empty
PBS	phosphate buffered saline
PBST	phosphate buffered saline with tween-20
PCR	polymerase chain reaction
PEG	polyethylene glycol
PVDF	polyvinylidene fluoride
QTL	quantitative trait locus/loci
RIL	recombinant inbred line
RNA	ribonucleic acid
RNase	ribonuclease
SC	synthetic complete
SDS	sodium dodecyl sulphate
SNP	single nucleotide polymorphism
T-DNA	transfer deoxyribonucleic acid
TE	tris-EDTA
Tris	tris(hydroxymethyl)aminomethane
v/v	volume per volume
w/v	weight per volume
YPD	yeast peptone dextrose

References

ABRAHAM, M. C., METHEETRAIRUT, C. & IRISH, V. F. 2013. Natural Variation Identifies Multiple Loci Controlling Petal Shape and Size in Arabidopsis thaliana. *PloS one,* 8**,** 1932-6203.

ACHARD, P., GUSTI, A., CHEMINANT, S., ALIOUA, M., DHONDT, S., COPPENS, F., BEEMSTER, G. T. & GENSCHIK, P. 2009. Gibberellin Signaling Controls Cell Proliferation Rate in Arabidopsis. *Current biology,* 19**,** 1188-1193.

ADAMSKI, N. M., ANASTASIOU, E., ERIKSSON, S., O'NEILL, C. M. & LENHARD, M. 2009. Local maternal control of seed size by KLUH/CYP78A5-dependent growth signaling. *Proceedings of the National Academy of Sciences,* 106**,** 20115-20120.

AGGARWAL, P., GUPTA, M. D., JOSEPH, A. P., CHATTERJEE, N., SRINIVASAN, N. & NATH, U. 2010. Identification of specific DNA binding residues in the TCP family of transcription factors in Arabidopsis. *The Plant Cell Online,* 22**,** 1174-1189.

AGUILAR-MARTÍNEZ, J. A., POZA-CARRIÓN, C. & CUBAS, P. 2007. Arabidopsis BRANCHED1 acts as an integrator of branching signals within axillary buds. *The Plant Cell Online,* 19**,** 458-472.

AGULNICK, A. D., TAIRA, M., BREEN, J. J., TANAKA, T., DAWID, I. B. & WESTPHAL, H. 1996. Interactions of the LIM-domain-binding factor Ldbl with LIM homeodomain proteins. 384**,** 270-272.

AIDA, M., ISHIDA, T., FUKAKI, H., FUJISAWA, H. & TASAKA, M. 1997. Genes involved in organ separation in Arabidopsis: an analysis of the cup-shaped cotyledon mutant. *The Plant Cell Online,* 9**,** 841-857.

AL-HAKIM, A., ZAGORSKA, A., CHAPMAN, L., DEAK, M., PEGGIE, M. & ALESSI, D. 2008. Control of AMPK-related kinases by USP9X and atypical Lys29/Lys33-linked polyubiquitin chains. *Biochem. J,* 411**,** 249-260.

AL-HAKIM, A. K., ZAGORSKA, A., CHAPMAN, L., DEAK, M., PEGGIE, M. & ALESSI, D. R. 2010. Control of AMPK-related kinases by USP9X and atypical Lys29/Lys33-linked polyubiquitin chains. *Biochemical Journal,* 411**,** 249-260.

ALLEN, J. F. 2003. Cyclic, pseudocyclic and noncyclic photophosphorylation: new links in the chain. *Trends in plant science,* 8**,** 15-19.

ALONSO, J. M., HIRAYAMA, T., ROMAN, G., NOURIZADEH, S. & ECKER, J. R. 1999. EIN2, a bifunctional transducer of ethylene and stress responses in Arabidopsis. *Science,* 284**,** 2148-2152.

ALVAREZ, J. P., GOLDSHMIDT, A., EFRONI, I., BOWMAN, J. L. & ESHED, Y. 2009. The NGATHA distal organ development genes are essential for style specification in Arabidopsis. *The Plant Cell Online,* 21**,** 1373-1393.

ALVEY, L. & HARBERD, N. P. 2005. DELLA proteins: integrators of multiple plant growth regulatory inputs? *Physiologia Plantarum,* 123**,** 153-160.

ANASTASIOU, E., KENZ, S., GERSTUNG, M., MACLEAN, D., TIMMER, J., FLECK, C. & LENHARD, M. 2007. Control of plant organ size by KLUH/CYP78A5-dependent intercellular signaling. *Developmental Cell,* 13**,** 843-856.

ANDRIANKAJA, M., DHONDT, S., DE BODT, S., VANHAEREN, H., COPPENS, F., DE MILDE, L., MÜHLENBOCK, P., SKIRYCZ, A., GONZALEZ, N. & BEEMSTER, G. T. 2012. Exit from Proliferation during Leaf Development in Arabidopsis thaliana: A Not-So-Gradual Process. *Developmental cell,* 22**,** 64-78.

ATWELL, S., HUANG, Y. S., VILHJÁLMSSON, B. J., WILLEMS, G., HORTON, M., LI, Y., MENG, D., PLATT, A., TARONE, A. M. & HU, T. T. 2010. Genome-wide association study of 107 phenotypes in Arabidopsis thaliana inbred lines. *Nature,* 465**,** 627-631.

AUTRAN, D., JONAK, C., BELCRAM, K., BEEMSTER, G. T., KRONENBERGER, J., GRANDJEAN, O., INZÉ, D. & TRAAS, J. 2002. Cell numbers and leaf development in Arabidopsis: a functional analysis of the STRUWWELPETER gene. *The EMBO Journal,* 21**,** 6036-6049.

AZPIROZ, R., WU, Y., LOCASCIO, J. C. & FELDMANN, K. A. 1998. An Arabidopsis brassinosteroid-dependent mutant is blocked in cell elongation. *The Plant Cell Online,* 10**,** 219-230.

BAIMA, S., NOBILI, F., SESSA, G., LUCCHETTI, S., RUBERTI, I. & MORELLI, G. 1995. The expression of the Athb-8 homeobox gene is restricted to provascular cells in Arabidopsis thaliana. *Development,* 121**,** 4171-4182.

BAIMA, S., POSSENTI, M., MATTEUCCI, A., WISMAN, E., ALTAMURA, M. M., RUBERTI, I. & MORELLI, G. 2001. The Arabidopsis ATHB-8 HD-zip protein acts as a differentiation-promoting transcription factor of the vascular meristems. *Plant Physiology,* 126**,** 643-655.

BALSEMÃO-PIRES, E., ANDRADE, L. R. & SACHETTO-MARTINS, G. 2013. Functional study of TCP23 in Arabidopsis thaliana during plant development. *Plant Physiology and Biochemistry,* 67**,** 120-125.

BARTRINA, I., OTTO, E., STRNAD, M., WERNER, T. & SCHMÜLLING, T. 2011. Cytokinin regulates the activity of reproductive meristems, flower organ size, ovule formation, and thus seed yield in Arabidopsis thaliana. *The Plant Cell Online,* 23**,** 69-80.

BEEMSTER, G. T., FIORANI, F. & INZÉ, D. 2003. Cell cycle: the key to plant growth control? *Trends in plant science,* 8**,** 154-158.

BELKHADIR, Y. & CHORY, J. 2006. Brassinosteroid signaling: a paradigm for steroid hormone signaling from the cell surface. *Science,* 314**,** 1410-1411.

BELL, M. A. & TRAVIS, M. P. 2005. Hybridization, transgressive segregation, genetic covariation, and adaptive radiation. *Trends in ecology & evolution,* 20**,** 358-361.

BEMER, M. & GROSSNIKLAUS, U. 2012. Dynamic regulation of Polycomb group activity during plant development. *Current opinion in plant biology,* 15**,** 523-529.

BERGELSON, J. & ROUX, F. 2010. Towards identifying genes underlying ecologically relevant traits in Arabidopsis thaliana. *Nature Reviews Genetics,* 11**,** 867-879.

BERGER, F., HAMAMURA, Y., INGOUFF, M. & HIGASHIYAMA, T. 2008. Double fertilization-caught in the act. *Trends in plant science,* 13**,** 437-443.

BHARATHAN, G., GOLIBER, T. E., MOORE, C., KESSLER, S., PHAM, T. & SINHA, N. R. 2002. Homologies in leaf form inferred from KNOXI gene expression during development. *Science,* 296**,** 1858-1860.

BI, D., JOHNSON, K. C., ZHU, Z., HUANG, Y., CHEN, F., ZHANG, Y. & LI, X. 2011. Mutations in an atypical TIR-NB-LRR-LIM resistance protein confer autoimmunity. *Frontiers in plant science,* 2**,** 1-10.

BIEDERMANN, S. & HELLMANN, H. 2011. WD40 and CUL4-based E3 ligases: lubricating all aspects of life. *Trends in plant science,* 16**,** 38-46.

BIEGERT A, MAYER C, REMMERT M, SÖDING J & A, L. 2006. The MPI Toolkit for protein sequence analysis. *Nucleic Acids Res,* 34**,** 335-339.

BLECKMANN, A., WEIDTKAMP-PETERS, S., SEIDEL, C. A. & SIMON, R. 2010. Stem cell signaling in Arabidopsis requires CRN to localize CLV2 to the plasma membrane. *Plant physiology,* 152**,** 166-176.

BOCOCK, J. P., CARMICLE, S., SIRCAR, M. & ERICKSON, A. H. 2010. Trafficking and proteolytic processing of RNF13, a model PA-TM- RING family endosomal membrane ubiquitin ligase. *FEBS Journal,* 278**,** 69-77.

BÖGRE, L., MAGYAR, Z. & LÓPEZ-JUEZ, E. 2008. New clues to organ size control in plants. *Genome Biology,* 9**,** 226-232.

BOND, J. S. & BEYNON, R. J. 1995. The astacin family of metalloendopeptidases. *Protein Science,* 4**,** 1247-1261.

BOU-TORRENT, J., SALLA-MARTRET, M., BRANDT, R., MUSIELAK, T., PALAUQUI, J.-C., MARTÍNEZ-GARCÍA, J. F. & WENKEL, S. 2012. ATHB4 and HAT3, two class II HD-ZIP transcription factors, control leaf development in Arabidopsis. *Plant signaling & behavior,* 7**,** 1382-1387.

BOWMAN, J. L., SMYTH, D. R. & MEYEROWITZ, E. M. 1991. Genetic interactions among floral homeotic genes of Arabidopsis. *Development,* 112**,** 1-20.

BRACHI, B., FAURE, N., HORTON, M., FLAHAUW, E., VAZQUEZ, A., NORDBORG, M., BERGELSON, J., CUGUEN, J. & ROUX, F. 2010. Linkage and association mapping of Arabidopsis thaliana flowering time in nature. *PLoS Genetics,* 6**,** e1000940.

BREUNINGER, H. & LENHARD, M. 2010. Chapter Seven-Control of Tissue and Organ Growth in Plants. *Current topics in developmental biology,* 91**,** 185-220.

BROWN, M. S. & GOLDSTEIN, J. L. 1997. The SREBP Pathway: Regulation Review of Cholesterol Metabolism by Proteolysis of a Membrane-Bound Transcription Factor. *Cell,* 89**,** 331-340.

BUDHIRAJA, R., HERMKES, R., MÜLLER, S., SCHMIDT, J., COLBY, T., PANIGRAHI, K., COUPLAND, G. & BACHMAIR, A. 2009. Substrates related to chromatin and to RNA-dependent processes are modified by Arabidopsis SUMO isoforms that differ in a conserved residue with influence on desumoylation. *Plant physiology,* 149**,** 1529-1540.

BUDIHARDJO, I., OLIVER, H., LUTTER, M., LUO, X. & WANG, X. 1999. Biochemical pathways of caspase activation during apoptosis. *Annual review of cell and developmental biology,* 15**,** 269-290.

BURCHELL, L., CHAUGULE, V. K. & WALDEN, H. 2012. Small, N-Terminal Tags Activate Parkin E3 Ubiquitin Ligase Activity by Disrupting Its Autoinhibited Conformation. *PLoS ONE,* 7**,** e34748.

BURKE, R. & BASLER, K. 1996. Dpp receptors are autonomously required for cell proliferation in the entire developing Drosophila wing. *Development,* 122**,** 2261-2269.

CALDANA, C., FERNIE, A. R., WILLMITZER, L. & STEINHAUSER, D. 2012. Unraveling retrograde signaling pathways: finding candidate signaling molecules via metabolomics and systems biology driven approaches. *Frontiers in plant science,* 3**,** 267.

CALLIS, J., CARPENTER, T., SUN, C.-W. & VIERSTRA, R. D. 1995. Structure and evolution of genes encoding polyubiquitin and ubiquitin-like proteins in Arabidopsis thaliana ecotype Columbia. *Genetics,* 139**,** 921-939.

CAPDEVILA, J. & GUERRERO, I. 1994. Targeted expression of the signaling molecule decapentaplegic induces pattern duplications and growth alterations in Drosophila wings. *The EMBO journal,* 13**,** 4459-4468.

CAPRON, A., ÖKRÉSZ, L. & GENSCHIK, P. 2003. First glance at the plant APC/C, a highly conserved ubiquitin–protein ligase. *Trends in plant science,* 8**,** 83-89.

CARABELLI, M., SESSA, G., BAIMA, S., MORELLI, G. & RUBERTI, I. 1993. The Arabidopsis Athb‐2 and‐4 genes are strongly induced by far‐red‐rich light. *The Plant Journal,* 4**,** 469-479.

CARDONE, M. H., ROY, N., STENNICKE, H. R., SALVESEN, G. S., FRANKE, T. F., STANBRIDGE, E., FRISCH, S. & REED, J. C. 1998. Regulation of cell death protease caspase-9 by phosphorylation. *Science,* 282**,** 1318-1321.

CASAMITJANA-MARTINEZ, E., HOFHUIS, H. F., XU, J., LIU, C.-M., HEIDSTRA, R. & SCHERES, B. 2003. Root-Specific CLE19 Overexpression and the sol1/2 Suppressors Implicate a CLV-like Pathway in the Control of Arabidopsis Root Meristem Maintenance. *Current Biology,* 13**,** 1435-1441.

CASSMAN, K. G. 1999. Ecological intensification of cereal production systems: Yield potential, soil quality, and precision agriculture. *Proceedings of the National Academy of Sciences,* 96**,** 5952-5959.

CASTAÑO-MIQUEL, L., SEGUÍ, J., MANRIQUE, S., TEIXEIRA, I., CARRETERO-PAULET, L., ATENCIO, F. & LOIS, L. M. 2013. Diversification of SUMO activating enzyme in Arabidopsis: implications in SUMO conjugation. *Molecular plant,* 6**,** 1646-1660.

CENTURY, K., REUBER, T. L. & RATCLIFFE, O. J. 2008. Regulating the regulators: the future prospects for transcription-factor-based agricultural biotechnology products. *Plant Physiology,* 147**,** 20-29.

CHAKRAVORTY, D., TRUSOV, Y., ZHANG, W., ACHARYA, B. R., SHEAHAN, M. B., MCCURDY, D. W., ASSMANN, S. M. & BOTELLA, J. R. 2011. An atypical heterotrimeric G‐protein γ‐subunit is involved in guard cell K+‐channel regulation and morphological development in Arabidopsis thaliana. *The Plant Journal,* 67**,** 840-851.

CHALFUN-JUNIOR, A., FRANKEN, J., MES, J. J., MARSCH-MARTINEZ, N., PEREIRA, A. & ANGENENT, G. C. 2005. ASYMMETRIC LEAVES2-LIKE1gene, a member of the AS2/LOB family, controls proximal–distal patterning in Arabidopsis petals. *Plant molecular biology,* 57**,** 559-575.

CHANG, D. F., BELAGULI, N. S., IYER, D., ROBERTS, W. B., WU, S.-P., DONG, X.-R., MARX, J. G., MOORE, M. S., BECKERLE, M. C. & MAJESKY, M. W. 2003. Cysteine-rich LIM-only proteins CRP1 and CRP2 are potent smooth muscle differentiation cofactors. *Developmental cell,* 4**,** 107-118.

CHANVIVATTANA, Y., BISHOPP, A., SCHUBERT, D., STOCK, C., MOON, Y.-H., SUNG, Z. R. & GOODRICH, J. 2004. Interaction of Polycomb-group proteins controlling flowering in Arabidopsis. *Development,* 131**,** 5263-5276.

CHEN, J.-G., ULLAH, H., YOUNG, J. C., SUSSMAN, M. R. & JONES, A. M. 2001. ABP1 is required for organized cell elongation and division in Arabidopsis embryogenesis. *Genes & Development,* 15**,** 902-911.

CHENG, R., ABNEY, M., PALMER, A. A. & SKOL, A. D. 2011. QTLRel: an R package for genome-wide association studies in which relatedness is a concern. *BMC genetics,* 12**,** 66.

CHENG, R. & PALMER, A. A. 2013. A Simulation Study of Permutation, Bootstrap, and Gene Dropping for Assessing Statistical Significance in the Case of Unequal Relatedness. *Genetics,* 193**,** 1015-1018.

CHENG, Y., CAO, L., WANG, S., LI, Y., SHI, X., LIU, H., LI, L., ZHANG, Z., FOWKE, L. C. & WANG, H. 2013a. Downregulation of multiple CDK inhibitor ICK/KRP genes upregulates the E2F pathway and increases cell proliferation, and organ and seed sizes in Arabidopsis. *The Plant Journal,* 75**,** 642-655.

CHENG, Y.-C., LIN, T.-Y. & SHIEH, S.-Y. 2013b. Candidate tumor suppressor BTG3 maintains genomic stability by promoting Lys63-linked ubiquitination and activation of the checkpoint kinase CHK1. *Proceedings of the National Academy of Sciences,* 110**,** 5993-5998.

CHEW, K. C. M., MATSUDA, N., SAISHO, K., LIM, G. G. Y., CHAI, C., TAN, H. M., TANAKA, K. & LIM, K. L. 2012. Parkin Mediates Apparent E2-Independent Monoubiquitination In Vitro and Contains an Intrinsic Activity That Catalyzes Polyubiquitination. *PLoS ONE,* 6**,** e19720.

CHINCHILLA, D., BAUER, Z., REGENASS, M., BOLLER, T. & FELIX, G. 2006. The Arabidopsis receptor kinase FLS2 binds flg22 and determines the specificity of flagellin perception. *The Plant Cell Online,* 18**,** 465-476.

CHINCHILLA, D., ZIPFEL, C., ROBATZEK, S., KEMMERLING, B., NÜRNBERGER, T., JONES, J. D., FELIX, G. & BOLLER, T. 2007a. A flagellin-induced complex of the receptor FLS2 and BAK1 initiates plant defence. *Nature,* 448**,** 497-500.

CHINCHILLA, D., ZIPFEL, C., ROBATZEK, S., KEMMERLING, B., NÜRNBERGER, T., JONES, J. D. G., FELIX, G. & BOLLER, T. 2007b. A flagellin-induced complex of the receptor FLS2 and BAK1 initiates plant defence. *Nature,* 448**,** 497-500.

CHO, H.-T. & COSGROVE, D. J. 2000. Altered expression of expansin modulates leaf growth and pedicel abscission in Arabidopsis thaliana. *Proceedings of the National Academy of Sciences,* 97**,** 9783-9788.

CHOE, S., FUJIOKA, S., NOGUCHI, T., TAKATSUTO, S., YOSHIDA, S. & FELDMANN, K. A. 2001. Overexpression of DWARF4 in the brassinosteroid biosynthetic pathway results in increased vegetative growth and seed yield in Arabidopsis. *The Plant Journal,* 26**,** 573-582.

CHURCHMAN, M. L., BROWN, M. L., KATO, N., KIRIK, V., HÜLSKAMP, M., INZÉ, D., DE VEYLDER, L., WALKER, J. D., ZHENG, Z. & OPPENHEIMER, D. G. 2006. SIAMESE, a plant-specific cell cycle regulator, controls endoreplication onset in Arabidopsis thaliana. *The Plant Cell Online,* 18**,** 3145-3157.

CLARK, S. E., WILLIAMS, R. W. & MEYEROWITZ, E. M. 1997. The CLAVATA1 gene encodes a putative receptor kinase that controls shoot and floral meristem size in Arabidopsis. *Cell,* 89**,** 575-585.

CLOUGH, M. V., HAMLINGTON, J. D. & MCINTOSH, I. 1999. Restricted distribution of loss‐of‐function mutations within the LMX1B genes of nail‐patella syndrome patients. *Human mutation,* 14**,** 459-465.

CLOUSE, S. D., LANGFORD, M. & MCMORRIS, T. C. 1996. A brassinosteroid-insensitive mutant in Arabidopsis thaliana exhibits multiple defects in growth and development. *Plant Physiology,* 111**,** 671-678.

COLL-GARCIA, D., MAZUCH, J., ALTMANN, T. & MÜSSIG, C. 2004. EXORDIUM regulates brassinosteroid-responsive genes. *FEBS letters,* 563**,** 82-86.

CUBAS, P., LAUTER, N., DOEBLEY, J. & COEN, E. 1999. The TCP domain: a motif found in proteins regulating plant growth and development. *The Plant Journal,* 18**,** 215-222.

CURTIS, M. D. & GROSSNIKLAUS, U. 2003. A gateway cloning vector set for high-throughput functional analysis of genes in planta. *Plant Physiology,* 133**,** 462-469.

DAI, N., WANG, W., PATTERSON, S. E. & BLEECKER, A. B. 2013. The TMK Subfamily of Receptor-Like Kinases in Arabidopsis Display an Essential Role in Growth and a Reduced Sensitivity to Auxin. *PloS one,* 8**,** e60990.

DAVIÈRE, J.-M. & ACHARD, P. 2013. Gibberellin signaling in plants. *Development,* 140**,** 1147-1151.

DE CASTRO E, SIGRIST CJA, GATTIKER A, BULLIARD V, LANGENDIJK-GENEVAUX PS, GASTEIGER E, BAIROCH A & N, H. 2006. ScanProsite: detection of PROSITE signature matches and ProRule-associated functional and structural residues in proteins. *Nucleic Acids Res,* 34**,** W362-W365.

DE LUCIA, F., CREVILLEN, P., JONES, A. M., GREB, T. & DEAN, C. 2008. A PHD-polycomb repressive complex 2 triggers the epigenetic silencing of FLC during vernalization. *Proceedings of the National Academy of Sciences,* 105**,** 16831-16836.

DE VEYLDER, L., BEECKMAN, T., BEEMSTER, G. T., KROLS, L., TERRAS, F., LANDRIEU, I., VAN DER SCHUEREN, E., MAES, S., NAUDTS, M. & INZÉ, D. 2001. Functional analysis of cyclin-dependent kinase inhibitors of Arabidopsis. *The Plant Cell Online,* 13**,** 1653-1668.

DELESSERT, C., KAZAN, K., WILSON, I. W., STRAETEN, D. V. D., MANNERS, J., DENNIS, E. S. & DOLFERUS, R. 2005. The transcription factor ATAF2 represses the expression of pathogenesis‐related genes in Arabidopsis. *The Plant Journal,* 43**,** 745-757.

DEPROST, D., YAO, L., SORMANI, R., MOREAU, M., LETERREUX, G., NICOLAÏ, M., BEDU, M., ROBAGLIA, C. & MEYER, C. 2007. The Arabidopsis TOR kinase links plant growth, yield, stress resistance and mRNA translation. *EMBO reports,* 8**,** 864-870.

DEVAULT, A., SALES, V., NAULT, C., BEAUMONT, A., ROQUES, B., CRINE, P. & BOILEAU, G. 1988. Exploration of the catalytic site of endopeptidase 24.11 by site-directed mutagenesis Histidine residues 583 and 587 are essential for catalysis. *FEBS letters,* 231**,** 54-58.

DEWITTE, W. & MURRAY, J. A. 2003. The plant cell cycle. *Annual Review of Plant Biology,* 54**,** 235-264.

DEWITTE, W., SCOFIELD, S., ALCASABAS, A. A., MAUGHAN, S. C., MENGES, M., BRAUN, N., COLLINS, C., NIEUWLAND, J., PRINSEN, E. & SUNDARESAN, V. 2007. Arabidopsis CYCD3 D-type cyclins link cell proliferation and endocycles and are rate-limiting for cytokinin responses. *Proceedings of the National Academy of Sciences,* 104**,** 14537.

DHARMASIRI, N., DHARMASIRI, S., WEIJERS, D., KARUNARATHNA, N., JURGENS, G. & ESTELLE, M. 2007. AXL and AXR1 have redundant functions in RUB conjugation and growth and development in Arabidopsis. *The Plant Journal,* 52**,** 114-123.

DIÉVART, A. & CLARK, S. E. 2003. Using mutant alleles to determine the structure and function of leucine-rich repeat receptor-like kinases. *Current opinion in plant biology,* 6**,** 507-516.

DILL, A., THOMAS, S. G., HU, J., STEBER, C. M. & SUN, T.-P. 2004. The Arabidopsis F-box protein SLEEPY1 targets gibberellin signaling repressors for gibberellin-induced degradation. *The Plant Cell Online,* 16**,** 1392-1405.

DINNENY, J. R., WEIGEL, D. & YANOFSKY, M. F. 2006. NUBBIN and JAGGED define stamen and carpel shape in Arabidopsis. *Development,* 133**,** 1645-1655.

DINNENY, J. R., YADEGARI, R., FISCHER, R. L., YANOFSKY, M. F. & WEIGEL, D. 2004. The role of JAGGED in shaping lateral organs. *Development,* 131**,** 1101-1110.

DISCH, S., ANASTASIOU, E., SHARMA, V. K., LAUX, T., FLETCHER, J. C. & LENHARD, M. 2006. The E3 ubiquitin ligase BIG BROTHER controls Arabidopsis organ size in a dosage-dependent manner. *Current Biology,* 16**,** 272-279.

DITTMAR, G. A., WILKINSON, C. R., JEDRZEJEWSKI, P. T. & FINLEY, D. 2002. Role of a ubiquitin-like modification in polarized morphogenesis. *Science,* 295**,** 2442-2446.

DITTRICH-REED, D. R. & FITZPATRICK, B. M. 2012. Transgressive Hybrids as Hopeful Monsters. *Evolutionary Biology,* 40**,** 310-315.

DIXIT, R. 2013. Plant Cytoskeleton: DELLA Connects Gibberellins to Microtubules. *Current Biology,* 23**,** 479-481.

DONG, J., FELDMANN, G., HUANG, J., WU, S., ZHANG, N., COMERFORD, S. A., GAYYED, M. F., ANDERS, R. A., MAITRA, A. & PAN, D. 2007. Elucidation of a Universal Size-Control Mechanism in Drosophila and Mammals. *Cell,* 130**,** 1120-1133.

DONNELLY, P. M., BONETTA, D., TSUKAYA, H., DENGLER, R. E. & DENGLER, N. G. 1999. Cell cycling and cell enlargement in developing leaves of Arabidopsis. *Developmental Biology,* 215**,** 407-419.

DOWNES, B. & VIERSTRA, R. 2005. Post-translational regulation in plants employing a diverse set of polypeptide tags. *Biochemical Society Transactions,* 33**,** 393-400.

DOWNES, B. P., STUPAR, R. M., GINGERICH, D. J. & VIERSTRA, R. D. 2003. The HECT ubiquitin‐protein ligase (UPL) family in Arabidopsis: UPL3 has a specific role in trichome development. *The Plant Journal,* 35**,** 729-742.

DREZE, M., CARVUNIS, A.-R., CHARLOTEAUX, B., GALLI, M., PEVZNER, S. J., TASAN, M., AHN, Y.-Y., BALUMURI, P., BARABÁSI, A.-L. & BAUTISTA, V. 2011. Evidence for network evolution in an Arabidopsis interactome map. *Science,* 333**,** 601-607.

DUBOIS, M., SKIRYCZ, A., CLAEYS, H., MALEUX, K., DHONDT, S., DE BODT, S., BOSSCHE, R. V., DE MILDE, L., YOSHIZUMI, T. & MATSUI, M. 2013. ETHYLENE RESPONSE FACTOR6 Acts as a Central Regulator of Leaf Growth under Water-Limiting Conditions in Arabidopsis. *Plant physiology,* 162**,** 319-332.

DUDA, D. M., BORG, L. A., SCOTT, D. C., HUNT, H. W., HAMMEL, M. & SCHULMAN, B. A. 2008. Structural insights into NEDD8 activation of cullin-RING ligases: conformational control of conjugation. *Cell,* 134**,** 995-1006.

DUNN, R. & HICKE, L. 2001. Multiple Roles for Rsp 5 p-dependent Ubiquitination at the Internalization Step of Endocytosis. *Journal of Biological Chemistry,* 276**,** 25974-25981.

EBERLE, D., HEGARTY, B., BOSSARD, P., FERRÉ, P. & FOUFELLE, F. 2004. SREBP transcription factors: master regulators of lipid homeostasis. *Biochimie,* 86**,** 839-848.

ECKER, J. R. 1995. The ethylene signal transduction pathway in plants. *Science,* 268**,** 667-675.

EDGAR, B. A. & DATAR, S. A. 1996. Zygotic degradation of two maternal Cdc25 mRNAs terminates Drosophila's early cell cycle program. *Genes & Development,* 10**,** 1966-1977.

EDGAR, B. A., KIEHLE, C. P. & SCHUBIGER, G. 1986. Cell cycle control by the nucleo-cytoplasmic ratio in early Drosophila development. *Cell,* 44**,** 365-372.

EDGAR, B. A., SPRENGER, F., DURONIO, R. J., LEOPOLD, P. & O'FARRELL, P. H. 1994. Distinct molecular mechanism regulate cell cycle timing at successive stages of Drosophila embryogenesis. *Genes & Development,* 8**,** 440-452.

EFRONI, I., ESHED, Y. & LIFSCHITZ, E. 2010. Morphogenesis of simple and compound leaves: a critical review. *The Plant Cell Online,* 22**,** 1019-1032.

ELLEDGE, S. J. 1996. Cell cycle checkpoints: preventing an identity crisis. *Science,* 274**,** 1664-1672.

ELOY, N. B., DE FREITAS LIMA, M., VAN DAMME, D., VANHAEREN, H., GONZALEZ, N., DE MILDE, L., HEMERLY, A. S., BEEMSTER, G. T., INZÉ, D. & FERREIRA, P. C. 2011. The APC/C subunit 10 plays an essential role in cell proliferation during leaf development. *The Plant Journal,* 68**,** 351-363.

EMANUELE, M. J., ELIA, A. E., XU, Q., THOMA, C. R., IZHAR, L., LENG, Y., GUO, A., CHEN, Y.-N., RUSH, J. & HSU, P. W.-C. 2011. Global identification of modular cullin-RING ligase substrates. *Cell,* 147**,** 459-474.

EMERY, J. F., FLOYD, S. K., ALVAREZ, J., ESHED, Y., HAWKER, N. P., IZHAKI, A., BAUM, S. F. & BOWMAN, J. L. 2003. Radial Patterning of Arabidopsis Shoots by Class III HD-ZIP and KANADI Genes. *Current Biology,* 13**,** 1768-1774.

ERIKSSON, S., STRANSFELD, L., ADAMSKI, N. M., BREUNINGER, H. & LENHARD, M. 2010. KLUH/CYP78A5-Dependent Growth Signaling Coordinates Floral Organ Growth in Arabidopsis. *Current Biology,* 20**,** 527-532.

ESHED, Y., BAUM, S. F., PEREA, J. V. & BOWMAN, J. L. 2001. Establishment of polarity in lateral organs of plants. *Current Biology,* 11**,** 1251-1260.

ESHED, Y., IZHAKI, A., BAUM, S. F., FLOYD, S. K. & BOWMAN, J. L. 2004. Asymmetric leaf development and blade expansion in Arabidopsis are mediated by KANADI and YABBY activities. *Development,* 131**,** 2997-3006.

EYÜBOGLU, B., PFISTER, K., HABERER, G., CHEVALIER, D., FUCHS, A., MAYER, K. & SCHNEITZ, K. 2007. Molecular characterisation of the STRUBBELIG-RECEPTOR FAMILY of genes encoding putative leucine-rich repeat receptor-like kinases in Arabidopsis thaliana. *BMC plant biology,* 7**,** 16.

FANG, S., JENSEN, J. P., LUDWIG, R. L., VOUSDEN, K. H. & WEISSMAN, A. M. 2000. Mdm2 is a RING finger-dependent ubiquitin protein ligase for itself and p53. *Journal of Biological Chemistry,* 275**,** 8945-8951.

FANG, W., WANG, Z., CUI, R., LI, J. & LI, Y. 2012. Maternal control of seed size by EOD3/CYP78A6 in Arabidopsis thaliana. *The Plant Journal,* 70**,** 929-939.

FELKER, F. C., PETERSON, D. M. & NELSON, O. E. 1985. Anatomy of immature grains of eight maternal effect shrunken endosperm barley mutants. *American Journal of Botany,* 72**,** 248-256.

FENG, G., QIN, Z., YAN, J., ZHANG, X. & HU, Y. 2011. Arabidopsis ORGAN SIZE RELATED1 regulates organ growth and final organ size in orchestration with ARGOS and ARL. *New Phytologist,* 191**,** 635-646.

FERJANI, A., HORIGUCHI, G., YANO, S. & TSUKAYA, H. 2007. Analysis of leaf development in fugu mutants of Arabidopsis reveals three compensation modes that modulate cell expansion in determinate organs. *Plant physiology,* 144**,** 988-999.

FIELDS, S. & SONG, O.-K. 1989. A novel genetic system to detect protein protein interactions.

FILIAULT, D. L. & MALOOF, J. N. 2012. A genome-wide association study identifies variants underlying the Arabidopsis thaliana shade avoidance response. *PLoS genetics,* 8**,** e1002589.

FISHER, R. D., WANG, B., ALAM, S. L., HIGGINSON, D. S., ROBINSON, H., SUNDQUIST, W. I. & HILL, C. P. 2003. Structure and ubiquitin binding of the ubiquitin-interacting motif. *Journal of Biological Chemistry,* 278**,** 28976-28984.

FIUME, E. & FLETCHER, J. C. 2012. Regulation of Arabidopsis embryo and endosperm development by the polypeptide signaling molecule CLE8. *The Plant Cell Online,* 24**,** 1000-1012.

FLEMING, A. J., CADERAS, D., WEHRLI, E., MCQUEEN-MASON, S. & KUHLEMEIER, C. 1999. Analysis of expansin-induced morphogenesis on the apical meristem of tomato. *Planta,* 208**,** 166-174.

FLEMING, A. J., MCQUEEN-MASON, S., MANDEL, T. & KUHLEMEIER, C. 1997. Induction of leaf primordia by the cell wall protein expansin. *Science,* 276**,** 1415-1418.

FLEMMING, A. J., SHEN, Z.-Z., CUNHA, A., EMMONS, S. W. & LEROI, A. M. 2000. Somatic polyploidization and cellular proliferation drive body size evolution in nematodes. *Proceedings of the National Academy of Sciences,* 97**,** 5285-5290.

FLICK, K., RAASI, S., ZHANG, H., YEN, J. L. & KAISER, P. 2006. A ubiquitin-interacting motif protects polyubiquitinated Met4 from degradation by the 26S proteasome. *Nature cell biology,* 8**,** 509-515.

FOOTITT, S., CORNAH, J. E., PRACHAROENWATTANA, I., BRYCE, J. H. & SMITH, S. M. 2007. The Arabidopsis 3-ketoacyl-CoA thiolase-2 (kat2-1) mutant exhibits increased flowering but reduced reproductive success. *Journal of experimental botany,* 58**,** 2959-2968.

FOX, J. W. & SERRANO, S. M. 2005. Structural considerations of the snake venom metalloproteinases, key members of the M12 reprolysin family of metalloproteinases. *Toxicon,* 45**,** 969-985.

FU, Y., XU, L., XU, B., YANG, L., LING, Q., WANG, H. & HUANG, H. 2007. Genetic interactions between leaf polarity-controlling genes and ASYMMETRIC LEAVES1 and 2 in Arabidopsis leaf patterning. *Plant and cell physiology,* 48**,** 724-735.

FÜLÖP, K., TARAYRE, S., KELEMEN, Z., HORVÁTH, G., KEVEI, Z., NIKOVICS, K., BAKÓ, L., BROWN, S., KONDOROSI, A. & KONDOROSI, E. 2005. Arabidopsis anaphase-promoting complexes: multiple activators and wide range of substrates might keep APC perpetually busy. *Cell cycle,* 4**,** 4084-4092.

FUTREAL, P. A., LIU, Q., SHATTUCK-EIDENS, D., COCHRAN, C., HARSHMAN, K., TAVTIGIAN, S., BENNETT, L. M., HAUGEN-STRANO, A., SWENSEN, J. & MIKI, Y. 1994. BRCA1 mutations in primary breast and ovarian carcinomas. *Science,* 266**,** 120-122.

GAGNE, J. M., SMALLE, J., GINGERICH, D. J., WALKER, J. M., YOO, S.-D., YANAGISAWA, S. & VIERSTRA, R. D. 2004. Arabidopsis EIN3-binding F-box 1 and 2 form ubiquitin-protein ligases that repress ethylene action and promote growth by directing EIN3 degradation. *Proceedings of the National Academy of Sciences of the United States of America,* 101**,** 6803-6808.

GALVEZ‐VALDIVIESO, G. & MULLINEAUX, P. M. 2010. The role of reactive oxygen species in signalling from chloroplasts to the nucleus. *Physiologia Plantarum,* 138**,** 430-439.

GAN, X., STEGLE, O., BEHR, J., STEFFEN, J. G., DREWE, P., HILDEBRAND, K. L., LYNGSOE, R., SCHULTHEISS, S. J., OSBORNE, E. J. & SREEDHARAN, V. T. 2011. Multiple reference genomes and transcriptomes for Arabidopsis thaliana. *Nature,* 477**,** 419-423.

GARCIA, D., GERALD, F., JONATHAN, N. & BERGER, F. 2005. Maternal control of integument cell elongation and zygotic control of endosperm growth are coordinated to determine seed size in Arabidopsis. *The Plant Cell Online,* 17**,** 52-60.

GARCIA, D., SAINGERY, V., CHAMBRIER, P., MAYER, U., JÜRGENS, G. & BERGER, F. 2003. Arabidopsis haiku mutants reveal new controls of seed size by endosperm. *Plant physiology,* 131**,** 1661-1670.

GELDNER, N., HYMAN, D. L., WANG, X., SCHUMACHER, K. & CHORY, J. 2007. Endosomal signaling of plant steroid receptor kinase BRI1. *Genes & Development,* 21**,** 1598-1602.

GENDALL, A. R., LEVY, Y. Y., WILSON, A. & DEAN, C. 2001. The VERNALIZATION 2 Gene Mediates the Epigenetic Regulation of Vernalization in Arabidopsis. *Cell,* 107**,** 525-535.

GIEFFERS, C., DUBE, P., HARRIS, J. R., STARK, H. & PETERS, J.-M. 2001. Three-dimensional structure of the anaphase-promoting complex. *Molecular cell,* 7**,** 907-913.

GLICKMAN, M. H. & CIECHANOVER, A. 2002. The ubiquitin-proteasome proteolytic pathway: destruction for the sake of construction. *Physiological reviews,* 82**,** 373-428.

GODGE, M. R., KUMAR, D. & KUMAR, P. P. 2008. Arabidopsis HOG1 gene and its petunia homolog PETCBP act as key regulators of yield parameters. *Plant cell reports,* 27**,** 1497-1507.

GÖHRE, V., SPALLEK, T., HÄWEKER, H., MERSMANN, S., MENTZEL, T., BOLLER, T., DE TORRES, M., MANSFIELD, J. W. & ROBATZEK, S. 2008. Plant pattern-recognition receptor FLS2 is directed for degradation by the bacterial ubiquitin ligase AvrPtoB. *Current Biology,* 18**,** 1824-1832.

GÓMEZ-GÓMEZ, L. & BOLLER, T. 2000. FLS2: an LRR receptor-like kinase involved in the perception of the bacterial elicitor flagellin in Arabidopsis. *Molecular cell,* 5**,** 1003-1011.

GÓMEZ‐GÓMEZ, L., FELIX, G. & BOLLER, T. 1999. A single locus determines sensitivity to bacterial flagellin in Arabidopsis thaliana. *The Plant Journal,* 18**,** 277-284.

GONZALEZ, N., DE BODT, S., SULPICE, R., JIKUMARU, Y., CHAE, E., DHONDT, S., VAN DAELE, T., DE MILDE, L., WEIGEL, D. & KAMIYA, Y. 2010. Increased leaf size: different means to an end. *Plant Physiology,* 153**,** 1261-1279.

GORITSCHNIG, S., ZHANG, Y. & LI, X. 2007. The ubiquitin pathway is required for innate immunity in Arabidopsis. *The Plant Journal,* 49**,** 540-551.

GOTTLIEB, T. M. & OREN, M. p53 and apoptosis. Seminars in cancer biology, 1998. Elsevier, 359-368.

GOUJON, M., MCWILLIAM, H., LI, W., VALENTIN, F., SQUIZZATO, S., PAERN, J. & LOPEZ, R. 2010. A new bioinformatics analysis tools framework at EMBL–EBI. *Nucleic acids research,* 38**,** W695-W699.

GOWEN, L. C., AVRUTSKAYA, A. V., LATOUR, A. M., KOLLER, B. H. & LEADON, S. A. 1998. BRCA1 required for transcription-coupled repair of oxidative DNA damage. *Science,* 281**,** 1009-1012.

GREB, T., MYLNE, J. S., CREVILLEN, P., GERALDO, N., AN, H., GENDALL, A. R. & DEAN, C. 2007. The PHD Finger Protein VRN5 Functions in the Epigenetic Silencing of Arabidopsis FLC. *Current biology,* 17**,** 73-78.

GROSSNIKLAUS, U., SPILLANE, C., PAGE, D. R. & KÖHLER, C. 2001. Genomic imprinting and seed development: endosperm formation with and without sex. *Current opinion in plant biology,* 4**,** 21-27.

GROSSNIKLAUS, U., VIELLE-CALZADA, J.-P., HOEPPNER, M. A. & GAGLIANO, W. B. 1998. Maternal control of embryogenesis by MEDEA, a polycomb group gene in Arabidopsis. *Science,* 280**,** 446-450.

GUO, M., THOMAS, J., COLLINS, G. & TIMMERMANS, M. C. 2008. Direct repression of KNOX loci by the ASYMMETRIC LEAVES1 complex of Arabidopsis. *The Plant Cell Online,* 20**,** 48-58.

GUO, X., LU, W., MA, Y., QIN, Q. & HOU, S. 2013. The BIG gene is required for auxin-mediated organ growth in Arabidopsis. *Planta***,** 1-13.

GUZZO, C. M., BERNDSEN, C. E., ZHU, J., GUPTA, V., DATTA, A., GREENBERG, R. A., WOLBERGER, C. & MATUNIS, M. J. 2012. RNF4-dependent hybrid SUMO-ubiquitin chains are signals for RAP80 and thereby mediate the recruitment of BRCA1 to sites of DNA damage. *Science signaling,* 5**,** ra88.

HA, C. M., JUN, J. H., NAM, H. G. & FLETCHER, J. C. 2004. BLADE-ON-PETIOLE1 encodes a BTB/POZ domain protein required for leaf morphogenesis in Arabidopsis thaliana. *Plant and cell physiology,* 45**,** 1361-1370.

HAAS, A., BRIGHT, P. & JACKSON, V. 1988. Functional diversity among putative E2 isozymes in the mechanism of ubiquitin-histone ligation. *Journal of Biological Chemistry,* 263**,** 13268-13275.

HAGLUND, K., SIGISMUND, S., POLO, S., SZYMKIEWICZ, I., DI FIORE, P. P. & DIKIC, I. 2003. Multiple monoubiquitination of RTKs is sufficient for their endocytosis and degradation. *Nature cell biology,* 5**,** 461-466.

HAGLUND, K. & STENMARK, H. 2006. Working out coupled monoubiquitination. *Nature cell biology,* 8**,** 1218-1219.

HAMLINGTON, J. D., JONES, C. & MCINTOSH, I. 2001. Twenty‐two novel LMX1B mutations identified in nail patella syndrome (NPS) patients. *Human mutation,* 18**,** 458-458.

HANKE, G. T., KIMATA-ARIGA, Y., TANIGUCHI, I. & HASE, T. 2004. A post genomic characterization of Arabidopsis ferredoxins. *Plant physiology,* 134**,** 255-264.

HAREVEN, D., GUTFINGER, T., PARNIS, A., ESHED, Y. & LIFSCHITZ, E. 1996. The making of a compound leaf: genetic manipulation of leaf architecture in tomato. *Cell,* 84**,** 735-744.

HARPER, J. W. & SCHULMAN, B. A. 2006. Structural complexity in ubiquitin recognition. *Cell,* 124**,** 1133-1136.

HARTWELL, L. H. & KASTAN, M. B. 1994. Cell cycle control and cancer. *Science,* 266**,** 1821-1828.

HASE, Y., TANAKA, A., BABA, T. & WATANABE, H. 2000. FRL1 is required for petal and sepal development in Arabidopsis. *The Plant Journal,* 24**,** 21-32.

HATFIELD, P. M., GOSINK, M. M., CARPENTER, T. B. & VIERSTRA, R. D. 1997. The ubiquitin‐activating enzyme (E1) gene family in Arabidopsis thaliana. *The Plant Journal,* 11**,** 213-226.

HAUVERMALE, A. L., ARIIZUMI, T. & STEBER, C. M. 2012. Gibberellin signaling: a theme and variations on DELLA repression. *Plant physiology,* 160**,** 83-92.

HAY, A., BARKOULAS, M. & TSIANTIS, M. 2006. ASYMMETRIC LEAVES1 and auxin activities converge to repress BREVIPEDICELLUS expression and promote leaf development in Arabidopsis. *Development,* 133**,** 3955-3961.

HE, J.-X., GENDRON, J. M., SUN, Y., GAMPALA, S. S., GENDRON, N., SUN, C. Q. & WANG, Z.-Y. 2005. BZR1 is a transcriptional repressor with dual roles in brassinosteroid homeostasis and growth responses. *Science Signaling,* 307**,** 1634.

HE, J.-X., GENDRON, J. M., YANG, Y., LI, J. & WANG, Z.-Y. 2002. The GSK3-like kinase BIN2 phosphorylates and destabilizes BZR1, a positive regulator of the brassinosteroid signaling pathway in Arabidopsis. *Proceedings of the National Academy of Sciences,* 99**,** 10185-10190.

HEERY, D. M., KALKHOVEN, E., HOARE, S. & PARKER, M. G. 1997. A signature motif in transcriptional co-activators mediates binding to nuclear receptors. *Nature,* 387**,** 733-736.

HÉMATY, K., SADO, P.-E., VAN TUINEN, A., ROCHANGE, S., DESNOS, T., BALZERGUE, S., PELLETIER, S., RENOU, J.-P. & HÖFTE, H. 2007. A Receptor-like Kinase Mediates the

Response of Arabidopsis Cells to the Inhibition of Cellulose Synthesis. *Current Biology,* 17**,** 922-931.

HERRADOR, A., LEON, S., HAGUENAUER-TSAPIS, R. & VINCENT, O. 2013. A mechanism for protein monoubiquitination dependent on a trans-acting ubiquitin binding domain. *Journal of Biological Chemistry,* 288**,** 16206-16211.

HERRIDGE, R., DAY, R., BALDWIN, S. & MACKNIGHT, R. 2011. Rapid analysis of seed size in Arabidopsis for mutant and QTL discovery. *Plant Methods,* 7**,** 3.

HERSHKO, A. & CIECHANOVER, A. 1998. The ubiquitin system. *Annual review of biochemistry,* 67**,** 425-479.

HERVÉ, C., DABOS, P., BARDET, C., JAUNEAU, A., AURIAC, M. C., RAMBOER, A., LACOUT, F. & TREMOUSAYGUE, D. 2009. In vivo interference with AtTCP20 function induces severe plant growth alterations and deregulates the expression of many genes important for development. *Plant physiology,* 149**,** 1462-1477.

HETTEMA, E. H., VALDEZ-TAUBAS, J. & PELHAM, H. R. 2004. Bsd2 binds the ubiquitin ligase Rsp5 and mediates the ubiquitination of transmembrane proteins. *The EMBO journal,* 23**,** 1279-1288.

HIBARA, K.-I., KARIM, M. R., TAKADA, S., TAOKA, K.-I., FURUTANI, M., AIDA, M. & TASAKA, M. 2006. Arabidopsis CUP-SHAPED COTYLEDON3 regulates postembryonic shoot meristem and organ boundary formation. *The Plant Cell Online,* 18**,** 2946-2957.

HICKE, L., SCHUBERT, H. L. & HILL, C. P. 2005. Ubiquitin-binding domains. *Nature Reviews Molecular Cell Biology,* 6**,** 610-621.

HIGUCHI, M., PISCHKE, M. S., MÄHÖNEN, A. P., MIYAWAKI, K., HASHIMOTO, Y., SEKI, M., KOBAYASHI, M., SHINOZAKI, K., KATO, T. & TABATA, S. 2004. In planta functions of the Arabidopsis cytokinin receptor family. *Proceedings of the National Academy of Sciences of the United States of America,* 101**,** 8821-8826.

HIRATSU, K., MATSUI, K., KOYAMA, T. & OHME‐TAKAGI, M. 2003. Dominant repression of target genes by chimeric repressors that include the EAR motif, a repression domain, in Arabidopsis. *The Plant Journal,* 34**,** 733-739.

HIRNER, B., FISCHER, W. N., RENTSCH, D., KWART, M. & FROMMER, W. B. 1998. Developmental control of H+/amino acid permease gene expression during seed development of Arabidopsis. *The Plant Journal,* 14**,** 535-544.

HOCHSTRASSER, M. 1996. Ubiquitin-dependent protein degradation. *Annual review of genetics,* 30**,** 405-439.

HOCHSTRASSER, M. 2009. Origin and function of ubiquitin-like proteins. *Nature,* 458**,** 422-429.

HOELLER, D., CROSETTO, N., BLAGOEV, B., RAIBORG, C., TIKKANEN, R., WAGNER, S., KOWANETZ, K., BREITLING, R., MANN, M. & STENMARK, H. 2006. Regulation of ubiquitin-binding proteins by monoubiquitination. *Nature cell biology,* 8**,** 163-169.

HOFMANN, K. & FALQUET, L. 2001. A ubiquitin-interacting motif conserved in components of the proteasomal and lysosomal protein degradation systems. *Trends in Biochemical Sciences,* 26**,** 347-350.

HONG, S.-Y., KIM, O.-K., KIM, S.-G., YANG, M.-S. & PARK, C.-M. 2011. Nuclear import and DNA binding of the ZHD5 transcription factor is modulated by a competitive peptide inhibitor in Arabidopsis. *Journal of Biological Chemistry,* 286**,** 1659-1668.

HORIGUCHI, G., FERJANI, A., FUJIKURA, U. & TSUKAYA, H. 2006a. Coordination of cell proliferation and cell expansion in the control of leaf size in Arabidopsis thaliana. *Journal of plant research,* 119**,** 37-42.

HORIGUCHI, G., FUJIKURA, U., FERJANI, A., ISHIKAWA, N. & TSUKAYA, H. 2006b. Large‐scale histological analysis of leaf mutants using two simple leaf observation methods: identification of novel genetic pathways governing the size and shape of leaves. *The Plant Journal,* 48**,** 638-644.

HORIGUCHI, G., KIM, G. T. & TSUKAYA, H. 2005. The transcription factor AtGRF5 and the transcription coactivator AN3 regulate cell proliferation in leaf primordia of Arabidopsis thaliana. *The Plant Journal,* 43**,** 68-78.

HORTON, M. W., HANCOCK, A. M., HUANG, Y. S., TOOMAJIAN, C., ATWELL, S., AUTON, A., MULIYATI, N. W., PLATT, A., SPERONE, F. G. & VILHJÁLMSSON, B. J. 2012. Genome-wide patterns of genetic variation in worldwide Arabidopsis thaliana accessions from the RegMap panel. *Nature genetics,* 44**,** 212-216.

HORVATH, B. M., MAGYAR, Z., ZHANG, Y., HAMBURGER, A. W., BAKO, L., VISSER, R. G., BACHEM, C. W. & BÖGRE, L. 2006. EBP1 regulates organ size through cell growth and proliferation in plants. *The EMBO journal,* 25**,** 4909-4920.

HOTTON, S. K., EIGENHEER, R. A., CASTRO, M. F., BOSTICK, M. & CALLIS, J. 2011. AXR1-ECR1 and AXL1-ECR1 heterodimeric RUB-activating enzymes diverge in function in Arabidopsis thaliana. *Plant molecular biology,* 75**,** 515-526.

HU, Y., POH, H. M. & CHUA, N. H. 2006. The Arabidopsis ARGOS‐LIKE gene regulates cell expansion during organ growth. *The Plant Journal,* 47**,** 1-9.

HU, Y., XIE, Q. & CHUA, N.-H. 2003. The Arabidopsis auxin-inducible gene ARGOS controls lateral organ size. *The Plant Cell Online,* 15**,** 1951-1961.

HUANG, S., RAMAN, A. S., REAM, J. E., FUJIWARA, H., CERNY, R. E. & BROWN, S. M. 1998. Overexpression of 20-oxidase confers a gibberellin-overproduction phenotype in Arabidopsis. *Plant Physiology,* 118**,** 773-781.

ICHIHASHI, Y., HORIGUCHI, G., GLEISSBERG, S. & TSUKAYA, H. 2010. The bHLH transcription factor SPATULA controls final leaf size in Arabidopsis thaliana. *Plant and cell physiology,* 51**,** 252-261.

IKEDA, F. & DIKIC, I. 2008. Atypical ubiquitin chains: new molecular signals. *EMBO reports,* 9**,** 536-542.

INGOUFF, M., JULLIEN, P. E. & BERGER, F. 2006. The female gametophyte and the endosperm control cell proliferation and differentiation of the seed coat in Arabidopsis. *The Plant Cell Online,* 18**,** 3491-3501.

INZÉ, D. & DE VEYLDER, L. 2006. Cell cycle regulation in plant development 1. *Annu. Rev. Genet.,* 40**,** 77-105.

IRNIGER, S., PIATTI, S., MICHAELIS, C. & NASMYTH, K. 1995. Genes involved in sister chromatid separation are needed for B-type cyclin proteolysis in budding yeast. *Cell,* 81**,** 269-277.

ISHIDA, T., FUJIWARA, S., MIURA, K., STACEY, N., YOSHIMURA, M., SCHNEIDER, K., ADACHI, S., MINAMISAWA, K., UMEDA, M. & SUGIMOTO, K. 2009. SUMO E3 ligase HIGH PLOIDY2 regulates endocycle onset and meristem maintenance in Arabidopsis. *The Plant Cell Online,* 21**,** 2284-2297.

IYER, L. M., KOONIN, E. V. & ARAVIND, L. 2004. Report Novel Predicted Peptidases with a Potential Role in the Ubiquitin Signaling Pathway. *Cell Cycle,* 3**,** 1440-1450.

JACKSON, D., VEIT, B. & HAKE, S. 1994. Expression of maize KNOTTED1 related homeobox genes in the shoot apical meristem predicts patterns of morphogenesis in the vegetative shoot. *Development,* 120**,** 405-413.

JACOBSON, A. D., ZHANG, N.-Y., XU, P., HAN, K.-J., NOONE, S., PENG, J. & LIU, C.-W. 2009. The lysine 48 and lysine 63 ubiquitin conjugates are processed differently by the 26 S proteasome. *Journal of Biological Chemistry,* 284**,** 35485-35494.

JAMES, P., HALLADAY, J. & CRAIG, E. A. 1996. Genomic libraries and a host strain designed for highly efficient two-hybrid selection in yeast. *Genetics,* 144**,** 1425-1436.

JENTSCH, S. & PYROWOLAKIS, G. 2000. Ubiquitin and its kin: how close are the family ties? *Trends in cell biology,* 10**,** 335-342.

JIANG, C.-Z. 2004. Method for modifying plant biomass. Google Patents.

JIN, J., LI, X., GYGI, S. P. & HARPER, J. W. 2007. Dual E1 activation systems for ubiquitin differentially regulate E2 enzyme charging. *Nature,* 447**,** 1135-1138.

JOHNSON, K. & LENHARD, M. 2011. Genetic control of plant organ growth. *New Phytologist,* 191**,** 319-333.

JONES, A. M., IM, K. H., SAVKA, M. A., WU, M. J., DEWITT, N. G., SHILLITO, R. & BINNS, A. N. 1998. Auxin-dependent cell expansion mediated by overexpressed auxin-binding protein 1. *Science,* 282**,** 1114-1117.

JONGENEEL, C. V., BOUVIER, J. & BAIROCH, A. 1989. A unique signature identifies a family of zinc-dependent metallopeptidases. *FEBS letters,* 242**,** 211-214.

JORDE, L. 2000. Linkage disequilibrium and the search for complex disease genes. *Genome research,* 10**,** 1435-1444.

JOUBES, J. & CHEVALIER, C. 2000. Endoreduplication in higher plants. *Plant Molecular Biology,* 43**,** 735-745.

JOUBES, J., CHEVALIER, C., DUDITS, D., HEBERLE-BORS, E., INZÉ, D., UMEDA, M. & RENAUDIN, J.-P. 2000. CDK-related protein kinases in plants. *Plant Molecular Biology,* 43**,** 607-620.

KADRMAS, J. L. & BECKERLE, M. C. 2004. The LIM domain: from the cytoskeleton to the nucleus. *Nature Reviews Molecular Cell Biology,* 5**,** 920-931.

KANG, H. M., ZAITLEN, N. A., WADE, C. M., KIRBY, A., HECKERMAN, D., DALY, M. J. & ESKIN, E. 2008. Efficient control of population structure in model organism association mapping. *Genetics,* 178**,** 1709-1723.

KANG, J. & DENGLER, N. 2002. Cell cycling frequency and expression of the homeobox gene ATHB-8 during leaf vein development in Arabidopsis. *Planta,* 216**,** 212-219.

KANG, X., LI, W., ZHOU, Y. & NI, M. 2013. A WRKY Transcription Factor Recruits the SYG1-Like Protein SHB1 to Activate Gene Expression and Seed Cavity Enlargement. *PLoS Genetics,* 9**,** e1003347.

KARLOVA, R. & DE VRIES, S. C. 2006. Advances in understanding brassinosteroid signaling. *Science's STKE,* 2006**,** p.pe36.

KATZ, A., OLIVA, M., MOSQUNA, A., HAKIM, O. & OHAD, N. 2004. FIE and CURLY LEAF polycomb proteins interact in the regulation of homeobox gene expression during sporophyte development. *The Plant Journal,* 37**,** 707-719.

KAVSAK, P., RASMUSSEN, R. K., CAUSING, C. G., BONNI, S., ZHU, H., THOMSEN, G. H. & WRANA, J. L. 2000. Smad7 binds to Smurf2 to form an E3 ubiquitin ligase that targets the TGFβ receptor for degradation. *Molecular cell,* 6**,** 1365-1375.

KAWAI, T. & AKIRA, S. 2010. The role of pattern-recognition receptors in innate immunity: update on Toll-like receptors. *Nature immunology,* 11**,** 373-384.

KAZAMA, T., ICHIHASHI, Y., MURATA, S. & TSUKAYA, H. 2010. The mechanism of cell cycle arrest front progression explained by a KLUH/CYP78A5-dependent mobile growth factor in developing leaves of Arabidopsis thaliana. *Plant and cell physiology,* 51**,** 1046-1054.

KEINATH, N. F., KIERSZNIOWSKA, S., LOREK, J., BOURDAIS, G., KESSLER, S. A., ASANO, H., GROSSNIKLAUS, U., SCHULZE, W., ROBATZEK, S. & PANSTRUGA, R. 2011. PAMP-induced changes in plasma membrane compartmentalization reveal novel components of plant immunity. *Journal of Biological Chemistry*.

KEMMERLING, B., SCHWEDT, A., RODRIGUEZ, P., MAZZOTTA, S., FRANK, M., QAMAR, S. A., MENGISTE, T., BETSUYAKU, S., PARKER, J. E. & MÜSSIG, C. 2007. The BRI1-associated kinase 1, BAK1, has a brassinolide-independent role in plant cell-death control. *Current Biology,* 17**,** 1116-1122.

KERSCHER, O., FELBERBAUM, R. & HOCHSTRASSER, M. 2006. Modification of proteins by ubiquitin and ubiquitin-like proteins. *Annu. Rev. Cell Dev. Biol.,* 22**,** 159-180.

KERSTETTER, R. A., BOLLMAN, K., TAYLOR, R. A., BOMBLIES, K. & POETHIG, R. S. 2001. KANADI regulates organ polarity in Arabidopsis. *Nature,* 411**,** 706-709.

KESSLER, S. & SINHA, N. 2004. Shaping up: the genetic control of leaf shape. *Current opinion in plant biology,* 7**,** 65-72.

KIEBER, J. J., ROTHENBERG, M., ROMAN, G., FELDMANN, K. A. & ECKER, J. R. 1993. CTR1, a negative regulator of the ethylene response pathway in arabidopsis, encodes a member of the Raf family of protein kinases. *Cell,* 72**,** 427-441.

KIEFFER, M., MASTER, V., WAITES, R. & DAVIES, B. 2011. TCP14 and TCP15 affect internode length and leaf shape in Arabidopsis. *The Plant Journal,* 68**,** 147-158.

KIERZKOWSKI, D., NAKAYAMA, N., ROUTIER-KIERZKOWSKA, A.-L., WEBER, A., BAYER, E., SCHORDERET, M., REINHARDT, D., KUHLEMEIER, C. & SMITH, R. S. 2012. Elastic domains regulate growth and organogenesis in the plant shoot apical meristem. *Science Signaling,* 335**,** 1096-1099.

KIM, G.-T., TSUKAYA, H. & UCHIMIYA, H. 1998a. The CURLY LEAF gene controls both division and elongation of cells during the expansion of the leaf blade in Arabidopsis thaliana. *Planta,* 206**,** 175-183.

KIM, G.-T., TSUKAYA, H. & UCHIMIYA, H. 1998b. The ROTUNDIFOLIA3 gene of Arabidopsis thalianaencodes a new member of the cytochrome P-450 family that is required for the regulated polar elongation of leaf cells. *Genes & development,* 12**,** 2381-2391.

KIM, G. T., SHODA, K., TSUGE, T., CHO, K. H., UCHIMIYA, H., YOKOYAMA, R., NISHITANI, K. & TSUKAYA, H. 2002. The ANGUSTIFOLIA gene of Arabidopsis, a plant CtBP gene, regulates leaf-cell expansion, the arrangement of cortical microtubules in leaf cells and expression of a gene involved in cell-wall formation. *EMBO Journal,* 21**,** 1267-1279.

KIM, J. H., CHOI, D. & KENDE, H. 2003. The AtGRF family of putative transcription factors is involved in leaf and cotyledon growth in Arabidopsis. *The Plant Journal,* 36**,** 94-104.

KIM, J. H. & KENDE, H. 2004. A transcriptional coactivator, AtGIF1, is involved in regulating leaf growth and morphology in Arabidopsis. *Proceedings of the National Academy of Sciences of the United States of America,* 101**,** 13374-13379.

KIM, S., PLAGNOL, V., HU, T. T., TOOMAJIAN, C., CLARK, R. M., OSSOWSKI, S., ECKER, J. R., WEIGEL, D. & NORDBORG, M. 2007. Recombination and linkage disequilibrium in Arabidopsis thaliana. *Nature genetics,* 39**,** 1151-1155.

KIM, T. & WANG, Z. Y. 2010. Brassinosteroid Signal Transduction from Receptor Kinases to Transcription Factors. *Annual Review of Plant Biology,* 61**,** 681-704.

KING, R. W., DESHAIES, R. J., PETERS, J.-M. & KIRSCHNER, M. W. 1996. How proteolysis drives the cell cycle. *Science,* 274**,** 1652-1659.

KINOSHITA, T., CAÑO-DELGADO, A., SETO, H., HIRANUMA, S., FUJIOKA, S., YOSHIDA, S. & CHORY, J. 2005. Binding of brassinosteroids to the extracellular domain of plant receptor kinase BRI1. *Nature,* 433**,** 167-171.

KIRISAKO, T., KAMEI, K., MURATA, S., KATO, M., FUKUMOTO, H., KANIE, M., SANO, S., TOKUNAGA, F., TANAKA, K. & IWAI, K. 2006. A ubiquitin ligase complex assembles linear polyubiquitin chains. *The EMBO journal,* 25**,** 4877-4887.

KOBAYASHI, Y., KANESAKI, Y., TANAKA, A., KUROIWA, H., KUROIWA, T. & TANAKA, K. 2009. Tetrapyrrole signal as a cell-cycle coordinator from organelle to nuclear DNA replication in plant cells. *Proceedings of the National Academy of Sciences,* 106**,** 803-807.

KÖHLER, C., HENNIG, L., BOUVERET, R., GHEYSELINCK, J., GROSSNIKLAUS, U. & GRUISSEM, W. 2003. Arabidopsis MSI1 is a component of the MEA/FIE Polycomb group complex and required for seed development. *The EMBO journal,* 22**,** 4804-4814.

KÖHLER, C. & MAKAREVICH, G. 2006. Epigenetic mechanisms governing seed development in plants. *EMBO reports,* 7**,** 1223-1227.

KOMANDER, D., CLAGUE, M. J. & URBE, S. 2009. Breaking the chains: structure and function of the deubiquitinases. *Nature Reviews Molecular Cell Biology,* 10**,** 550-563.

KOORNNEEF, M. & VAN DER VEEN, J. 1980. Induction and analysis of gibberellin sensitive mutants in Arabidopsis thaliana (L.) Heynh. *Theoretical and Applied genetics,* 58**,** 257-263.

KOSUGI, S. & OHASHI, Y. 1997. PCF1 and PCF2 specifically bind to cis elements in the rice proliferating cell nuclear antigen gene. *The Plant Cell Online,* 9**,** 1607-1619.

KOSUGI, S. & OHASHI, Y. 2002. DNA binding and dimerization specificity and potential targets for the TCP protein family. *The Plant Journal,* 30**,** 337-348.

KOVER, P. X. & MOTT, R. 2012. Mapping the genetic basis of ecologically and evolutionarily relevant traits in Arabidopsis thaliana. *Current opinion in plant biology,* 15**,** 212-217.

KOVER, P. X., VALDAR, W., TRAKALO, J., SCARCELLI, N., EHRENREICH, I. M., PURUGGANAN, M. D., DURRANT, C. & MOTT, R. 2009. A multiparent advanced generation inter-cross to fine-map quantitative traits in Arabidopsis thaliana. *PLoS genetics,* 5**,** e1000551.

KOYAMA, T., FURUTANI, M., TASAKA, M. & OHME-TAKAGI, M. 2007. TCP transcription factors control the morphology of shoot lateral organs via negative regulation of the expression of boundary-specific genes in Arabidopsis. *The Plant Cell Online,* 19**,** 473-484.

KOYAMA, T., MITSUDA, N., SEKI, M., SHINOZAKI, K. & OHME-TAKAGI, M. TCP Transcription Factors Regulate the Activities of ASYMMETRIC LEAVES1 and miR164, as Well as the Auxin Response, during Differentiation of Leaves in Arabidopsis. *The Plant Cell Online,* 22**,** 3574-3588.

KOYAMA, T., MITSUDA, N., SEKI, M., SHINOZAKI, K. & OHME-TAKAGI, M. 2010a. TCP Transcription Factors Regulate the Activities of ASYMMETRIC LEAVES1 and miR164, as Well as the Auxin Response, during Differentiation of Leaves in Arabidopsis. *The Plant Cell Online,* 22**,** 3574-3588.

KOYAMA, T., SATO, F. & OHME-TAKAGI, M. 2010b. A role of TCP1 in the longitudinal elongation of leaves in Arabidopsis. *Bioscience, biotechnology, and biochemistry,* 74**,** 2145-2147.

KRIZEK, B. A., LEWIS, M. W. & FLETCHER, J. C. 2006. RABBIT EARS is a second‐whorl repressor of AGAMOUS that maintains spatial boundaries in Arabidopsis flowers. *The Plant Journal,* 45**,** 369-383.

KUREPA, J. & SMALLE, J. A. 2008. Structure, function and regulation of plant proteasomes. *Biochimie,* 90**,** 324-335.

KWON, Y. R., LEE, H. J., KIM, K. H., HONG, S.-W., LEE, S. J. & LEE, H. 2008. Ectopic expression of Expansin3 or Expansin β1 causes enhanced hormone and salt stress sensitivity in Arabidopsis. *Biotechnology letters,* 30**,** 1281-1288.

LARKIN, M., BLACKSHIELDS, G., BROWN, N., CHENNA, R., MCGETTIGAN, P. A., MCWILLIAM, H., VALENTIN, F., WALLACE, I. M., WILM, A. & LOPEZ, R. 2007. Clustal W and Clustal X version 2.0. *Bioinformatics,* 23**,** 2947-2948.

LARKIN MA, BLACKSHIELDS G, BROWN NP, CHENNA R, MCGETTIGAN PA, MCWILLIAM H, VALENTIN F, WALLACE IM, WILM A, LOPEZ R, THOMPSON JD, GIBSON TJ & DG, H. 2007. Clustal W adn Clustal X version 2.0. 23**,** 2947-2948.

LARSON-RABIN, Z., LI, Z., MASSON, P. H. & DAY, C. D. 2009. FZR2/CCS52A1 expression is a determinant of endoreduplication and cell expansion in Arabidopsis. *Plant physiology,* 149**,** 874-884.

LECHNER, E., XIE, D., GRAVA, S., PIGAGLIO, E., PLANCHAIS, S., MURRAY, J. A., PARMENTIER, Y., MUTTERER, J., DUBREUCQ, B. & SHEN, W.-H. 2002. The AtRbx1 protein is part of plant SCF complexes, and its down-regulation causes severe growth and developmental defects. *Journal of Biological Chemistry,* 277**,** 50069-50080.

LECUIT, T., BROOK, W. J., NG, M., CALLEJA, M., SUN, H. & COHEN, S. M. 1996. Two distinct mechanisms for long-range patterning by Decapentaplegic in the Drosophila wing. *Nature,* 381**,** 387-393.

LEE, B. H., KO, J.-H., LEE, S., LEE, Y., PAK, J.-H. & KIM, J. H. 2009. The Arabidopsis GRF-INTERACTING FACTOR gene family performs an overlapping function in determining

organ size as well as multiple developmental properties. *Plant physiology,* 151**,** 655-668.

LEE, S. S., CHO, H. S., YOON, G. M., AHN, J. W., KIM, H. H. & PAI, H. S. 2003. Interaction of NtCDPK1 calcium‐dependent protein kinase with NtRpn3 regulatory subunit of the 26S proteasome in Nicotiana tabacum. *The Plant Journal,* 33**,** 825-840.

LEISTER, D. 2012. Retrograde signaling in plants: from simple to complex scenarios. *Frontiers in plant science,* 3**,** 135.

LENHARD, M. 2012. All's Well that Ends Well: Arresting Cell Proliferation in Leaves. *Developmental cell,* 22**,** 9-11.

LÉON, S. & HAGUENAUER-TSAPIS, R. 2009. Ubiquitin ligase adaptors: regulators of ubiquitylation and endocytosis of plasma membrane proteins. *Experimental cell research,* 315**,** 1574-1583.

LEPORE, L. S., ROELVINK, P. R. & GRANADOS, R. R. 1996. Enhancin, the granulosis virus protein that facilitates nucleopolyhedrovirus (NPV) infections, is a metalloprotease. *Journal of invertebrate pathology,* 68**,** 131-140.

LEVIN, J. Z. & MEYEROWITZ, E. M. 1995. UFO: an Arabidopsis gene involved in both floral meristem and floral organ development. *The Plant Cell Online,* 7**,** 529-548.

LI, C., POTUSCHAK, T., COLÓN-CARMONA, A., GUTIÉRREZ, R. A. & DOERNER, P. 2005a. Arabidopsis TCP20 links regulation of growth and cell division control pathways. *Proceedings of the National Academy of Sciences of the United States of America,* 102**,** 12978-12983.

LI, J., WEN, J., LEASE, K. A., DOKE, J. T., TAX, F. E. & WALKER, J. C. 2002a. BAK1, an Arabidopsis LRR receptor-like protein kinase, interacts with BRI1 and modulates brassinosteroid signaling. *Cell,* 110**,** 213-222.

LI, J., YANG, H., PEER, W. A., RICHTER, G., BLAKESLEE, J., BANDYOPADHYAY, A., TITAPIWANTAKUN, B., UNDURRAGA, S., KHODAKOVSKAYA, M. & RICHARDS, E. L. 2005b. Arabidopsis H+-PPase AVP1 regulates auxin-mediated organ development. *Science,* 310**,** 121-125.

LI, M., CHEN, D., SHILOH, A., LUO, J., NIKOLAEV, A. Y., QIN, J. & GU, W. 2002b. Deubiquitination of p53 by HAUSP is an important pathway for p53 stabilization. *Nature,* 416**,** 648-653.

LI, X., CLARKE, J. D., ZHANG, Y. & DONG, X. 2001. Activation of an EDS1-mediated R-gene pathway in the snc1 mutant leads to constitutive, NPR1-independent pathogen resistance. *Molecular plant-microbe interactions,* 14**,** 1131-1139.

LI, Y., ZHENG, L., CORKE, F., SMITH, C. & BEVAN, M. W. 2008. Control of final seed and organ size by the DA1 gene family in Arabidopsis thaliana. *Genes & Development,* 22**,** 1331-1336.

LI, Z. Y., LI, B. & DONG, A. W. 2012. The Arabidopsis transcription factor AtTCP15 regulates endoreduplication by modulating expression of key cell-cycle genes. *Molecular plant,* 5**,** 270-280.

LIN, W.-C., SHUAI, B. & SPRINGER, P. S. 2003. The Arabidopsis LATERAL ORGAN BOUNDARIES–domain gene ASYMMETRIC LEAVES2 functions in the repression of KNOX gene expression and in adaxial-abaxial patterning. *The Plant Cell Online,* 15**,** 2241-2252.

LIPSHITZ, H. D. 2009. Follow the mRNA: a new model for Bicoid gradient formation. *Nature Reviews Molecular Cell Biology,* 10**,** 509-512.

LIU, X., KIM, Y. J., MÜLLER, R., YUMUL, R. E., LIU, C., PAN, Y., CAO, X., GOODRICH, J. & CHEN, X. 2011. AGAMOUS terminates floral stem cell maintenance in Arabidopsis by directly repressing WUSCHEL through recruitment of Polycomb Group proteins. *The Plant Cell Online,* 23**,** 3654-3670.

LIU, Z. & MEYEROWITZ, E. M. 1995. LEUNIG regulates AGAMOUS expression in Arabidopsis flowers. *Development,* 121**,** 975-991.

LONG, J. A., MOAN, E. I., MEDFORD, J. I. & BARTON, M. K. 1996. A member of the KNOTTED class of homeodomain proteins encoded by the STM gene of Arabidopsis. *Nature,* 379**,** 66-69.

LOPES, M. A. & LARKINS, B. A. 1993. Endosperm origin, development, and function. *The Plant Cell,* 5**,** 1383-1339.

LU, D., LIN, W., GAO, X., WU, S., CHENG, C., AVILA, J., HEESE, A., DEVARENNE, T. P., HE, P. & SHAN, L. 2011. Direct ubiquitination of pattern recognition receptor FLS2 attenuates plant innate immunity. *Science Signaling,* 332**,** 1439.

LU, H., SALIMIAN, S., GAMELIN, E., WANG, G., FEDOROWSKI, J., LACOURSE, W. & GREENBERG, J. T. 2009. Genetic analysis of acd6‐1 reveals complex defense networks and leads to identification of novel defense genes in Arabidopsis. *The Plant Journal,* 58**,** 401-412.

LUO, M., BILODEAU, P., KOLTUNOW, A., DENNIS, E. S., PEACOCK, W. J. & CHAUDHURY, A. M. 1999. Genes controlling fertilization-independent seed development in Arabidopsis thaliana. *Proceedings of the National Academy of Sciences,* 96**,** 296-301.

MACLEAN, D. Z., C unpublished.

MAGYAR, Z., HORVÁTH, B., SAFINA KHAN, B. M., HENRIQUES, R., DE VEYLDER, L., BAKÓ, L., SCHERES, B. & BÖGRE, L. 2012. Arabidopsis E2FA stimulates proliferation and endocycle separately through RBR-bound and RBR-free complexes. *The EMBO journal,* 31**,** 1480-1493.

MALINOWSKI, R., KASPRZEWSKA, A. & FLEMING, A. J. 2011. Targeted manipulation of leaf form via local growth repression. *The Plant Journal,* 66**,** 941-952.

MALLERY, D. L., VANDENBERG, C. J. & HIOM, K. 2002. Activation of the E3 ligase function of the BRCA1/BARD1 complex by polyubiquitin chains. *The EMBO Journal,* 21**,** 6755-6762.

MAO, Y., SENIC-MATUGLIA, F., DI FIORE, P. P., POLO, S., HODSDON, M. E. & DE CAMILLI, P. 2005. Deubiquitinating function of ataxin-3: insights from the solution structure of the Josephin domain. *Proceedings of the National Academy of Sciences of the United States of America,* 102**,** 12700-12705.

MARINO, D., PEETERS, N. & RIVAS, S. 2012. Ubiquitination during plant immune signaling. *Plant physiology,* 160**,** 15-27.

MARMOR, M. D. & YARDEN, Y. 2004. Role of protein ubiquitylation in regulating endocytosis of receptor tyrosine kinases. *Oncogene,* 23**,** 2057-2070.

MARTÍN-TRILLO, M. & CUBAS, P. 2010. TCP genes: a family snapshot ten years later. *Trends in plant science,* 15**,** 31-39.

MASON, S. D. & JOYCE, J. A. 2011. Proteolytic networks in cancer. *Trends in cell biology,* 21**,** 228-237.

MASUDA, H. P., CABRAL, L. M., DE VEYLDER, L., TANURDZIC, M., DE ALMEIDA ENGLER, J., GEELEN, D., INZÉ, D., MARTIENSSEN, R. A., FERREIRA, P. C. & HEMERLY, A. S. 2008. ABAP1 is a novel plant Armadillo BTB protein involved in DNA replication and transcription. *The EMBO journal,* 27**,** 2746-2756.

MATTHEWS, B., COLMAN, P., JANSONIUS, J., TITANI, K., WALSH, K. & NEURATH, H. 1972. Structure of thermolysin. *Nature,* 238**,** 41-43.

MATTSSON, J., CKURSHUMOVA, W. & BERLETH, T. 2003. Auxin signaling in Arabidopsis leaf vascular development. *Plant Physiology,* 131**,** 1327-1339.

MAUL, R. S., SONG, Y., AMANN, K. J., GERBIN, S. C., POLLARD, T. D. & CHANG, D. D. 2003. EPLIN regulates actin dynamics by cross-linking and stabilizing filaments. *The Journal of cell biology,* 160**,** 399-407.

MAYER, K. F., SCHOOF, H., HAECKER, A., LENHARD, M., JÜRGENS, G. & LAUX, T. 1998. Role of WUSCHEL in Regulating Stem Cell Fate in the Arabidopsis Shoot Meristem. *Cell,* 95**,** 805-815.

MAZZUCOTELLI, E., BELLONI, S., MARONE, D., DE LEONARDIS, A., GUERRA, D., DI FONZO, N., CATTIVELLI, L. & MASTRANGELO, A. 2006. The E3 ubiquitin ligase gene family in plants: regulation by degradation. *Current genomics,* 7**,** 509-522.

MCCARTHY, M. I., ABECASIS, G. R., CARDON, L. R., GOLDSTEIN, D. B., LITTLE, J., IOANNIDIS, J. P. & HIRSCHHORN, J. N. 2008. Genome-wide association studies for complex traits: consensus, uncertainty and challenges. *Nature Reviews Genetics,* 9**,** 356-369.

MCGINNIS, K. M., THOMAS, S. G., SOULE, J. D., STRADER, L. C., ZALE, J. M., SUN, T.-P. & STEBER, C. M. 2003. The Arabidopsis SLEEPY1 gene encodes a putative F-box subunit of an SCF E3 ubiquitin ligase. *The Plant Cell Online,* 15**,** 1120-1130.

MCGWIRE, B. S. & CHANG, K.-P. 1996. Posttranslational Regulation of a Leishmania HEXXH Metalloprotease (gp63). The effects of site-specific mutagenesis of catalytic, zinc binding, N-glycosylation, and glycosyl phosphatidylinositol addition sites on N-terminal end cleavage, intracellular stability, and extracellular exit. *Journal of Biological Chemistry,* 271**,** 7903-7909.

MCINTOSH, I., DREYER, S. D., CLOUGH, M. V., DUNSTON, J. A., EYAID, W., ROIG, C. M., MONTGOMERY, T., ALA-MELLO, S., KAITILA, I. & WINTERPACHT, A. 1998. Mutation Analysis of LMX1B Gene in Nail-Patella Syndrome Patients. *The American Journal of Human Genetics,* 63**,** 1651-1658.

MELARAGNO, J. E., MEHROTRA, B. & COLEMAN, A. W. 1993. Relationship between endopolyploidy and cell size in epidermal tissue of Arabidopsis. *The Plant Cell Online,* 5**,** 1661-1668.

MENG, L.-S., SUN, X.-D., LI, F., LIU, H.-L., FENG, Z.-H. & ZHU, J. 2010. Modification of flowers and leaves in Cockscomb (Celosia cristata) ectopically expressing Arabidopsis ASYMMERTIC LEAVES2-LIKE38 (ASL38/LBD41) gene. *Acta Physiologiae Plantarum,* 32**,** 315-324.

MERLET, J., BURGER, J., GOMES, J.-E. & PINTARD, L. 2009. Regulation of cullin-RING E3 ubiquitin-ligases by neddylation and dimerization. *Cellular and molecular life sciences,* 66**,** 1924-1938.

MESQUITA, D., DEKANTY, A. & MILÁN, M. 2010. A dp53-dependent mechanism involved in coordinating tissue growth in Drosophila. *PLoS biology,* 8**,** e1000566.

MEULMEESTER, E., KUNZE, M., HSIAO, H. H., URLAUB, H. & MELCHIOR, F. 2008. Mechanism and consequences for paralog-specific sumoylation of ubiquitin-specific protease 25. *Molecular cell,* 30**,** 610-619.

MIKI, Y., SWENSEN, J., SHATTUCK-EIDENS, D., FUTREAL, P. A., HARSHMAN, K., TAVTIGIAN, S., LIU, Q., COCHRAN, C., BENNETT, L. M. & DING, W. 1994. A strong candidate for the breast and ovarian cancer susceptibility gene BRCA1. *Science,* 266**,** 66-71.

MITCHELL, P. L. & SHEEHY, J. E. 2006. Supercharging rice photosynthesis to increase yield. *New Phytologist,* 171**,** 688-693.

MITCHELL-OLDS, T. 2010. Complex-trait analysis in plants. *Genome Biol,* 11**,** 423.

MIURA, K. & HASEGAWA, P. M. 2010. Sumoylation and other ubiquitin-like post-translational modifications in plants. *Trends in cell biology,* 20**,** 223-232.

MIURA, K., JIN, J. B., LEE, J., YOO, C. Y., STIRM, V., MIURA, T., ASHWORTH, E. N., BRESSAN, R. A., YUN, D.-J. & HASEGAWA, P. M. 2007. SIZ1-mediated sumoylation of ICE1 controls CBF3/DREB1A expression and freezing tolerance in Arabidopsis. *The Plant Cell Online,* 19**,** 1403-1414.

MIURA, K., LEE, J., JIN, J. B., YOO, C. Y., MIURA, T. & HASEGAWA, P. M. 2009. Sumoylation of ABI5 by the Arabidopsis SUMO E3 ligase SIZ1 negatively regulates abscisic acid signaling. *Proceedings of the National Academy of Sciences,* 106**,** 5418-5423.

MIURA, K., LEE, J., MIURA, T. & HASEGAWA, P. M. 2010. SIZ1 controls cell growth and plant development in Arabidopsis through salicylic acid. *Plant and cell physiology,* 51**,** 103-113.

MIYOSHI, K., AHN, B.-O., KAWAKATSU, T., ITO, Y., ITOH, J.-I., NAGATO, Y. & KURATA, N. 2004. PLASTOCHRON1, a timekeeper of leaf initiation in rice, encodes cytochrome P450. *Proceedings of the National Academy of Sciences of the United States of America,* 101**,** 875-880.

MIZUKAMI, Y. 2001. A matter of size: developmental control of organ size in plants. *Current opinion in plant biology,* 4**,** 533-539.

MIZUKAMI, Y. & FISCHER, R. L. 2000. Plant organ size control: AINTEGUMENTA regulates growth and cell numbers during organogenesis. *Proceedings of the National Academy of Sciences,* 97**,** 942-947.

MOES, D., GATTI, S., HOFFMANN, C., DIETERLE, M., MOREAU, F., NEUMANN, K., SCHUMACHER, M., DIEDERICH, M., GRILL, E. & SHEN, W.-H. 2012. A LIM Domain Protein from Tobacco Involved in Actin-Bundling and Histone Gene Transcription. *Molecular Plant,* 6**,** 483-502.

MOFFAT, C. S., INGLE, R. A., WATHUGALA, D. L., SAUNDERS, N. J., KNIGHT, H. & KNIGHT, M. R. 2012. ERF5 and ERF6 play redundant roles as positive regulators of JA/Et-mediated defense against Botrytis cinerea in Arabidopsis. *PLoS One,* 7**,** e35995.

MOON, J. & HAKE, S. 2011. How a leaf gets its shape. *Current opinion in plant biology,* 14**,** 24-30.

MORELLI, G. & RUBERTI, I. 2002. Light and shade in the photocontrol of Arabidopsis growth. *Trends in plant science,* 7**,** 399-404.

MORIMOTO, M., NISHIDA, T., HONDA, R. & YASUDA, H. 2000. Modification of Cullin-1 by Ubiquitin-like Protein Nedd8 Enhances the Activity of SCFskp2 toward p27 kip1. *Biochemical and biophysical research communications,* 270**,** 1093-1096.

MOTT, R. 2000. *HAPPY: a software package for Multipoint QTL Mapping in Genetically Heterogeneous Animals* [Online]. Available: http://www.well.ox.ac.uk/~rmott/happy.html.

MOTT, R., KOVER, P. X., CLARK, R., RAETSCH, G., TOOMAJIAN, C., STEGLE, O. & GAN, X. 2011. *Association Analysis in Arabidopsis thaliana MAGIC recombinant inbred lines* [Online]. Available: http://mus.well.ox.ac.uk/19genomes/magic.html.

MOTT, R., TALBOT, C. J., TURRI, M. G., COLLINS, A. C. & FLINT, J. 2000. A method for fine mapping quantitative trait loci in outbred animal stocks. *Proceedings of the National Academy of Sciences,* 97**,** 12649-12654.

MUKHTAR, M. S., CARVUNIS, A. R., DREZE, M., EPPLE, P., STEINBRENNER, J., MOORE, J., TASAN, M., GALLI, M., HAO, T. & NISHIMURA, M. T. 2011. Independently evolved virulence effectors converge onto hubs in a plant immune system network. *Science,* 333**,** 596-601.

MULLEN, J. R., CHEN, C.-F. & BRILL, S. J. 2010. Wss1 is a SUMO-dependent isopeptidase that interacts genetically with the Slx5-Slx8 SUMO-targeted ubiquitin ligase. *Molecular and cellular biology,* 30**,** 3737-3748.

MYOUGA, F., HOSODA, C., UMEZAWA, T., IIZUMI, H., KUROMORI, T., MOTOHASHI, R., SHONO, Y., NAGATA, N., IKEUCHI, M. & SHINOZAKI, K. 2008. A heterocomplex of iron superoxide dismutases defends chloroplast nucleoids against oxidative stress and is essential for chloroplast development in Arabidopsis. *The Plant Cell Online,* 20**,** 3148-3162.

NAG, A., KING, S. & JACK, T. 2009. miR319a targeting of TCP4 is critical for petal growth and development in Arabidopsis. *Proceedings of the National Academy of Sciences,* 106**,** 22534-22539.

NAGATA, K., OHASHI, K., YANG, N. & MIZUNO, K. 1999. The N-terminal LIM domain negatively regulates the kinase activity of LIM-kinase 1. *Biochemical Journal,* 343**,** 99-105.

NAGL, W. 1976. DNA endoreduplication and polyteny understood as evolutionary strategies. *Nature,* 261**,** 614-615.

NAKAJIMA, K., SENA, G., NAWY, T. & BENFEY, P. N. 2001. Intercellular movement of the putative transcription factor SHR in root patterning. *Nature,* 413**,** 307-311.

NAKAYA, M., TSUKAYA, H., MURAKAMI, N. & KATO, M. 2002. Brassinosteroids control the proliferation of leaf cells of Arabidopsis thaliana. *Plant and cell physiology,* 43**,** 239-244.

NAKAYAMA, K. I. & NAKAYAMA, K. 2006. Ubiquitin ligases: cell-cycle control and cancer. *Nature Reviews Cancer,* 6**,** 369-381.

NAM, K. H. & LI, J. 2002. BRI1/BAK1, a receptor kinase pair mediating brassinosteroid signaling. *Cell,* 110**,** 203-212.

NAM, K. H. & LI, J. 2004. The Arabidopsis transthyretin-like protein is a potential substrate of BRASSINOSTEROID-INSENSITIVE 1. *The Plant Cell Online,* 16**,** 2406-2417.

NANBA, D., MAMMOTO, A., HASHIMOTO, K. & HIGASHIYAMA, S. 2003. Proteolytic release of the carboxy-terminal fragment of proHB-EGF causes nuclear export of PLZF. *The Journal of cell biology,* 163**,** 489-502.

NATH, U., CRAWFORD, B. C., CARPENTER, R. & COEN, E. 2003. Genetic control of surface curvature. *Science Signaling,* 299**,** 1404-1407.

NEBERT, D. W. & RUSSELL, D. W. 2002. Clinical importance of the cytochromes P450. *The Lancet,* 360**,** 1155-1162.

NISHIMURA, C., OHASHI, Y., SATO, S., KATO, T., TABATA, S. & UEGUCHI, C. 2004. Histidine kinase homologs that act as cytokinin receptors possess overlapping functions in the regulation of shoot and root growth in Arabidopsis. *The Plant Cell Online,* 16**,** 1365-1377.

NORBERG, M., HOLMLUND, M. & NILSSON, O. 2005. The BLADE ON PETIOLE genes act redundantly to control the growth and development of lateral organs. *Development,* 132**,** 2203-2213.

NOTT, A., JUNG, H.-S., KOUSSEVITZKY, S. & CHORY, J. 2006. Plastid-to-nucleus retrograde signaling. *Annu. Rev. Plant Biol.,* 57**,** 739-759.

OGUNJIMI, A. A., BRIANT, D. J., PECE-BARBARA, N., LE ROY, C., DI GUGLIELMO, G. M., KAVSAK, P., RASMUSSEN, R. K., SEET, B. T., SICHERI, F. & WRANA, J. L. 2005. Regulation of Smurf2 ubiquitin ligase activity by anchoring the E2 to the HECT domain. *Molecular cell,* 19**,** 297-308.

OHAD, N., YADEGARI, R., MARGOSSIAN, L., HANNON, M., MICHAELI, D., HARADA, J. J., GOLDBERG, R. B. & FISCHER, R. L. 1999. Mutations in FIE, a WD polycomb group gene, allow endosperm development without fertilization. *The Plant Cell Online,* 11**,** 407-415.

OHNO, C. K., REDDY, G. V., HEISLER, M. G. & MEYEROWITZ, E. M. 2004. The Arabidopsis JAGGED gene encodes a zinc finger protein that promotes leaf tissue development. *Development,* 131**,** 1111-1122.

OKAMOTO, Y., OZAKI, T., MIYAZAKI, K., AOYAMA, M., MIYAZAKI, M. & NAKAGAWARA, A. 2003. UbcH10 is the cancer-related E2 ubiquitin-conjugating enzyme. *Cancer research,* 63**,** 4167-4173.

OKUSHIMA, Y., MITINA, I., QUACH, H. L. & THEOLOGIS, A. 2005. AUXIN RESPONSE FACTOR 2 (ARF2): a pleiotropic developmental regulator. *The Plant Journal,* 43**,** 29-46.

OLDHAM, C. E., MOHNEY, R. P., MILLER, S. L. H., HANES, R. N. & O'BRYAN, J. P. 2002. The ubiquitin-interacting motifs target the endocytic adaptor protein epsin for ubiquitination. *Current Biology,* 12**,** 1112-1116.

OPEN_BIOSYSTEMS. *Arabidopsis thaliana amiRNA Library* [Online]. Available: http://www.biocat.com/bc/pdf/Arabidopsis_manual.pdf.

OVERVOORDE, P. J., OKUSHIMA, Y., ALONSO, J. M., CHAN, A., CHANG, C., ECKER, J. R., HUGHES, B., LIU, A., ONODERA, C. & QUACH, H. 2005. Functional genomic analysis of the AUXIN/INDOLE-3-ACETIC ACID gene family members in Arabidopsis thaliana. *The Plant Cell Online,* 17**,** 3282-3300.

OZKAYNAK, E., FINLEY, D., SOLOMON, M. & VARSHAVSKY, A. 1987. The yeast ubiquitin genes: a family of natural gene fusions. *The EMBO journal,* 6**,** 1429-1439.

PAGNUSSAT, G. C., YU, H.-J., NGO, Q. A., RAJANI, S., MAYALAGU, S., JOHNSON, C. S., CAPRON, A., XIE, L.-F., YE, D. & SUNDARESAN, V. 2005. Genetic and molecular identification of genes required for female gametophyte development and function in Arabidopsis. *Development,* 132**,** 603-614.

PALATNIK, J. F., ALLEN, E., WU, X., SCHOMMER, C., SCHWAB, R., CARRINGTON, J. C. & WEIGEL, D. 2003. Control of leaf morphogenesis by microRNAs. *Nature,* 425**,** 257-263.

PAN, D. 2007. Hippo signaling in organ size control. *Genes & development,* 21**,** 886-897.

PARKER, J. E., SZABÒ, V., STASKAWICZ, B. J., LISTER, C., DEAN, C., DANIELS, M. J. & JONES, J. D. 1993. Phenotypic characterization and molecular mapping of the Arabidopsis thaliana locus RPP5, determining disease resistance to Peronospora parasitica. *The Plant Journal,* 4**,** 821-831.

PATEL, R. A. 2012. *Characterisation of TCP genes in Arabidospis Thaliana.* Doctoral, University of Toronto.

PEAUCELLE, A., BRAYBROOK, S. A., LE GUILLOU, L., BRON, E., KUHLEMEIER, C. & HÖFTE, H. 2011. Pectin-Induced Changes in Cell Wall Mechanics Underlie Organ Initiation in Arabidopsis. *Current Biology,* 21**,** 1720-1726.

PEAUCELLE, A., LOUVET, R., JOHANSEN, J. N., HÖFTE, H., LAUFS, P., PELLOUX, J. & MOUILLE, G. 2008. Arabidopsis Phyllotaxis Is Controlled by the Methyl-Esterification Status of Cell-Wall Pectins. *Current Biology,* 18**,** 1943-1948.

PELLMAN, D. & CHRISTMAN, M. F. 2001. Separase anxiety: dissolving the sister bond and more. *Nature cell biology,* 3**,** E207-E209.

PENG, J., CAROL, P., RICHARDS, D. E., KING, K. E., COWLING, R. J., MURPHY, G. P. & HARBERD, N. P. 1997. The Arabidopsis GAI gene defines a signaling pathway that negatively regulates gibberellin responses. *Genes & Development,* 11**,** 3194-3205.

PENG, J., SCHWARTZ, D., ELIAS, J. E., THOREEN, C. C., CHENG, D., MARSISCHKY, G., ROELOFS, J., FINLEY, D. & GYGI, S. P. 2003. A proteomics approach to understanding protein ubiquitination. *Nature biotechnology,* 21**,** 921-926.

PENG, Y., MA, W., CHEN, L., YANG, L., LI, S., ZHAO, H., ZHAO, Y., JIN, W., LI, N. & BEVAN, M. W. 2013. Control of Root Meristem Size by DA1-RELATED PROTEIN2 in Arabidopsis. *Plant physiology,* 161**,** 1542-1556.

PÉREZ-PÉREZ, J. M., CANDELA, H., ROBLES, P., LÓPEZ-TORREJÓN, G., DEL POZO, J. C. & MICOL, J. L. 2010. A role for AUXIN RESISTANT3 in the coordination of leaf growth. *Plant and cell physiology,* 51**,** 1661-1673.

PETERS, J.-M. 2006. The anaphase promoting complex/cyclosome: a machine designed to destroy. *Nature Reviews Molecular Cell Biology,* 7**,** 644-656.

PETERSON, K. M., RYCHEL, A. L. & TORII, K. U. 2010. Out of the mouths of plants: the molecular basis of the evolution and diversity of stomatal development. *The Plant Cell Online,* 22**,** 296-306.

PETROSKI, M. D. & DESHAIES, R. J. 2003. Context of multiubiquitin chain attachment influences the rate of Sic1 degradation. *Molecular cell,* 11**,** 1435-1444.

PICKART, C. M. & FUSHMAN, D. 2004. Polyubiquitin chains: polymeric protein signals. *Current opinion in chemical biology,* 8**,** 610-616.

PINOT, F. & BEISSON, F. 2011. Cytochrome P450 metabolizing fatty acids in plants: characterization and physiological roles. *Febs Journal,* 278**,** 195-205.

PLATT, A., HORTON, M., HUANG, Y. S., LI, Y., ANASTASIO, A. E., MULYATI, N. W., ÅGREN, J., BOSSDORF, O., BYERS, D. & DONOHUE, K. 2010. The scale of population structure in Arabidopsis thaliana. *PLoS genetics,* 6**,** e1000843.

PODUST, V. N., BROWNELL, J. E., GLADYSHEVA, T. B., LUO, R.-S., WANG, C., COGGINS, M. B., PIERCE, J. W., LIGHTCAP, E. S. & CHAU, V. 2000. A Nedd8 conjugation pathway is

essential for proteolytic targeting of p27Kip1 by ubiquitination. *Proceedings of the National Academy of Sciences,* 97**,** 4579-4584.

PRASAD, K., ZHANG, X., TOBÓN, E. & AMBROSE, B. A. 2010. The Arabidopsis B‐sister MADS‐box protein, GORDITA, represses fruit growth and contributes to integument development. *The Plant Journal,* 62**,** 203-214.

PRIGGE, M. J., OTSUGA, D., ALONSO, J. M., ECKER, J. R., DREWS, G. N. & CLARK, S. E. 2005. Class III homeodomain-leucine zipper gene family members have overlapping, antagonistic, and distinct roles in Arabidopsis development. *The Plant Cell Online,* 17**,** 61-76.

QI, R. & JOHN, P. C. L. 2007. Expression of genomic AtCYCD2; 1 in Arabidopsis induces cell division at smaller cell sizes: implications for the control of plant growth. *Plant physiology,* 144**,** 1587-1597.

R.D. FINN, J. MISTRY, J. TATE, P. COGGILL, A. HEGER, J.E. POLLINGTON, O.L. GAVIN, P. GUNESEKARAN, G. CERIC, K. FORSLUND, L. HOLM, E.L. SONNHAMMER, S.R. EDDY & BATEMAN, A. 2012. The Pfam protein families database. *Nucleic Acids Res,* 40.

RAZ, V., BERGERVOET, J. & KOORNNEEF, M. 2001. Sequential steps for developmental arrest in Arabidopsis seeds. *Development,* 128**,** 243-252.

READ, M. A., BROWNELL, J. E., GLADYSHEVA, T. B., HOTTELET, M., PARENT, L. A., COGGINS, M. B., PIERCE, J. W., PODUST, V. N., LUO, R.-S. & CHAU, V. 2000. Nedd8 modification of Cul-1 activates SCFβTrCP-dependent ubiquitination of IκBα. *Molecular and cellular biology,* 20**,** 2326-2333.

REINHARDT, D., PESCE, E.-R., STIEGER, P., MANDEL, T., BALTENSPERGER, K., BENNETT, M., TRAAS, J., FRIML, J. & KUHLEMEIER, C. 2003. Regulation of phyllotaxis by polar auxin transport. *Nature,* 426**,** 255-260.

REMMERT, M., BIEGERT, A., HAUSER, A. & SÖDING, J. 2011. HHblits: lightning-fast iterative protein sequence searching by HMM-HMM alignment. *Nature methods,* 9**,** 173-175.

RIESER, E., CORDIER, S. M. & WALCZAK, H. 2013. Linear ubiquitination: a newly discovered regulator of cell signalling. *Trends in biochemical sciences,* 38**,** 94-102.

ROBATZEK, S., CHINCHILLA, D. & BOLLER, T. 2006. Ligand-induced endocytosis of the pattern recognition receptor FLS2 in Arabidopsis. *Genes & Development,* 20**,** 537-542.

RODRIGUEZ, R. E., MECCHIA, M. A., DEBERNARDI, J. M., SCHOMMER, C., WEIGEL, D. & PALATNIK, J. F. 2010. Control of cell proliferation in Arabidopsis thaliana by microRNA miR396. *Development,* 137**,** 103-112.

ROGULJA, D. & IRVINE, K. D. 2005. Regulation of cell proliferation by a morphogen gradient. *Cell,* 123**,** 449-461.

ROGULJA, D., RAUSKOLB, C. & IRVINE, K. D. 2008. Morphogen control of wing growth through the Fat signaling pathway. *Developmental cell,* 15**,** 309-321.

ROJAS, C. A., ELOY, N. B., DE FREITAS LIMA, M., RODRIGUES, R. L., FRANCO, L. O., HIMANEN, K., BEEMSTER, G. T. S., HEMERLY, A. S. & FERREIRA, P. C. G. 2009. Overexpression of the Arabidopsis anaphase promoting complex subunit CDC27a increases growth rate and organ size. *Plant Molecular Biology,* 71**,** 307-318.

ROJO, E., MARTÍN, R., CARTER, C., ZOUHAR, J., PAN, S., PLOTNIKOVA, J., JIN, H., PANEQUE, M., SÁNCHEZ-SERRANO, J. J. & BAKER, B. 2004. VPEγ exhibits a caspase-like activity that contributes to defense against pathogens. *Current Biology,* 14**,** 1897-1906.

ROJO, E., ZOUHAR, J., CARTER, C., KOVALEVA, V. & RAIKHEL, N. V. 2003. A unique mechanism for protein processing and degradation in Arabidopsis thaliana. *Proceedings of the National Academy of Sciences,* 100**,** 7389-7394.

SABLOWSKI, R. 2011. Plant stem cell niches: from signalling to execution. *Current opinion in plant biology,* 14**,** 4-9.

SADANANDOM, A., BAILEY, M., EWAN, R., LEE, J. & NELIS, S. 2012. The ubiquitin–proteasome system: central modifier of plant signalling. *New Phytologist,* 196**,** 13-28.

SADOWSKI, I., MA, J., TRIEZENBERG, S. & PTASHNE, M. 1988. GAL4-VP16 is an unusually potent transcriptional activator. *Nature,* 335**,** 563-564.

SAMPEDRO, J. & COSGROVE, D. J. 2005. The expansin superfamily. *Genome biology,* 6**,** 242.

SARACCO, S. A., HANSSON, M., SCALF, M., WALKER, J. M., SMITH, L. M. & VIERSTRA, R. D. 2009. Tandem affinity purification and mass spectrometric analysis of ubiquitylated proteins in Arabidopsis. *The Plant Journal,* 59**,** 344-358.

SARVEPALLI, K. & NATH, U. 2011. Hyper‐activation of the TCP4 transcription factor in Arabidopsis thaliana accelerates multiple aspects of plant maturation. *The Plant Journal,* 67**,** 595-607.

SAVALDI-GOLDSTEIN, S., PETO, C. & CHORY, J. 2007. The epidermis both drives and restricts plant shoot growth. *NATURE-LONDON-,* 446**,** 199.

SCANLON, M. J. 2003. The polar auxin transport inhibitor N-1-naphthylphthalamic acid disrupts leaf initiation, KNOX protein regulation, and formation of leaf margins in maize. *Plant Physiology,* 133**,** 597-605.

SCHENA, M., LLOYD, A. & DAVIS, R. 1993. The HAT4 gene of Arabidopsis encodes a developmental regulator. *Genes & development,* 7**,** 367-379.

SCHIESSL, K., KAUSIKA, S., SOUTHAM, P., BUSH, M. & SABLOWSKI, R. 2012. JAGGED Controls Growth Anisotropy and Coordination between Cell Size and Cell Cycle during Plant Organogenesis. *Current Biology,* 22**,** 1739-1746.

SCHMEICHEL, K. L. & BECKERLE, M. C. 1994. The LIM domain is a modular protein-binding interface. *Cell,* 79**,** 211-219.

SCHOOF, H., LENHARD, M., HAECKER, A., MAYER, K. F., JÜRGENS, G. & LAUX, T. 2000. The Stem Cell Population of Arabidopsis Shoot Meristems Is Maintained by a Regulatory Loop between the CLAVATA and WUSCHEL Genes. *Cell,* 100**,** 635-644.

SCHRUL, B., KAPP, K., SINNING, I. & DOBBERSTEIN, B. 2010. Signal peptide peptidase (SPP) assembles with substrates and misfolded membrane proteins into distinct oligomeric complexes. *Biochemical Journal,* 427**,** 523-534.

SCHULTZ J, MILPETZ F, BORK P & CP, P. 1998. SMART, a simple modular architecture research tool: Identification of signaling domains. *Proceedings of the National Academy of Sciences,* 95**,** 5857-5864.

SCHWAB, R., OSSOWSKI, S., RIESTER, M., WARTHMANN, N. & WEIGEL, D. 2006. Highly specific gene silencing by artificial microRNAs in Arabidopsis. *The Plant Cell Online,* 18**,** 1121-1133.

SCHWARTZ, D. C. & HOCHSTRASSER, M. 2003. A superfamily of protein tags: ubiquitin, SUMO and related modifiers. *Trends in biochemical sciences,* 28**,** 321-328.

SCOTT, F. L., DENAULT, J.-B., RIEDL, S. J., SHIN, H., RENATUS, M. & SALVESEN, G. S. 2005. XIAP inhibits caspase-3 and-7 using two binding sites: evolutionarily conserved mechanism of IAPs. *The EMBO journal,* 24**,** 645-655.

SEMIARTI, E., UENO, Y., TSUKAYA, H., IWAKAWA, H., MACHIDA, C. & MACHIDA, Y. 2001. The ASYMMETRIC LEAVES2 gene of Arabidopsis thaliana regulates formation of a symmetric lamina, establishment of venation and repression of meristem-related homeobox genes in leaves. *Development,* 128**,** 1771-1783.

SEPÚLVEDA-GARCÍA, E. & ROCHA-SOSA, M. 2012. The Arabidopsis F-box protein AtFBS1 interacts with 14-3-3 proteins. *Plant Science,* 195**,** 36-47.

SHAO, M., ZHENG, H., HU, Y., LIU, D., JANG, J.-C., MA, H. & HUANG, H. 2004. The GAOLAOZHUANGREN1 gene encodes a putative glycosyltransferase that is critical for normal development and carbohydrate metabolism. *Plant and cell physiology,* 45**,** 1453-1460.

SHEWRY, P. R., NAPIER, J. A. & TATHAM, A. S. 1995. Seed storage proteins: structures and biosynthesis. *The plant cell,* 7**,** 945-956.

SHIRASAKI, R. & PFAFF, S. L. 2002. Transcriptional codes and the control of neuronal identity. *Annual review of neuroscience,* 25**,** 251-281.

SHIU, S.-H. & BLEECKER, A. B. 2003. Expansion of the receptor-like kinase/Pelle gene family and receptor-like proteins in Arabidopsis. *Plant Physiology,* 132**,** 530-543.

SHPAK, E. D., LAKEMAN, M. B. & TORII, K. U. 2003. Dominant-negative receptor uncovers redundancy in the Arabidopsis ERECTA leucine-rich repeat receptor–like kinase signaling pathway that regulates organ shape. *The Plant Cell Online,* 15**,** 1095-1110.

SKIRYCZ, A., REICHELT, M., BUROW, M., BIRKEMEYER, C., ROLCIK, J., KOPKA, J., ZANOR, M. I., GERSHENZON, J., STRNAD, M. & SZOPA, J. 2006. DOF transcription factor AtDof1. 1 (OBP2) is part of a regulatory network controlling glucosinolate biosynthesis in Arabidopsis. *The Plant Journal,* 47**,** 10-24.

SMITH, L. G., GREENE, B., VEIT, B. & HAKE, S. 1992. A dominant mutation in the maize homeobox gene, Knotted-1, causes its ectopic expression in leaf cells with altered fates. *Development,* 116**,** 21-30.

SOARES, A. S., DRISCOLL, S. P., OLMOS, E., HARBINSON, J., ARRABAÇA, M. C. & FOYER, C. H. 2008. Adaxial/abaxial specification in the regulation of photosynthesis and stomatal opening with respect to light orientation and growth with CO2 enrichment in the C4 species Paspalum dilatatum. *New Phytologist,* 177**,** 186-198.

SOBHIAN, B., SHAO, G., LILLI, D. R., CULHANE, A. C., MOREAU, L. A., XIA, B., LIVINGSTON, D. M. & GREENBERG, R. A. 2007. RAP80 targets BRCA1 to specific ubiquitin structures at DNA damage sites. *Science,* 316**,** 1198-1202.

SÖDING, J. 2005. Protein homology detection by HMM–HMM comparison. *Bioinformatics,* 21**,** 951-960.

SÖDING, J., BIEGERT, A. & LUPAS, A. N. 2005. The HHpred interactive server for protein homology detection and structure prediction. *Nucleic acids research,* 33**,** W244-W248.

SONG, L., SHI, Q.-M., YANG, X.-H., XU, Z.-H. & XUE, H.-W. 2009. Membrane steroid-binding protein 1 (MSBP1) negatively regulates brassinosteroid signaling by enhancing the endocytosis of BAK1. *Cell research,* 19**,** 864-876.

SONG, X. J., HUANG, W., SHI, M., ZHU, M. Z. & LIN, H. X. 2007. A QTL for rice grain width and weight encodes a previously unknown RING-type E3 ubiquitin ligase. *Nature genetics,* 39**,** 623-630.

SONODA, Y., SAKO, K., MAKI, Y., YAMAZAKI, N., YAMAMOTO, H., IKEDA, A. & YAMAGUCHI, J. 2009. Regulation of leaf organ size by the Arabidopsis RPT2a 19S proteasome subunit. *The Plant Journal,* 60**,** 68-78.

SPREITZER, R. J. & SALVUCCI, M. E. 2002. Rubisco: structure, regulatory interactions, and possibilities for a better enzyme. *Annual review of plant biology,* 53**,** 449-475.

STEINDLER, C., MATTEUCCI, A., SESSA, G., WEIMAR, T., OHGISHI, M., AOYAMA, T., MORELLI, G. & RUBERTI, I. 1999. Shade avoidance responses are mediated by the ATHB-2 HD-zip protein, a negative regulator of gene expression. *Development,* 126**,** 4235-4245.

STEINER, E., EFRONI, I., GOPALRAJ, M., SAATHOFF, K., TSENG, T. S., KIEFFER, M., ESHED, Y., OLSZEWSKI, N. & WEISS, D. 2012. The Arabidopsis O-Linked N-Acetylglucosamine Transferase SPINDLY Interacts with Class I TCPs to Facilitate Cytokinin Responses in Leaves and Flowers. *The Plant Cell Online,* 24**,** 96-108.

STEVENSON, L. F., SPARKS, A., ALLENDE-VEGA, N., XIRODIMAS, D. P., LANE, D. P. & SAVILLE, M. K. 2007. The deubiquitinating enzyme USP2a regulates the p53 pathway by targeting Mdm2. *The EMBO journal,* 26**,** 976-986.

STIMPSON, H. E., LEWIS, M. J. & PELHAM, H. R. 2006. Transferrin receptor-like proteins control the degradation of a yeast metal transporter. *The EMBO journal,* 25**,** 662-672.

STONE, S. L., WILLIAMS, L. A., FARMER, L. M., VIERSTRA, R. D. & CALLIS, J. 2006. KEEP ON GOING, a RING E3 ligase essential for Arabidopsis growth and development, is involved in abscisic acid signaling. *The Plant Cell Online,* 18**,** 3415-3428.

SU, D. & HOCHSTRASSER, M. 2010. A WLM protein with SUMO-directed protease activity. *Molecular and cellular biology,* 30**,** 3734-3736.

SUGIMOTO-SHIRASU, K. & ROBERTS, K. 2003. "Big it up": endoreduplication and cell-size control in plants. *Current opinion in plant biology,* 6**,** 544-553.

SUMMERS, M. K., PAN, B., MUKHYALA, K. & JACKSON, P. K. 2008. The unique N terminus of the UbcH10 E2 enzyme controls the threshold for APC activation and enhances checkpoint regulation of the APC. *Molecular cell,* 31**,** 544-556.

SUN, S., WANG, H., YU, H., ZHONG, C., ZHANG, X., PENG, J. & WANG, X. 2013. GASA14 regulates leaf expansion and abiotic stress resistance by modulating reactive oxygen species accumulation. *Journal of experimental botany,* 64**,** 1637-1647.

SUN, Y. 2003. Targeting E3 ubiquitin ligases for cancer therapy. *Cancer biology & therapy,* 2**,** 623-629.

SUN, Y. 2006. E3 ubiquitin ligases as cancer targets and biomarkers. *Neoplasia (New York, NY),* 8**,** 645-654.

SUTTERLÜTY, H., CHATELAIN, E., MARTI, A., WIRBELAUER, C., SENFTEN, M., MÜLLER, U. & KREK, W. 1999. p45SKP2 promotes p27Kip1 degradation and induces S phase in quiescent cells. *Nature Cell Biology,* 1**,** 207-214.

SZÉCSI, J., JOLY, C., BORDJI, K., VARAUD, E., COCK, J. M., DUMAS, C. & BENDAHMANE, M. 2006. BIGPETALp, a bHLH transcription factor is involved in the control of Arabidopsis petal size. *The EMBO journal,* 25**,** 3912-3920.

TAIRA, M., OTANI, H., SAINT-JEANNET, J.-P. & DAWID, I. B. 1994. Role of the LIM class homeodomain protein Xlim-1 in neural and muscle induction by the Spemann organizer in Xenopus. *Nature,* 372**,** 677-679.

TAO, Q., GUO, D., WEI, B., ZHANG, F., PANG, C., JIANG, H., ZHANG, J., WEI, T., GU, H. & QU, L.-J. 2013. The TIE1 Transcriptional Repressor Links TCP Transcription Factors with TOPLESS/TOPLESS-RELATED Corepressors and Modulates Leaf Development in Arabidopsis. *The Plant Cell Online,* 25**,** 421-437.

TEALE, W. D., PAPONOV, I. A. & PALME, K. 2006. Auxin in action: signalling, transport and the control of plant growth and development. *Nature Reviews Molecular Cell Biology,* 7**,** 847-859.

TETZLAFF, M. T., YU, W., LI, M., ZHANG, P., FINEGOLD, M., MAHON, K., HARPER, J. W., SCHWARTZ, R. J. & ELLEDGE, S. J. 2004. Defective cardiovascular development and elevated cyclin E and Notch proteins in mice lacking the Fbw7 F-box protein. *Proceedings of the National Academy of Sciences of the United States of America,* 101**,** 3338-3345.

THORNBERRY, N. A. & LAZEBNIK, Y. 1998. Caspases: enemies within. *Science,* 281**,** 1312-1316.

THROWER, J. S., HOFFMAN, L., RECHSTEINER, M. & PICKART, C. M. 2000. Recognition of the polyubiquitin proteolytic signal. *The EMBO journal,* 19**,** 94-102.

TORII, K. U., MITSUKAWA, N., OOSUMI, T., MATSUURA, Y., YOKOYAMA, R., WHITTIER, R. F. & KOMEDA, Y. 1996. The Arabidopsis ERECTA gene encodes a putative receptor protein kinase with extracellular leucine-rich repeats. *The Plant Cell Online,* 8**,** 735-746.

TRANQUE, P., CROSSIN, K. L., CIRELLI, C., EDELMAN, G. M. & MAURO, V. P. 1996. Identification and characterization of a RING zinc finger gene (C-RZF) expressed in chicken embryo cells. *Proceedings of the National Academy of Sciences,* 93**,** 3105-3109.

TURCHI, L., CARABELLI, M., RUZZA, V., POSSENTI, M., SASSI, M., PEÑALOSA, A., SESSA, G., SALVI, S., FORTE, V. & MORELLI, G. 2013. Arabidopsis HD-Zip II transcription factors control apical embryo development and meristem function. *Development,* 140**,** 2118-2129.

TZAFRIR, I., PENA-MURALLA, R., DICKERMAN, A., BERG, M., ROGERS, R., HUTCHENS, S., SWEENEY, T. C., MCELVER, J., AUX, G. & PATTON, D. 2004. Identification of genes required for embryo development in Arabidopsis. *Plant Physiology,* 135**,** 1206-1220.

UBEDA-TOMÁS, S., FEDERICI, F., CASIMIRO, I., BEEMSTER, G. T., BHALERAO, R., SWARUP, R., DOERNER, P., HASELOFF, J. & BENNETT, M. J. 2009. Gibberellin Signaling in the Endodermis Controls Arabidopsis Root Meristem Size. *Current Biology,* 19**,** 1194-1199.

UBERTI-MANASSERO, N. G., LUCERO, L. E., VIOLA, I. L., VEGETTI, A. C. & GONZALEZ, D. H. 2012. The class I protein AtTCP15 modulates plant development through a pathway that overlaps with the one affected by CIN-like TCP proteins. *Journal of Experimental Botany,* 63**,** 809-823.

UMEDA, M., MANABE, Y. & UCHIMIYA, H. 1997. Phosphorylation of the C2 subunit of the proteasome in rice (Oryza sativa L.). *FEBS letters,* 403**,** 313-317.

VAN DELFT, S., GOVERS, R., STROUS, G. J., VERKLEIJ, A. J. & EN HENEGOUWEN, P. M. V. B. 1997. Epidermal growth factor induces ubiquitination of Eps15. *Journal of Biological Chemistry,* 272**,** 14013-14016.

VAN DEN HEUVEL, S. 2005. *Cell-cycle regulation, WormBook*.

VAN DER BIEZEN, E. A., FREDDIE, C. T., KAHN, K. & JONES, J. D. 2002. Arabidopsis RPP4 is a member of the RPP5 multigene family of TIR‐NB‐LRR genes and confers downy mildew resistance through multiple signalling components. *The Plant Journal,* 29**,** 439-451.

VANNESTE, S., MAES, L., DE SMET, I., HIMANEN, K., NAUDTS, M., INZE, D. & BEECKMAN, T. 2005. Auxin regulation of cell cycle and its role during lateral root initiation. *Physiologia Plantarum,* 123**,** 139-146.

VAROTTO, C., PESARESI, P., MEURER, J., OELMÜLLER, R., STEINER‐LANGE, S., SALAMINI, F. & LEISTER, D. 2000. Disruption of the Arabidopsis photosystem I gene psaE1 affects photosynthesis and impairs growth. *The Plant Journal,* 22**,** 115-124.

VERMEULEN, K., VAN BOCKSTAELE, D. R. & BERNEMAN, Z. N. 2003. The cell cycle: a review of regulation, deregulation and therapeutic targets in cancer. *Cell proliferation,* 36**,** 131-149.

VERT, G. & CHORY, J. 2006. Downstream nuclear events in brassinosteroid signalling. *Nature,* 441**,** 96-100.

VIERSTRA, R. D. 1996. Proteolysis in plants: mechanisms and functions. *Plant molecular biology,* 32**,** 275-302.

VILLANUEVA, J. M., BROADHVEST, J., HAUSER, B. A., MEISTER, R. J., SCHNEITZ, K. & GASSER, C. S. 1999. INNER NO OUTER regulates abaxial–adaxial patterning in Arabidopsis ovules. *Genes & Development,* 13**,** 3160-3196.

VIOLA, I., UBERTI, M. N., RIPOLL, R. & GONZALEZ, D. 2011. The Arabidopsis class I TCP transcription factor AtTCP11 is a developmental regulator with distinct DNA-binding properties due to the presence of a threonine residue at position 15 of the TCP domain. *Biochem. J,* 435**,** 143-155.

VLACH, J., HENNECKE, S., ALEVIZOPOULOS, K., CONTI, D. & AMATI, B. 1996. Growth arrest by the cyclin-dependent kinase inhibitor p27Kip1 is abrogated by c-Myc. *The EMBO Journal,* 15**,** 6595-6604.

VOGES, D., ZWICKL, P. & BAUMEISTER, W. 1999. The 26S proteasome: a molecular machine designed for controlled proteolysis. *Annual review of biochemistry,* 68**,** 1015-1068.

VOIGT, C., OSTER, U., BÖRNKE, F., JAHNS, P., DIETZ, K. J., LEISTER, D. & KLEINE, T. 2010. In‐depth analysis of the distinctive effects of norflurazon implies that tetrapyrrole biosynthesis, organellar gene expression and ABA cooperate in the GUN‐type of plastid signalling. *Physiologia plantarum,* 138**,** 503-519.

WAGNER, R. & PFANNSCHMIDT, T. 2006. Eukaryotic transcription factors in plastids—Bioinformatic assessment and implications for the evolution of gene expression machineries in plants. *Gene,* 381**,** 62-70.

WANG, B., MATSUOKA, S., BALLIF, B. A., ZHANG, D., SMOGORZEWSKA, A., GYGI, S. P. & ELLEDGE, S. J. 2007. Abraxas and RAP80 form a BRCA1 protein complex required for the DNA damage response. *Science,* 316**,** 1194-1198.

WANG, F., ZHU, D., HUANG, X., LI, S., GONG, Y., YAO, Q., FU, X., FAN, L.-M. & DENG, X. W. 2009. Biochemical insights on degradation of Arabidopsis DELLA proteins gained from a cell-free assay system. *The Plant Cell Online,* 21**,** 2378-2390.

WANG, P. & GRANADOS, R. R. 1997. An intestinal mucin is the target substrate for a baculovirus enhancin. *Proceedings of the National Academy of Sciences,* 94**,** 6977-6982.

WANG, T.-W., LU, L., ZHANG, C.-G., TAYLOR, C. & THOMPSON, J. E. 2003a. Pleiotropic effects of suppressing deoxyhypusine synthase expression in Arabidopsis thaliana. *Plant molecular biology,* 52**,** 1223-1235.

WANG, X. & CHORY, J. 2006. Brassinosteroids regulate dissociation of BKI1, a negative regulator of BRI1 signaling, from the plasma membrane. *Science,* 313**,** 1118-112.

WANG, Y., HENRIKSSON, E., SÖDERMAN, E., HENRIKSSON, K. N., SUNDBERG, E. & ENGSTRÖM, P. 2003b. The arabidopsis homeobox gene, ATHB16, regulates leaf development and the sensitivity to photoperiod in Arabidopsis. *Developmental biology,* 264**,** 228-239.

WANG, Y., RIBOT, C., REZZONICO, E. & POIRIER, Y. 2004. Structure and expression profile of the Arabidopsis PHO1 gene family indicates a broad role in inorganic phosphate homeostasis. *Plant Physiology,* 135**,** 400-411.

WEIGEL, D. 2012. Natural variation in Arabidopsis: from molecular genetics to ecological genomics. *Plant physiology,* 158**,** 2-22.

WEIGEL, D. & MOTT, R. 2009. The 1001 genomes project for Arabidopsis thaliana. *Genome Biol,* 10**,** 107.

WHITE, D. W. R. 2006. PEAPOD regulates lamina size and curvature in Arabidopsis. *Proceedings of the National Academy of Sciences,* 103**,** 13238-13243.

WIBORG, J., O'SHEA, C. & SKRIVER, K. 2008. Biochemical function of typical and variant Arabidopsis thaliana U-box E3 ubiquitin-protein ligases. *Biochem. J,* 413**,** 447-457.

WIBORG, O., PEDERSEN, M., WIND, A., BERGLUND, L., MARCKER, K. & VUUST, J. 1985. The human ubiquitin multigene family: some genes contain multiple directly repeated ubiquitin coding sequences. *The EMBO journal,* 4**,** 755-759.

WIESNER, S., OGUNJIMI, A. A., WANG, H.-R., ROTIN, D., SICHERI, F., WRANA, J. L. & FORMAN-KAY, J. D. 2007. Autoinhibition of the HECT-type ubiquitin ligase Smurf2 through its C2 domain. *Cell,* 130**,** 651-662.

WILMOTH, J. C., WANG, S., TIWARI, S. B., JOSHI, A. D., HAGEN, G., GUILFOYLE, T. J., ALONSO, J. M., ECKER, J. R. & REED, J. W. 2005. NPH4/ARF7 and ARF19 promote leaf expansion and auxin‐induced lateral root formation. *The Plant Journal,* 43**,** 118-130.

WINBORN, B. J., TRAVIS, S. M., TODI, S. V., SCAGLIONE, K. M., XU, P., WILLIAMS, A. J., COHEN, R. E., PENG, J. & PAULSON, H. L. 2008. The deubiquitinating enzyme ataxin-3, a polyglutamine disease protein, edits Lys63 linkages in mixed linkage ubiquitin chains. *Journal of Biological Chemistry,* 283**,** 26436-26443.

WOELK, T., OLDRINI, B., MASPERO, E., CONFALONIERI, S., CAVALLARO, E., DI FIORE, P. P. & POLO, S. 2006. Molecular mechanisms of coupled monoubiquitination. *Nature cell biology,* 8**,** 1246-1254.

WOOD, C. C., ROBERTSON, M., TANNER, G., PEACOCK, W. J., DENNIS, E. S. & HELLIWELL, C. A. 2006. The Arabidopsis thaliana vernalization response requires a polycomb-like protein complex that also includes VERNALIZATION INSENSITIVE 3. *Proceedings of the National Academy of Sciences,* 103**,** 14631-14636.

WU, F.-H., SHEN, S.-C., LEE, L.-Y., LEE, S.-H., CHAN, M.-T. & LIN, C.-S. 2009. Tape-Arabidopsis Sandwich-a simpler Arabidopsis protoplast isolation method. *Plant Methods,* 5**,** 16.

XIA, T. L., NA;DUMENIL, JACK; LI, JIE; BEVAN, MICHAEL W; LI, YUNHAI 2013. DA2, an E3 ubiquitin ligase, interacts with the ubiquitin receptor DA1 to control seed size in Arabidopsis thaliana. *The plant cell,* 25**,** 3347-3359.

XIE, Q., FRUGIS, G., COLGAN, D. & CHUA, N.-H. 2000. Arabidopsis NAC1 transduces auxin signal downstream of TIR1 to promote lateral root development. *Genes & Development,* 14**,** 3024-3036.

XING, S., ROSSO, M. G. & ZACHGO, S. 2005. ROXY1, a member of the plant glutaredoxin family, is required for petal development in Arabidopsis thaliana. *Development,* 132**,** 1555-1565.

XING, S. & ZACHGO, S. 2008. ROXY1 and ROXY2, two Arabidopsis glutaredoxin genes, are required for anther development. *The Plant Journal,* 53**,** 790-801.

XU, L., XU, Y., DONG, A., SUN, Y., PI, L., XU, Y. & HUANG, H. 2003. Novel as1 and as2 defects in leaf adaxial-abaxial polarity reveal the requirement for ASYMMETRIC LEAVES1 and 2 and ERECTA functions in specifying leaf adaxial identity. *Development,* 130**,** 4097-4107.

XU, R. & LI, Y. 2011. Control of final organ size by Mediator complex subunit 25 in Arabidopsis thaliana. *Development,* 138**,** 4545-4554.

XU, R. & LI, Y. 2012. The Mediator complex subunit 8 regulates organ size in Arabidopsis thaliana. *Plant Signaling & Behavior,* 7**,** 182-183.

YANG, H., SHI, Y., LIU, J., GUO, L., ZHANG, X. & YANG, S. 2010. A mutant CHS3 protein with TIR-NB-LRR-LIM domains modulates growth, cell death and freezing tolerance in a temperature-dependent manner in Arabidopsis. *The Plant Journal,* 63**,** 283-296.

YE, Y. & RAPE, M. 2009. Building ubiquitin chains: E2 enzymes at work. *Nature reviews Molecular cell biology,* 10**,** 755-764.

YI, H. & RICHARDS, E. J. 2007. A cluster of disease resistance genes in Arabidopsis is coordinately regulated by transcriptional activation and RNA silencing. *The Plant Cell Online,* 19**,** 2929-2939.

YOUNG, P., DEVERAUX, Q., BEAL, R. E., PICKART, C. M. & RECHSTEINER, M. 1998. Characterization of two polyubiquitin binding sites in the 26 S protease subunit 5a. *Journal of Biological Chemistry,* 273**,** 5461-5467.

YUAN, T., FUJIOKA, S., TAKATSUTO, S., MATSUMOTO, S., GOU, X., HE, K., RUSSELL, S. D. & LI, J. 2007. BEN1, a gene encoding a dihydroflavonol 4 ‐ reductase (DFR) ‐ like protein, regulates the levels of brassinosteroids in Arabidopsis thaliana. *The Plant Journal,* 51**,** 220-233.

ZECCA, M., BASLER, K. & STRUHL, G. 1996. Direct and Long-Range Action of a Wingless Morphogen Gradient. *Cell,* 87**,** 833-844.

ZHADANOV, A. B., BERTUZZI, S., TAIRA, M., DAWID, I. B. & WESTPHAL, H. 1995. Expression pattern of the murine LIM class homeobox gene Lhx3 in subsets of neural and neuroendocrine tissues. *Developmental dynamics,* 202**,** 354-364.

ZHANG, H., HACKBARTH, C., CHANSKY, K. & CHAMBERS, H. 2001. A proteolytic transmembrane signaling pathway and resistance to beta-lactams in staphylococci. *Science Signaling,* 291**,** 1962-1965.

ZHANG, X., GARRETON, V. & CHUA, N.-H. 2005. The AIP2 E3 ligase acts as a novel negative regulator of ABA signaling by promoting ABI3 degradation. *Genes & Development,* 19**,** 1532-1543.

ZHANG, Y., GORITSCHNIG, S., DONG, X. & LI, X. 2003. A gain-of-function mutation in a plant disease resistance gene leads to constitutive activation of downstream signal transduction pathways in suppressor of npr1-1, constitutive 1. *The Plant Cell Online,* 15**,** 2636-2646.

ZHAO, B., LI, L., LEI, Q. & GUAN, K.-L. 2010. The Hippo–YAP pathway in organ size control and tumorigenesis: An updated version. *Genes & development,* 24**,** 862-874.

ZHENG, J., YANG, X., HARRELL, J. M., RYZHIKOV, S., SHIM, E.-H., LYKKE-ANDERSEN, K., WEI, N., SUN, H., KOBAYASHI, R. & ZHANG, H. 2002. CAND1 binds to unneddylated CUL1 and regulates the formation of SCF ubiquitin E3 ligase complex. *Molecular cell,* 10**,** 1519-1526.

ZHOU, Y. & NI, M. 2010. SHORT HYPOCOTYL UNDER BLUE1 truncations and mutations alter its association with a signaling protein complex in Arabidopsis. *The Plant Cell Online,* 22**,** 703-715.

ZHOU, Y., ZHANG, X., KANG, X., ZHAO, X., ZHANG, X. & NI, M. 2009. SHORT HYPOCOTYL UNDER BLUE1 associates with MINISEED3 and HAIKU2 promoters in vivo to regulate Arabidopsis seed development. *The Plant Cell Online,* 21**,** 106-117.

ZHUANG, M., GUAN, S., WANG, H., BURLINGAME, A. L. & WELLS, J. A. 2012. Substrates of IAP ubiquitin ligases identified with a designed orthogonal E3 ligase, the NEDDylator. *Molecular cell,* 49**,** 273-282.

ZIPFEL, C., KUNZE, G., CHINCHILLA, D., CANIARD, A., JONES, J. D., BOLLER, T. & FELIX, G. 2006. Perception of the Bacterial PAMP EF-Tu by the Receptor EFR Restricts *Agrobacterium*-Mediated Transformation. *Cell,* 125**,** 749-760.